The impact of maternal HIV infection on uninfected neonate brain structure

By

Abdulmumin Ibrahim

Presented for the Degree of

DOCTOR OF PHILOSOPHY

In the Department of Human Biology

Faculty of Health Sciences

UNIVERSITY OF CAPE TOWN

Supervisor: Dr. Martha Holmes

Co-supervisors: Prof. Ernesta Meintjes, Dr. Fleur Warton

February 2022

Abstract

Successful prevention of mother-to-child HIV transmission (PMTCT) programs have reduced the risk of infant HIV infection in South Africa from 8% in 2008 to an estimated 1.4% in 2015, resulting in an increasing population of HIV-exposed uninfected (HEU) children. However, the long-term effects of HIV and antiretroviral therapy (ART) exposure on the developing brain is not well understood. While HEU children perform better than their counterparts living with HIV, they continue to demonstrate greater neurodevelopmental delay than HIV-unexposed uninfected (HUU) children. As a result, neuroimaging studies have looked at the developing brain in this population, however there is little consensus about typical exposure related effects. In addition, it is unclear whether previously reported exposure-related results are directly related to *in utero* exposure to HIV, or indirectly via family and/or environmental factors. Research focused on newborns allows one to eliminate possible contributions from other factors, clarifying the influence of ART and HIV exposure on the developing brain.

This dissertation employs neuroimaging and neurocognitive data in a well-characterized infant cohort to better understand the influence of maternal HIV infection on the uninfected brain. HEU infants were exposed to ART in utero between 3 and 9 months, allowing for the study of potential ART exposure effects of as well as HIV exposure. This dissertation will identify HIV and ART exposure effects on brain structure. In addition, the relationship between neonate brain structural outcomes and cognitive abilities at 9-12 months will be determined to identify potential functional consequences of early structural abnormalities.

Chapter two presents an analysis of manually traced subcortical volumes in 120 unexposed uninfected (HUU) and exposed uninfected (HEU) neonates. HEU neonates demonstrated significantly reduced mean caudate volumes bilaterally and left mean putamen volumes relative to HUU neonates. Further analysis revealed the observed differences in basal nuclei volumes were related to duration of ART in utero. Infants exposed to ART throughout pregnancy had similar caudate and putamen volumes compared to their HU counterparts. While infants exposed to ART post conception (from 3 – 8 months in utero) had significantly smaller mean caudate volumes bilaterally, and a trending smaller left putamen volume compared to HUU infants.

Chapter three examines the potential functional consequences of HIV/ART volumetric reductions. We modelled manually traced neonatal subcortical volumes with neuropsychological outcomes at 9 – 12

months. Among HUU infants, bilateral pallidum volumes predicted neuropsychological measures across all domains. All volumes, with the exception of bilateral thalamus and vermis, predicted the general quotient score in HUU infants. In contrast, among the HEU infants, volumes did not relate to neuropsychological outcomes with the exception of the caudate, putamen and vermis predicting locomotion scores in the preconception group. While no HIV exposure differences were present in neuropsychological domains, HEU infants recruit alternative subcortical structures compared to typically developing unexposed infants.

Chapter four presents a DTI-tractographic analysis of white matter connections between subcortical structures manually traced. HEU demonstrate white matter alterations in two tracts – higher FA between right putamen and left thalamus and higher MD between caudate and thalamus on the right hemisphere. The WM alterations observed in HEU appear to be from roles of both HIV and ART exposure. In contrast to ART dependent subcortical grey matter reductions, the observed white matter alterations are independent of maternal treatment initiation. In addition, we also find associations between unaltered white matter connections and both maternal immune health and ART duration during pregnancy. These results suggest white matter is influenced to varying degrees by HIV and ART exposure, as well as maternal health in pregnancy.

Chapter five looks at the possible functional consequences of the reported alterations in white matter integrity. We modelled white matter connections between manually traced neonatal subcortical volumes with neuropsychological outcomes at 9 – 12 months. Similar to chapter 3, within HUU infants, we observed a number of white matter connections predictive of neuropsychological outcomes across all domains. And almost no white matter tracts predicted neuropsychological measures in HEU infants. These results again point to HEU infants recruiting different pathways to perform basic tasks.

In conclusion, the results documented in this thesis point to the influence of HIV exposure, ART duration and maternal immune health on fetal brain development. However, these factors impact grey and white matter differently. ART initiated pre-conception was protective of subcortical grey matter volumes but did not protect two white matter connections. Despite few localized grey and white matter alterations, HEU infants demonstrated a lack of structural associations with neuropsychological outcomes later in infancy. While there were no exposure related differences across neuropsychological domains, the long-term functional consequences of altered structural recruitment is unknown. Finally, this thesis adds to the body of literature that early ART in pregnancy

is neuroprotective, and that HIV exposure related structural alterations are evident as early as 2 - 4 weeks after birth.

Acknowledgements

This research was funded by NIH grant RO1HD085813 (Fogarty International Centre and the Eunice Kennedy Shriver National Institute of Child Health and Human Development). To principal, Ernesta M. Meintjes and to collaborative investigators.

A special thanks to my supervisor, DR. Martha J. Holmes for her supervisory, advisory and mentorship roles. I have indeed learnt a great deal and I am forever grateful. To my co-supervisors, Ernesta M. Meintjes and Fleur F. Warton for their contributions to this thesis. To Marcin Jankiewics, for his constructive criticism and technical advice to make this thesis a success. I am indeed very grateful. Many thanks to Barbara Laughton for her immense contribution to the neuropsychological component of this thesis.

I also want to acknowledge my colleagues in the lab, especially Farai Mberi, Joanah Madzime, Isaac Kubo, and Amy Graham for their support during the course of my PhD study. My profound gratitude to Steven Randall for his support and advice regarding submission technicality.

A special thanks to a friend like a brother Gabriel Oluwadare Adeyemo who engineered my first visit to Cape Town and introduced me to Sofia Osawe who in turn introduced me to Mohammadou. These three wonderful people were instrumental for my admission into UCT.

To my lovely wife Amina Ibidunni Sedick for her patience, understanding, love, and prayers. To my children; Yasser, Nadia, and the twins (Ibrahim & Suwaiba) who constantly missed daddy while away from home. I love you forever. To my senior brothers, Professor Isah Ibrahim and Mr. Shuaib Ibrahim for their constant support and prayers. To my late parents, Mr & Mrs Ibrahim, may you continue to rest in peace.

To my South African sister and family, Kentse and her husband, Itumeleng for making me feel at home throughout my studies. To my friends and families, Alhaji Baba Abdulkadir, Usman Abdulraheem, Ahmed Isa, Sofiullahi Abubakar, Aisha Olagunju, Aminu Imam and Samuel Bayi.

To my mentor, Prof. William Fifer (Uncle Bill) for taken a fatherly role during and after this work. I appreciate your moral and financial support. Your support always comes when I desperately needed it. Thank you always.

Plagiarism declaration

1. I acknowledge and understand that plagiarism is a serious academic dishonesty.
2. I have read the document about avoiding plagiarism, I am familiar with its contents, and I have avoided all forms of plagiarism mentioned there.
3. I hereby attest to the originality of this work and I have cited properly all the references used including using quotation marks where I have used the word of others.

Table of Contents

List of Abbreviations

AD: axial diffusivity

AFNI: analysis of functional neuro-imaging

AP: anteroposterior

ART: antiretroviral therapy

ARV: antiretrovirals

CNS: central nervous system

DT: diffusion tensor

DTI: diffusion tensor imaging

DW: diffusion weighted

DWI: diffusion weighted imaging

EPI: echo planar imaging

FA: fractional anisotropy

FACT: fibre assessment by continuous tracking

FACTID: fibre assessment by continuous tracking including diagonals

FID: free induction decay

FLASH: fast low angle shot

fMRI: functional magnetic resonance imaging

GM: grey matter

HEU: HIV-exposed uninfected

HIV: Human immunodeficiency virus

HUU: HIV-unexposed uninfected

MD: mean diffusivity

MRI: magnetic resonance imaging

MRS: magnetic resonance spectroscopy

PA: posteroanterior

PD: proton density

RF: radio frequency

RD: radial diffusivity

ROI: region of interest

SNR: signal-to-noise ratio

TE: time to echo

TR: repetition time

VL: viral load

WM: white matter

WM-ROI: white matter region of interest

CHAPTER ONE

1.1 introduction and problem identification

The increased availability of non-invasive imaging techniques has led to a better understanding of the human brain in health and disease. Certain populations are more difficult to image, such as infants, and more research is necessary to fill this gap. There is a particular need for research on typical developing infants globally, to provide a benchmark of healthy development that is locally relevant. There is a growing awareness of the long-term influence of maternal health during pregnancy on the developing brain. As such, there is an interest in studying infant development through the lens of maternal health.

Preventative efforts by scientists and policymakers worldwide have reduced perinatal transmissions of the human immunodeficiency virus (HIV). Sub-Saharan Africa is the region most affected by the HIV pandemic and has put much effort into programs focused on preventing HIV transmission. South African National prevention of mother-to-child transmission of HIV (PMTCT) strategies have brought the risk of infant HIV infection down from 8% in 2008 to 1.4% in 2015and below 1.0% in 2019 (National Department of Health, 2019). Between 2010 and 2016 the South African PMTCT programme prevented approximately 80 000-85 000 newborn babies yearly from early HIV infection (assuming 1 million live births, 31% infant HIV exposure and 30% MTCT in the absence of PMTCT interventions) (SAMRC, 2016). The reduction in new perinatal infections was due to the continued promotion of combination ART in pregnancy (van Schalkwyk et al., 2013, Aizire et al., 2013, Shetty and Maldonado, 2013, Phelps et al., 2013). One outcome of this achievement is an increasing population of HIV-exposed-uninfected (HEU) infants. While perinatal HIV and antiretroviral therapy (ART) exposure are not as damaging as HIV infection for the developing infant, research suggests there are possible long-term exposure related developmental delays and damage especially in resource-poor settings (Le Doare et al., 2012).

Neurocognitive studies provide an indirect assessment of the central nervous system through measures of cognitive functions including behaviour and language acquisition. Neuroimaging studies use direct quantitative measures of brain structure and function (Le Doare et al., 2012). In combination, these methods can provide insight into the biological underpinnings of cognitive abnormalities. To date, both imaging and neurocognitive studies report mixed findings on the effect

of HIV/ART exposure on neurodevelopmental outcomes. Of the forty-one neurocognitive studies including HEU infants/children, fifteen report HIV/ART exposure related differences (Forehand et al., 1998, Esposito et al., 1999, Dorsey et al., 1999, Sanmaneechai et al., 2005, Van Rie et al., 2009, Van Rie et al., 2008, Boivin et al., 1995, Brahmbhatt et al., 2014, Alcock et al., 2016, Familiar et al., 2018, Wu et al., 2018, le Roux et al., 2018, Wedderburn et al., 2019, Ntozini et al., 2020, Madlala et al., 2020). Within these studies, HEU children had a lower mean score in at least one neuropsychological domain. Seven of nine imaging studies reported subtle changes in metabolite levels and white matter integrity across different brain regions, in HEU children compared to their HIV-unexposed uninfected (HUU) counterparts (Cortey et al., 1994, Tran et al., 2016, Robertson et al., 2018, Graham et al., 2020, Madzime et al., 2021, Jankiewicz et al., 2017, Yadav et al., 2020).

Previously reported HIV/ART exposure related neurodevelopmental changes in infants and children are likely associated with clinical and developmental outcomes. Since the second and third trimester of pregnancy and the first two years of postnatal life (Stile & Jernigan 2010) are critical periods of brain development, it is important to monitor brain changes in HEU children. Neurodevelopment may be influenced by exposure to the virus and ART in utero and postnatally. Other factors, like duration of ART exposure and maternal immune health may be important drivers *in utero* and early postnatal life.

Given the lack of consensus among neurodevelopmental studies in infants and children exposed to HIV and ART, more work is needed within this population. It is unclear whether previously reported exposure-related results are directly related to *in utero* exposure to HIV, or indirectly via family and/or environmental factors. Research focused on newborns allows one to eliminate possible contributions from other factors, clarifying the influence of ART and HIV exposure on the developing brain.

This thesis involves neuroimaging and neuropsychological data from a birth cohort of 186 mother-infant pairs. The thesis adds to the small body of literature on this topic. The work presented is unique in that it includes both magnetic resonance imaging (MRI) of the brain and neuropsychological measures in infancy. In addition, data is available on the length of ART exposure in utero allowing for study of its effects independent of HIV exposure. Within the neonate brain, this thesis focused on subcortical structures and cerebellum. The first analysis (chapter two) presents manually traced neonate subcortical volumes (basal ganglia (caudate, putamen and pallidum), thalamus and cerebellum including cerebellar vermis), performing statistical analysis to identify potential effects of HIV and ART exposure. The second analysis (chapter three) examines the potential consequences of

HIV associated volumetric changes by looking at relationships with neuropsychological outcomes at 9 months postnatal life. Chapter four builds on the first analysis (chapter two) by quantifying structural connectivity among manually traced subcortical structures and cerebellum. Lastly, the fifth chapter examines the potential consequences of HIV associated structural connectivity changes in neonates by looking at relationships with neuropsychological outcomes at 9 months postnatal life.

1.1.1 Research questions:

1. Does maternal HIV infection influence subcortical grey and white matter development in newborns?
2. Does initiation of ARV before conception protect subcortical grey and white matter development in newborns?
3. Do HIV and/or ART exposure associated subcortical grey and white matter changes in newborns affect neurocognitive abilities at 9 months?

1.1.2 Hypotheses:

1. Compared to HUU neonates, HEU newborns will have smaller mean subcortical volumes.
2. Compared to HUU neonates, HEU newborns will have altered white matter connectivity between exposure affected subcortical structures.
3. Maternal ART provides neuroprotection for the developing fetus. Duration of ART in pregnancy will be positively associated with subcortical volumes in HEU newborns.
4. Smaller volumes and lower FA/higher MD will be associated with poor neuropsychological outcomes scores at 9-month postnatal life. e.g. reduced basal ganglia volumes will be associated with deficits in the measures of fine and gross motor abilities.

1.1.3 Specific objectives:

1. Manual segmentation of subcortical structures (thalamus, basal nuclei – caudate nuclei, putamen and pallidus, and cerebellar hemispheres and cerebellar vermis) from neonate anatomical MRI data; assessment of relevant confounders for model building; use linear regression models to identify HIV-exposure related differences in segmented subcortical structures.
2. Pre/process DTI data; perform tractography using manually traced volumes as seeds; statistical analysis to determine HIV-exposure group differences in DTI measures

Statistical modelling of relationship between neonate structural MRI outcomes (volumes, structural connectivity) and neuropsychological tests performed at 9 months.

1.2 Background and literature

1.2.1 Typical human brain development

The human brain starts to develop shortly after conception and continues through adolescence until early adulthood. The brain develops in a time dependent sequential pattern. The fetal brain begins to develop during the third week of gestation starting with the appearance of neural progenitor cells which then differentiate into neurons and glia – the two cell types that form the basis of nervous system. The birth of new neurons and glia is referred to as neurogenesis and gliogenesis, respectively. Neurons are responsible for communicating messages throughout the entire brain and glial cells provide neurons with structural and chemical support (Stiles, 2008, Stiles and Jernigan, 2010, Martin, 2013).

The brain is small and smooth in appearance by the ninth week of gestation. As pregnancy progresses, the growing brain forms the characteristics folds that designate distinct brain regions. Anatomical changes reflect underlying alterations at the cellular level. At this stage, communication between nerve cells is enhanced as neurons start to release chemical signalling molecules. This is therefore followed by the formation of fibre pathways forming the brain's communication networks. "Cells that make up the neocortex – the part of the brain that coordinates sight, sound, spatial reasoning, conscious thought, and language – begin to communicate" (Kostović and Jovanov-Milosević, 2006).

Although the brain's foundation is assembled prenatally, its functional connectivity development continues postnatally, underpinned by sensory input. The neural connectivity is remarkable in the first years of life. "After age 2 years, the number of neural connections decreases. In a process known as synaptic pruning, the brain organizes its connectome to perform more efficiently, removing inefficient connections to maximize performance" (Innocenti and Price, 2005, Stiles and Jernigan, 2010, van den Heuvel et al., 2015).

The sequelae of normal brain development from conception to birth and into early adulthood are: i) neurulation and proliferation ii) neuronal migration iii) synaptogenesis and synaptic reorganisation iv) pruning (neural regression) and v) myelination. Fig 1.1

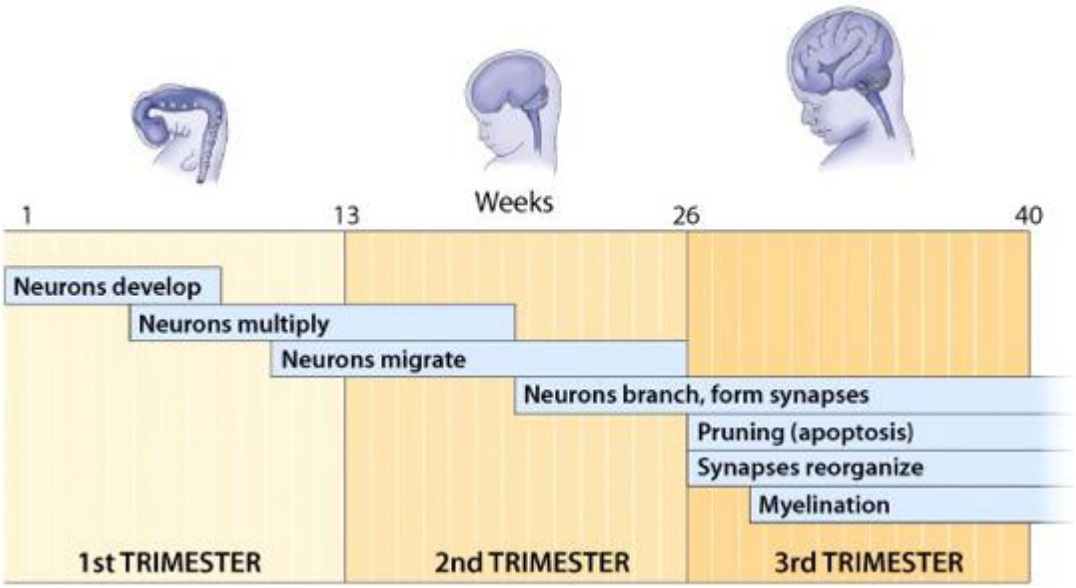

Figure 1.1 sequelae of brain development (Duke University, 2016).

1.2.2 Neurulation (neurons develop) and proliferation (neurons multiply)

Neurulation is the formation of the neural tube. The neural tube is the first brain structure to appear during the third week of gestation, between embryonic day 20 – 27. Neurulation is preceded by gastrulation (differentiation of neural progenitor cells) – the first step in brain development which begins on embryonic day thirteen. The process of gastrulation is signalled by the appearance of a slit-like opening in the upper layer of the embryo called the primitive streak. This development transforms the embryo from a single layer of cells (blastula) to three primary germ layers (trilaminar embryo) – endoderm, mesoderm, and ectoderm. The primary germ layers give rise to specific parts of the organism. The cells of the ectoderm will be transformed into two types of ectodermal stem cells – epidermal ectodermal stem cells which give rise structures such as skin, nails and sweat glands, while neurectoderm stem cells (neural progenitor cells) give rise to the brain and central nervous system. At the end of gastrulation, the cells along the midline of the upper layer of the embryo have transformed into neural progenitor cells. Neural progenitor cells differentiate into neural progenitor that will produce precursor cells for forebrain structures and for hindbrain or spinal cord structures (Stiles, 2008, Stiles and Jernigan, 2010, Martin, 2013).

The next major step in brain development after the differentiation of neural progenitor cells involves the formation of the first well-defined neural structure, the neural tube. The neural progenitor cells

have developed and are positioned along the rostral-caudal midline of the upper layer of the three-layered embryo near the conclusion of gastrulation (Stiles and Jernigan 2010). The neural plate is the part of the embryo that contains the neural progenitor cells on around embryonic day 21. Between the two ridges are the brain progenitor cells. The ridges rise, invaginate, and merge over many days to produce a hollow tube. Fusion starts in the growing tube's centre and moves in both rostral and caudal directions. On embryonic day 25 and 27, the anterior neuropore at the tube's most rostral end and the posterior neuropore at the caudal end are the last segments to close (Stiles and Jernigan 2010). The neural progenitors create a single layer of cells that lines the middle of the neural tube, immediately adjacent to its hollow centre, after the neural tube is complete. The hollow centre of the neural tube is cylindrical in the embryo, but as the brain grows larger and more sophisticated, the shape of the hollow cavity changes as well, eventually producing the brain's ventricular system. The "ventricular zone" is so named because neural progenitors are found in the region that will eventually become the ventricles (VZ). The brain will be formed by neural progenitor cells located in the most rostral portion of the neural tube, whereas the hindbrain and spinal column will be formed by cells located more caudally. (Copp et al., 2003, Stiles, 2008, Stiles and Jernigan, 2010).

When the neural tube closes, the diameter of the ventral end of the tube increases, forming the three major brain vesicles, or pouches. The "prosencephalon," which will create the future forebrain, is the ventrally positioned embryonic brain vesicles. The "mesencephalon," which will become the future midbrain, is in the middle, and the "rhombencephalon," which will become the hindbrain, is in the back. These three segments progressively subdivide, resulting in five secondary brain vesicles by the end of the embryonic stage. The prosencephalon is divided into "telencephalon" and "diencephalon," while the rhombencephalon is divided into "metencephalon" and "myelencephalon." The mesencephalon does not divide any further. These five subdivisions are arranged along the embryo's rostral-caudal axis. These five subdivisions are positioned along the embryo's rostral-caudal axis and form the central nervous system's basic arrangement. (Stiles, 2008, Stiles and Jernigan, 2010, Martin, 2013) See table 1.1.

Table 1.1. Major subdivisions of the embryonic central nervous system with their associated mature structures.

Neural Tube (Week 3)	Primary Vesicles (Week 4)	Secondary Vesicles (week 5)	Adult Structures
neural plate neural groove neural tube **Brain**	Prosencephalon (forebrain)	Telencephalon	Cerebral (cortex), **basal ganglia**, hippocampus, amygdala, olfactory bulb, rhinencephalon, pituitary, lateral ventricles
		Diencephalon	Epithalamus, **thalamus**, subthalamus, pineal, posterior commissure, pretectum, third ventricle
	Mesencephalon (midbrain)	Mesencephalon	Tectum, cerebral peduncle, cerebral aqueduct, pons
	Rhombencephalon (hindbrain)	Metencephalon	**Cerebellum,** pons, upper part of 4th ventricle
		Myelencephalon	Medulla oblongata, isthmus, lower part of 4th ventricle
Spinal cord, pyramidal decussation, central canal			

Adapted from Wikipedia. The bolded are the structures of interest.

1.2.3 Neuronal migration

Most neurons are birthed in the VZ and migrate radially from the centre of the brain out to the developing neocortex. The migration of neurons into the developing cortex results in the formation of an orderly six-layered structure. Most of these neurons migrate actively in a radial pattern along a scaffold of glial cells such that earlier neurons form the deeper layers of the cortex while those of later generations form successfully more superficial layers. The preplate is the first visible cortical layer, formed by the first sets of migrating neurons around 5 to 8 weeks of gestation. Once the preplate is established at 7 – 11 weeks of gestation, the next wave of migrating neurons splits the preplate into two separate regions, the marginal zone (MZ) and subplate (SP). The neurons that split the preplate begin to form a new region between the MZ and SP called cortical plate (CP). The cells that will form cortical layer 6, the deepest layer of cortex, are the first to arrive in the CP, followed by migrating cells that will form progressively more superficial layers of cortex – each new wave of neurons bypasses the previous wave of neurons, assuming the most superficial position within the developing cortex.

Neuronal migration along the radial scaffold is thought to be most likely regulated by complex molecular interactions between neuronal and glial cells. Young neurons produce axons and dendrites to become part of the information processing networks once they reach their target region of cortex. Neurons communicate with each other via axons and dendrites. Dendrites are significant places for receiving input from neighbouring neurons, while axons are the primary means of conveying signals from the neuron. Each cell possesses a large number of dendrites that create thick "arbors" in the near area, as well as a single axon that can reach a long distance out from the cell. An axon grows and elongates as it follows molecular cues to its destination area. Synapses are generated between an axon and its target cell once it reaches its target location. Synapses allow electrical information to be transmitted between neurons in the brain, allowing for communication. (Supèr et al., 1998, Hatten, 1999, de Graaf-Peters and Hadders-Algra, 2006, Stiles, 2008, Stiles and Jernigan, 2010).

1.2.4 Synapse formation (synaptogenesis)

Synaptogenesis is a crucial event in the neonatal cortex. Cellular differentiation and organisation of the cortex occurs with increasing synaptogenesis. The moment a neuron arrived at its prescribed location; it develops connections with other neurons. Developing axons are guided by their terminal growth cones, which respond to chemoattractant or chemorepellent cues to form projections. Axons may form shorter projections like in interneurons, or significantly lengthier connections, such as those found in long-distance bundles – monoaminergic system, corpus callosum, or corticofugal pathways (Judas et al., 2003). Dendritic tree development occurs during the first two trimesters, and accelerates during the third trimester, with those of the subplate and deep cortical neurons maturing earlier than the more superficial cortical dendrites (Judas et al., 2003). As the dendritic and axonal connections develop, synaptogenesis increases. The first synapses form in the spinal cord during the sixth gestational week (Shimizu et al., 1984), and in the cortex at around 7 weeks (Zecevic, 1998). Synaptic density increases homogeneously in the cortex until around 22 weeks, after which it rapidly accelerates in a region-specific manner until well after birth. Maximum synaptic density in the primary sensory areas occurs at 3 postnatal months, while in the prefrontal cortex maximum density is not reached until 15 months of age (Huttenlocher and Dabholkar, 1997).

1.2.5 Neural regression

The multiplication of neuronal components is the most common neurodevelopmental event. However, in order to manage the population of neurons and glia cells, two crucial processes involving

significant loss of neural components are required. These two processes include naturally occurring cell death, which involves the typical loss of half or more of the neurons in a brain region, and synaptic exuberance and pruning, which involves tremendous excess connection formation followed by systematic deletion of up to half of those connections. (Stiles and Jernigan, 2010). For shaping local connection, synaptic pruning is critical. Neural apoptosis occurs during the prenatal period. Both apoptosis and synaptic pruning are nonpathological phenomena that play a crucial part in the formation of the developing brain's intricate network. (Rakic and Zecevic, 2000, Stiles and Jernigan, 2010).

1.2.6 Glial cells and Myelination

Glial cells are nonneural cells that develop from the same embryonic origin as neurons, forming from neural progenitor cells. Within the CNS, neural stem cells generate neurons followed by most of the central glia cells. Glial cells provide mechanical support and nutrition for neurons. The two main forms of glial cells are the microglia and macroglia (de Graaf-Peters and Hadders-Algra, 2006, Martin, 2013). Microglia penetrate the brain during the fifth week of pregnancy, colonizing and clustering in various areas of the brain throughout the next few weeks. They are microphages and are responsible for providing immunity for the brain (de Graaf-Peters and Hadders-Algra, 2006). Additionally, they are involved in neuronal development, neuronal connection, neural vasculature, and axonal myelination during development (Pierre et al., 2017). Glial cell apoptosis occurs over a long period of time, mostly postnatally.

Macroglia is the general term used for glia cells other than microglia, including radial glia, astrocytes, oligodendrocytes, and Schwann cells (Hill, 2022, February 9). The first three, including microglia, act in the CNS and have common embryonic origin – neural progenitor cells (Liu and Rao, 2004). Schwann cells have a different embryonic origin (neural crest cells) and act in the peripheral nervous system (PNS)(Knobloch et al., 2008). The main forms of macroglia cells are astrocytes and oligodendrocytes. Astrocytes are the most common glial cells in the brain. They are star-shaped and form an important component of the BBB. They serve as conduit through which nutrients from the arterial blood riches the neurons for optimum functionality. (Hill, 2022, February 9). Astrocytes help in extracellular regulation, neurotransmitter removal and modulation of synaptic structure and function. Oligodendrocytes develop after astrocytes and are responsible for the myelination of axons in the CNS (Altman and Bayer, 1984). Schwann cells perform similar function in the PNS. Radial glia play an

important role in nervous system development, guiding newly formed neurons from their birth zone outward to their destined adult position (de Graaf-Peters and Hadders-Algra, 2006).

Myelination is the process of close wrapping around a neural axon by a glia cell. Upon reaching its destination, an oligodendrocyte progenitor cell begins to differentiate by extending processes and increasing myelin protein expression. Microglia promote differentiation and maturation of oligodendrocytes by interacting with it, via releasing a broad spectrum of cytokines especially IL-1β and IL-6 (Shigemoto-Mogami et al., 2014). Microglia has also been demonstrated to induce survival and differentiation of oligodendrocyte progenitor cells and mature oligodendrocytes (Pang et al., 2013). The processes then begin to form membrane wraps around nearby axons. Eventually the oligodendrocyte forms tightly wrapped multi-layered sheaths from which most of the cytoplasm has been extruded. Even though oligodendrocyte progenitors form during embryonic period (E8), their proliferation and transformation into mature oligodendrocytes only begins at around E20 (Back et al., 2001). Myelination is regionally dependent and based primarily on the hierarchy processing needs within cortical connections – regions of cortex responsible for low-level processing mature earlier than those involve in high-level and more complex functions (Paus et al., 2001, Sowell et al., 2002).

1.2.7 Region of interests (ROIs)

In this study, our regions of interest included cerebellum and select subcortical structures – thalamus and basal ganglia (caudate nucleus, putamen and globus pallidus). Subcortical grey matter structures are clusters of grey matter/nuclei embedded under the cortex of the brain. The subcortical grey matter structures include the diencephalon (thalamus and hypothalamus), pituitary gland, amygdala and hippocampus (limbic structures), and basal ganglia (caudate, putamen, globus pallidus, substantial nigra, and subthalamic nucleus). Functions of these structures include complex activities such as memory, emotion, and pleasure. They act as information hubs of the nervous system, relaying and modulating information to different areas of the brain.

1.2.8 Anatomy and functions of the ROI structures

1.2.8.1 Cerebellum

The cerebellum “little brain”, develops from metencephalon, an upper derivative of rhombencephalon. The cerebellum is located within the posterior cranial fossa, immediately inferior to the occipital and temporal lobes. A tough layer of dura matter called the tentorium cerebelli

separate it from these lobes. It lies at the same level of and posterior to the pons, from which it is separated by the fourth ventricle.

Although the cerebellum is a tenth of the volume of the total brain, it contains as many as half of the whole number of brain neurons. Anatomically, it is roughly divided into two hemispheres, vermis – a narrow, worm-like midline area, and the flucculonodular lobe. Like other structures in the central nervous system, the surface of the cerebellum consists of grey matter. It is tightly folded, forming the cerebellar cortex. It also includes white matter, located underneath the cerebellar cortex. Embedded in the white matter are the four cerebellar nuclei (the dentate, emboliform, globose, and fastigial nuclei).

The cerebellum has three anatomical lobes (the anterior, posterior, and floculonodular lobes) and three cerebellar zones (the vermis in the midline, intermediate zone on either side of the vermis, and lateral hemispheres lateral to the intermediate zone). There is no difference in gross structure between the lateral hemispheres and intermediate zones.

The cerebellum has three functional areas and this include 1) The cerebrocerebellum – It is the largest of the three functional sections of the cerebellum. It is involved in movement planning and motor control. It receives afferent signals from the cerebral cortex and pontine nucleus and transmits motor fibres to the thalamus and midbrain red nucleus. 2) The spinocerebellum is comprised of the vermis and intermediate zone of the cerebellar hemispheres. It forms part of proprioceptive pathways, regulating movements of the body. 3) The vestibulocerebellum or flocculonodular lobe. It forms pathway with the vestibular system, receiving fibres from this system and sending outputs to the vestibular nuclei of the system. This division is associated with balance and ocular reflexes (Martin, 2013).

1.2.8.2 Thalamus

The thalamus is a large mass cylindrical-shaped grey matter structure that lies close to the third ventricle. It is located deep in the forebrain between the brainstem and the telencephalon. It is the largest subcortical structure. Its anterior part lies behind the interventricular foramen. The posterior end is called the pulvinar. The pulvinar is superolateral to the superior colliculus of the midbrain. Inferiorly, the surface of the thalamus is continuous with the tegmentum of the midbrain.

The thalamus consists of mainly of grey matter and it's made up of three laminae: 1) The stratum zonale – a thin layer of white matter that covers the superior surface of the thalamus. 2) The external medullary lamina – covers the lateral surface of the thalamus. Lastly, the internal medullary lamina (a Y-shaped white matter sheet) which divides the grey matter of the thalamus into three, the anterior, medial and lateral parts. The anterior part of the thalamic-grey matter contains the anterior thalamic nuclei. The mamillary nuclei, cingulate gyrus, and hypothalamus send input fibres to these nuclei, which send output fibres to the cingulate gyrus and hypothalamus. The dorsomedial nucleus of the thalamus is located in the medial region, and it receives and sends fibres to the prefrontal cortex, hypothalamus, and thalamus. All other thalamic nuclei transmit and receive fibres through it. The lateral part is grouped into dorsal and ventral tiers. Intralaminar nuclei, geniculate bodies – medial and lateral, and reticular nuclei are the other types of thalamic nuclei. The interior medullary lamina contains intralaminar nuclei. They receive information from the spinothalamic and trigeminal-thalamic tracts and send them to other thalamic nuclei. Between the exterior medullary lamina and the posterior limb of the capsule, there is a thin layer of reticular nuclei. They receive reticular formation and cerebral cortex fibres and send efferent fibres to the other thalamic nuclei. A swelling on the posterior surface of the thalamus, directly behind the pulvinar, is known as the medial geniculate body. It's a component of the auditory system. It receives fibres from the inferior colliculus via the inferior brachium to the auditory system. Another swelling right under the pulvinar is the lateral geniculate body. It forms the visual pathway. It receives impulses from the optic chiasma and transmits efferent fibres to the primary visual cortex(Memory, 2020)

The thalamic nuclei control a wide range of bodily processes, including sensory and motor signal transmission, awareness, sleep, and alertness management. The thalamic nuclei in charge of this functions are the relay nuclei, intralaminar nuclei, and the reticular nucleus. (Sherman, 2006, Tortora and Anagnostakos, 1987, Sciacca and Jones).

1.2.8.3 Basal ganglia

The basal ganglia, also known as basal nuclei, are masses of grey matter nuclei embedded in the cerebral cortex. The basal ganglia components include, caudate nucleus, putamen, globus pallidus, substantia nigra and subthalamic nucleus. Functionally, the substantia nigra and subthalamic nucleus are considered part of basal ganglia components – with the substantia nigra being a midbrain structure, and subthalamic nucleus as part of the subthalamus fund in the thalamus.

The putamen and caudate nucleus together are also known as the striatum, and they are separated by a sheet of white matter called internal capsule – a white matter tracts connecting the thalamus and cerebral cortex. The putamen and globus pallidus form the lentiform nucleus. The globus pallidus consist of internal and external segments. Globus pallidus and substantia nigra give rise to the major basal ganglia output projections.

1.2.8.3.1 Caudate nucleus

The caudate nucleus is C-shaped. It consists of the head, body, and tail. With its structures, it participates in the construction of the lateral brain chambers. On the inside of the caudate nucleus is the thalamus. Between these two structures is the stria terminalis, and the vein of the thalamostriata is positioned above. The corpus callosum is positioned above the caudate nucleus. At the tip of caudate nucleus is the amygdala. The anterior limb of the inner medulla separates the caudate nucleus and lentiform nucleus.

1.2.8.3.2 Lentiform nucleus (Putamen and globus pallidus)

The lentiform nucleus is comprised of putamen and globus pallidus and is located medially from the insular cortex. Although anatomically related, functionally they are different. The putamen forms the lateral aspect of the lentiform nucleus. On its concave inner surface lies the most exterior structure of the globus pallidus, GPe, and the most internal structure is the GPi. The putamen is separated from the GPe by the lateral medullary lamina, and the medial medullary lamina separates the GPe and GPi. Lateral to the putamen is another collection of white matter fibres known as the external capsule. Lateral to the external capsule is a thin bundle of grey matter called the claustrum, historically considered part of the basal ganglia. More lateral to the claustrum is the extreme capsule, which are white matter tracts separating the claustrum from the insula cortex.

1.2.8.3.3 Components and functional connections of basal ganglia

The striatum (caudate, putamen, and nucleus accumbens), the subthalamic nucleus, the globus pallidus (GPe and GPi), and the substantia nigra are all part of the basal ganglia (pass compacta and pars reticulata). The limbic components of the basal ganglia circuitry are the nucleus accumbens and the ventral section of the globus pallidus.

Extrinsic input to the basal ganglia is mostly received via the striatum. Almost all of the cerebral cortices send excitatory signals to the striatum. Cortical input is carried by the neurotransmitter

glutamate and is mostly terminated on the heads of medium spiny neurons' dendritic spines. Around 95% of all striatal neurons are medium spiny striatal neurons. They project outside the striatum and receive a variety of inputs, the most notable of which are excitatory glutamatergic inputs from the thalamus; cholinergic input from striatal interneurons; GABA-ergic input from adjacent medium spiny neurons.

The primary basal ganglia output arises from GPi, a GPi-like component of ventral pallidum (VP), and the substantia nigra pars reticulata (SNpr). The GPi and SNpr receive excitatory input from the subthalamic nucleus (STN) and inhibitory input from the striatum. They also receive inhibitory input from the GPe. The output from GPi, VP, and SNpr is inhibitory and uses the neurotransmitter GABA. The primary output is projected to the thalamic nuclei which in turn project to the frontal lobes of the cerebral cortex, with the strongest output going to the motor area.

Figure 1.2 shows basal ganglia circuitry involving two pathways – direct (D1) and indirect (D2) pathways. In the direct pathway, the cerebral cortex sends excitatory projections to the striatum. The striatum then sends inhibitory signals to the GPi and SNr. In turn, the GPi sends inhibitory signals to the thalamus which is usually in an active state. This results in selective disinhibition of thalamocortical neurons, and from the thalamus excitatory signals to the cortex where they affect the planning of movement. In the indirect pathway, the cerebral cortex also sends excitatory projections to the striatum but instead of sending axons directly to the GPi and SNr, they project to the GPe. GPi then sends inhibitory impulses to the STN instead of sending directly to the thalamus (this is why this pathway is called indirect). From the STN, signals are sent to the GPi and SNr and then continue as the direct pathway. (Mink, 1996, Nambu et al., 2000, Mink, 2003).

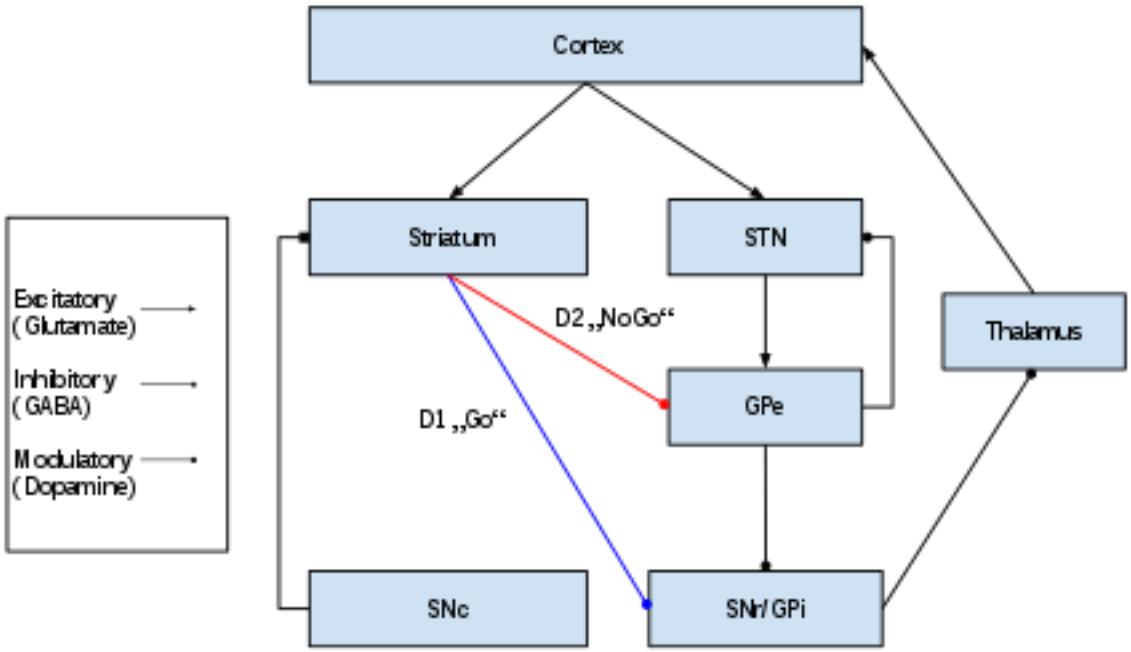

Figure 1.2. Diagrammatic representation of the major connections of the basal ganglia. The blue line (D1) indicates the path of the direct pathway, while the red line (D2) indicates the path of the indirect pathway is depicted by red lines. STN = subthalamic neuron; SNc = substantial nigra pars compacta; SNr = substantial nigra pars reticulata; GPe = globus pallidus external segment; GPi = globus pallidus internal segment. (Wikipedia)

1.2.9 Techniques for studying the developing human brain

Due to its complexity and ethical issues surrounding human research, tools, or technologies to investigate the developing brain need to be non-invasive. Recent advancements in technology resulted in improved techniques for mapping the human brain. Imaging and neuropsychological methods provide complementary measurements related to the structure and functionality of the brain. Combining both techniques in a single study is ideal as together they will provide more insights into the link between pathology and developing cognition and behaviour.

1.2.9.1 Imaging techniques

Structural imaging provides static anatomical information whereas functional imaging provides dynamic physiological information (Symms et al., 2004). Structural MRI and DTI are well-suited modalities for studying brain structure. For brain function, functional MRI (fMRI), positron emission tomography (PET), electroencephalography (EEG), magnetoencephalography (MEG), and trans-cranial magnetic stimulation (TMS) provide relevant measures.

1.2.9.1.1 Principles of MRI

The first commercial MRI scanners have been available since early 1980s. It is a powerful tool in clinical and research because it is radiation free and non-invasive.

MRI is based on two principles. First principle, says that atoms with an odd number of protons or neutrons in their nuclei have a non-zero magnetic-momentum/magnetisation (spin) that can interact with a large static magnetic field (B0). The human body contains many such atoms that can serve as good MR nuclei (1H, 13C, 19F, 23Na). The abundance of water molecules (each containing two hydrogen atoms) makes hydrogen the most common MR imaging contrast. In a lack of external static magnetic field (Figure 1.3a), spins in the body will be oriented randomly, cancelling out any net magnetisation. In the presence of external static magnetic field (Figure 1.3b) protons will orient themselves processing in a parallel and anti-parallel direction of that static magnetic field. The number of anti-parallel and parallel spins isn't equal (due to quantum-mechanical effects) creating an effective net magnetisation vector. The second principle, says that protons which up to now processed along direction of the B0 field can be excited by radio-frequency (RF) pulses (emitted by a transmit coil), effectively changing a direction of their net-magnetisation (Figure 1.4a). The RF pulse applied in a direction perpendicular to the direction of the static-magnetic field B0 causes longitudinal component of the magnetization to diminish creating a transversal magnetization component. When the RF pulse is switched off (Figure 1.4b), the protons have to release their excess of energy, by returning to their ground state, this energy is released in a form of an RF signal that can be measured by a receiver coil. This release of energy isn't linear but inverse-exponential govern by two times constants T1 (as spin-lattice relaxation time) and T2 (spin-spin relaxation). Mathematically, T1 is defined as a time that takes longitudinal component of the magnetisation vector to return to 63 percent of its initial value (pre-excitation by an RF pulse). T2 relaxation time is defined as a time needed for transverse component of the magnetisation vector to decay exponentially to 37% of initial magnitude. What's important is the fact that these relaxation time constants uniquely characterise different tissue types. In an MRI experiment, the RF pulse is being repeated multiple times to excite spins at different spatial locations (this is accomplished with additional magnetic fields, called gradient fields).

In an MRI experiment we can control the contrast (emphasis) on different tissue types, by controlling two basic MR sequence parameters parameters TR and TE. TR (repetition time) is the time between

two consecutive excitation pulses. TE (echo time) is a time between RF excitation pulse and signal echo, i.e., a time when the signal is measured. T1-weighted images are obtained with MR sequences with a short TR and a short TE time. T2-weighted images are obtained with sequences with longer TR and longer TE times. Short and long times are with respect to the T1/T2 values of a specific tissue. Table 1.2 below depicts the appearance of central nervous system tissues in different MR images.

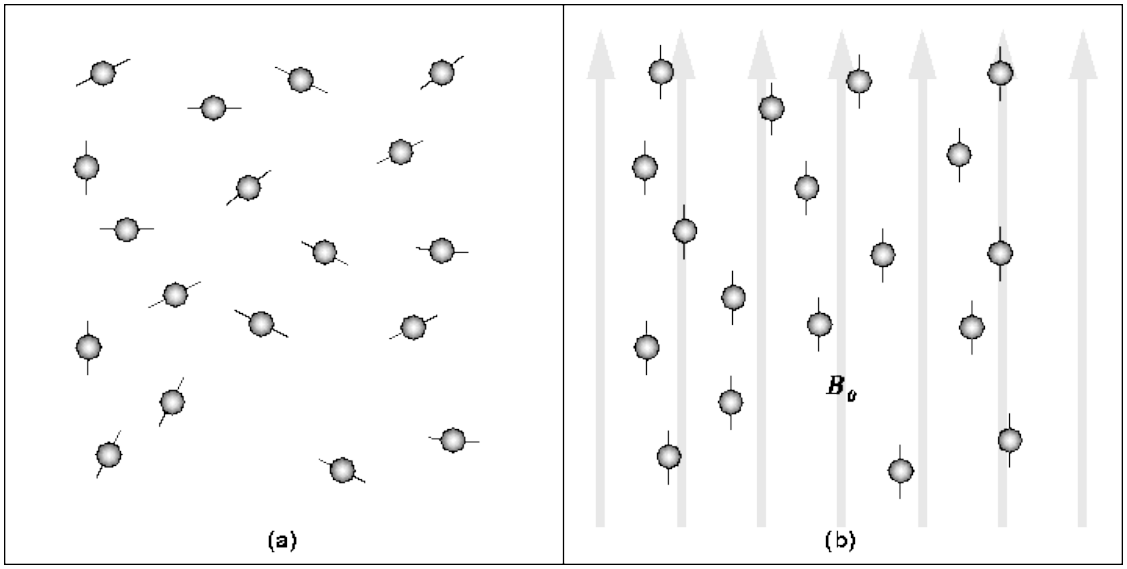

Figure 1.3: In the absence of a strong magnetic field, hydrogen nuclei are randomly aligned as in (a). When the strong magnetic field, B_0, is applied, the hydrogen nuclei process about the direction of the field as in (b).

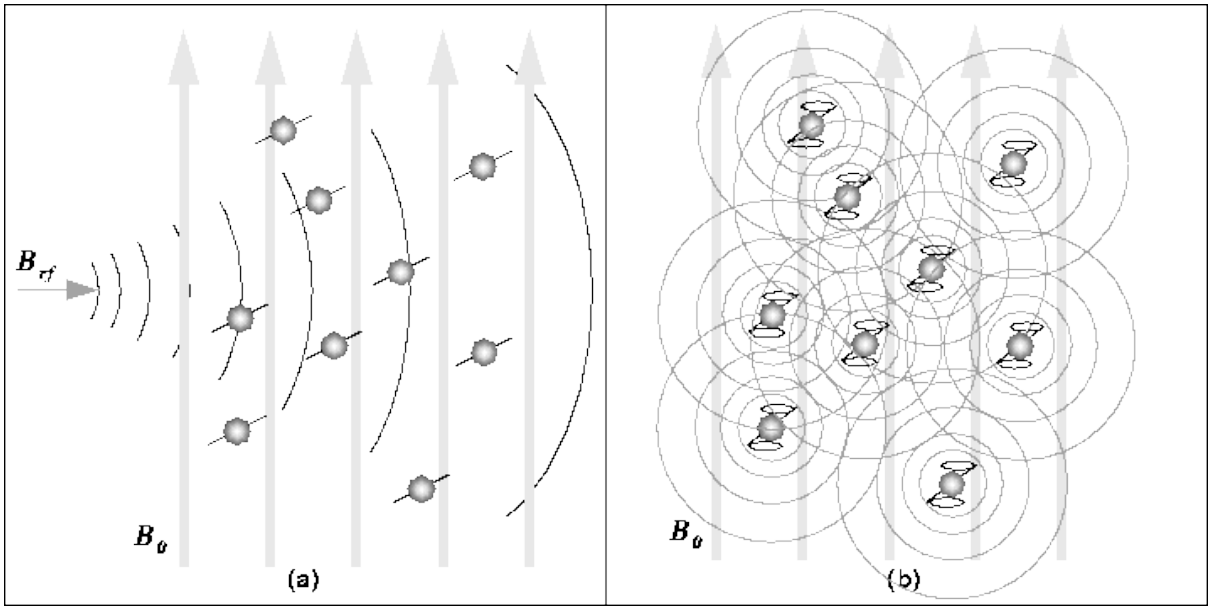

Figure 1.4: (a) The RF pulse, B_{rf}, causes the net magnetic moment of the nuclei, *M*, to tilt away from B_0. (b) When the RF pulse stops, the nuclei return to equilibrium such that *M* is again parallel to B_0. During realignment, the nuclei lose energy and a measurable RF signal. (Mackiewich, 2005)

Table 1.2. Relaxation times for tissue types of interest and their appearance for different contrast weightings.

			T1-weighted		**T2-weighted**	
	T1	**T2**	**Adult**	**Infant**	**Adult**	**Infant**
White matter	Intermediate	Intermediate	Bright	Intermediate	Dark	Intermediate
Gray matter	Intermediate	Intermediate	Intermediate	Bright	Intermediate	Dark
Cerebrospinal fluid (CSF)	Long	Long	Dark	Dark	Bright	Bright

Adapted from (Xue et al., 2007, Hashemi et al., 2010)

1.2.9.1.2 Structural MRI: Imaging grey and white matter

With structural MRI, researchers can visually distinguish between grey and white matter because of their compositional differences in water and fat, which have different magnetic properties (relaxation times). Grey matter is where information processing happens as it contains the cell bodies and dendrites of the neuron. White matter contains axons, which transmits electrical impulses between

neurons and their myelin sheaths. Myelin sheaths have a high fat content and act as insulator for axons.

Structural imaging has been used for decades in both clinical and research settings to describe the anatomy of the human brain in health and diseases as well as the effects of aging. Structural MRI is based on T2-and T1-weighted images. High resolution T1-and T2-weighted images have been used to measure local or regional brain volumes and/or assessing structural changes in HIV (Randall et al., 2017, Chang and Shukla, 2018, Yu et al., 2019), and other diseases/disorders such as epilepsy (Alvarez-Linera Prado, 2012, Peng et al., 2014, Huang et al., 2015, Avalos et al., 2019), Alzheimer's disease (Marzban et al., 2020)**,** and Parkinson's disease (De Micco et al., 2018).

1.2.9.1.3 Principle of Diffusion Tensor Imaging

MRI can be used to measure the diffusion of water – that is, the random motion of water molecules. This advanced MRI technique is known as diffusion tensor imaging (DTI). Water molecules exhibit constant random motion due to heat energy. In the brain tissue, movement of water molecules is mostly restricted. We can measure diffusion of water molecules by modifying MR sequence with and additional components called diffusion gradients. If diffusion encoding gradients are applied, the MR signal in the presence of diffusion experiences attenuation of amplitude. Acquiring images with diffusion weighting (known as diffusion-weighted imaging, DWI) allows the diffusion coefficient to be measured. By repeating the experiment with different strengths of the diffusion gradients we can measure components of the diffusion tensor, which leads us to DTI. Despite the promise of DTI, some of its methodological challenges makes its clinical usefulness limited. These challenges include its dependency on noise and on the inaccurate assumption that water molecules obey Gaussian diffusion in biological tissues (Inglese & Bester 2010). A major important challenge of DTI is the DT model failure to describe the formation of voxel that contain multiple fibre with different orientations (such as crossing fibres). This is because DTI is independent of the tissue architecture, the diffusion properties of each voxel are always average by a single diffusion ellipsoid.

Diffusion in brain tissue (e.g. CSF) can be isotropic i.e., water can diffuse equally in each direction, or it can be anisotropic, such as white matter tracts where diffusion is less restricted along the long axis of the white matter tract than it is in direction perpendicular to the tract (Symms et al., 2004). it has also been thought that grey matter of the cortex in adults also exhibit isotropic diffusion (Pierpaoli and Basser, 1996, Shimony et al., 2006). Overall, diffusion is more restricted along white matter

bundles than in grey matter. Therefore, DTI uses anisotropy to estimate the axonal organisation of the brain. There are four scalar parameters which are used in DTI to estimate and determine axonal integrity. Namely, fractional anisotropy (FA), mean diffusivity (MD), axial diffusivity (AD) and radial diffusivity (RD). The four scaler (FA, MD, AD and RD) parameters are calculated from the eigenvalues (λ_1, λ_2, λ_3) of the diffusion tensor (O'Donnell and Westin, 2011). Each eigenvalue corresponds to one of the eigenvectors (e_1, e_2, e_3). Geometrically, the diffusion tensor forms all ellipsoid with three main axes oriented in that directions (defined by the eigenvectors) that translate to the extent (defined by eigenvalues) of diffusivity in that direction (O'Donnell and Westin, 2011).

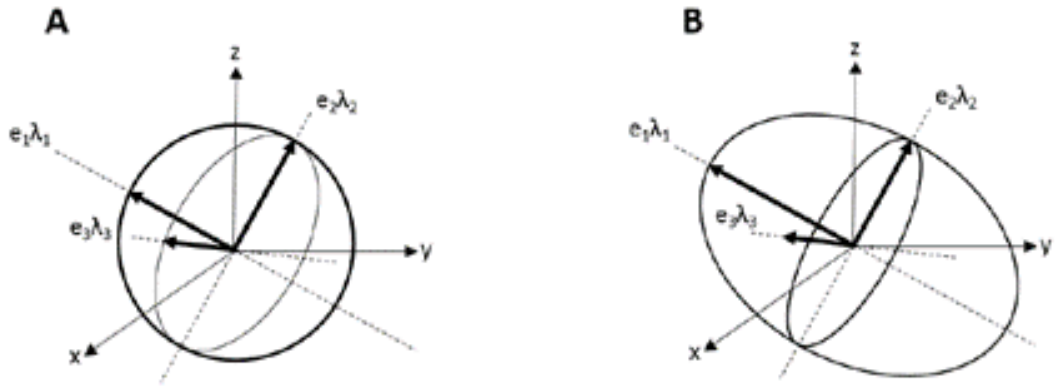

Figure 1.5. The diffusivity in three dimensions is modelled as an ellipsoid whose orientation is characterised by the eigenvectors e_1, e_2 and e_3, and whose shape is defined by the eigenvalues λ_1, λ_2 and λ_3. Completely isotropic diffusion within a voxel is modelled by a perfect sphere (A), while anisotropy is shown by the eccentricity of the ellipsoid (B). (Jellison et al., 2004).

Even though FA and MD are the most used DTI scalers as earlier mentioned, analysis of WM integrity will not be complete without including the other two indices (AD and RD). This is because examining diffusivity along the principal axis (AD) and the diffusion in orthogonal/perpendicular directions (RD) complement FA and MD and because they provide more in-depth interpretation of FA and MD related changes. FA, which is used as index of diffusion anisotropy (O'Donnell and Westin, 2011, Dietrich et al., 2010, Hagmann et al., 2006), is generally used as an indicator of WM integrity (relating to axon myelination, the diameter of axons, and/or the density); increase FA is an indication of WM maturation, increase myelination and dense axonal packing. Lower FA may be an indication of axonal damage and/or de(dys)myelination (Tromp, 2016, Hoeft et al., 2007). MD, which is independent of

anisotropy, demonstrates the average movement of water within the WM voxel and can be interpreted as a general indicator of WM maturation and/or injury (Basser and Pierpaoli, 1996). In contrast to FA, decreases in MD relate to WM maturation, increased myelination, and denser axonal packing whereas its increase may affect WM maturation, decrease myelination, and reduce axonal packing density. Even though FA and MD are both individually sensitive to microstructural changes, their interpretation alone is not enough to determine axonal and myelin related changes – interpretation of FA and MD in relation to AD and RD provide an in-depth interpretation of FA and MD. AD is related to WM maturation and axonal damage and it complement FA in these regards. Increase AD points at WM maturation while its decrease is related to axonal damage. AD has not been shown to be related to myelination or axonal density (Tromp, 2016). RD describes the amount of diffusion perpendicular to the WM axons and may affect neurons in the way MD does (Tromp, 2016). Myelin, which surrounds an axon, hinders perpendicular diffusion. Thus, high RD values indicate WM damage due to de(dys)myelination (Feldman et al., 2010).

The second objective of this study was to determine and compare the diffusion indices of the tracts connecting the ROIs of HEU and HUU infants. Diffusion indices such as MD is a measure of cellular state, while diffusion anisotropy give insights about the structure of white matter. Overall, DTI measures describe the structural organization of white matter of the brain. DTI has been used to study brain development from as early as first trimester (Feldman et al., 2010), through postnatal period – childhood to adulthood (Lebel et al., 2008). It has been used to demonstrate localized white matter differences in HEU infants and children as compared to their uninfected peers (Jankiewicz et al., 2017, Tran et al., 2016, Madzime et al., 2021). Over the years, DTI has been an effective modality in studying brain injury disorders such as acute stroke (Chen et al., 2008), multiple sclerosis (Sbardella et al., 2013, Kolasa et al., 2019) and epilepsy (Leyden et al., 2015).

1.2.9.1.4 Tractography

Diffusion tensor tractography is a technique for tracking white fibre bundles that is non-invasive. It connects distant locations by integrating voxel-by-voxel orientations into a pathway (Garcia and Anaya 2016). Tractography can be considered a subtype of DTI (Anaya García et al., 2015). The basics of both techniques are the same, though tractography is a further step to DTI – the tensors of cerebral white matter can be reconstructed to track 3-dimensional (3D) macroscopic fibre orientation in the brain.

Therefore, tractography provides information that cannot be achieved by conventional anatomical MRI.

The translation of the long axis of the tensor (v1) (figure 1.6, 1.7 and 1.8) into neural trajectories can be achieved by various algorisms. These algorisms are broadly classified into two, deterministic and probabilistic. Deterministic is the most used of the two algorithms. Mori et al created one of the first deterministic algorism, the FACT (fibre assignment by continuous tracking) (Mori et al., 1999, Xue et al., 1999). These are also called line propagation or streamline techniques (fig 2.7) (Yamada et al., 2009). Neural connections are mapped by designating at least 2 arbitrary regions of interest (ROI) in 3D space. Tracking is terminated when a pixel with low FA or predetermined trajectory curvature between two contagious vectors is reached (figure 2.8). These are often called "stop criteria". Probabilistic algorism is based on global energy minimization to find the most favourable energetic pathway between two pixels (Mori and van Zijl, 2002).

The main application of tractography is the 3D visualization of white matter trajectories, particularly in relation to brain pathology (Alexander et al., 2007, Catani and Thiebaut de Schotten, 2008). Tractography has been used in research settings to study both developing and aging brains, which has help clinicians to detect abnormalities in the brain and to diagnose neurological conditions such as epilepsy, metabolic disorders, mental illnesses, and brain tumors (Anaya García et al., 2015).

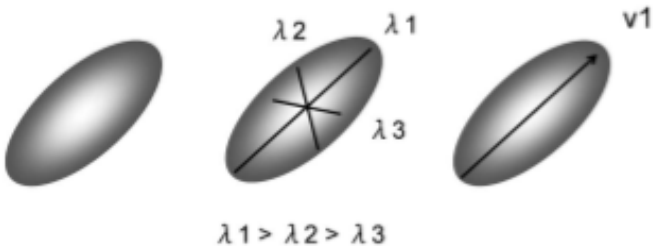

Figure 1.6. Diffusion constants of a given ellipsoid are shown. λ1 represents diffusivity in the longest axis of this tensor. V1 represents the vector orientation of λ_1

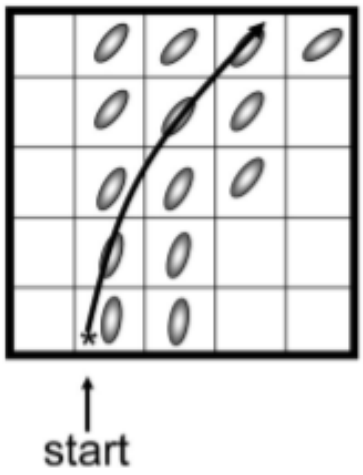

Figure 1.7. Tracking starts at a pixel (or region of interest [ROI]). The fibre assignment by continuous tracking (FACT) program tracks the ellipsoids as long as the adjacent vectors are strongly aligned.

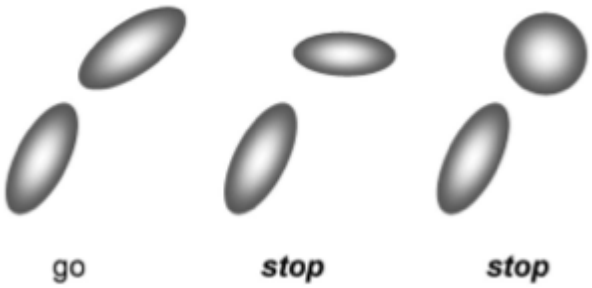

Figure 1.8. (Left) tracking between two neighbouring voxels. Stop criteria: When diffusion vectors of neighbouring voxels become random or meet predefined set of conditions, as quantitatively established by an inner product of these diffusion vectors, tracking is terminated (middle). The algorithm also terminates when the diffusion ellipsoids approach as a spherical shape (right).

1.2.9.2 Neuropsychological techniques

Neuropsychological tests measure a psychological function associated with a brain structure or pathway (Boyle et al., 2012). These tests are used in research and clinical settings to learn more about brain function and diagnose brain impairments. The principle of neuropsychological assessments or tools is to generate a hypothesis about a region or area of the brain (of interest) that is involved in a

particular behaviour or function and then apply an appropriate behavioural or cognitive test(s) to evaluate the hypothesis (Sciences, 2000). The tests usually involve the systematic administration of clearly defined tasks. Ideally, it is possible to dissociate one behaviour from another (for example, explicit from implicit memory) by using a cluster of tasks or applying such tasks to both normative and clinical populations. Data from a normative population are usually stratified by age, level of education, and ethnicity, especially when empirical evidence has proven that these factors affected the performance of a particular test. Controlling for these factors allows for a person's performance to be compared to a suitable control group and thus provide a fair assessment of their current cognitive function. (Seidman, 1998, Habben and Millberg, 2009, Lezak et al., 2012).

Neuropsychological tests can be categorized into different forms based on the type of brain function they assess (Lezak et al., 2012). No brain part or region works in isolation. Most forms of cognition usually involve multiple functions working in unison. However, some tests are organized to predominantly assess specific cognitive functions such as intelligence, memory, language, executive function, visuospatial, etc. Others are designed to measure multiple cognitive functions, such as those used to measure neurodevelopment.

Different types of neuropsychological tools are available depending on the age strata under study (see table 1.3). These tools have been adapted and normalized for Africans. Of the 42 related studies listed in table 1.3, Bayley Scales of Infant Development (BSID) (both as a stand-alone or in combination with other neuropsychological tools) appears to be the widely used tool overall. BSID is the most used test in North American and African (table 1.3). BSID was first developed in 1933 for assessing infant behaviour and predict later development. The first edition of these scales only provided test procedures and scores for the first 18 months, which is why the scales did not comply with important psychological testing pre-requisites. It was re-standard in 1993 to assess children between ages one and four months (BSID II) (Bayley, 1993). Bayley III assesses a child in five developmental domains - cognitive, language, motor, social-emotional and adaptive behaviour (Bayley, 2006).

1.2.10 Disruptions of typical brain development

The fetal and early neonatal period involves critical processes in the developing brain. Brain maturation is controlled by complex interactions among signalling receptors, genetic/epigenetic factors, and environmental influences. The sequence of brain development during the gestational period are – neurulation (weeks 3 – 4), porencephalic development (months 2 – 3), neuronal

proliferation (3 – 5 months), neuronal organization (5 months postnatal period) and myelination (begins in the second trimester, spike in in the immediate neonatal period, and continues postnatally into adulthood) (Cordeiro et al 2015). Disruption of this developmental processes during this critical period may result in irreversible brain damage or even death.

Maternal health plays an important role in healthy brain development in utero during pregnancy. Maternal infections (viruses, bacterial, parasites) have been linked to the disruption of normal brain development.

1.2.11 Infections and brain development

Several independent studies provide empirical evidence of the link between infections during pregnancy and altered brain development. Viral infections such as influenza (Ellman et al., 2009, Parboosing et al., 2013), HIV (Msellati et al., 1993, Nozyce et al., 1994, Nozyce et al., 2014), Hepatitis (Salemi et al., 2014), and cytomegalovirus (Fowler et al., 1992, Nigro et al., 2005) are the most reported. Infections cause disruptions or alterations in normal brain development via the activation of inflammatory cascades, leading to the release of proinflammatory markers and ultimately structural and functional changes. For the scope of this study, we will limit our review to the impact of maternal HIV infection and antiretroviral (ARV) treatment on fetal brain development in HEU children.

1.2.12 HIV/ART exposure and brain development

It is difficult to dissociate the effects of HIV and ARVs on the developing brain of HEU children since ART is widely used to protect both the mother and the fetus. ART programs for pregnant women and their infants are designed to improve maternal health and reduce vertical transmission, as well as prevent negative effects of HIV infection on the developing fetus. The impact of this treatment/prevention program is evidenced by the dramatic reduction in vertical transmission and the increased population of HEU children. However, some pharmacovigilant studies have shown that ART is not completely safe for the fetus. Some of the adverse effects reported include prematurity, growth retardation and metabolic disturbances (Powis et al., 2011, Jao and Abrams, 2014, Hofer et al., 2016). Mitochondrial abnormalities (Blanche et al., 1999, Barret et al., 2003, Brogly et al., 2007) and delay in language acquisition (Sirois et al., 2013, Rice et al., 2013, Himes et al., 2015, Desmonde et al., 2016) have also been documented. Overall, it is safe to say that the benefits of ART in the prevention of vertical transmission outweighs its adverse effects because the reported adverse effects are subtler in HEU than in children living with HIV.

Researchers, clinicians, and policy makers have grown more interested in HEU infants and children because studies suggest this growing population experience developmental delays (Wu et a., 2018). Since it is difficult to separate the effects of HIV and ART exposure on fetal brain development in the current era, the next few paragraphs will focus on how HIV/ART impact on the developing fetal brain. Prenatally, HEU children are exposed to HIV virus and may be exposed to ART. Postnatally, HEU infants may be exposed to ART through breastfeeding (Le Doare et al., 2012). Since HEU children are exposed to HIV/ART but not infected by HIV virus, it is important to monitor their developmental milestones to be able to detect any developmental disorder or delay involving cognitive abilities including behaviour, learning and language acquisitions as it affects their day-to-day life endeavours.

The methods employed in the study of human brain development include indirect methods, which measure cognitive functions, and direct methods, such as imaging techniques which quantify aspects of brain structure and function. Both methods have been used, separately or in combination, to gain more understanding about HIV/ART exposure effects on fetal/infant brain development and/or impairment.

Tables 1.3 and 1.4 below summarize the studies using indirect and direct methods to study the impact of ART and HIV exposure on the brain in HEU as compared to HUU children. Overall, the findings are inconsistent, which may be due to variations in age, study designs, study location, socioeconomic status, ARV regimens, and other factors. In table 1.3, a total of 41 studies using neuropsychological methods were included – we excluded studies with subjects above the age of 12 years as teenage period is marked with dramatic changes in neural activities. Of these 41 studies, 27 (66.0%) were performed in Africa (Boivin et al., 1995, Drotar et al., 1999, Bagenda et al., 2006, Van Rie et al., 2008, Van Rie et al., 2009, Ngoma et al., 2014, Chaudhury et al., 2017, Springer et al., 2018, le Roux et al., 2018, Wedderburn et al., 2019, Boivin et al., 2019, Msellati et al., 1993, Kandawasvika et al., 2011, Laughton et al., 2012, Brahmbhatt et al., 2014, Alcock et al., 2016, Familiar et al., 2018, Kacanek et al., 2018, Debeaudrap et al., 2018, Laughton et al., 2018, Springer et al., 2020, Rotheram-Borus et al., 2019, White et al., 2020, Strehlau et al., 2020, Gruver et al., 2020, Ntozini et al., 2020, Madlala et al., 2020), seven (17.0%) from North America (Mellins et al., 1994, Forehand et al., 1998, Culnane et al., 1999, Dorsey et al., 1999, Alimenti et al., 2006, Williams et al., 2010, Sirois et al., 2013) with two studies each appearing to be with the same group from Africa (Van Rie et al., 2008, Van Rie et al., 2009) and North America (Forehand et al., 1998, Dorsey et al., 1999) respectively. Four (10.0%) studies from Asia

(Sanmaneechai et al., 2005, Wu et al., 2018, Kerr et al., 2014, Rajan et al., 2017), two (5.0%) from South America (Gomez et al., 2009, Spaulding et al., 2016), and one (2.0%) from Europe (Esposito et al., 1999). In all, fifteen (about 40%) studies reported lower scores in at least one measure of the assessed domains – HEU children have deficits in cognition, motor function, expressive and receptive language, and behavior (Boivin et al., 1995, Forehand et al., 1998, Dorsey et al., 1999, Esposito et al., 1999, Sanmaneechai et al., 2005, Van Rie et al., 2008, Brahmbhatt et al., 2014, Alcock et al., 2016, Familiar et al., 2018, Wu et al., 2018, le Roux et al., 2018, Wedderburn et al., 2019, Ntozini et al., 2020, Madlala et al., 2020). Lower scores on reading and various aspects of language are common to HIV affected children in African countries (Van Rie et al., 2009, Brahmbhatt et al., 2014, Alcock et al., 2016, Wedderburn et al., 2019, Ntozini et al., 2020). Table 1.4 summarize studies using brain imaging methods in HEU and HUU infants and children. To date only nine studies have used imaging in the context of HEU. Six (67.0%) studies were conducted in South Africa. And seven (78.0%) reported subtle brain changes in HEU compared to HUU children (Cortey et al., 1994, Tran et al., 2016, Jankiewicz et al., 2017, Robertson et al., 2018, Graham et al., 2020, Madzime et al., 2021, Yadav et al., 2020).

Neuroimaging measures provide detailed information on the structure and biology of the CNS. However, imaging outcomes do not provide much insight into the consequences of observed abnormalities. Taken together, a combination of neuroimaging and neuropsychological measures may provide greater insight into the consequences of HIV/ART exposure on the infant brain.

Table 1.3 Neuropsychological studies on the effects of HIV/ART exposure on HEU children's brain

Ref	Country	Study type	Scale	ART Received by the pregnant Woman	Neurodevelopmental Assessment Age (months)	Sample Size		Mean score difference (MD); *p*-Value
						HEU	HUU	
(Msellati et al., 1993)	Rwanda		DDST	Not reported	6 – 24	133	193	No difference HEU vs HUU
(Mellins et al., 1994)	USA	Cross-sectional	DDST BSID	Not reported	2 – 30	30	23	p= ns
(Boivin et al., 1995)	Zaire	Cross-sectional	K-ABC ECSP	Not reported	3-18 0ver 24	20	16	**HEU had poorer global cognitive scores on K-ABC**
(Forehand et al., 1998)	USA	Cross-sectional	ABS CBCL CDI, PRS WRAT-R	Not reported	72-132	87	132	MD = 1.87; **p<0.05** HEU had difficulty in all domains of psychological adjustments.
(Drotar et al., 1999)	Uganda	Cross-sectional	BSID PDMS	Not reported	0-24	234	115	MD= -1.5; p=ns

(Culnane et al., 1999)	USA	Cross-sectional	BSID-II	AZT	30	64	73	MD= ,0.2; p=0.84 No significant difference
(Dorsey et al., 1999)	USA	Cross-sectional	ABS, CBCL CDI	Not reported	72-132	87	132	MD=not reported; **p<0.05** HEU children had behavioural difficulties
(Esposito et al., 1999)	Italy	Cross-sectional	ABS, CBCL CDI	Not reported	72-132	39	78	**P<0.05**. HEU had worse scores in most of the behavioural domains
(Sanmaneechai et al., 2005)	Thailand	Cross-sectional	CBCL TIA	ZDV	36-60	30	35	MD=n/s; **p= 0.03**. HEU had lower cognitive function
(Alimenti et al., 2006)	Canada	Cross-sectional	BSID-II	AZT, 3TC, NVP, NFV	18-36	39	24	MD= -3.2; p=not reported. p= ns
(Bagenda et al., 2006)	Uganda	Cross-sectional	K-ABC	Not reported	72-144	42	37	p= ns
(Van Rie et al., 2008)	DRC	Cross-sectional	BSID II, SON, PDMS	Not reported	18-72	35	90	**HEU had poorer motor and expressive language**
(Van Rie et al., 2009)	DRC	Cross-sectional	BSID SON	Not reported	18-71	35	90	**p< 0.001** at 6 and 12 months HEU had poorer motor scores

(Gomez et al., 2009)	Colombia	Longitudinal	BSID II	AZT, 3TC, NVP, LPV/r, NFV	3, 6, 9, 12, 18, 24	7	6	MD= -7.0; p= 0.90 No significant difference
(Williams et al., 2010)	USA and Puerto Rico	Longitudinal	BSID II	AZT	6, 12, 18, 24, 30, 36	169	146	MD= -5.0; p= 0.82 No significant difference
(Kandawasvika et al., 2011)	Zimbabwe	-	BINS	Not reported	12	188	287	No difference HEU vs HUU
(Sirois et al., 2013)	USA	Cross-sectional	BSID III	AZT, 3TC, TDF, ATV, LPV/r, NFV	9-15	309	62	MD= 0.4; p= 0.82
(Laughton et al., 2012)	South Africa	Cross-sectional	GMDS	cART	10 – 12	28	34	No difference HEU vs HUU
(Ngoma et al., 2014)	Zambia	Cross-sectional	FSDQ	AZT, LPV/r, NVP	15-36	97	103	No difference, MD= 4.7; p= Not reported
(Brahmbhatt et al., 2014)	Uganda	Cross-sectional	MSEL	AZT/cART	0 – 6	105	108	**HEU had poorer receptive language**
(Kerr et al., 2014)	Thailand &Cambodia	Cross-sectional	WISC-III, WPPSI-III, Beery VMI, CBCL	Not reported	24-132	160	167	HEU had lower score in FSIQ (MD = -5.07; p=0.03), Verbal IQ (MD = -6.09; p= 0.004), and Bead memory (MD = -3.78; **p= 0.01**
(Alcock et al., 2016)	Kenya	Cross-sectional	Kilifi CDI	Not reported	8 – 30	14	161	**HEU had poorer language**

(Spaulding et al., 2016)	Latin America Brazil,&Carib Bean	Cross-sectional	Neurological 1, motor clinical examination	c ART	6	1400	-	No neurological abnormalities observed
(Chaudhury et al., 2017)	Botswana	Cross-sectional	BSID III	AZT, 3TC, FTC, TDF, EFV	24	313	357	MD= 0.59; No difference HEU had lower cognitive score, and expressive language (p= 0.09)
(Rajan et al., 2017)	India	-	DAC-I	c ART	6 – 18	50	9	No difference
(Familiar et al., 2018)	Uganda	-	MSEL	cART	6 – 12	75	140	**HEU had lower cognitive scores**
(Springer et al., 2018)	South Africa	Cross-sectional	BSID III	cART or AZT	12	58	38	No significant difference, p = ns
(Wu et al., 2018)	China	Cross-sectional	BSID III	cART	6-30	250	250	**HEU had lower cognitive and adaptive scores**
(le Roux et al., 2018)	South Africa	Cross-sectional	BSID III	TDF, FTC, EFV	11-18	215	306	HEU and HUU had similar scores in all domains, **but HEU children had higher odds of been diagnosed with**

								cognitive delay and motor development.
(Kacanek et al., 2018)	Botswana	Prospective cohort	DMC, BSID II	cART	24	197	-	No abnormalities
(Debeaudrap et al., 2018)	Cameroon	Prospective cohort	K-ABC II, SDQ	Not reported	24 – 36	101	110	No difference HEU vs HUU
(Laughton et al., 2018)	South Africa	Prospective cohort	GMDS-ER, CBCL, Beery	cART	24 – 36	34	39	No difference HEU vs HUU
(Springer et al., 2020)	South Africa	Prospective cohort	BSID III	cART or AZT	30 – 42	32	27	No significant difference, p = ns
(Wedderburn et al., 2019)	South Africa	Prospective cohort	BSID-III	TDF, FCT, EFV	6, 24	61	199	HEU had higher proportions with expressive **(p= 0.02**) and receptive language (**0.03**) delays
(Boivin et al., 2019)	Uganda & Malawi	Prospective cohort	MSEL, KABC-II	TDF, FCT, EFV	12, 24, 48, 60	199	146	No significant difference between HEU and HUU at all timepoint
(Rotheram-Borus et al., 2019)	South Africa	Prospective cohort	BSID, CBCL, SDQ, K-ABC	Not reported	2 weeks, 6, 18, 36	345	732	No difference HEU vs HUU

(White et al., 2020)	South Africa	Prospective/cross-sectional	GMCD	Not reported	4 – 12, 12 – 20 wks	14	8	p = ns No difference was reported
(Madlala et al., 2020)	South Africa	Longitudinal	ASQ	Not reported	12 – 24	355	-	**HEU delayed development in gross and fine movement. p-value not reported**
(Strehlau et al., 2020)	South Africa	Cross-sectional	BSID III	Not reported	12	49	-	No developmental delay found in HEU children
(Gruver et al., 2020)	South Africa	Cross-sectional	GCS, K-ABC II, R-DLS III	Not reported	4 – 6 years	257	627	No different across all domains between HEU and HUU
(Ntozini et al., 2020)	Zimbabwe	-	MDAT, CDI, A-not-B test, self-control task	Not reported	24	205 1175		**HEU lower total child development and vocabulary scores**

AZT—zidovudine; 3TC—lamivudine; NVP—nevirapine; NFV—nelfinavir; LPV/r—lopinavir/ritonavir; TDF—tenofovir; ATV—atazanavir; EVF—evaferenze. BSID-II—Bayley Scales of Infant Development second edition; BSID-III—Bayley Scales of Infant Development third edition; FSDQ— Full-Scale Developmental Quotient; CBCL – Aggressive Behavioural Subscale; CDI – Children's Depression Inventory; WRAT – Wide Range Achievement Test; PDMS – Peabody Development Motor Scale; PRS – Parent Rating Scale; ECSP – Early Childhood Screening Profile; K-ABS- Kaufman Assessment Battery for Children; DDST – Denver Development Screening Test; GCMD – The Guide for Monitoring Child Development; ASG – Ages and Stages Questionnaire; R-DLS – Reynell Developmental Language Scales; GCS – Grover-Counter Scale of Cognitive Development; MDST – Malawi Developmental Assessment Tool; DAC-I – Developmental assessment scale for Indian infants; GMDS – Griffiths Mental Developmental Scale.

Table 1.4 MRI brain imaging studies on the effects of HIV/ART exposure in HEU children

Ref	Country	Study type	Imaging modality	ROIs	ART in pregnancy	Age at scans	Sample Size		Findings suggestive of neurodevelopmental alterations in HEU children
							HEU	HUU	
(Cortey et al., 1994)	USA	Cross-sectional	MRS	parietooccipital white matter (WM)	Not reported	1-10 days	5	5	**choline-to-creatine ratio is higher (p=0.001) in HEU; NAA/creatine ratio is lower in HEU** (p=0.01)
(Jahanshad et al., 2015)	Thailand	Cross-sectional	DTI	Whole WM, Corpus Callosum	Not reported	2-15 years	30	33	No group differences
(Tran et al., 2016)	South Africa	Cross-sectional	DTI	Cerebral, brainstem and cerebellum WM bundles	Not reported	2-4 weeks	15	22	**HEU had Higher FA in middle cerebella peduncles (p=0.003)**
(Jankiewicz et al., 2017)	South Africa	Cross-sectional	DTI		AZT, NVP	7 years	19	27	**HEU had increases in FA in a cluster of corticospinal tracts**
(Holmes et al., 2017)	South Africa	Longitudinal	MRS	MFGM, basal ganglia and peritrigonal WM	AZT, NVP	5, 7 and 9 years	29	35	No group differences
(Robertson et al., 2018)	South Africa	Cross-sectional	MRS	Basal ganglia	AZT, NVP	7 and 9 years	14	21	At age 7yrs, no group differences

									At age 9yrs, HEU had lower NAA, glutamate, / choline, and creatine ($p < 0.05$)
(Graham et al., 2020)	South Africa	Cross-sectional	MRS	Basal ganglia, MFGM, PWM	AZT, NVP	11 years	30	30	HEU had lower levels of NAA and Glu in the MFGM, and NAA and NAA where low in PWM compared to HUU
(Yadav et al., 2020)	India	Cross-sectional	DTI	Multiple brain regions	Not reported	10 years	8	22	**HEU had lower FAs; increased/decreased MDS**
(Madzime et al., 2021)	South Africa	Cross-sectional	DTI	Default mode network, visual, somatosensory network, salience, auditory, basal ganglia	AZT, NVP	7 years	19	27	**HEU had Higher FA than HUU**

AZT—zidovudine; NVP – nevirapine; MRS—magnetic resonance spectroscopy; DTI—diffusion tensor imaging; magnetic resonance imaging; WM—white matter; MFGM—midfrontal grey matter; PWM – peritrigonal white matter; FA—functional anisotropy.

1.2.13 HIV/ART exposure and breastfeeding

Optimal breastfeeding practices have been shown to favor cognitive outcomes (Horta et al., 2015), as well as intelligence, educational attainment, and income (Horta et al., 2015). At the same time, breastfeeding is one of the common routes through which HIV can be transmitted from mother-to-child. However, when taken during pregnancy and after giving birth, ART reduces vertical transmission of HIV through this route and other common routes like during pregnancy, labour, or delivery. While PMTCT has been promising in the fight against vertical transmission, it is not completely safe for mothers living with HIV to breastfeed their infants. For example, in the United States, where there is access to clean and portable water, and affordable infants' formula, the CDC and the American Academy of Pediatrics recommend that HIV-infected mothers completely avoid breastfeeding their infants, regardless of ART and maternal viral loads, this may be because there still a small risk of transmission. This can also be said of the rest of the developed world. In contrast, in resource-limited settings such as some parts of Africa, WHO recommend that HIV-infected mothers should breastfed exclusively for six months of life (starting as early and within 1 hour after birth), and continue for at least 12 months, with the addition of complementary foods. The benefits of breastfeeding outweighed the risks of transmission as it has been shown that suboptimal breastfeeding is linked to morbidity and mortality especially in resource-limited settings (Victora et al., 2016). Examining neuroimaging measures a few weeks after birth has the advantage of identifying the effects of maternal HIV/ART exposure before parenting differences and/or breast versus formula feeding may confound brain outcomes.

1.2.14 Changes in brain structure and functions from birth to early infancy

Investigating normative brain trajectories from early postnatal life onward is especially important in identifying deviations from typical development. Structural and/or functional alterations may be associated with cognition and language development.

Since the earliest periods of postnatal development are the most dynamic (Gilmore et al., 2007), much research has been focused on understanding typical changes in the brain during this period. Deviation from typical maturation may indicate cognitive, psychological and/or behavioural disorders. MRI is one of the most reliable and safest tools to longitudinally investigate healthy brain development. Before imaging techniques emerged, clinicians relied on approaches such as measuring head

circumference as surrogate for brain development (C TE, 1967, World-Health-Oganization, 2007, Daymont et al., 2010).

Structural MRI allows one to study the anatomical development of the brain, structural properties such as cortical thickness and gyrification as well as structural connectivity (Haartsen et al., 2016). A neonate brain weighs between 380 to 420g (Huppi et al., 1998), which is one-fourth to one-third of its matured volume. At 2 to 4 weeks postnatal life, total brain volume is approximately 36%, and it is about 72% of adult volume at 1 year of age (Knickmeyer et al., 2008). The rate of cerebral growth slows down after age 2, reaching 80% of its adult size at 3 years and approaches 90 to 92% at 9 years (range 7 to 11 years) (Caviness et al., 1996a, Caviness et al., 1996b, Caviness et al., 1996c). Overall, intracranial volume increases by about 300 mL between 3 months and 10 years (Pfefferbaum et al., 1994). Sexual dimorphism has been documented, with males having a larger average cerebral volume than females (Holland et al., 2014, Choe et al., 2013, Lenroot et al., 2007).

Regional structural growth rates have also been demonstrated. Choe and colleagues (2013) computed subcortical grey matter growth rates from three-months postnatal age to 13-month at three different age groups and intervals: 3 -to- 4 -months, 6 -to-7 -month and 12 -to- 13 -months ages groups. The rate of thalamic growth was steady for the entire assessment periods – 3.8 % increase between the first and second assessment periods and 5.0% between the second and third assessment periods, even though the interval between the second and third assessment periods is twice (6 months) that of interval between the first and second assessment periods (3 months). Conversely, growth rates of basal ganglia structures (caudate, putamen and globus pallidus) were higher between the first and second assessment periods. With regards to laterality, globus pallidus, cerebrum and cerebellar hemispheres were reported to be significantly larger on the left whereas caudate, hippocampus and ventral diencephalon were rightward symmetry for all ages combine (i.e. 3 -to- 13 month) (Choe et al., 2013). At age 3 months, thalamus, putamen, globus pallidus and hippocampus were larger on the right (Holland et al., 2014). Choe et al (2013) reported larger thalamus and putamen on the left hemisphere in the 3 -to-4 -month age group. In the 6-to-7 -month age group, cerebrum, globus pallidus, lateral ventricles, and cerebellar hemisphere larger on the left than on the right, while caudate, hippocampus and ventral diencephalon were larger on the right than on the left. At 3-month, male infants have larger cerebellum, thalamus, caudate, putamen and amygdala than female infants. Globus pallidus and hippocampus were larger in females than in male infants (Holland et al., 2014).

It has been established that the growth rates of cortical thickness and cortical surface area differ across brain regions (Lyall et al., 2015), with cortical thickness maturing earlier than cortical surface areas in most brain regions. Though both cortical thickness and surface area are larger during the first year of postnatal life than in the second year. At age 2 years, the cortical thickness approaches 97% of adult values, whereas the cortical surface area only reaches 69% of adult values at this age (Haartsen et al., 2016). Cortical gyrification is also age dependent, with larger folding rates at age 1 year than at age 2 years (Moeskops et al., 2015).

Regional brain connectivity also follows developmental trajectory. White matter tracks or fibre bundles/networks structurally connect brain regions with each other to allow for communication of various modalities for optimum functioning of the CNS. Tractography imaged by diffusion DTI is used to trace these connections (Ball et al., 2013, Brown et al., 2014, Huang et al., 2015). *In utero*, it has been shown that connections in the frontal and occipital lobes were higher than in the other regions (Brown et al., 2014). These connections are part of networks that are already highly efficient and clustered at term age, but show increased efficiency, clustering and small-worldness with increasing age (Haartsen et al., 2016). Brain regional connectivity increases with age suggesting an increased in white matter tracts with higher fractional anisotropy values (Huang et al., 2015).

1.3 Study introduction

Between 2017 and 2021, 226 Xhosa-speaking women (144 living with HIV; 82 uninfected controls), 18 years or older, with low-risk pregnancies were recruited at $\leq$ 31 weeks of gestation from community antenatal clinics in Cape Town, South Africa where HIV sero-prevalence approaches 30% (SANAC, 2018). Of the pregnant women living with HIV (PWLH), 78 had initiated ART before conception, exposing the fetus to ARVs for the entire pregnancy, while 66 started ART after conception of the current pregnancy (Figure 1).

Study exclusion criteria were underlying chronic disorders (e.g. diabetes, epilepsy, tuberculosis, hypertension), poor obstetric history (*e.g. any previous second trimester miscarriage, stillbirth, neonatal deaths, hypertension, gestational diabetes, previous premature delivery*), active tuberculosis or a known tuberculosis contact, current pregnancy related medical conditions (*e.g. hypertension or diabetes*); medication other than required pregnancy supplements (ferrous sulphate, folic acid, calcium carbonate) or ART, cotrimoxazole or isoniazid; among women with HIV poor adherence to

ART, non-standard ART regimens or nondisclosure of HIV status to family members; alcohol consumption $\geq$ 7 drinks per week or $\geq$ 4 drinks per occasion, illicit drug use, or language criteria not met.

All women enrolled provided written informed consent in person in their preferred language before enrolling into the study. The study was conducted according to protocols that had been approved by the Health Sciences Human Research Ethics Committees of Stellenbosch University (M16/10/041) and the University of Cape Town (UCT; 801/2016). Mothers also provided consent for their infants to participate in the study.

At enrolment demographic information was recorded. Women had monthly study visits to coincide with planned routine antenatal clinic visits at the same site. Study visits included health monitoring (co-infections and concomitant medications). Mothers were also interviewed at each clinic visit regarding their smoking (cigarettes/day), alcohol and drug use using the timeline follow-back approach (Jacobson et al., 2008, Jacobson et al., 2002). Urine was tested for recreational drug use (cannabis, methamphetamine and methaqualone) at study visits closest to 20 and 33 weeks of gestation. Gestational age (GA) was estimated by a combination of date of last menstrual period, fundal height and early antenatal ultrasound performed at the clinic. Following delivery, the GA at antenatal time points were adjusted according to the GA estimate at birth, taking into consideration the above factors and repeat ultrasound examination.

For women living with HIV, VL and CD4 counts within 6 months of pregnancy and delivery were obtained from clinic records. As per standard care for all pregnant women in South Africa, HIV status is confirmed at the antenatal clinic mostly using HIV Rapid test. VL and CD4 counts are measured yearly in previously diagnosed PWLH, and during pregnancy for those newly diagnosed. Only PWLH on fixed drug combination ART (Tenofovir/ Efavirenz/Emtricitabine) were included in the study. An ART adherence questionnaire was administered at each study visit by an adherence counselor.

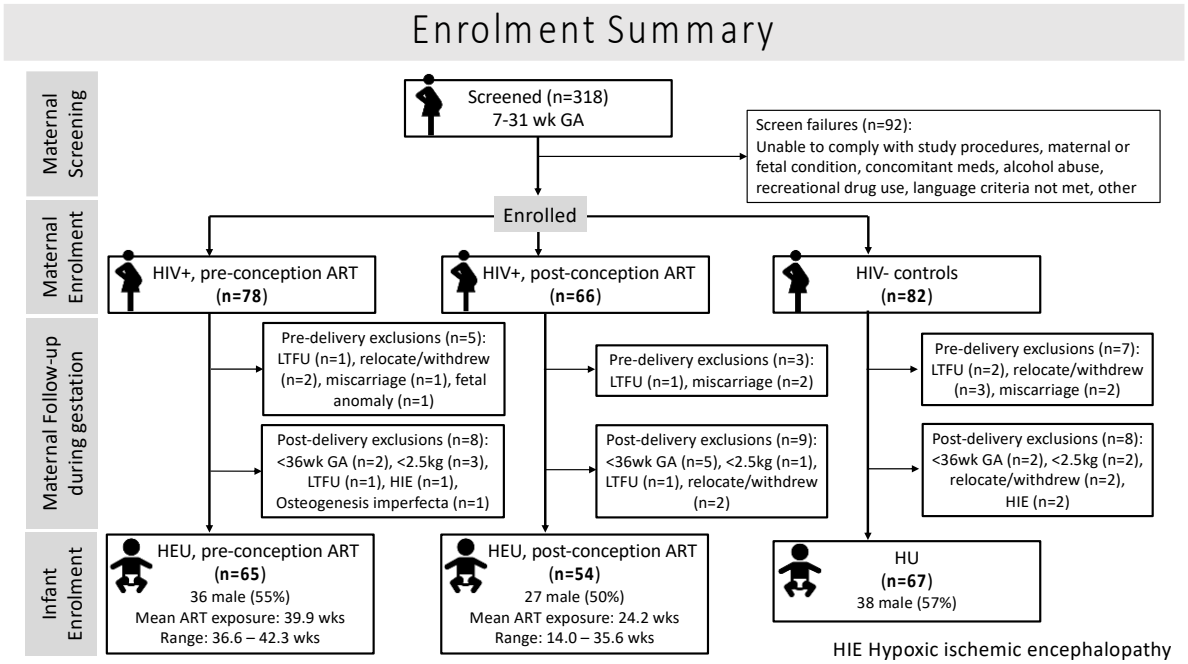

Figure 1.9 Enrolment summary

Infants born to PWLH were given Nevirapine if considered low risk and Zidovudine added if high risk of vertical transmission of HIV. Infants were considered at high risk if maternal VL >1000 copies/mL at 32 weeks gestation.

Infant exclusion criteria included preterm delivery <36 weeks GA, neonatal hospital admission, birth weight <2500g, positive on HIV-1 PCR, or conditions that could influence neurodevelopmental outcomes, such as severe congenital malformations or chromosomal abnormalities, neonatal asphyxia, persistent hypoglycaemia, or severe neonatal jaundice. Details of pre- and post-delivery exclusions are provided in Figure 1.9

After exclusions, 186 mother-infant pairs were enrolled in the study, of which 67 infants were HUU, 65 HEU with ART exposure throughout gestation (HEU-pre), and 54 HEU but exposed to ART for only part of their gestational period (HEU-post).

1.3.1 MR data acquisition

New-borns and their mothers were transported to the Cape Universities Body Imaging Centre (CUBIC) located adjacent to the UCT Faculty of Health Sciences in Cape Town, South Africa for MRI at a mean GA of 41.6 weeks (range 39 – 45 weeks). A paediatrician, blind to HIV and ART exposure status, weighed, examined, and administered the Dubowitz Infant Neurological Examination (Dubowitz et al., 2005) roughly one hour before the scheduled scan. Infants were then fed, had their diaper changed, sponge earplugs inserted in their ears which were then covered with mini-muffs and a beanie, and a pulse oximeter attached to one of their feet to monitor oxygen saturation. They were tightly swaddled, put to sleep supine on an MRI-compatible vacuum cushion containing Styrofoam beads (Vac Fix®, S&S Par Scientific, Houston, TX) in the Siemens 16-channel paediatric head and neck coil, and imaged without sedation on a 3 T Skyra MRI (Siemens, Erlangen, Germany). The protocol included a high-resolution T1-weighted 3D echo-planar imaging (EPI) navigated multi echo magnetization prepared rapid gradient echo (MEMPRAGE) acquisition (FOV 192x192 mm^2, TR 2540 ms, TI 1450 ms, TE's = 1.69/3.55/5.41/7.27 ms, bandwidth 650 Hz/px, 144 sagittal slices, 1.0x1.0x1.0 mm^3; GRAPPA factor 2). Two diffusion-weighted imaging (DWI) sets with opposite (Anterior-Posterior, Posterior-Anterior; AP/PA) phase encoding directions were acquired with a multi-band (Setsompop *et al.*, 2012) twice refocused spin-echo EPI sequence: TR 4800 ms, TE 84 ms, matrix 62 axial slices of 96x96 voxels (each voxel 2x2x2 mm^3), 6/8 partial Fourier encoding, BW 1628 Hz/px, with slice-acceleration factor 2 and GRAPPA factor 2. Each acquisition contained six b = 0 s mm^{-2} (b0) reference scans and 30 DW gradient directions with b = 1000 s mm^{-2}.

Of the 186 enrolled infants, 184 visited CUBIC (2 HEU-pre infants missed their visit) and 165 (58 HEU-pre; 48 HEU-post; 59 HUU) provided imaging data. Scans were visually inspected for image quality and a subset of 120 high-quality scans selected for manual tracing.

1.3.2 Manual segmentation of target ROIs

The caudate nucleus, putamen and globus pallidus of the basal ganglia, thalamus, cerebellar hemispheres, and cerebellar vermis (Figure 1.10) were manually traced using Freeview software (FreeSurfer v7.1.0 image analysis suite, http://surfer.nmr.mgh.harvard.edu/) on a Lenovo ThinkPad Yoga370 tablet. Each ROI structure contour was manually traced in the coronal plane and corrected on axial and sagittal planes on a slice-by-slice basis by a single expert neuroanatomist (AI). The tracer was blinded to participants' exposure status. Traced volumes were visually checked and verified by a

senior neuroanatomist (FW). Total intracranial volume (ICV) for each subject was calculated using an in-house script adapted from FreeSurfer. Manual tracing was preferred over automated segmentation because of difficulty in segmenting neonate brains. Automated tools cannot clearly demarcate between grey and white matter at this early stage as the brain is still undergoing rapid changes and development.

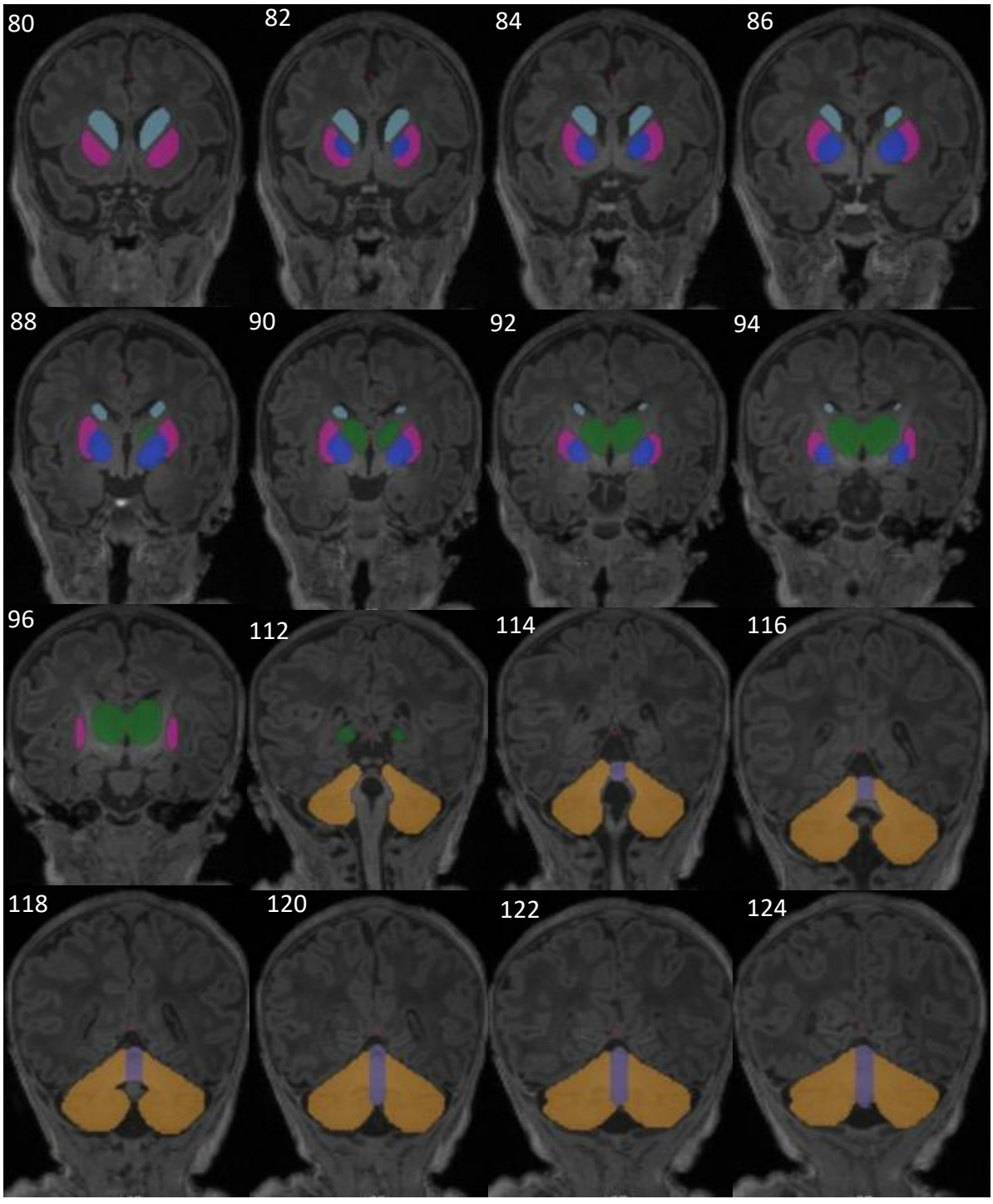

Figure 1.10 Coronal view of neonatal brain showing the manually segmented structures: Basal ganglia (caudate (sky blue), putamen (magenta), pallidum (dark blue)), thalamus (green), cerebellar hemispheres (yellow), and cerebellar vermis (purple). The slices shown here are from one of the HUU infants' images (slices 80 to 124).

1.3.3 Image processing for DTI

Structural and DWI data were converted from DICOM format to NiFTi format using AFNI's dcm2niix_afni tool. All diffusion-weighted volumes from both AP and PA acquisitions were visually inspected. Any volume with slices showing distortion or signal drop-out was removed from both the AP and PA acquisitions of that subject. Only subjects with at least 15 remaining diffusion directions, and at least one b0 image, were retained for further analyses. DIFF_PREP and DR_BUDDI tools within TORTOISE v3.1.0 (Pierpaoli et al., 2010; Iefanoglu et al., 2015) were used to correct for motion and eddy distortions and DWI distortion, respectively. We used the *fat_proc_dwi_to_dt* function in AFNI for an estimating the diffusion tensor and DTI parameters (FA, MD, etc). The masks of the traced volumes (with tracings performed in the structural space) were aligned to the diffusion space, using 12 parameter affine transformation performed in AFNI's 3dAllineate. This was possible because TORTOISE postprocessing step the DW were distortion-free and non-linear warping of the structural to diffusion space was unnecessary. Finally, the ROIs were inflated by 2mm using 3dROIMaker.

1.3.4 Tractography analyses

Full-probabilistic tractography was performed using 3dTrackID in AFNI (Taylor and Saad, 2013) with the following stop criteria (section 1.2.15.1.5): angle threshold of 60 degrees, a mask of FA > 0.01, as proxy for white matter in infants (Dubois et al., 2006), minimal streamline length threshold of 15mm, number of seeds per voxel Monte Carlo iteration set to 5, number of Monte Carlo iterations = 1000. Finally, tracks with a minimum of 5 streamlines connecting a pair of GM seeds were kept and interpreted as a WM-tract. Only WM-tracts common to the entire set of subjects were kept for further analyses. The DTI parameters FA, MD, AD, and RD for each of the WM-tracts were exported into R statistical software (R Core Team, 2019) for further analyses.

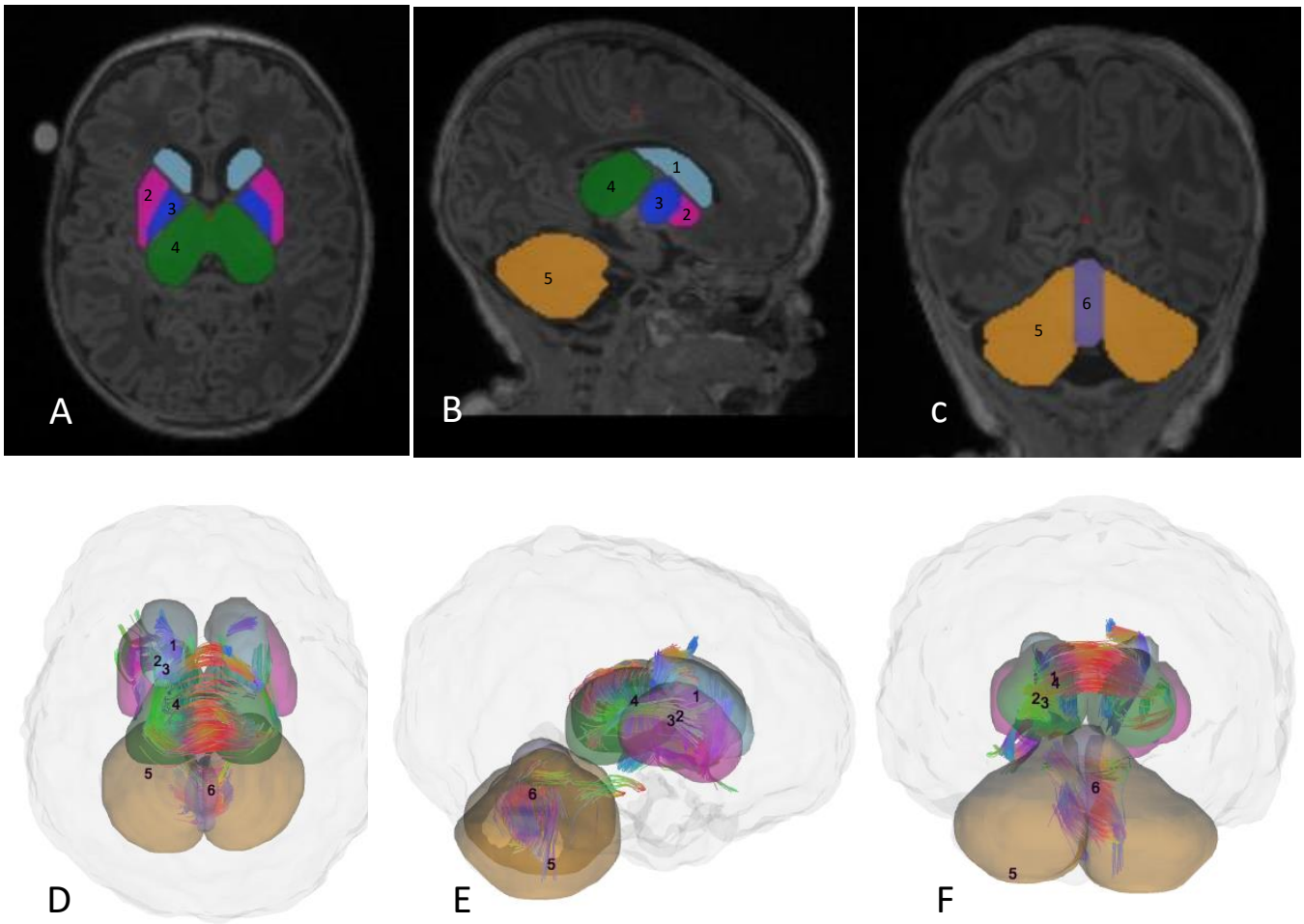

Figure 1.11. **Top row (A, B, C):** Manually traced structures used as seeds and targets for probabilistic tractography. A = axial view; B = sagittal view; C = coronal view. **Bottom row (D, E, F)** = Axial, sagittal and coronal views of white matter tracts from probabilistic tractography that connect the manually traced seeds/targets. Seeds/targets: 1) caudate; 2) putamen; 3) pallidum; 4) thalamus; 5) cerebellar hemisphere; 6) cerebellar vermis. Regions are numbered in one hemisphere only but were traced bilaterally.

1.3.5 Neurodevelopmental assessments

The Griffiths Mental Developmental Scales (GMDS) assesses all developmental areas of child development. The GMDS extended revised version (birth to age 2 years) was performed in the cohort at 9 to 12 months. The GMDS assesses neurodevelopment on the subscales: locomotor, personal social, language, eye & hand coordination, and performance (Table 1.5). A separate raw score was allocated to each subscale. The raw scores of the various subtests were added up and processed to obtain quotients. Obtaining scores for each subscale allowed one to determine the section of the subscale of the measuring instrument the infant is demonstrating delay. Standardized translations into IsiXhosa were used. We converted raw scores into age equivalents using standardized norms and calculate a quotient as a percentage of each infant's chronological age, using the United Kingdom norms with a mean of 100 and standard deviation of 15. A quotient of less than 70 signifies developmental delay.

Table 1.5 Griffiths mental developmental scales

Subscales	Description of abilities assessed
Locomotor	Balance, co-ordinate and control movements - crawling, sitting, standing, pulling itself up by using furniture, and walking.
Personal social	Independence and personal-social development - *inter alia,* smiling, holding a spoon, drinking from an open cup, reaction to strangers, finger feeding, giving affection and playing interactive games.
Language	Receptive and expressive language - babbling, singing of tunes, the number of words the infant can utter, identifying and naming of objects.
Eye & hand coordination	Co-ordination between eyes and hands and its ability to skilfully manipulate objects - holding of objects, throwing of objects, pointing with the index finger, the holding of pencil as if to mark on paper, and pushing cars along.
Performance	Skills regarding manipulation, speed and precision - manipulation of more than one object, reacting to paper, rattling of box, open lid of box, and completion of form boards
General Quotient	Average of the 5 subscales above

1.3.6 Statistical analysis

All statistical analyses were performed in R statistical software (R Core Team, 2019). Student's t-test/ANOVA and chi-square test for continuous and categorical variables, respectively, were used to compare sample characteristics between unexposed and HEU groups.

We used linear regression models to examine group differences: HUU vs HEU, HUU vs HEU-pre, and HUU vs HEU-post. To determine the most salient confounders for each model, we calculated Pearson correlation coefficients between potential confounders and outcome volumes. Possible confounders included 4 maternal indices (age at delivery, weight change per week, absolute alcohol consumption per day averaged across pregnancy, and education), infant sex and 3 infant indices at scan (GA, weight, and head circumference). Potential confounders related at $p<0.10$ to any outcome were included in regression models with that outcome. Pearson correlation and linear regression were also used to examine associations of regional brain volumes among HEU infants with maternal clinical and treatment variables. We used false discovery rate (FRD) for multiple comparisons.

CHAPTER TWO

Maternal HIV/ART exposure and neonate subcortical volumes

2.1 Introduction

Maternal HIV likely contributes to developmental delays in HEU infants and children through changes to the mother's immune system during pregnancy. While ART keeps the virus at bay by increasing CD4+ T cells, it may also be neurotoxic to the fetus (Lanman et al., 2021). Human and animal models provide evidence that maternal viral infections influence fetal and infant brain development (Choi et al., 2016, Salemi et al., 2014, Bauman et al., 2014, Parboosing et al., 2013, Visentin et al., 2012, Ellman et al., 2009), and an increased inflammatory response has been posited as a possible mechanism (Sappenfield et al., 2013). As it is still not well understood how viruses – including HIV – affect the developing fetus, it is important to monitor brain maturation in HEU infants.

While neuroimaging has been used to identify the effects of HIV exposure in infants and children, little work has focused on anatomical changes. The only previous study to examine HIV exposure-related structural brain changes was conducted in 10-year-old children and did not find any volumetric differences using tensor-based morphometry (Jahanshad et al., 2015). In addition, little work has examined subcortical structures. While most HIV-exposure imaging studies use DTI to study white matter, an MRS study reported altered metabolite levels in the basal ganglia in 9-year-old HEU children [reference Frances' paper here]. This result suggest in utero exposure alters subcortical development, at least in the basal ganglia. Segmentation of the basal ganglia may help refine the location of regional effects of HIV exposure.

This is the first study to examine regional brain volume changes in early infancy within an HEU population. Previous studies have demonstrated the vulnerability of basal ganglia in HIV infected and exposed subjects. This vulnerability is attributed to the proximity of basal ganglia to the ventricular system of the brain (Sarma et al., 2014, Castelo et al., 2007). We also include the thalamus and cerebellum because they are equally proximal to the ventricular system of the brain. While basal ganglia nuclei are proximal to the lateral ventricles, the thalamus and cerebellum are proximal to the third ventricle and fourth ventricle, respectively (Martin, 2013).

The basal ganglia and cerebellum are also involved in motor control and coordination. HEU infants have been found to have poorer fine and gross motor scores compared to their HUU counterparts.

We hypothesized smaller volumes in the basal ganglia and cerebellum in HEU neonates compared to HUU. Since no effect of ART initiation timing was previously seen on gross and fine motor function (Madlala et al., 2020), we hypothesized that volumes would not be impacted by duration of *in utero* ART exposure.

2.2 Results

We present volumes for 120 infants (79 HEU; mean age at scan ± standard deviation = 41.5 ± 1.0 weeks GA; 59 female). Of the 79 HEU infants, 40 were exposed to ART throughout gestation (HEU-pre) and 39 only for part of their gestational period (HEU-post). Post-conception mothers initiated ART at a mean GA of 15.4 (±5.7) weeks. Sample characteristics are summarized in Table 2.1. Overall, maternal and infant indices were similar across groups, except that mothers in the HIV pre-conception group were roughly 3 years older than their post-conception and HIV-negative counterparts. Mothers in the HIV pre-conception group had higher CD4+ cell counts and lower VLs within 6 months of enrolment than the post-conception mothers. There were only 10 mothers with positive drug tests – 4 for cannabis (3 HUU; 1 HEU-pre), 5 for methamphetamine (3 HUU; 2 HEU-post) and 1 methaqualone in the HUU group. Only 1 HUU mother reported smoking. Approximately 50% of mothers across groups reported very low levels (all < 0.10 oz AA/day) drinking during pregnancy.

Figure 2.1 shows regional volumes by group, together with results from pairwise group comparisons using independent two-tailed Student's t-test. Associations of potential confounders with regional volumes are summarized in APPENDIX (supplementary analysis 1 Table 2). In no regions were volumes associated with infant sex, maternal age at delivery or maternal education.

In Table 2.2 we present regression coefficients for the effect of group on regional volumes, controlling for potential confounding by covariates weakly related to the volumetric outcome being examined. As a group, HEU infants demonstrated significantly smaller left putamen compared to HUU. However, this difference falls below conventional levels of significance within each of the HEU sub-groups when compared separately to HUU. In contrast, we observe smaller caudates bilaterally in infants in the HEU-post group compared to HUU, which are not seen in the HEU-pre group, nor when comparing all HEU infants combined to HUU. Both left and right caudate surviving FDR correction for multiple comparisons, while the significant difference observed in the left putamen does not remain after correction.

In the APPENDIX (Supplementary analysis 1 table 3 and figure 1) we present associations of regional volumes among HEU infants with maternal clinical and treatment variables. In both the left and right caudate, increasing duration of ART exposure is associated with increasing volume (figure 2.2), effects that remain significant after control for potential confounding by infant weight. Moreover, higher maternal CD4 within 6 months of enrolment is associated with larger left caudates. Although we do not find association of volumes with maternal VL in any of the regions studied here, either among mothers with detectable VL or all mothers living with HIV, infants in the HEU-post group with detectable VL demonstrate smaller left thalamic volumes than those with undetectable VL (mean ± sd, detectable VL = 4225.8±369.2; undetectable VL = 4513.0±329.7; p = 0.02). Although below conventional levels of significance, a similar result is seen in the right thalamus (detectable VL = 4322.6±318.3; undetectable VL = 4554.8±376.1; p = 0.06) (APPENDIX: Supplementary analysis 1 table 4 and figure 2).

Table 2.1 Sample characteristics (N = 120)

	HUU (n = 41)		HEU (n = 79)					
			Pre-conception ART (n = 40)		Post-conception ART (n = 39)			
	Mean±SD	**Range**	**Mean±SD**	**Range**	**Mean±SD**	**Range**	**X^2 or t or F**	***P (for* X^2 or t or F**
Maternal indices								
Age at delivery (years)	28.2 ± 5.7	19.6 – 44.1	31.4 ± 5.4	20.6 – 46.3	28.5 ± 4.8	19.6 – 40.9	4.45	**0.01**
GA at enrolment (weeks)	19.7 ± 5.5	8.1 – 28.0	20.9 ± 6.1	7.1 – 35.1	21.3 ± 6.1	9.1 – 30.7	0.83	0.44
Highest school level completed (n, %)								
Grade 6	0 (0)	-	1 (2.5 %)	-	0 (0)	-		
Grade 8	2 (4.9 %)	-	1 (2.5 %)	-	0 (0)	-		
Grade 9	0 (0)	-	3 (7.5 %)	-	1 (2.6 %)	-		
Grade 10	1 (2.4 %)	-	3 (7.5 %)	-	4 (10.3 %)	-	11.47	0.32
Grade 11	12 (29.3 %)	-	15 (37.5 %)	-	14 (35.9 %)	-		
Grade 12	26 (63.4 %)	-	17 (42.5 %)	-	20 (51.3 %)	-		
CD4 within 6 mo of enrolment (cells/μL)[1]	N/A	N/A	576 ± 172	108 – 887	436 ± 195	52 – 913	3.33	**0.001**
VL within 6 mo of enrolment								
Undetectable (n, %)	N/A	N/A	31 (77.5 %)	-	25 (64.1 %)	-	1.13	0.29
Detectable (n, %)	N/A	N/A	9 (22.5 %)	-	14 (35.9 %)	-		
VL (copies/mL)[2] Median [IQR]	N/A	N/A	30 [27 – 55]	26 – 238	259 [45– 443]	22 – 16787	7.99	**0.009**

Substance use across pregnancy								
Alcohol (n; %)	20 (48.8%)	-	18 (45.0%)	-	22 (56.4%)	-	1.07	0.59
AA/day (oz)[3]	0.04 ± 0.03	0.057 x10^{-3} – 0.096	0.03 ± 0.02	0.012 – 0.072	0.04 ± 0.02	0.009 – 0.072	0.79	0.46
Cannabis (n; %)[4]	3 (7.3 %)	-	1 (2.5 %)	-	0 (0)	-	3.45	0.18
Methamphetamine (n; %)[4]	3 (7.3 %)	-	0 (0)	-	2 (5.1 %)	-	2.85	0.24
Methaqualone (n; %)[4]	1 (2.4 %)	-	0 (0)	-	0 (0)	-	1.94	0.38
Smoking (n; %)	1 (2.4 %)	-	0 (0)	-	0 (0)	-	1.94	0.38
Infant indices								
Sex (n Female; %)	21 (51.2%)	-	19 (47.5%)	-	19 (48.7%)	-	0.12	0.94
Delivery route:								
Vaginal (n, %)	35 (85.4 %)	-	30 (75.0 %)		26 (66.7 %)	-	3.84	0.15
Caesarean (n, %)	6 (14.6 %)	-	10 (25.0 %)		13 (33.3 %)	-		
Birth indices:								
GA (weeks)	39.8 ± 1.2	36.7 – 42.1	39.7 ± 1.4	36.6 – 42.1	39.7 ± 1.5	36.9 – 42.3	0.04	0.96
Weight (g)	3265 ± 388	2575 – 4180	3235 ± 347	2575 – 4255	3241 ± 387	2500 – 4230	0.07	0.93
Crown-to-heel length (cm)	49.9 ± 2.7	45.0 – 58.0	49.6 ± 2.2	44.0 – 54.0	50.1 ± 2.8	43.0 – 56.0	0.29	0.75
Head circumference (cm)	34.1 ± 1.2	32 – 37	34.0 ± 1.2	31 – 36	33.5 ± 1.5	31 – 39	2.09	0.13
ART exposure length (weeks)	N/A	N/A	39.7 ± 1.4	36.6 – 42.1	24.8 ± 5.7	14.0 – 35.6	16.1	**<0.001**
MRI indices:								
GA Equivalent (weeks)	41.6 ± 0.9	40.0 – 43.9	41.3 ± 1.0	39.0 – 44.4	41.5 ± 1.2	39.0 – 43.4	0.50	0.61

Weight (g)[5]	3491 ± 405	2500 – 4250	3440 ± 421	2700 – 4500	3465 ± 397	2750 – 4450	0.15	0.86
Head circumference (cm)[5]	35.0 ± 1.3	32 – 37	35.5 ± 1.3	33 – 37	34.9 ± 1.2	31 – 36.5	2.48	0.09
Total ICV (x 10^5 mm^3)	4.95 ± 0.71	3.84 – 7.55	5.28 ± 0.59	3.99 – 6.41	5.07 ± 0.74	3.44 – 7.68	1.69	0.19

[1]CD4 count missing for 2 mothers who started ART pre-conception; [2]Based only on mothers with detectable VL levels (9 mothers who started ART pre-conception; 14 mothers who started ART post-conception); [3]Based only on mothers who consumed alcohol; 1 oz absolute alcohol (AA) is equivalent to 2 standard drinks; [4]Numbers based on urine tests; 5Data missing for 1 infant in the pre-conception group and 2 HUU infants. Bold indicates significance at $p \leq 0.05$. [a]Fisher exact test.

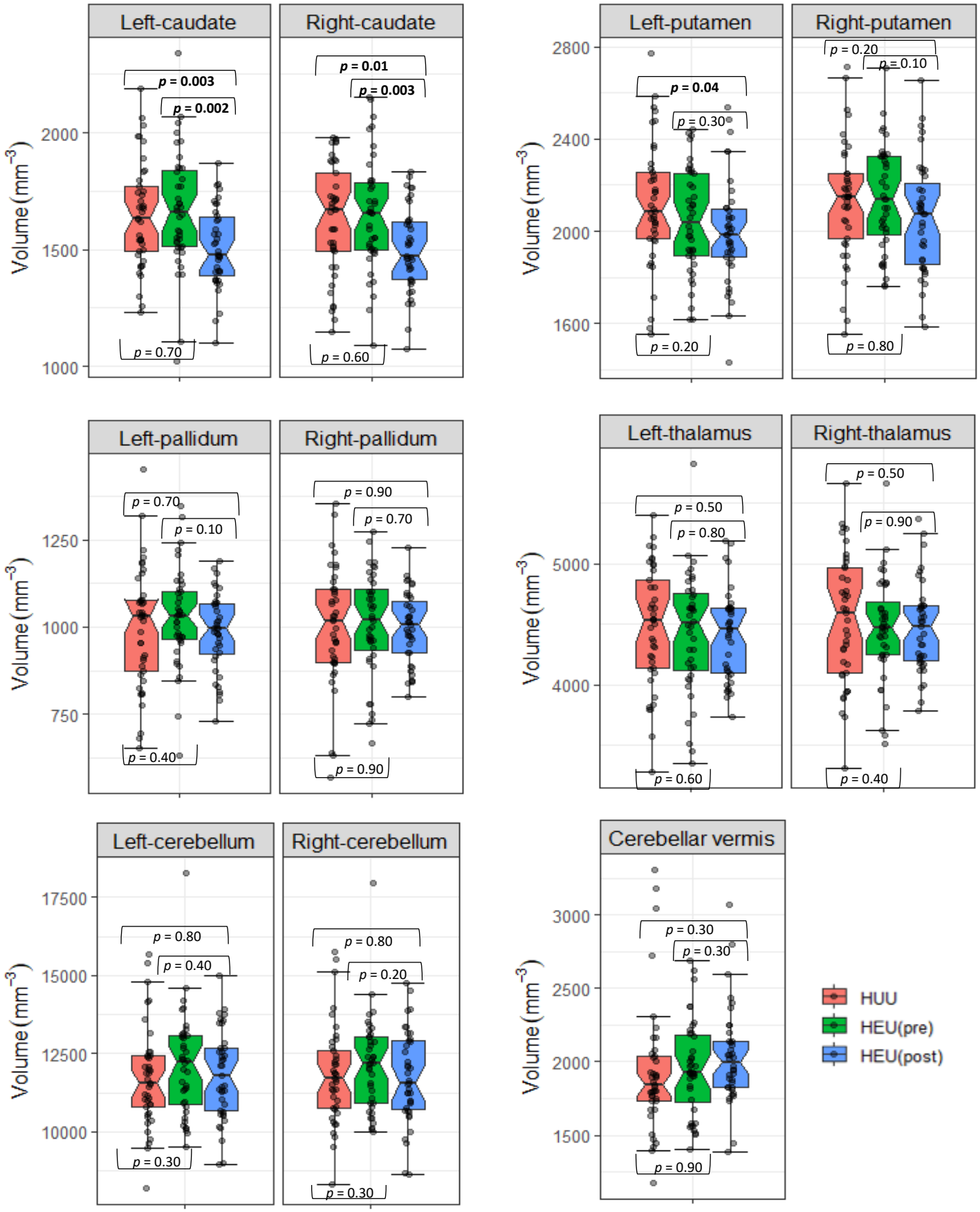

Figure 2.1. Comparison of regional volumes by group. The HEU group comprised exposed uninfected infants born to mothers who had either initiated ART **pre**-conception or during gestation (**post**-conception); HUU are unexposed uninfected controls. Hourglasses show median and interquartile ranges; whiskers are upper and lower extremes. Values above and below the whiskers are outliers, defined as data points more than 1.5 times the interquartile range above (or below) the upper (or lower) quartile. *p* values from independent one-tail student t-tests.

Table 2.2 Comparison of regional volumes between infants who had (HEU) and had not (HUU) been exposed to HIV prenatally. We also separately compare infants who had been exposed to ART either throughout gestation (pre-conception ART) or for a shorter period (post-conception ART) to unexposed infants. Values are unstandardized regression coefficients (**β**) and standard errors (SE).

Region	**HUU vs HEU**		**HUU vs HEU pre-conception ART**		**HUU vs HEU post-conception ART**	
	β (SE)	***P***	**β (SE)**	***p***	**β (SE)**	***P***
Left caudate[2]	-65.8 (44.2)	0.14	18.1 (48.7)	0.71	-149.4 (48.7)	**0.003**
Right caudate[2]	-54.5 (45.0)	0.22	22.2 (50.4)	0.66	-131.0 (50.1)	**0.01**
Left putamen[2,3,4]	-91.3 (46.3)	**0.05**	-89.1 (53.7)	0.10	-93.5 (55.6)	0.08
Right putamen[2,3]	-40.1 (44.1)	0.45	-12.8 (52.0)	0.81	-64.6 (50.6)	0.20
Left pallidum[3]	3.4 (27.6)	0.90	21.9 (32.2)	0.50	-14.2 (31.8)	0.66
Right pallidum[3,4]	-3.9 (27.6)	0.89	-2.0 (32.7)	0.93	-4.7 (31.8)	0.88
Left thalamus[2]	-52.7 (83.2)	0.53	-35.0 (96.4)	0.72	-70.5 (96.3)	0.47
Right thalamus[2,3]	-55.8 (82.0)	0.51	-53.8 (96.4)	0.58	-56.4 (96.1)	0.56
Left cerebellum[2,3]	328.9 (265.5)	0.22	531.4 (305.8)	0.09	128.9 (304.8)	0.67
Right cerebellum[2,3]	211.9 (265.3)	0.43	472.6 (304.0)	0.12	-45.5 (303.1)	0.88
Vermis[2,3]	63.1 (69.6)	0.37	29.7 (80.4)	0.71	96.9 (80.7)	0.23

The model includes potential confounders related to the outcome at $p<0.10$: 1 = equivalent GA of infant at MRI; 2 = infant weight at MRI; 3 = infant head circumference at MRI; 4 = maternal weight change per week;. Bold indicates significance at $p\leq0.05$.

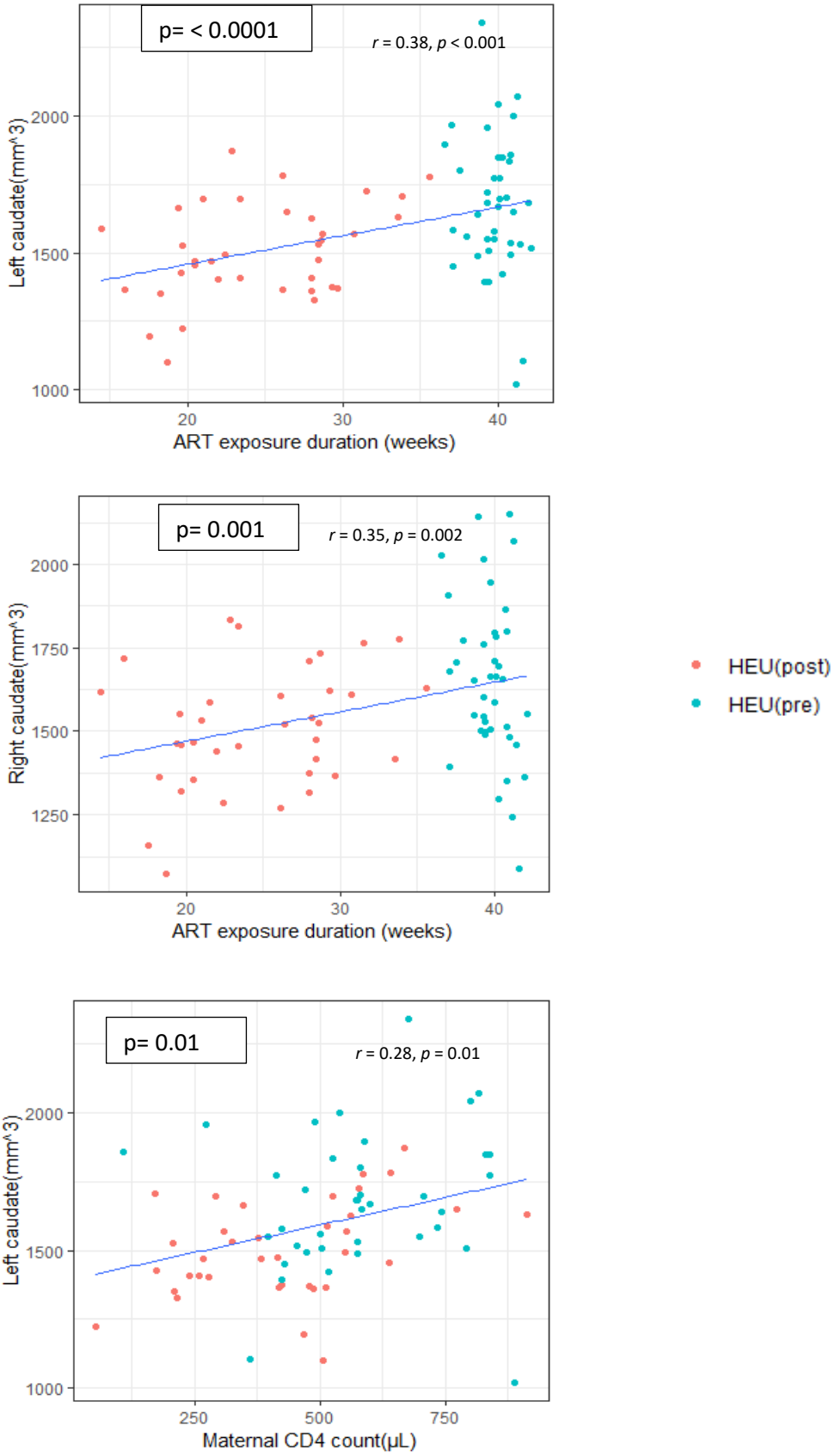

Figure 2.2. plots showing associations of the regional volumes among infants with maternal clinical and treatment variables.

2.3 Discussion

To our knowledge, this is the first study to quantify the influence of maternal HIV infection and prenatal ART exposure duration on subcortical and cerebellar volumes in uninfected newborns. We found HIV exposure-related volume reductions in the left putamen and bilateral caudates. The fact that the reductions in caudate volumes were evident only in infants from the HEU-post group, suggests that maternal ART protects the caudates of the developing fetal brain from HIV-related damage. This is further supported by the associations between caudate volumes and duration of prenatal ART exposure. The observed fetal neuroprotection may be related to maternal immune health, as maternal CD4 count was positively associated with left caudate volumes. However, reductions in the left putamen were not related to ART duration or maternal immune health during pregnancy suggesting different mechanisms are involved.

Exposure to maternal HIV infection

The reduction in the left putamen volume among HEU neonates suggests that HIV infection, even with ART, still influences the developing fetal brain. Exposure to maternal infection likely impacts the fetal brain indirectly via maternal inflammation cascades at the level of placentation. Proinflammatory cytokines secreted from maternal decidua immune cells are elevated in pregnant mothers living with HIV compared to their uninfected counterparts (Vyas et al., 2021a, Lee et al., 2001). The increasing number of proinflammatory cytokines may disrupt immune equilibrium at the maternofetal interface. The maternal and fetal immune systems synergistically interact during pregnancy to support typical fetal development and prevent adverse outcomes (Arck and Hecher, 2013). The maternal aggravated immune response to HIV infection may skew immune responses toward inflammation, and this may provoke the fetal part of the placenta to initiate its own responses. HEU infants demonstrate an increased frequency of activated T cells compared to HUU. (Bunders et al., 2014a, Vigano et al., 2007, Clerici et al., 2000).

A study in rhesus macaque found reduced grey and white matter volumes in offspring whose mothers were infected with influenza virus. The authors show that the virus had not entered the fetal compartment nor elicited a primary response. Further, MRI at 1 year demonstrated reductions in most of the grey matter volumes and decreased white matter volume in the parietal cortex compared to controls. The authors posit that fetuses did not need to be directly infected with the virus before it impacts their brains. The atrophy reported appeared to be the consequence of secondary mediators generated by the maternal immune response (Short et al., 2010).

Therefore, neural abnormalities in uninfected neonates may be a result of a maternal immune response rather than directly from fetal primary responses. Studies in rodents and mice mimicking

inflammation in pregnancy demonstrate the impact of increasing proinflammatory cytokines on the placenta with subsequent effects on fetal neurodevelopment (Meyer, 2014, Smith et al., 2007). Proinflammatory cytokines IL6 can enter the fetal circulation via amniotic fluid by disrupting the functions of the placenta (Smith et al., 2007). Cytokines generated in the placenta can in turn excite the synthesis of fetal cytokines (Gilmore et al., 2003, Urakubo et al., 2001). Both cytokines and circulating leucocytes can permeate the developing blood-brain barrier (BBB) and brain parenchyma leading to neurodevelopmental dysfunctions (Meyer et al., 2006, Rees and Harding, 2004). However, the exact mechanisms underlying the basal ganglia volume reductions observed in this study are unclear.

The sequence of events leading to grey matter atrophy following the entrance of cytokines and circulating leucocytes into these regions in HEU populations is lacking. A large body of literature has linked structural atrophy to inflammation and gliosis (Cavaliere et al., 2020, Guzman-Martinez et al., 2019, Walker, 2018, Bachiller et al., 2018, Pekny and Pekna, 2016). A substantial number of studies have implicated basal ganglia in HIV infection with the majority of studies reporting grey matter atrophy (Li et al., 2018, Becker et al., 2011, Küper et al., 2011, Di Sclafani et al., 1997, Aylward et al., 1993). A few studies reported hypertrophy in these HIV affected regions, and attributed these increased volumes to increased accumulation of HIV-infected mononucleated cells and toxins in the structures closer to the ventricular system due to easier penetration (acute), and slow metabolic waste removal (due to chronic exposure) in more distal regions such as putamen and nucleus accumbens (Randall et al., 2017, Sarma et al., 2014, Castelo et al., 2007).

Juxtaposing with studies reporting grey matter reductions above, the mechanism underpinning the basal ganglia reduction in HEU babies is likely similar to children living with HIV. The common preconditioning denominator is inflammation. However, the cascades of events leading to neuroinflammation in both cases are different. While the primary response to HIV infection triggers the release of proinflammatory cytokines in children living with HIV, neuroinflammation in HEU is due to a secondary effect from the maternal primary response.

Exposure to maternal HIV infection and variable ART duration

We find significantly reduced caudate volumes in the HEU post-conception group compared to HUU infants. In addition, HEU infants' caudate volumes were positively associated with *in utero* ART exposure duration.

Despite evidence of improved prevention of vertical transmission of HIV among mothers who initiated ART preconception compared to those who started ART during pregnancy (Agabu et al., 2020, Mandelbrot et al., 2015), pre-conception ART has been linked with increased risk of still births,

preterm delivery (PTD), small for gestational age or low birth weight infants (Snijdewind et al., 2018, Uthman et al., 2017, Chen et al., 2012). However, we are not aware of any studies that have reported negative effects of longer prenatal ART exposure on infant neurodevelopmental outcomes. In contrast to the poorer birth outcomes reported in the above studies, the numbers of miscarriages/fetal anomalies among mothers enrolled in our study were similar across groups, as were the number of infants excluded due to PTD, low birth weight or a medical diagnosis (8.0% HUU; 9.6% HEU-pre; 9.5% HEU-post). Moreover, all infant indices at birth were similar across groups. Discrepancies with previous studies may be attributable to optimised ART regimens in the current study, where all women living with HIV were on a fixed drug combination ART (Tenofovir/ Efavirenz/Emtricitabine).

To date, it is not clear what the optimal period and timing of ART treatment during pregnancy is to minimise HIV-related damage to the fetus. A cell line study by Divi and colleagues examining mitochondrial pathology in cultured human cells exposed to zidovudine over a protracted period, found a transient zidovudine-induced abnormal proliferation of mitochondria in cells exposed to zidovudine for half of the experimental period (early to mid-passages). In contrast, cells of the later passages showed irreversible wide-spread mitochondrial morphological damage and severe mitochondrial DNA depletion (Divi et al., 2007). Extrapolating to the whole human organism, this suggests that exposure to ART from conception to mid-pregnancy might be sufficient to prevent HIV-related neural damage even in zidovudine-based combination therapy where concerns have been raised regarding its safety to developing fetus (Zuena et al., 2013).

Since the development of neurons and glial cells (responsible for providing nutrients, support and protection) is accelerated during the first trimester when the foundation of brain structures and functions are laid (Tiwari et al., 2018, Reemst et al., 2016, Stiles and Jernigan, 2010), any disturbances over this period may have severe long-term consequences. Pre-conception ART may mitigate HIV-related neural damage by lowering maternal viral loads and preventing an aggressive aggravated maternal immune response (Maharaj et al., 2017). Conversely, in women who start ART later during pregnancy, elevations of proinflammatory cytokines in the placenta and eventually in the fetal brain during early pregnancy may trigger or precipitate brain mal-development and related aberrations in cognition and behaviour later in life. Indeed, epidemiological data suggest that maternal infection during early-to-mid human pregnancy is more likely to be associated with long-term developmental brain and behavioural abnormality in the offspring (Brown et al., 2004, Rodier and Hyman, 1998, Mednick et al., 1988)Meyer 2006). Corroborating with the postulated theory of easier penetrability of certain debris (foreign substances) including infected microphages and circulating leucocytes via the BBB into structures that are in close proximity with the ventricular system of the brain (Andronikou et

al., 2014), suggests why caudate is heavily impacted. The invasion of the caudate nuclei by these proinflammatory cytokines possibly elicits the volume reductions found in these structures via inflammation and gliosis. The precursors of basal ganglia, the lateral and medial ganglionic eminences first appear at embryonic stage 14. The basal ganglia, however, assumes its adult shape at embryonic stage 21. The caudate and the future nucleus accumbens area appear first at stage 19 while putamen and pallidum appear at stage 20 (Nunta-aree et al., 2001). This may suggest why the caudate is more susceptible. The introduction of ART at any stage during pregnancy would prevent a further crossing of these proinflammatory cytokines into the fetal brain thereby preventing the exacerbation of its sequelae and in turn averting further damage to the developing brain. Notably, the timing of maternal inflammation has been shown to impact the cytokine response in the fetal brain, as well as the pathological consequences on brain and behaviour (Meyer et al., 2006, Rees and Harding, 2004).

Effects of maternal immune health

Maternal health is crucial for optimal fetal development. Pregnant women experience physiological changes that are necessary to allow for implantation and subsequent fetal development. These changes in maternal physiology are in tandem with maternal immune suppression, though this altered immune system in pregnancy was recently reported to be timed (Aghaeepour et al., 2017). Mothers living with HIV may be more vulnerable during pregnancy compared to HIV-uninfected mothers since they face HIV-related immunocompromise in addition to pregnancy-related immune alteration (Vyas et al., 2021a, Pfeifer and Bunders, 2016, Abu-Raya et al., 2016b). Fetuses of HIV-infected mothers may therefore be at greater developmental risk with or without maternal ART. In this study, we profiled maternal $CD4^+$ cell count and viral loads during pregnancy as a measure of maternal immune health. We found a positive association of the left caudate volume with maternal $CD4^+$ cell count (table 5, figure 4). This is not unexpected as lower $CD4^+$ counts have been linked with weak immune health (Battistini Garcia and Guzman, 2021), and compromised maternal immune health may indicate higher decidual inflammatory cytokines. These in turn can passively be delivered to the fetus and may disrupt the fetal innate immunity (Dzanibe et al., 2019, Clerici et al., 2000, Rich et al., 1997), with consequent impact on the developing brain. We did not find an association between viral loads and volumes in any of the regions studied – this may be due to the time at which the viral loads are measured. Further, we stratified post-conception neonates into those whose mothers had detectable viral loads and those whose mothers had undetectable viral loads to determine whether neonates born to mothers who had undetectable viral loads had better volumetric outcomes. Within the postconception group, we found significantly lower left thalamic volume in neonates whose mothers have detectable VL relative to their counterparts whose mothers had undetectable VL (figure 2). Overall, this may point to a potential role maternal wellness may play in the developmental outcomes of HEU children.

Despite maternal ART, HEU infants demonstrate smaller basal nuclei volumes compared to HUU. However, these volumetric changes are largely driven by the timing of maternal ART initiation.

CHAPTER THREE

Neonate subcortical volumes predicting cognitive ability at 9-12 months

3.1 Introduction

In the previous chapter, we reported reduced bilateral caudate nuclei volumes in HIV exposed neonates dependent on ART exposure duration and HIV exposure reductions in the left putamen regardless of ART exposure duration. A body of evidence has shown that individuals with delayed structural developmental milestones are at risk of cognitive impairments at later ages (Melillo, 2011).

Decreased cerebral and cerebellar GM volumes have been associated with poorer cognitive scores during normal aging (Ramanoël et al., 2018).While structural MRI can identify the parts of the brain impacted by HIV/ART exposure, it provides limited insight into the consequences of altered volumes. Neuropsychological studies give information about functional abilities. Research combining both are ideal for linking neural alterations to potential functional consequences. However, little work has been done using both techniques within HEU populations. To date, two studies have examined the association between imaging outcomes and neurodevelopmental outcomes (Yadav et al., 2020, Tran et al., 2016). They report lower scores in HEU compared to HUU, with associations between DTI metric and children (at age 10 years) and infants' cognitive battery respectively (Yadav et al., 2020, Tran et al., 2016).

Several neurodevelopmental studies have reported deficits or delays in several functional domains in HEU infants and children (Ntozini et al., 2020, Wedderburn et al., 2019, Madlala et al., 2020). Grey matter is the central processing unit of the brain, and consists of neural cell bodies, dendrites, unmyelinated axons, glial cells, synapses, and capillaries (Purves et al., 2008). In HIV, reduced basal ganglia volumes are associated with neurocognitive impairments (Qi et al., 2021, Yadav et al., 2017, Wright et al., 2016) and dementia (Hestad et al., 1993). Hypertrophy of basal ganglia volume is also associated with cognitive impairment (Castelo et al., 2007). With growing evidence of association between altered grey matter volumes and neurocognitive impairment in patients living with HIV (Kato et al., 2020, Lewis-de los Angeles et al., 2017), it is important to examine this relationship in the context of HIV exposure. Examining the associations between basal ganglia volume and neurocognitive outcomes in infants will contribute to our understanding of how HIV exposure-related structural alterations may affect cognitive functions at later ages.

Basal ganglia are involved in motor control and learning. Its dysfunctions have been implicated in many motors related impairments. Beyond the known motor role of basal ganglia, a number of studies have provided evidence linking basal ganglia to other functional domains, such as cognition, linguistic ability and reasoning. It is also involved in emotion and reward systems via its connection to the limbic system

(Leisman et al., 2014). The input components of the BG circuit include caudate nuclei, putamen, and nucleus accumbens. These structures receive excitatory input from the cortex. The input components then project mainly inhibitory signals to the intrinsic BG components – the external segment of globus pallidus, subthalamic nucleus, and pars compacta of the substantial nigra of the midbrain. The major BG output nuclei are the internal segment of the globus pallidus and pars reticulata of substantial nigra of the midbrain. The output component of BG project to the thalamus for subsequent projections back to the cortex for the modulation of motor activity (Lanciego et al., 2012, DeLong and Wichmann, 2010, Wichmann and Delong, 2007). Atrophy or hypertrophy of these structures may contribute to the underlying causes of motor and cognitive dysfunctions in non-imaging studies among HIV exposed children and infants. Specifically, in adults, atrophy involving putamen and caudate nuclei have been implicated in Parkinsonism – a movement disorder. Since the focus of this chapter is on the components of basal ganglia volumes and its prospective associations with neurodevelopmental outcomes, looking at typically developing infants' will provide a benchmark of healthy development.

This chapter aimed to examine prospective associations between subcortical volumes in the neonatal period and subsequent neuropsychological scores at 9-12 months. Neuropsychological outcomes were determined using the GMDS. The GMDS have been used previously in the South Africa context (Amod et al., 2007a, Cockcroft et al., 2008, Laughton et al., 2010, Molteno et al., 2014). In South Africa and within the context of HIV exposure, Laughton and colleagues have used GMDS for two different studies to assess the neurodevelopment of HIV and HEU children at ages 10 - 12 months (Laughton et al., 2019) and 5 years (Laughton et al., 2018). Out of these two studies, only one included HEU children (Laughton et al., 2018). Scores were similar on GMDS, however HEU children scored lower relative to HUU on the Beery visual perception scale.

Based on our findings reported in the previous chapter, and the role of basal ganglia in motor and cognitive functions, we hypothesized lower volumes would be associated with poorer neuropsychological scores in HEU infants.

3.2 Results

A total of 84 newborn infants had manually segmented subcortical volumes and successfully underwent neuropsychological testing at 9-month (56 HEU; mean age at neuropsychological assessments ± SD = 9.8 ± 1.2 months GA; 28 female).

Of the 56 HEU infants, 26 were exposed to ARV throughout gestation (HEU-preconception), and 30 only for part of their gestational period (HEU-postconception). Mothers in the post-conception group had initiated ART at a mean GA of 15.4 (±5.7) weeks. Sample characteristics are summarized in Table 3.1. Overall, maternal and infant indices were similar across groups, except that mothers in the HIV

pre-conception group were roughly 3 years and about 5 years older than their post-conception and HIV-negative counterparts respectively. Not surprisingly, mothers in the HIV pre-conception group had higher CD4+ cell counts and lower VLs within 6 months of enrolment than the post-conception mothers. There were 7 mothers with positive drug tests. Five of the seven were HIV uninfected – 2 tested positive for cannabis, 3 for methamphetamines and 1 for methaqualone. Two mothers living with HIV tested positive for Methamphetamine. None of the mothers reported smoking. Half of mothers across groups reported very low levels of drinking in during pregnancy (all < 0.04 oz AA/day).

Neuropsychological outcome scores were similar for all infants across all domains assessed at an average range.

In table 3.2 and figure 3.1 we present the associations of the infants' subcortical volumes at one-month, and GMDS scores at 9- to 12-months postnatal life. Our analysis finds significant associations primarily in the HUU infants.

In typically developing infants (HUU), we found several negative associations between subcortical volumes with neuropsychological domains. Specifically, locomotor scores were negatively associated with bilateral pallidal volumes. Personal social scores were negatively associated with bilateral caudate and pallidum and left cerebellar volumes. Language scores were negatively associated with bilateral pallidal and right cerebellar volumes. Eye & Hand coordination scores were negatively associated with bilateral pallidum, left cerebellum and right caudate and putamenal volumes. Performance scores were negatively associated with left pallidal volumes and at trending level with right pallium. General quotient scores were negatively associated with bilateral caudate, putamen, pallidum, and cerebellum. None of the observed significant associations of structural volume scores with neuropsychological subscales survive FDR correction for multiple comparisons except associations between Personal Social scores with bilateral caudate and bilateral pallidum. In addition, the observed significant association of Eye & Hand coordination also survived FDR correction.

In HEU infants, within the preconception group locomotor scores were positively associated with bilateral caudate and putamenal volumes, and vermis. However, none of these associations survived FDR correction for multiple comparisons.

Table 3.1 Sample characteristics (N = 84)

	HUU (n = 28)		HEU (n = 56)					
			Pre-conception ART (n = 26)		Post-conception ART (n = 30)			
	Mean±SD	**Range**	**Mean±SD**	**Range**	**Mean±SD**	**Range**	**X^2 or t or F**	***P (for* X^2 or t or F)**
Maternal indices								
Age at delivery (years)	27.5 ± 5.4	19.6 – 42.4	32.2 ± 5.5	20.6 – 46.3	28.9 ± 4.7	20.5 – 40.9	-0.97	0.34
GA at enrolment (weeks)	20.2 ± 5.2	10.7 – 28.0	19.5 ± 6.8	7.1 – 35.1	21.4 ± 6.0	9.3 – 30.7	0.75	0.48
Highest school level completed (n, %)								
Grade 6	0 (0)	-	1 (3.8 %)	-	0 (0)	-	19.57	0.14
Grade 8	1 (3.6 %)	-	0 (0)	-	0 (0)	-		
Grade 9	0 (0)	-	2 (7.7 %)	-	1 (3.4 %)	-		
Grade 10	0 (0)	-	0 (0)	-	4 (13.3 %)	-		
Grade 11	8 (28.6 %)	-	10 (38.5 %)	-	13 (43.3 %)	-		
Grade 12	19 (67. 8%)	-	13 (50.0 %)	-	12 (40.0 %)	-		
CD4 within 6 mo of enrolment (cells/µL)[1]	N/A	N/A	581 ± 193	108 – 887	411 ± 199	172 – 814	3.38	**0.001**
VL within 6 mo of enrolment								
Undetectable (n, %)	N/A	N/A	17 (65.4 %)	-	18 (66.7 %)	-	0.02	0.89
Detectable (n, %)	N/A	N/A	9 (34.6 %)	-	9 (33.3 %)	-		

VL (copies/mL)[2] Median[a] [IQR]	N/A	N/A	30 [27 – 55]	26 – 238	259 [45– 443]	22 – 16787	7.99	**0.009**
Substance use across pregnancy								
Alcohol (n; %)	16 (57.1 %)	-	10 (38.5 %)	-	16 (53.3 %)	-		
AA/day (oz)[3]	0.04 ± 0.02	0.06 x10^{-3} – 0.090	0.03 ± 0.02	0.014 – 0.072	0.04 ± 0.02	0.01 – 0.072	0.92	0.41
Cannabis (n; %)[4]	2 (7.1 %)	-	0 (0)	-	0 (0)	-	4.09	0.13
Methamphetamine (n; %)[4]	3 (10.7 %)	-	0 (0)	-	2 (6.7 %)	-	2.81	0.24
Methaqualone (n; %)[4]	1 (3.6 %)	-	0 (0)	-	0 (0)	-	2.02	0.36
Smoking (n; %)	0 (0)	-	0 (0)	-	0 (0)	-	-	NA
Infant indices								
Sex (n Female; %)	16 (%)	-	12 (%)	-	16 (%)	-	0.67	0.71
Delivery route:								
Vaginal (n, %)	23 (82.1 %)	-	20 (76.9 %)		21 (70.0 %)	-	1.19	0.55
Caesarean (n, %)	5 (17.9 %)	-	6 (23.1 %)		9 (30.0 %)	-		
Birth indices:								
GA (weeks)	39.5 ± 1.2	36.7 – 41.6	39.5 ± 1.5	36.6 – 41.6	39.8 ± 1.3	36.8 – 42.3	0.24	0.79
Weight (g)	3249 ± 400	2575 – 4180	3147 ± 312	2575 – 3750	3244 ± 407	2500 – 4230	0.62	0.54
Crown-to-heel length (cm)	49.8 ± 2.1	45.0 – 53.0	49.8 ± 2.0	46.0 – 54.0	50.1 ± 2.8	43.0 – 56.0	0.10	0.90
Head circumference (cm)	34.2 ± 1.3	32 – 37	33.9 ± 1.3	31 – 36	33.6 ± 1.6	31 – 39	1.31	0.27
ART exposure length (weeks)	N/A	N/A	39.5 ± 1.5	36.6 – 41.6	24.9 ± 5.5	14.0 – 35.6	13.07	**<0.0001**
MRI indices:								

GA Equivalent (weeks)	41.5 ± 0.9	40.0 – 43.8	41.3 ± 0.8	39.0 – 42.7	41.5 ± 1.1	39.3 – 43.1	0.59	0.56
Weight (g)[5]	3539 ± 395	2700 – 4250	3391 ± 405	2700 – 4200	3468 ± 394	2800 – 4450	0.90	0.41
Head circumference (cm)[5]	35.1 ± 1.2	33 – 37	35.5 ± 1.3	33 – 37	34.7 ± 1.3	31 – 36.5	2.16	0.12
Total ICV (x 10^5 mm^3)	4.80 ± 0.50	3.84 – 5.86	5.00 ± 0.60	3.99 – 6.40	5.06 ± 0.82	42.2 – 7.65	1.12	0.33
Age at Neuropsychological examination	9.64±1.09	8.60 – 13.10	9.79±1.25	8.96 – 13.50	10.14±1.41	8.70 – 13.0	1.20	0.31
Neuropsychological mean scores								
Locomotor	104.7±14.1	71 – 126	106.2±11.7	84 – 122	102.1±14.0	76 – 126	0.64	0.53
Personal Social	112.1±16.2	87 – 150	106.2±11.8	76 – 125	107.5±12.8	75 – 130	1.38	0.26
Language	107.0±12.4	85 – 138	107.0±11.9	77 – 131	107.6±12.6	89 – 138	0.02	0.98
Eye & Hand Coordination	107.8±16.2	74 – 150	106.7±15.3	78 – 133	102.9±13.5	78 – 133	0.86	0.42
Performance	91.6±14.4	67 – 133	92.1±12.2	72 – 120	91.7±15.1	50 – 110	0.01	1.00
General Quotient	108.0±17.9	82 – 177	104.9±8.9	86 – 125	103.6±10.1	82 – 124	0.90	0.41

Table 3.2 Associations grey matter volumes with GMDS neuropsychological scores

	Locomotion						**Personal Social**					
	HUU		**HEU-preconception**		**HEU-postconception**		**HUU**		**HEU-preconception**		**HEU-postconception**	
	β (std err.)	**p**	**β (std err.)**	**p**	**β (std err.)**	**p**	**β (std err.)**	**p**	**β (std err.)**	**p**	**β (std err.)**	**p**
L caudate	-0.012 (0.010)	0.23	**0.020 (0.009)**	**0.02**	0.006 (0.009	0.65	**-0.022 (0.009)**	**0.02**	2.463 (8.583)	0.97	0.003 (0.013)	0.76
L putamen	-0.008 (0.009)	0.37	**0.022 (0.011)**	**0.05**	0.004 (0.012)	0.69	-0.011 (0.008)	0.18	-0.012 (0.010)	0.21	2.607 (1.127)	0.99
L pallidum	**-0.028 (0.013)**	**0.04**	0.013 (0.017)	0.46	0.032 (0.023)	0.17	**-0.037 (0.012)**	**0.004**	-0.003 (0.016)	0.82	-0.033 (0.021)	0.11
L thalamus	0.004 (0.005)	0.38	0.002 (0.005)	0.66	0.004 (0.006)	0.54	-7.0.29 (4.927)	0.88	-3.129 (4.987)	0.95	-9.796 (6.383)	0.87
L cerebellum	-0.003 (0.001)	0.07	1.438 (1.460)	0.32	1.394 (2.186)	0.52	**-0.003 (0.001)**	**0.02**	-5.618 (1.352)	0.67	1.504 (2.024)	0.94
R caudate	-0.016 (0.010)	0.10	**0.019 (0.009)**	**0.04**	0.006 (0.012)	0.62	**-0.027 (0.009)**	**0.004**	-0.002 (0.008)	0.78	0.013 (0.011)	0.24
R putamen	-1.112 (9.199)	0.23	**0.021 (0.010)**	**0.04**	0.016 (0.010)	0.10	-0.008 (0.008)	0.33	-0.010 (0.010)	0.32	0.001 (0.009)	0.85
R pallidum	**-0.028 (0.014)**	**0.05**	0.027 (0.014)	0.06	0.042 (0.025)	0.10	**-0.039 (0.013)**	**0.005**	-0.005 (0.013)	0.67	-0.012 (0.024)	0.61
R thalamus	0.006 (0.004)	0.21	0.001 (0.005)	0.74	0.004 (0.007)	0.55	-0.000 (0.004)	0.88	-0.004 (0.005)	0.45	0.001 (0.006)	0.78
R cerebellum	-0.003 (0.002)	0.08	0.0012 (0.002)	0.46	0.0006 (0.0020)	0.80	-0.002 (0.015)	0.10	-0.0004(0.001)	0.30	0.0005 (0.0019)	0.80
Vermis	0.004 (0.006)	0.46	**0.019 (0.008)**	**0.02**	0.008 (0.009)	0.36	0.003 (0.006)	0.55	0.005 (0.007)	0.44	0.007 (0.008)	0.40

	Language						**Eye & Hand coordination**					
	HUU		**HEU-preconception**		**HEU-postconception**		**HUU**		**HEU-preconception**		**HEU-postconception**	
	β (std err.)	**p**	**β (std err.)**	**p**	**β (std err.)**	**p**	**β (std err.)**	**p**	**β (std err.)**	**p**	**β (std err.)**	p
L caudate	-0.012 (0.009)	0.20	-0.007 (0.008)	0.41	-9.727 (1.343)	0.94	-0.022 (0.011)	0.06	2.402 (1.053)	0.99	-0.018 (0.016)	0.24
L putamen	-0.005 (0.008)	0.54	-0.013 (0.010)	0.18	0.014 (0.011)	0.18	-0.012 (0.010)	0.26	-0.007 (0.012)	0.54	-0.002 (0.013)	0.84
L pallidum	**-0.024 (0.012)**	**0.05**	-0.020 (0.016)	0.21	-0.012 (0.022)	0.57	**-0.040 (0.015)**	**0.01**	-0.021 (0.020)	0.29	0.013 (0.026)	0.62
L thalamus	0.006 (0.004)	0.21	-7.546 (4.892)	0.87	0.004 (0.006)	0.49	-0.002 (0.005)	0.66	0.004 (0.006)	0.50	-0.007 (0.007)	0.34
L cerebellum	-7.455 (1.634)	0.65	-6.358 (1.387)	0.64	-9.356 (2.077)	0.65	**-0.004 (0.001)**	**0.02**	2.944 (1.648)	0.85	-0.002 (0.002)	0.34
R caudate	**-0.020 (0.009)**	**0.03**	-0.007 (0.008)	0.38	0.012 (0.011)	0.27	**-0.029 (0.011)**	**0.01**	-3.165 (1.061)	0.76	-2.598 (1.460)	0.85

R putamen	-0.004 (0.008)	0.59	-0.007 (0.010)	0.46	0.008 (0.009)	0.41	**-0.012 (0.010)**	0.25	-0.007 (0.012)	0.57	-0.011 (0.012)	0.35
R pallidum	**-0.030 (0.013)**	**0.03**	-0.012 (0.013)	0.37	0.017 (0.024)	0.47	**-0.035 (0.017)**	**0.03**	-0.014 (0.017)	0.41	-0.010 (0.030)	0.72
R thalamus	6.348 (4.402)	0.15	-0.002 (0.005)	0.64	6.451 (6.581)	0.33	-0.001 (0.005)	0.72	0.001 (0.006)	0.77	-2.393 (8.270)	0.97
R cerebellum	-0.0004 (0.001)	0.79	-0.001 (0.001)	0.85	-0.002 (0.002)	0.37	-3.508 (1.881)	0.06	-1.535 (1.822)	0.99	-3.323 (2.329)	0.15
Vermis	0.006 (0.006)	0.31	7.361 (7.840)	0.92	-6.804 (8.679)	0.93	0.011 (0.007)	0.11	0.009 (0.009)	0.30	-0.013 (0.010)	0.20
	Performance						**General quotient**					
	HUU		**HEU-preconception**		**HEU-postconception**		**HUU**		**HEU-preconception**		**HEU-postconception**	
	β (std err.)	**p**	**β (std err.)**	**p**	**β (std err.)**	**p**	**β (std err.)**	**p**	**β (std err.)**	**p**	**β (std err.)**	**p**
L caudate	-0.014 (0.011)	0.22	0.007 (0.010)	0.43	0.010 (0.015)	0.51	**-0.025 (0.009)**	**0.01**	0.005 (0.008)	0.48	-8.752 (1.307)	0.94
L putamen	-1.277 (1.011)	0.21	-0.009 (0.011)	0.41	-1.295 (1.302)	0.32	**-0.024 (0.008)**	**0.005**	-0.004 (0.010)	0.66	3.114 (1.093)	0.97
L pallidum	**-0.036 (0.014)**	**0.01**	-0.018 (0.019)	0.34	-0.021 (0.025)	0.39	**-0.050 (0.012)**	**<0.0001**	-0.009 (0.015)	0.53	-0.002 (0.020)	0.92
L thalamus	4.060 (5.649)	0.99	0.001 (0.005)	0.85	-0.007 (0.007)	0.34	-0.004 (0.004)	0.33	8.303 (4.960)	0.86	-0.001 (0.006)	0.87
L cerebellum	-1.751 (1.880)	0.35	0.001 (0.001)	0.41	-0.010 (2.390)	0.67	**-0.003 (0.001)**	**0.01**	2.154 (1.349)	0.87	-6.313 (2.020)	0.75
R caudate	-0.018 (0.011)	0.10	0.002 (0.010)	0.83	0.017 (0.013)	0.22	**-0.035 (0.008)**	**0.0001**	0.003 (0.008)	0.70	0.009 (0.011)	0.38
R putamen	-0.001 (0.010)	0.89	-0.005 (0.011)	0.62	-0.012 (0.011)	0.26	**-0.017 (0.008)**	**0.04**	-0.001 (0.010)	0.89	9.352 (9.811)	0.92
R pallidum	-0.027 (0.016)	0.09	-0.003 (0.016)	0.84	0.005 (0.028)	0.85	**-0.045 (0.013)**	**0.001**	-5.131 (1.353)	0.96	0.006 (0.023)	0.79
R thalamus	-6.027 (5.181)	0.90	6.922 (6.366)	0.91	-0.008 (0.007)	0.28	-0.003 (0.004)	0.38	-0.001 (0.005)	0.82	0.002 (0.006)	0.75
R cerebellum	-0.001 (0.001)	0.30	0.001 (0.001)	0.47	-5.912 (2.248)	0.79	**0.003 (0.001)**	**0.02**	-1.323 (1.488)	0.92	-1.060 (1.902)	0.57
Vermis	0.007 (0.006)	0.28	0.008 (0.008)	0.35	-0.007 (0.009)	0.44	0.006 (0.006)	0.28	0.008 (0.007)	0.29	-1.371 (8.663)	0.98

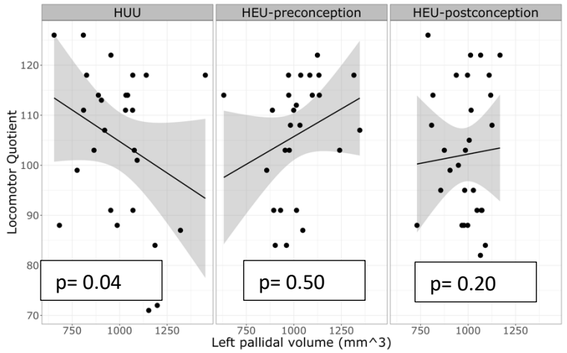
HUU
HEU-preconception
HEU-postconception
Locomotor Quotient
p= 0.04
p= 0.50
p= 0.20
Left pallidal volume (mm^3)

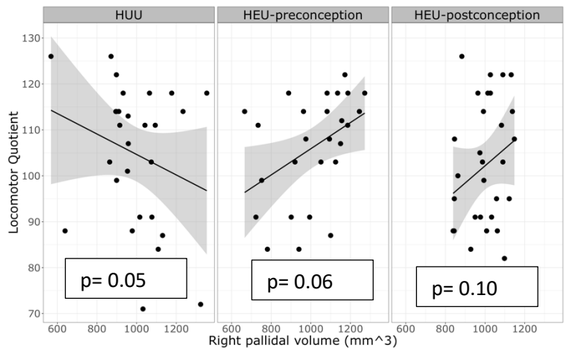
HUU
HEU-preconception
HEU-postconception
Locomotor Quotient
p= 0.05
p= 0.06
p= 0.10
Right pallidal volume (mm^3)

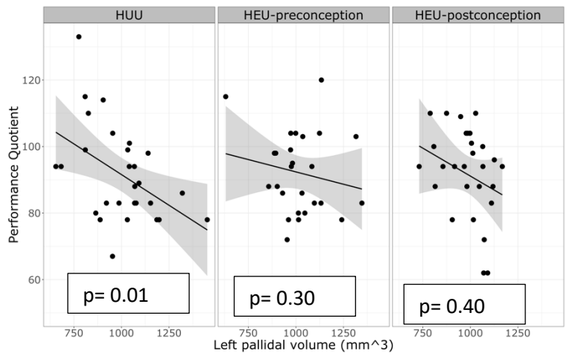
HUU
HEU-preconception
HEU-postconception
Performance Quotient
p= 0.01
p= 0.30
p= 0.40
Left pallidal volume (mm^3)

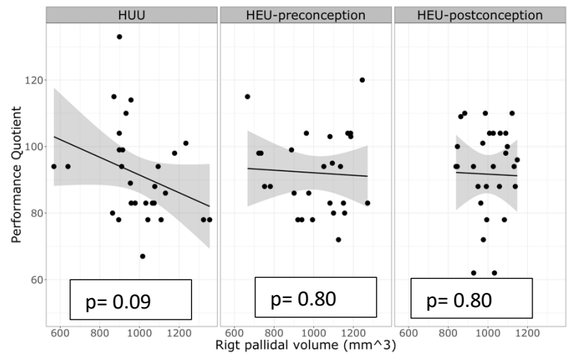
HUU
HEU-preconception
HEU-postconception
Performance Quotient
p= 0.09
p= 0.80
p= 0.80
Rigt pallidal volume (mm^3)

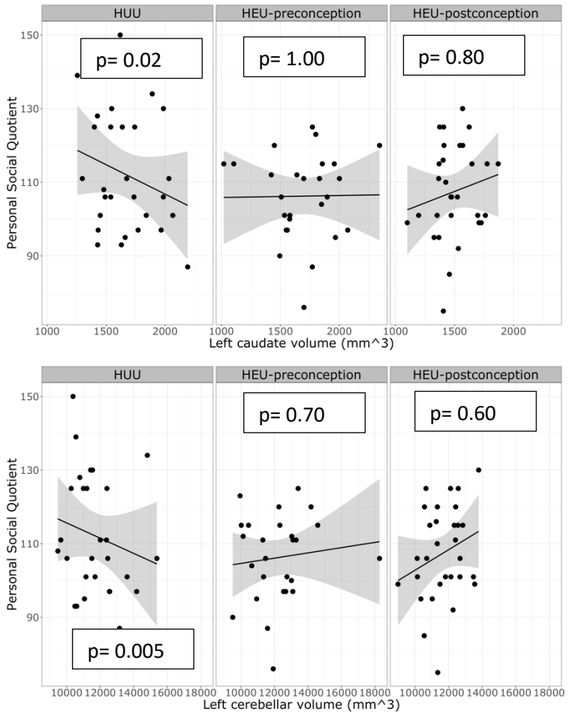
HUU
HEU-preconception
HEU-postconception
Personal Social Quotient
p= 0.02
p= 1.00
p= 0.80
p= 0.005
p= 0.70
p= 0.60
Left cerebellar volume (mm^3)

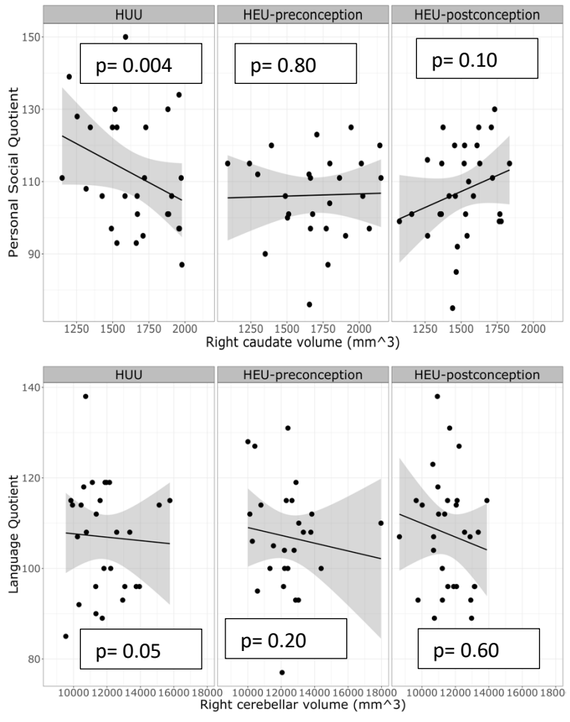
HUU
HEU-preconception
HEU-postconception
Personal Social Quotient
p= 0.004
p= 0.80
p= 0.10
Language Quotient
p= 0.05
p= 0.20
p= 0.60
Right caudate volume (mm^3)
Right cerebellar volume (mm^3)

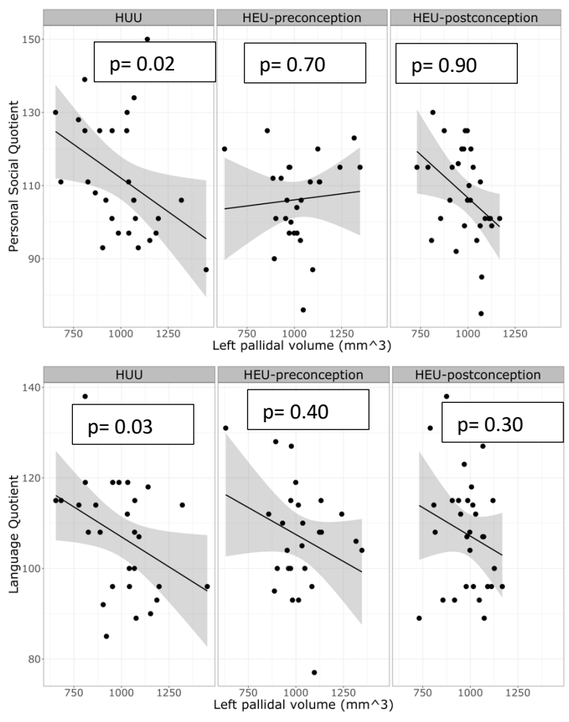
HUU
HEU-preconception
HEU-postconception
Personal Social Quotient
p= 0.02
p= 0.70
p= 0.90
Language Quotient
p= 0.03
p= 0.40
p= 0.30
Left pallidal volume (mm^3)

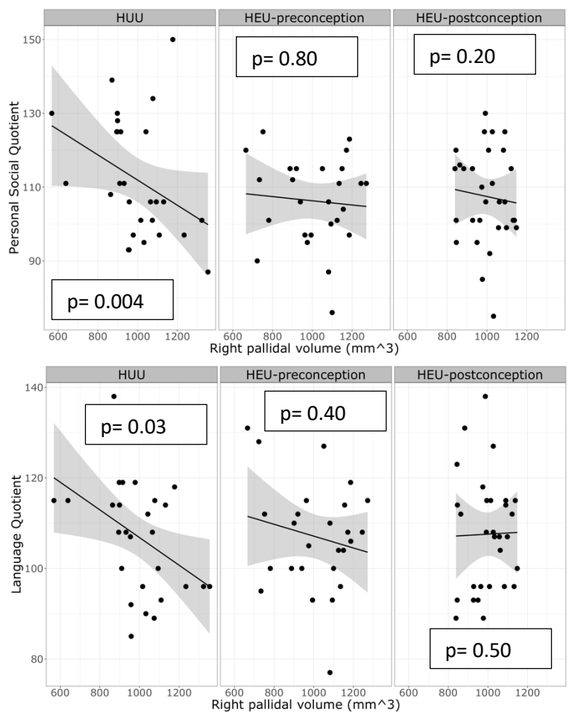
HUU
HEU-preconception
HEU-postconception
Personal Social Quotient
p= 0.004
p= 0.80
p= 0.20
Language Quotient
p= 0.03
p= 0.40
p= 0.50
Right pallidal volume (mm^3)

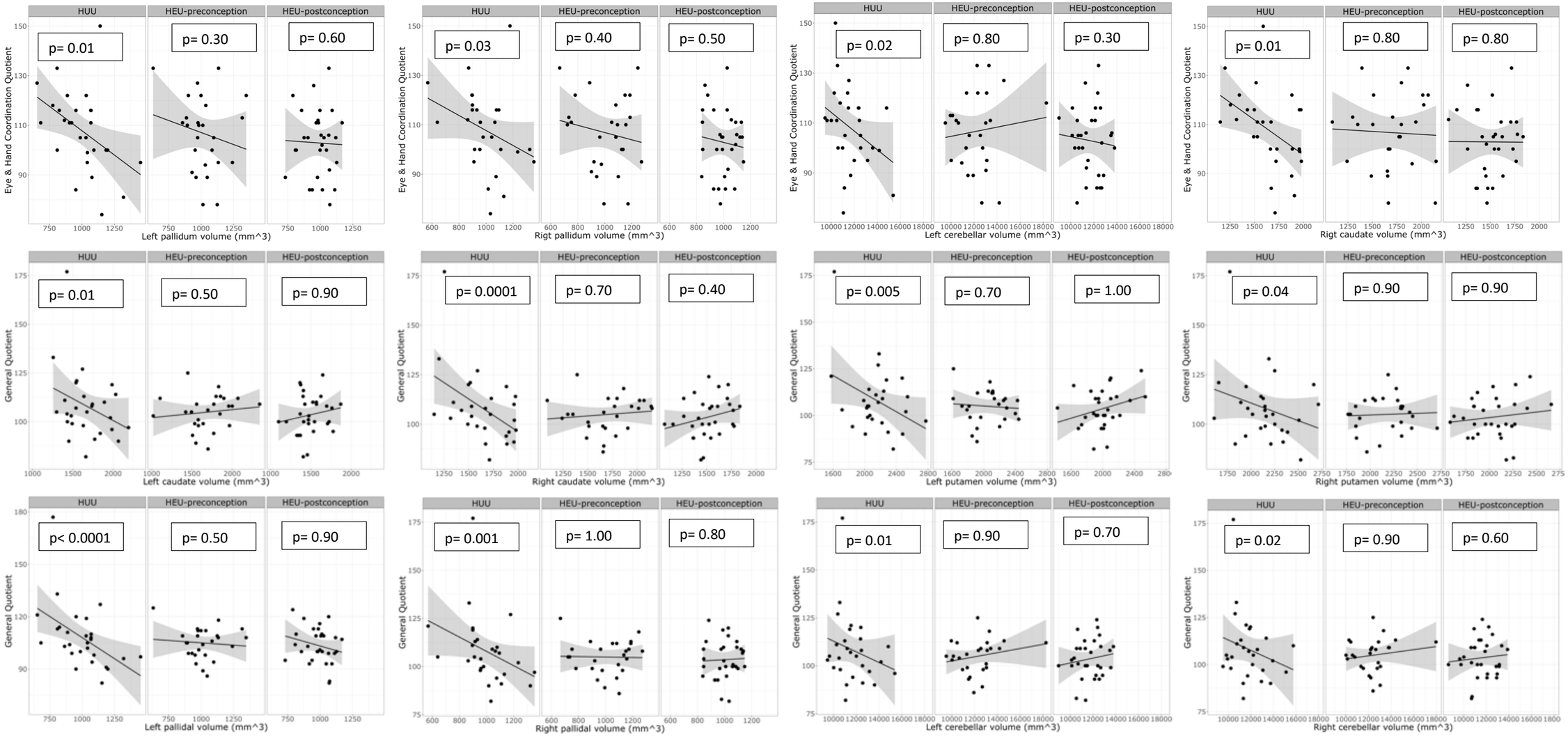

figure 3.1 Associations of grey matter volumes with GMDS neuropsychological scores.

3.3 Discussion

In this chapter, we examined the associations between grey matter volumes in the neonatal period with neuropsychological outcomes at late infancy. We hypothesized that smaller subcortical grey matter volumes would be associated with poorer neuropsychological scores. We observed positive associations between locomotor scores and caudate, putamen and vermis volumes in HEU infants in the pre-conception group. In line with our hypothesis, measures of locomotion are positively related to components of the basal ganglia and cerebellum. And, HEU infants had reduced mean left putamen volumes compared to their uninfected peers, and these reductions are related to lower locomotion abilities. However, we expected to observe these associations within the post-conception group as well.

Also contrary to our hypothesis, typically developing infants (HUU) demonstrated numerous negative associations across volumes and neuropsychological domains. Pallidal volume was negatively associated across all GMDS domains of, pointing at the involvement of pallidum in a wide range of neurodevelopmental functions in early infancy.

Associations in typically developing infants

Bilateral pallidal volumes were related to all GMDS subscales. Most associations were significant and would survive multiple comparison corrections. In addition to research linking the pallidum with motor function (Graves et al., 2017; Lanciego et al., 2012), there is growing evidence showing its involvement in cognition, behavior, and emotion (Aristieta and Gittis, 2021, Karube et al., 2019, Gillies et al., 2017). Our findings support the involvement of the pallidum in motor functions as well as other functional domains.

Typically developing infants' caudate nuclei was also related to personal social, eye & hand coordination and language scores. The associations with personal social were bilateral while the associations with language and eye & hand coordination was right hemispheric domiciled. These results suggest that the developing infants' prospective associations of neonatal caudate with personal social and eye & hand coordination domains at infancy is right hemispheric dominant. However, the lateralization of these functional domains in relation to caudate volumes may be transient as the brain continue to undergo remarkable changes until about 2 years postnatal life (Alimenti et al., 2006). Further, these results may be counterintuitive since 90% of the population are right-handed, and that brain sides control the opposite sides of the body (Guy-Evanas, 2021).

Associations in HEU infants

Bilaterally, we found a positive association between caudate, putaminal and vermis volumes and locomotor scores only in infants who were exposed to ART throughout pregnancy. In typically developing infants, the only structure associated with locomotor scores is the pallidum. Our findings suggest HEU infants may recruit different subcortical structures for locomotor function. It is interesting that HUU infants rely on the pallidum only, while the pre-conception HEU infants recruit caudate, putamen as well as the vermis.

Given the reduced putamen volumes in pre-conception infants, the finding that volumes predict locomotor scores is expected. However, the lack of volume reductions in the caudate and vermis in pre-conception neonates is surprising and suggests these structures may have altered development between the time of scan and neuropsychological testing.

The volumetric associations with GMDS subscales in typically developing infants were missing in their HIV/ART exposed counterparts. This result is particularly unexpected considering that HEU infants performed similarly across all neuropsychological domains. These findings suggest HEU neonates adequately recruit different structures to achieve the developmental milestones tested. It also suggests the volume reductions observed in the previous chapter in HEU pre and post conception neonates do not lead to delayed development in the domains tested at 9- to 12-months.

In conclusion, HUU infants demonstrate associations between structural volumes and neuropsychological outcomes. Whereas, within HEU neonates we do not observe similar associations. The lack of association may be due to the effect of HIV, ART or combination of both.

CHAPTER FOUR

Maternal HIV/ART exposure and white matter integrity

4.1 Introduction

The period between the second trimester of pregnancy and the first two years of postnatal life is critical for brain development. Fundamental processes of neurodevelopment including neuronal migration, cellular organization, cortical layering, and myelination are remarkable from second and third trimesters. These processes laid the structural foundation for efficient neural connectivity required for optimal cognitive functions (Stile & Jernigan 2010). Since maternal HIV likely contributes to developmental delays in HEU infants and children, studying the properties of white matter in early infancy gives us a window into the influence of in utero HIV/ART exposure on myelin and axonal maturation.

Common DTI metrics include FA and MD. FA is an indicator of WM integrity (relating to axon myelination, the diameter of axons, and/or the density). MD can be interpreted as an indicator of WM maturation and/or injury (Basser and Pierpaoli, 1996). In addition, AD and RD are frequently studied alongside FA and MD to aid with interpretation. AD is related to WM maturation and axonal damage and RD is related to myelination and dysmyelination or demyelination (Feldman et al., 2010).

Deviations from typical development due to HIV and ART exposure have been reported using DTI (Madzime et al., 2021, Yadav et al., 2020, Jankiewicz et al., 2017, Tran et al., 2016, Jahanshad et al., 2015). With only one of these studies using tractography (Madzime et al., 2021). Three of these studies reported higher FA (Madzime et al., 2021, Jankiewicz et al., 2017, Tran et al., 2016) , and one reported lower FA (Yadav et al., 2020). And the other reported no group diffreneces in HEU relative to their unexposed counterparts (Jahanshad et al., 2015). However, none of these studies included the effects of ART exposure in addition to HIV. Further, the only study that examined WM abnormalities using DTI in infancy has small sample size compared to our study's (Tran, 2016). They reported higher FA in the middle cerebellar peduncle.

In our cohort, we previously reported volume reductions in putamen and caudate nuclei in HEU compared to HUU children. Based on these findings, we hypothesized decreased FA and increased MD in the tracts connecting caudate and putamen to other ROIs in HEU neonates compared to HUU. Since the volume reductions we found in the first analysis is attributable to shorter *in utero* exposure to ART, we hypothesized that increased FA would be attributable to shorter duration of *in utero* ART exposure.

4.2 Results

DTI pre- and post-processing was successful in 86 of the 120 infants whose structural images had been manually traced. The remaining 34 subjects did not pass the quality control of both structural and DTI postprocessing. Of the 34 subjects that did not pass the quality control, 16 did not have a minimum 15 diffusion directions while in 18 subjects, mask of their traced volumes does not align to their respective diffusion space. A total of 30 WM tracts between seeds and targets were common to all the 86 subjects.

A total of 86 infants (57 HEU; mean age at scan ± SD = 41.5 ± 1.0 wks GA; 42 female) were included in this analysis. Of the 57 HEU infants, 29 were exposed to ARV throughout gestation (HEU-pre), and 28 only for part of their gestational period (HEU-post). Mothers in the post-conception group had initiated ART at a mean GA of 15.4 (±5.7) weeks. Sample characteristics are summarized in Table 4.1. Overall, maternal and infant indices were similar across groups, except that mothers in the HIV pre-conception group were roughly 3 years older than their post-conception and HIV-negative counterparts; and pre-conception infants had slightly larger head circumferences at the time of their scan than their post-conception and HUU counterparts. As expected, mothers in the HIV pre-conception group had higher CD4+ cell counts and lower VLs within 6 months of enrolment than the post-conception mothers. There were only 6 mothers with positive drug tests, and all were HIV uninfected – 3 tested positive for cannabis, 2 for methamphetamines and 1 for methaqualone. None of the mothers reported smoking. More than 40% of mothers across groups engaged in very low levels of drinking in pregnancy (all < 0.08 oz AA/day).

Figure 4.1 depicts WM tracts between the manually traced seeds and targets. APPENDIX (Supplementary analysis 2 Figure 1) shows WM tracts by group, together with results from pairwise group comparisons using independent one-tailed student t-tests. Associations of potential confounders with FA, MD, AD and RD in WM tracts are summarized in the APPENDIX, Supplementary analysis 2 Tables 2.1a, 2.1b, 2.1c and 2.1d.

In Tables 4.2 and 4.3 we present regression coefficients for the effect of group on DTI parameters in the WM tracts connecting our manually traced structures, controlling for potential confounding by covariates weakly related to the volumetric outcome being examined. As a group, HEU infants demonstrate significantly higher FA in the commissural connection between right putamen and left thalamus, although with no significant corresponding AD and RD was observed. The observed significant difference in FA survived FDR correction for multiple comparison at trending level (p_{FDR} = 0.06). Within HEU, the observed higher FA was significant for both subgroups when compared separately to HUU with none of these surviving FDR correction for multiple comparisons.

Similarly, as a group, compared to HUU, HEU infants demonstrate higher MD in the ipsilateral tract between caudate and thalamus in the right hemisphere with corresponding higher AD and RD, and higher MD in diagonal bundles of the left putamen and right pallidum with corresponding higher RDs only. When comparing each HEU subgroup to HUU, the higher MD in the right caudothalamic tract remain significant for both HEU subgroups with corresponding significant RDs and trending ADs. None of the observed significant values (both between and within groups) survive FDR correction for multiple comparisons for all the DTI metrics – MD, AD and RD.

In tables 2.2a, 2.2b and 2.2c (APPENDIX Supplementary analysis 2) we present associations of WM tracts among HEU infants with maternal clinical and treatment variables (2.2a = CD4 counts, 2.2b = VL, 2.2c = infant ART exposure duration). In none of the tracts where we found group differences in both FA and MD were associated with maternal clinical and treatment variables. However, we found tracts correlating with maternal clinical and treatment variables in other tracts. Left-putamen to right caudate tract's FA, AD and RD were all correlated with CD4 counts (figure 4.2). Left caudoputamen's FA and RD, left caudopallidum's MD and RD, and FA of the tracts connecting left putamopallidum, left putamen/right caudate, and left putamen/right thalamus were all correlated with maternal VL. MD, AD and RD of tract connecting right and left thalamus, right thalamocerebellar FA and right thalamovermis AD were all associated with ART exposure duration. Details in APPENDIX (Supplementary analysis 2 table 2.2c).

In the APPENDIX supplementary analysis 2, we stratified HEU combined into detectable and undetectable VL arms Table 2.3a, and in Table 2.3b, we stratified each of the HEU subgroups (pre and post conceptions) separately into detectable and undetectable VL arms. Within HEU combined, in none of the tracts did infant demonstrate group differences in FA. In contrast, infants on the detectable VL arm demonstrate higher MDs with corresponding increased ADs and RDs in the right-putamopallidum and interthalamic tracts. Within HEU pre-conception subgroup, in one tract connecting left-putamen to right-caudate, infants on the detectable VL strata demonstrate higer FA, lower MD and corresponding lower RD. More also, within preconception subgroup, infants in the detectable VL strata demonstrate higher FAs in four tracts (left-caudate-right thalamus, left putamen-right thalamus, left-pallidum-right thalamus and right-caudate-left thalamus) within the extrinsic basal ganglia connections, albeit with no corresponding significant ADs and RDs. In contrast, within the post-conception subgroup, infants in the detectable VL strata demonstrate higher MD with corresponding higher AD and higher RD in the fiber connection between right-putamen and left thalamus.

Table 4.1 Sample characteristics (N = 86)

	HUU (n = 29)		HEU (n = 57)					
			Pre-conception ART (n = 29)		Post-conception ART (n = 28)			
	Mean±SD	**Range**	**Mean±SD**	**Range**	**Mean±SD**	**Range**	**X^2 or t or F**	***P (for* X^2 or t or F)**
Maternal indices								
Age at delivery (years)	28.8±6.0	19.7 – 44.1	31.5±5.8	20.6 – 46.3	28.3±5.4	19.6 – 40.9	2.58	0.08
GA at enrolment (weeks)	20.0±6.2	8.1 – 28.0	20.9±6.4	7.1 – 35.1	21.6±6.4	9.3 – 30.7	0.44	0.64
Highest school level completed (n, %)								
Grade 6	0	-	1 (3.4 %)	-	0	-	9.66	0.47
Grade 8	1 (3.4 %)	-	1 (3.4 %)	-	0	-		
Grade 9	0	-	1 (3.4 %)	-	1 (3.6 %)	-		
Grade 10	0	-	3 (10.2 %)	-	3 (10.8 %)	-		
Grade 11	9 (31.1 %)	-	11 (38.0 %)	-	12 (42.8 %)	-		
Grade 12	19 (65.5 %)	-	12 (41.6 %)	-	12 (42.8 %)	-		
CD4 within 6 mo of enrolment (cells/µL)[1]	N/A	N/A	542.9±165.0	108 – 832	425.5±209.9	52 – 913	2.32	**0.02**
VL within 6 mo of enrolment								
Undetectable (n, %)	N/A	N/A	22 (75.9 %)	-	18 (64.3 %)	-	0.44	0.50
Detectable (n, %)	N/A	N/A	7 (24.1 %)	-	10 (35.7 %)	-		

VL (copies/mL)[2] Median [IQR]	N/A	N/A	34 [26 – 59]	26 – 238	259 [48 – 398]	22 – 16787	-0.92	**0.008**
Substance use across pregnancy								
Alcohol (n; %)	13 (44.8 %)	-	12 (41.4 %)	-	14 (50.0 %)	-	0.43	0.80
AA/day (oz)[3]	0.03±0.02	0.001 – 0.076	0.03±0.01	0.016 – 0.052	0.04±0.02	0.02 – 0.072	0.87	0.42
Cannabis (n; %)[4]	3 (10.3 %)	-	0 (0)	-	0 (0)	-	6.11	0.05
Methamphetamine (n; %)[4]	2 (6.8 %)	-	0 (0)	-	0 (0)	-	4.02	0.13
Methaqualone (n; %)[4]	1 (3.4 %)	-	0 (0)	-	0 (0)	-	2.0	0.37
Smoking (n; %)	0 (0)	-	0 (0)	-	0 (0)	-	N/A	N/A
Infant indices								
Sex (n Female; %)	15 (51.7 %)		15 (51.7 %)		12 (42.8 %)	-	0.59	0.74
Delivery route:								
Vaginal (n, %)	25 (86.2 %)	-	22 (75.9 %)		19 (67.9 %)	-	2.70	0.26
Caesarean (n, %)	4 (13.8 %)	-	7 (24.1 %)		9 (32.1 %)	-		
Birth indices:								
GA (weeks)	39.7±1.2	37.0 – 42.1	39.7±1.4	36.6 – 42.1	39.7±1.5	36.8 – 42.3	0.02	0.98
Weight (g)	3256.4±415.9	2575 – 4180	3286.9±291.2	2775 – 4055	3265.9±417.8	2500 – 4230	0.05	0.95
Crown-to-heel length (cm)	49.7±2.4	45 – 54	49.9±2.1	44 – 54	50.5±2.5	47 – 56	0.95	0.39
Head circumference (cm)	34.0±1.3	32 – 37	34.1±1.3	31 – 36	33.5±1.5	31 – 39	1.58	0.21
ART exposure length (weeks)	N/A	N/A	39.7±1.4	36.6 – 42.1	24.9±6.0	14.0 – 35.6	12.9	**<0.0001**
MRI indices:								

GA Equivalent (weeks)	41.6±1.0	40.0 – 43.8	41.4±1.0	39.1 – 44.4	41.6±1.1	39.3 – 43.4	0.40	0.67
Weight (g)[5]	3495.4±419.1	2500 – 4025	3525.2±408.3	2775 – 4200	3558.9±384.2	2850 – 4450	0.19	0.83
Head circumference (cm)[5]	35.0±1.3	32.0 – 37.0	35.8±1.1	33.5 – 37.0	35.0±1.3	31.0 – 36.5	4.50	**0.01**
Total ICV (x 10^5 mm^3)	4.98±0.70	4.16 – 7.55	5.07±0.45	4.10 – 6.05	5.28±1.15	3.44 – 7.68	0.93	0.39

[1]CD4 count missing for 1 mother who started ART pre-conception; [2]Based only on mothers with detectable VL levels (7 mothers who started ART pre-conception; 10 mothers who started ART post-conception); [3]Based only on mothers who consumed alcohol; 1 oz absolute alcohol (AA) is equivalent to 2 standard drinks; [4]Numbers based on urine tests; [5]Data missing for 1 infant in the pre-conception group and 2 HUU infants. Bold indicates significance at $p \leq 0.05$.

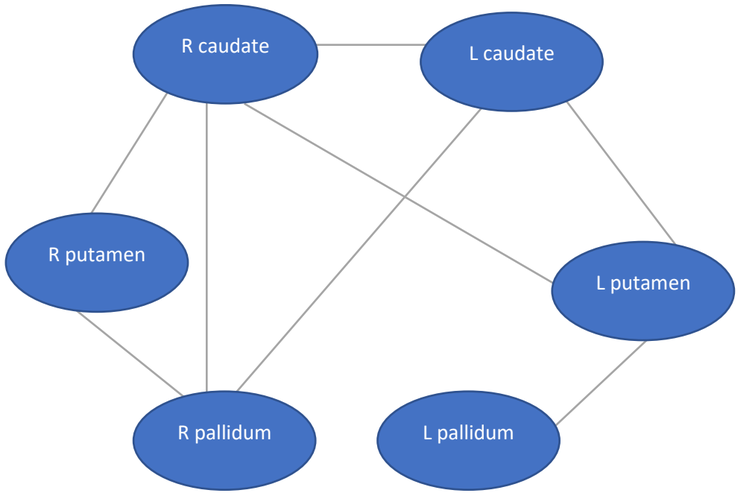

Intrinsic basal ganglia network connections

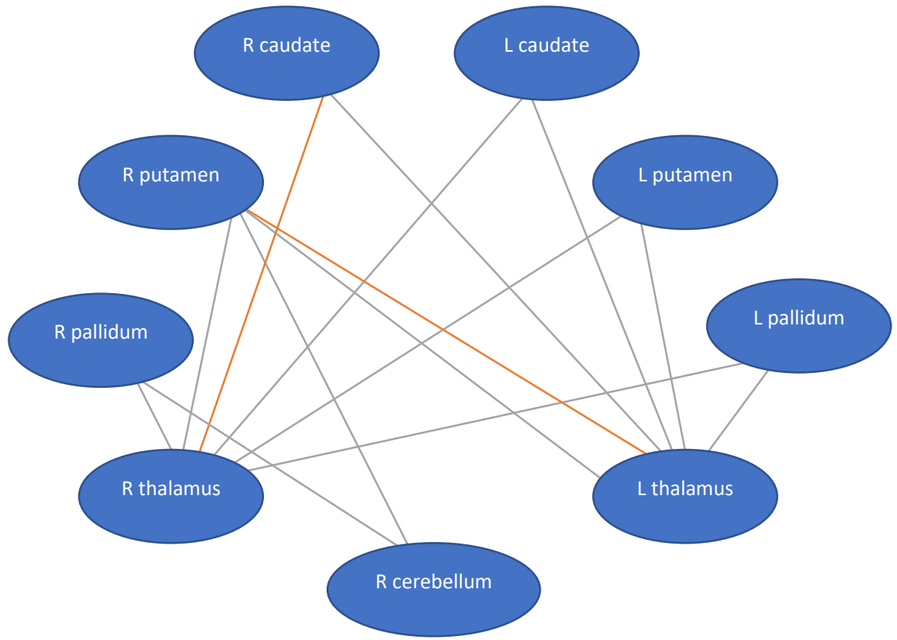

Extrinsic basal ganglia network connections

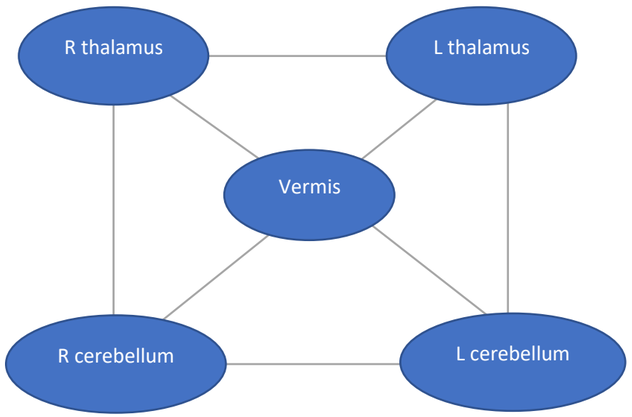

Thalamocerebellar network connections

Figure 4.1. Schematic showing WM tracts connecting manually traced gray matter seeds and targets. WM tracts have been grouped into three networks: (i) intrinsic basal ganglia network comprising tracts that connect basal ganglia structures, (ii) extrinsic basal ganglia network connecting basal ganglia seeds to cerebellar and thalamic targets, and (iii) a thalamocerebellar network connecting thalamic and cerebellar structures. Red lines show WM tracts where infants in the HEU group have higher FA (R put-L thal) or higher MD (R caud-R thal) than their HUU peers. Notably, these increases are evident in both infants whose mothers started ART pre- and post-conception. Higher MD is largely attributable to higher radial diffusivity. Left (L), right (R), caudate (caud), putamen (put), thalamus (thal), cerebellar hemisphere (cereb).

Table 4.2 Comparison of DTI parameters (FA, MD, AD and RD) in WM tracts connecting manually traced seeds/targets between infants who had (HEU) and had not (HUU) been exposed to HIV prenatally. Values are unstandardized regression coefficients (**β**) and standard errors (SE).

	FA		**MD**		**AD**		**RD**	
WM tract	**HEU vs HUU**		**HEU vs HUU**		**HEU vs HUU**		**HEU vs HUU**	
	β (SE)	***p***	**β (SE)**	***p***	**β (SE)**	***p***	**β (SE)**	***p***
Intrinsic basal ganglia connections								
L caudoputamen[2, a, b, *, †, §]	0.0005 (0.003)	0.80	0.013 (0.01)	0.20	0.009 (0.01)	0.50	0.010 (0.01)	0.20
L caudopallidum[2, †]	0.003 (0.003)	0.40	0.005 (0.01)	0.70	0.010 (0.02)	0.50	-0.0004 (0.01)	1.00
L putamopallidum[2, b, †]	0.005 (0.003)	0.10	0.013 (0.01)	0.30	0.015 (0.02)	0.40	0.015 (0.01)	0.10
R caudoputamen[2, e, †, ¶]	-0.001 (0.003)	0.60	0.011 (0.01)	0.30	0.014 (0.01)	0.30	0.013 (0.01)	0.20
R caudopallidum[2, #, ¶]	0.001 (0.003)	0.70	-0.001 (0.01)	0.90	-0.003 (0.01)	0.80	0.002 (0.01)	0.80
R putamopallidum[2]	0.005 (0.004)	0.20	-0.013 (0.01)	0.30	-0.014 (0.02)	0.40	-0.010 (0.01)	0.30
Inter-caudate[2, f]	-0.00005 (0.004)	1.00	-0.017 (0.02)	0.30	-0.021 (0.02)	0.30	-0.010 (0.01)	0.50
L putamen-R caudate[e]	0.003 (0.006)	0.50	-0.002 (0.01)	0.90	0.005 (0.01)	0.70	-0.006 (0.01)	0.70
Extrinsic basal ganglia connections								
L caudothalamus[2, a, b, d, A, *, †, §]	-0.001 (0.002)	0.70	0.013 (0.01)	0.20	0.020 (0.01)	0.10	0.014 (0.01)	0.10

L putamothalamus[2, a, b, d, A, *, †, §]	-0.001 (0.002)	0.70	0.013 (0.01)	0.20	0.019 (0.01)	0.10	0.014 (0.01)	0.10
L pallidothalamus[2, †]	0.001 (0.003)	0.70	0.013 (0.01)	0.20	0.018 (0.02)	0.30	0.013 (0.01)	0.20
R caudothalamus[2, a, b, f, B, F, †, #]	-0.002 (0.002)	0.50	0.025 (0.01)	**0.009**	0.024 (0.01)	**0.04**	0.025 (0.01)	**0.006**
R putamothalamus[2, f, F, †]	-0.0001 (0.002)	0.80	0.001 (0.01)	0.90	-0.004 (0.01)	0.80	0.007 (0.01)	0.40
R pallidothalamus[†, §]	0.001 (0.003)	0.70	0.004 (0.01)	0.70	0.003 (0.01)	0.80	0.015 (0.01)	0.20
L caudate-R thalamus[2, a, c, C, ‡]	0.001 (0.004)	0.80	0.006 (0.01)	0.60	0.013 (0.01)	0.40	0.010 (0.01)	0.40
L putamen-R thalamus[†]	0.001 (0.005)	0.90	0.007 (0.01)	0.60	-0.004 (0.02)	0.80	0.004 (0.01)	0.80
L pallidum-R thalamus[b, B, †]	0.003 (0.005)	0.60	0.011 (0.01)	0.40	0.026 (0.01)	0.10	0.017 (0.01)	0.20
R caudate-L thalamus	0.0001 (0.004)	1.00	0.017 (0.01)	0.20	0.028 (0.01)	0.07	0.005 (0.01)	0.70
R putamen-L thalamus[2, f, C, #]	0.014 (0.004)	**0.002**	0.0001 (0.01)	1.00	0.013 (0.02)	0.40	-0.009 (0.01)	0.40
R pallidum-L thalamus[2, 6, †]	0.006 (0.004)	0.20	0.011 (0.01)	0.40	0.007 (0.01)	0.60	0.009 (0.01)	0.50
R putamocerebellar[6, a, b, B, †]	-0.001 (0.004)	0.80	-0.008 (0.01)	0.50	-0.006 (0.01)	0.70	-0.004 (0.01)	0.70
R pallidocerebellar[1, b, B, †]	-0.002 (0.004)	0.50	-0.001 (0.01)	0.90	-0.005 (0.02)	0.70	-0.002 (0.01)	0.80
Cerebellothalamic group								
L thalamocerebellar[2, a, *, †, ‡]	0.004 (0.004)	0.30	0.005 (0.01)	0.60	0.010 (0.01)	0.50	0.006 (0.01)	0.60

R thalamocerebellar[1,2, b, B, †]	0.001 (0.003)	0.80	-0.002 (0.01)	0.80	0.001 (0.01)	0.90	0.001 (0.01)	0.90
L thalamo-vermis[†]	0.005 (0.005)	0.20	-0.004 (0.01)	0.70	0.006 (0.02)	0.80	-0.006 (0.01)	0.50
R thalamo-vermis[e, f, E, ¶]	-0.001 (0.004)	0.90	-0.004 (0.01)	0.80	0.003 (002)	0.90	-0.004 (0.01)	0.70
Interthalami[2, b, †]	0.002 (0.003)	0.60	0.002 (0.01)	0.80	0.006 (0.01)	0.60	0.009 (0.01)	0.40
L cerebello-vermis[1, a, b, B, F, *, †]	-0.004 (0.003)	0.20	0.010 (0.01)	0.40	0.003 (0.01)	0.80	0.013 (0.01)	0.30
R cerebello-vermis[1, 2, b, B, *, †]	-0.003 (0.003)	0.70	0.001 (0.01)	0.90	-0.007 (0.01)	0.60	0.004 (0.01)	0.70
Intercerebelli[1, a, b, A, *, †]	-0.004 (0.003)	0.10	0.0006 (0.01)	1.00	-0.0001 (0.01)	1.00	0.009 (0.01)	0.40

The model includes potential confounders related to the outcome at $p<0.1$: FA:- 1 = infant sex; 2 = Equivalent GA of infant at MRI; 3 = infant weight at MRI; 4 = infant head circumference at MRI; 5 = maternal weight change per week; 6 = maternal age at delivery; MD:- a = infant sex; b = Equivalent GA of infant at MRI; c = infant weight at MRI; d = infant head circumference at MRI; e maternal weight change per week; f = maternal age at delivery; AD:- A = infant sex; B = Equivalent GA of infant at MRI; C = infant weight at MRI; D = infant head circumference at MRI; E = maternal weight change per week; F = maternal age at delivery; RD:- ∗ = infant sex; † = Equivalent GA of infant at MRI; ‡ = infant weight at MRI, § = infant head circumference at MRI; ¶ = maternal weight change per week; # = maternal age at delivery; Bold indicates significance at $p \leq 0.05$

Table 4.3 Comparison of DT parameters (FA, MD, AD and RD) in WM tracts connecting manually traced seeds/targets) between infants who had not (HUU) been exposed to HIV prenatally and infants who had been exposed to ART either throughout gestation (pre-conception ART) or for a shorter period (post-conception ART) to unexposed infants. Values are unstandardized regression coefficients (**β**) and standard errors (SE).

	FA				**MD**				**AD**				**RD**			
WM-ROI	**HEU pre-conception vs HUU**		**HEU post-conception vs HUU**		**HEU pre-conception vs HUU**		**HEU post-conception vs HUU**		**HEU pre-conception vs HUU**		**HEU post-conception vs HUU**		**HEU pre-conception vs HUU**		**HEU post-conception vs HUU**	
	β (SE)	***p***	**β (SE)**	***p***	**β (SE)**	***p***	**β (SE)**	***p***	**β (SE)**	***p***	**β (SE)**	***p***	**β (SE)**	***p***	**β (SE)**	***p***
Intrinsic Basal ganglia connections																
L caudoputamen[2, a, b, *, †, §]	0.0006 (0.003)	0.80	0.0005 (0.003)	0.90	0.006 (0.01)	0.60	0.020 (0.01)	0.07	0.0002 (0.01)	1.00	0.018 (0.01)	0.20	0.0007 (0.01)	0.90	0.019 (0.01)	0.06
L caudopallidum[2, †]	0.002 (0.003)	0.60	0.003 (0.003)	0.30	0.001 (0.01)	0.90	0.009 (0.01)	0.50	0.002 (0.02)	0.90	0.018 (0.02)	0.30	-0.001 (0.01)	0.90	0.001 (0.01)	0.90
L putamopallidum[2, b, †]	0.005 (0.004)	0.20	0.005 (0.004)	0.20	0.005 (0.01)	0.70	0.022 (0.01)	0.10	0.005 (0.02)	0.80	0.024 (0.02)	0.30	0.007 (0.01)	0.50	0.022 (0.01)	**0.05**
R caudoputamen[2, e, †, ¶]	0.00003 (0.003)	1.00	-0.002 (0.003)	0.40	0.007 (0.01)	0.50	0.016 (0.01)	0.20	0.010 (0.01)	0.50	0.018 (0.02)	0.20	0.010 (0.01)	0.40	0.014 (0.01)	0.20
R caudopallidum[2, #, ¶]	0.003 (0.004)	0.50	0.0001 (0.004)	1.00	0.0001 (0.01)	1.00	-0.002 (0.01)	0.90	-0.005 (0.02)	0.70	-0.001 (0.02)	0.90	0.010 (0.01)	0.40	0.014 (0.01)	0.20
R putamopallidum[2]	0.007 (0.004)	0.10	0.003 (0.004)	0.50	-0.01 (0.015)	0.40	-0.01 (0.01)	0.30	-0.007 (0.02)	0.70	-0.021 (0.02)	0.30	-0.011 (0.01)	0.30	-0.009 (0.01)	0.40
Inter-caudate[2, f]	-0.0001 (0.005)	0.80	-0.001 (0.005)	0.80	-0.015 (0.02)	0.50	-0.018 (0.02)	0.40	-0.021 (0.02)	0.30	-0.020 (0.02)	0.30	-0.013 (0.01)	0.50	-0.006 (0.01)	0.70
L putamen-R caudate[e]	0.002 (0.006)	0.70	0.004 (0.006)	0.50	-0.009 (0.01)	0.50	-0.006 (0.01)	0.70	-0.005 (0.01)	0.80	0.016 (0.02)	0.30	-0.013 (0.01)	0.40	0.001 (0.01)	0.90
Extrinsic basal ganglia connections																
L caudothalamus[2, a, b, d, A, *, †, §]	-0.001 (0.003)	0.80	-0.001 (0.003)	0.70	0.008 (0.01)	0.50	0.017 (0.01)	0.10	0.015 (0.01)	0.30	0.020 (0.01)	0.10	0.012 (0.01)	0.20	0.016 (0.01)	0.10
L putamothalamus[2, a, b, d, A, *, †, §]	-0.001 (0.003)	0.80	-0.001 (0.003)	0.80	0.008 (0.01)	0.50	0.17 (0.01)	0.10	0.016 (0.01)	0.20	0.023 (0.01)	0.10	0.012 (0.01)	0.20	0.016 (0.01)	0.10
L pallidothalamus[2, †]	0.001 (0.003)	0.70	0.001 (0.003)	0.70	0.017 (0.01)	0.20	0.009 (0.01)	0.50	0.019 (0.02)	0.30	0.017 (0.02)	0.40	0.015 (0.01)	0.20	0.013 (0.01)	0.30
R caudothalamus[2, a, b, f, B, F, †, #]	-0.001 (0.003)	0.80	-0.002 (0.003)	0.30	0.022 (0.01)	**0.04**	0.027 (0.01)	**0.01**	0.024 (0.01)	0.08	0.024 (0.01)	0.09	0.023 (0.01)	**0.02**	0.026 (0.01)	**0.01**
R putamothalamus[2, f, F, †]	0.001 (0.003)	0.70	-0.002 (0.003)	0.40	-0.001 (0.01)	0.90	0.003 (0.01)	0.80	-0.005 (0.02)	0.70	-0.003 (0.02)	0.90	0.006 (0.01)	0.60	0.009 (0.01)	0.40
R pallidothalamus[†, §]	0.002 (0.003)	0.60	0.0001 (0.003)	1.00	0.006 (0.01)	0.60	0.001 (0.01)	0.90	0.010 (0.02)	0.50	0.006 (0.02)	0.70	0.010 (0.01)	0.40	0.019 (0.01)	0.10
L caudate-R thalamus[2, a, c, C, ‡]	0.002 (0.005)	0.70	-0.0003 (0.005)	0.90	0.0002 (0.01)	1.00	0.011 (0.01)	0.40	-0.003 (0.02)	0.90	0.030 (0.02)	0.10	0.005 (0.01)	0.70	0.015 (0.01)	0.20
L putamen-R thalamus[†]	0.003 (0.006)	0.60	-0.002 (0.006)	0.80	-0.0002 (0.02)	1.00	0.014 (0.02)	0.40	-0.011 (0.02)	0.60	0.003 (0.02)	0.80	-0.003 (0.01)	0.80	0.011 (0.01)	0.50
L pallidum-R thalamus[b, B, †]	0.006 (0.006)	0.30	0.0003 (0.006)	1.00	0.005 (0.02)	0.70	0.017 (0.02)	0.30	0.021 (0.18)	0.20	0.031 (0.02)	0.09	0.010 (0.01)	0.50	0.023 (0.01)	0.10
R caudate-L thalamus	-0.002 (0.005)	0.70	0.002 (0.005)	0.70	0.022 (0.01)	0.40	0.012 (0.01)	0.40	0.030 (0.02)	1.00	0.026 (0.02)	0.10	0.009 (0.01)	0.50	0.001 (0.01)	0.90

R putamen-L thalamus[2, f, C, #]	0.015 (0.005)	**0.004**	0.012 (0.005)	**0.02**	0.005 (0.01)	0.70	-0.005 (0.01)	0.70	0.022 (0.02)	0.20	0.001 (0.02)	0.80	-0.003 (0.01)	0.80	-0.015 (0.01)	0.20
R pallidum-L thalamus[2, 6, †]	0.006 (0.005)	0.20	0.005 (0.005)	0.30	0.020 (0.02)	0.20	0.001 (0.02)	1.00	0.017 (0.02)	0.30	-0.002 (0.02)	0.90	0.018 (0.01)	0.20	-0.0005 (0.01)	1.00
R putamocerebellar[6, a, b, B, †]	-0.001 (0.004)	0.80	-0.0006 (0.004)	0.90	-0.007 (0.01)	0.60	-0.008 (0.01)	0.50	-0.008 (0.02)	0.60	-0.004 (0.02)	0.80	-0.003 (0.01)	0.80	-0.004 (0.01)	0.70
R pallidocerebellar[1, b, B, †]	-0.002 (0.004)	0.70	-0.003 (0.004)	0.50	-0.003 (0.01)	0.80	-0.006(0.01)	0.60	-0.001 (0.02)	1.00	-0.010 (0.01)	0.60	0.001 (0.01)	0.90	-0.005 (0.01)	0.60
Cerebellothalamic group																
L thalamocerebellar[2, a, *, †, ‡]	0.004 (0.004)	0.30	0.003 (0.004)	0.50	0.010 (0.01)	0.40	-0.001 (0.01)	0.90	0.016 (0.02)	0.30	0.002 (0.02)	0.90	0.010 (0.01)	0.30	0.001 (0.01)	0.90
R thalamocerebellar[1,2, b, B, †]	0.004 (0.004)	0.30	-0.002 (0.004)	0.50	0.007 (0.01)	0.60	-0.011 (0.01)	0.30	0.021 (0.01)	0.20	-0.020 (0.02)	0.20	0.004 (0.01)	0.70	-0.002 (0.01)	0.90
L thalamo-vermis[†]	0.005 (0.005)	0.40	0.006 (0.005)	0.30	0.009 (0.01)	0.60	-0.017 (0.01)	0.30	0.025 (0.02)	0.30	-0.013 (0.02)	0.60	0.002 (0.01)	0.90	-0.014 (0.01)	0.20
R thalamo-vermis[e, f, E, ¶]	0.003 (0.005)	0.50	-0.002 (0.005)	0.60	0.007 (0.01)	0.60	-0.015 (0.01)	0.30	0.030 (0.02)	0.20	-0.028 (0.02)	0.20	0.001 (0.01)	0.90	-0.011 (0.01)	0.40
Interthalami[2, b, †]	0.002 (0.004)	0.50	0.001 (0.004)	0.80	-0.009 (0.01)	0.40	0.013 (0.01)	0.20	-0.006 (0.01)	0.70	0.018 (0.01)	0.20	-0.001 (0.01)	0.90	0.018 (0.01)	0.10
L cerebello-vermis[1, a, b, B, F, *, †]	-0.003 (0.003)	0.40	-0.004 (0.003)	0.20	0.004 (0.01)	0.70	0.016 (0.01)	0.20	-0.005 (0.02)	0.80	0.012 (0.01)	0.40	0.007 (0.01)	0.60	0.018 (0.01)	0.20
R cerebello-vermis[1, 2, b, B, *, †]	-0.0002 (0.003)	0.90	-0.002 (0.003)	0.50	-0.001 (0.01)	0.90	0.003 (0.01)	0.80	-0.013 (0.02)	0.40	0.0001 (0.02)	1.00	0.003 (0.01)	0.80	0.005 (0.01)	0.70
Intercerebelli[1, a, b, A, *, †]	-0.003 (0.003)	0.30	-0.005 (0.003)	0.10	0.001 (0.01)	0.90	0.0002 (0.01)	1.00	-0.002 (0.01)	0.90	-0.003 (0.01)	0.80	0.009 (0.01)	0.40	0.009 (0.01)	0.50

The model includes potential confounders related to the outcome at $p<0.1$: DT = diffusion tensor

FA:- 1 = infant sex; 2 = Equivalent GA of infant at MRI; 3 = infant weight at MRI; 4 = infant head circumference at MRI; 5 = maternal weight change per week; 6 = maternal age at delivery;

MD:- a = infant sex; b = Equivalent GA of infant at MRI; c = infant weight at MRI; d = infant head circumference at MRI; e maternal weight change per week; f = maternal age at delivery;

AD:- A = infant sex; B = Equivalent GA of infant at MRI; C = infant weight at MRI; D = infant head circumference at MRI; E = maternal weight change per week; F = maternal age at delivery;

RD:- ∗ = infant sex; † = Equivalent GA of infant at MRI; ‡ = infant weight at MRI, § = infant head circumference at MRI; ¶ = maternal weight change per week; # = maternal age at

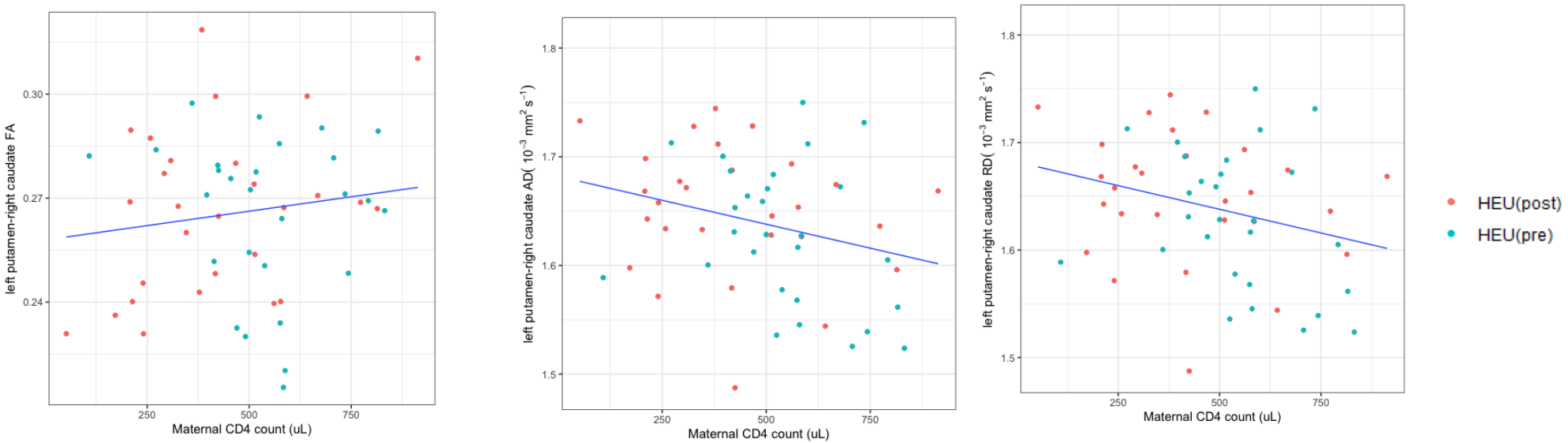

Figure 4.2. Plots showing associations of the some of the regional white matter measures among infants with maternal CD4 counts.

4.3 Discussion

We hypothesized white matter integrity would be altered among connections to/from subcortical volumes demonstrating HIV/ART exposure reductions. Our analysis identified two tracts within the extrinsic basal ganglia circuit. Contradictory to our hypothesis, we report higher mean FA in a tract between the right putamen and left thalamus in HEU infants. In line with our expectations, we also report higher mean MD in the tract connecting caudate nucleus (where we found reduced volumes due to HIV/ART exposure) and thalamus in the right hemisphere in HEU infants. We also hypothesized ART protection among the pre-conception group. However, the observed WM microstructural changes are independent of prenatal ART exposure duration. These findings suggest that even in the presence of ART, localized white matter development is vulnerable to HIV during pregnancy. In addition, we also observed white matter tracts without abnormalities influenced by ART duration and/or maternal immune health. Ultimately, our results point to maternal HIV, immune health and ART duration in pregnancy impact regional white matter growth in newborns.

Despite reduced bilateral caudate and left putamen volumes in HEU infants, almost all connections in the analysis including these structures were unaffected. Unlike the observed reductions in subcortical gray matter, which depended on ART duration, white matter alterations were independent of ART. The subcortical BG regions begin to develop around embryonic day 14 and assume adult shape around embryonic day 20 to 21 (Nunta-aree et al., 2001). White matter development accelerates after the gray matter foundation is laid (Tiwari et al., 2018, Reemst et al., 2016, Stiles and Jernigan, 2010), with most growth occurring systematically in the second and third trimesters. Maternal ART likely protected white matter since all newborns in our cohort were exposed during this period. Interestingly, the two HIV exposure group differences reported – increased FA in the right putamen/left thalamus connection and increased MD in right caudate/thalamus connection – suggest different underlying changes. FA represents anisotropy, which is interpreted as axonal density and/or myelination in the tract. Whereas MD represents the average shift of water molecules and is associated with white matter maturation.

We found higher FA in one commissural tract connecting the right putamen and left thalamus within the extrinsic basal ganglia circuit in HEU infants relative to their HUU counterparts. A few previous DTI studies in HEU infants and children have also reported higher FA in different brain regions (Madzime et al., 2021, Jankiewicz et al., 2017, Tran et al., 2016). While Jankiewicz et al. and Madzime et al. also reported concurrent changes in AD and RD in 7-year-old HEU children, the study by Tran et al. in newborns did not. We also did not find AD and/or RD differences in the corresponding implicated tract. Since changes in FA may be interpreted in terms of axons or myelin, looking at AD and/or RD provides essential complementary information. However, since the majority of literature discussing

the interpretation of DTI measures is in children and adults, they may need to be adjusted for the immature white matter of the newborn brain.

As part of healthy white matter maturation, FA typically increases with age during the second and third trimesters in utero and in infancy. Even though we had a small age range, FA values were positively associated with gestational age across most tracts in our analysis. Increased FA in non-typically developing infants may represent disruptions to typical development in the presence of disease or exposure to potential teratogenic agents, including HIV or ART. In this context, higher FA may represent accelerated myelination as posited. However, since neonatal WM is immature, the observed increased FA may be due to active axonal out-growth and initial enlistment of axons by premyelin sheaths, generated by immature oligodendrocytes (Haybes et al., 2005; Back et al., 2002). According to Wimberger et al, unmyelinated WM tracts still show signal intensity changes consistent with anisotropic water diffusion (Wimberger et al., 1995).

Higher mean FA is observed in certain neurodevelopmental disorders in children including attention-deficit hyperactivity disorders (ADHD), schizophrenia, autism syndrome, and developmental coordination disorder (DCD) (Andrews et al., 2019, Peterson et al., 2011, Davenport et al., 2010, Brown-Lum et al., 2020, Cascio et al., 2013). HEU children are at increased risk for autistic syndrome disorder, emotional disturbances, and hyperkinetic disorder (Piske et al., 2018).

We found higher MD with accompanying higher RD and AD (at trending level) in the ipsilateral connection between caudate and thalamus in the right hemisphere. In children, Jankiewicz et al. reported lower mean MD, RD and AD in HEU compared to HUU in the corticospinal tract (Jankiewicz et al., 2017), while Madzime et al. found no exposure related changes in MD. Yadav found both regional increase and decrease regions of mean MD with no reported changes in AD or RD (Yadav, 2020). In neonates, Tran et al. did not report changes in MD in their studied region of interest (Tran et al., 2016). Lower MD indicates well-organized WM structure and densely axonal packing, and MD typically decreases as the brain matures with age. Increased MD is interpreted as axonal degeneration and possible demyelination. RD is related to myelination, with higher values indicating de- or dys-myelination. Changes in the axonal diameters or density may also influence RD (Alexander et al., 2011, Feldman et al., 2010, Alexander et al., 2007). However, given the immature form of white matter, these may not best describe the observed alterations in MD, RD and AD. In typical development, Schneider and colleagues observed higher MD in the mid-third trimester which they attributed to larger extracellular space between fibers to allow for cellular migration which is still ongoing and very much needed at this time for normative development (Schneider et al., 2007). The observed increased

MD in HEU infants may reflect less mature white matter as a result of delayed cellular migration caused by HIV exposure.

Interestingly, within HEU newborns, some connections (APPPENDIX, supplementary results table 3.2a, b and c) that did not demonstrate HIV/ART group differences were associated with ART duration and/or maternal immune health. These associations may suggest maternal immune health and ART timing play a role in WM development. Within this cohort, we earlier reported an association between reduced grey matter volumes and shorter in utero ART exposure. Even though grey matter and WM have different underlying mechanisms, it is interesting that all the associations between WM indices and maternal immune health/treatments variables we observed involved ROIs grey matter seeds where we found reduced volumes (bilateral caudate and left putamen). Additionally, we also found associations between WM connections of the thalamus and ART exposure duration.

In individuals living with HIV on ART, reductions in both grey and white matter have been reported. While grey matter atrophy has been attributed to inflammation and gliosis (Cavaliere et al., 2020; Guzman-Martinez et al., 2019, Walker 2018), decreased WM has been linked to undifferentiated oligodendrocytes – glial cells responsible for myelination of WM, and/or stressed oligodendrocytes preconditioned by elevated levels of glutamate from infected macrophages (Lindsay et al., 2021). It is not yet clear how exposure to HIV and ART affects WM, however, we suggest that disruptions in extracellular matrix by infiltration of by-products of ART and circulating macrophages crossing the fetal's BBB might alter WM in HEU infants.

In conclusion, even in the presence of ART, HEU infants demonstrate altered white matter in two white mater tracts connecting thalamus and basal nuclei. In contrast with earlier findings of reduced grey matter volumes attributable to shorter in utero ART exposure duration within this cohort, the implicated tracts in this study were independent of ART exposure duration.

CHAPTER FIVE

Neonate white matter integrity predicting cognitive ability at 9-12 months

5.1 Introduction

In the previous chapter we reported changes in white matter structure in two tracts in HEU neonates, independent of ART exposure duration. In typical developments, white matter anisotropy continues to increase with age and this increase is dependent on myelination (Paus et al., 1999). In healthy populations, changes in white matter anisotropy have been directly linked to cognitive ability (Sousa et al., 2018; Cremmers et al., 2016; Petters et al., 2012; Bendlin et al., 2010). Given the emerging evidence of exposure related white matter alterations HEU population, it is important to examine the functional consequences of this HIV/ART related altered white matter.

Within the imaging studies including HEU infants/children, three combine imaging and cognitive outcomes (Madzime et al., 2021, Yadav et al., 2020, Tran et al., 2016). Madzime et al. found no cognitive associations with FA alterations in HEU children (Madzime et al., 2021). Yadav et al. reported decreased FA and altered MD in HEU school-age children in several brain regions compared to uninfected controls. Lower FA and, higher/lower MD were associated with poor neuropsychological scores (Yadav et al., 2020). Tran et al. also reported an association between altered WM and Dubowitz abnormal neurological scores in HEU infants compared to their control counterparts. Dubowitz abnormal neurological signs subscale scores were positively associated with FA in the left uncinate fasciculus and negatively correlated with MD in the inferior cerebellar peduncle (Tran et al., 2016).

Notably, apart from Madlala and colleagues' study, none of the imaging and non-imaging or combined studies above considered ART exposure duration relative to structural and functional brain changes. Maternal immune health during pregnancy may dictate the developmental outcome of the infant.

This chapter examined prospective associations between white matter metrics (FA and MD) in the neonatal period and subsequent neuropsychological scores at 9-12 months. In the previous chapter, we examined WM connections between components of the basal ganglia, thalamus, and cerebellum. The basal ganglia, thalamus and the grey matter components of the cerebellum forms the central processing units in which the long-range axons connecting to several regions of the brain originated.

Based on our findings reported in the previous chapter, and the role of basal ganglia in motor and cognitive functions, we hypothesized higher FA in the R putamen-L thalamus and higher MD in the R caudothalamus would be associated with lower neuropsychological scores, especially in motor-related domains, in HEU infants. We hypothesized these associations would be independent of the duration of in utero exposure to ART.

5.2 Results

A total of 61, a subset of 86 infants whose DTI tractographic metrics were obtained within the first month of postnatal life in the previous analysis, and successfully underwent neuropsychological testing at 9-month (40 HEU; mean age at neuropsychological assessments ± SD = 9.6 ± 1.0 months GA; 21 female) were included in this analysis.

Of the 40 HEU infants, 18 were exposed to ARV throughout gestation (HEU-preconception), and 22 only for part of their gestational period (HEU-postconception). Mothers in the post-conception group had initiated ART at a mean GA of 15.4 (±5.7) weeks. Sample characteristics are summarized in Table 5.1. Overall, maternal and infant indices were similar across groups, except that mothers in the HIV pre-conception group were about 3 years and four years older than their post-conception HIV-negative counterparts respectively; and post-conception infants had slightly lower head circumferences at the time of their scan than their post-conception and HUU counterparts. Not surprisingly, mothers in the HIV pre-conception group had higher CD4+ cell counts and lower VLs within 6 months of enrolment than the post-conception mothers. There were only 5 mothers with positive drug tests and all were HIV uninfected – 2 tested positive for cannabis, 2 for methamphetamines and 1 for methaqualone. None of the mothers reported smoking. In contrast to the virtual absence of drug use, more than 40% of mothers across groups reported drinking during pregnancy, albeit at very low levels (all < 0.04 oz AA/day). All infants were examined at about the same age. Neuropsychological outcome scores were similar for all infants across all domains assessed and were in the average range.

In Table 5.2 and figure 5.1 we present the associations of the infant's DTI-tractographic FA at one month and GMDS scores at 9-month postnatal life. In typical development (HUU):

Locomotor scores were positively associated with FA in two tracts of the cerebellothalamic group within the cerebellar connections – R cerebello-vermis and intercerebellar.

Personal Social scores were positively associated with FA in several tracts – caudoputamen, caudopallidum, and putamopallidum on the left hemisphere of the intrinsic BG connections; left putamothalamic, and bilateral caudothalamic and pallidothamic tracts of the extrinsic BG connections; and bilateral cerebellovermis and intercerebelli connections withing the cerebellar connections. All these associations survived FDR correction for multiple comparisons.

Language scores were positively associated with FA in the left caudothalamic, left putamothalamic, left pallidothalamic and right pallidocerebelli withing the extrinsinc BL coonections; bilateral

cerebellovermis and intercerebelli within the cerebellar connections. None of the associations survived FDR correction for multiple comparisons.

Eye & Head coordination scores were positively associated with caudoputamen, caudopallidum and putamopallidum on the left hemisphere withing the intrinsic BG circuit; right pallidocerebelli, left pallidothalami, and bilateral caudothalamic and putamothalamic of the exrinsinc BG circuit. In the cerebellothalamic group, Eye & Hand coordination was positively associated with bilateral cerebellovermis FAs, inetrcerebelli, and thalamocerebelli (at trenading level) on the right side of the brain. Intercerebelli and right thalamocerebelli FAs were also associated with Eye & Hand coordination in the preconception arm. Of the observed significant associations, only left caudothalamic, bilateral putamothalamic, left pallidothamic, left cerebello-vermis and intercerebelli tracts survived FDR corrections for multiple comparisons.

Performance scores was positively associated with FAs in the right putamothalamic and right-caudate-left thalamic tracts of the extrinsic BG circuit. In contrast, Perfomamce scores were negatively associated with FA in the right putamocerebelli, left thalamocerebelli, left thalamovermis, and left cerebellovermis tracts with none of these surviving FDR correction for multiple comparisons.

General quotient scores was positively associated with left caudoputamen, left pallidothalamic, right putamocerebelli, right pallidocerebelli, right thalamocerebelli, and bilateral caudothalamic and putamothalamic tracts with only left caudothalmus, left putamothalamus and right thalamocerebellar surviving FDR correction for multiple comparisons.

In Table 5.3 and figure 5.2 we present the associations of the infant's DTI-tractographic MD at one month and GDMS scores at 9-month postnatal life.

In typical development (HUU), three GDMS quotients were associated with MD; Locomotor – was positively associated with right putamothalamic, right- putamen- left thalamus, and left thalamovermis tracts; Language was negatively associated with intercerebelli connection; and Eye & Hand Coordination was negatively associated with intercaudate tract. In contrast to typical development, we found negative associations of GDMS domains with several WM tract's MDs in HEU infants except one commissural tract – left caudate- right thalamus which was positively associated with Locomotor score in the postcconception group. None of the significant associations observed survive multiple comparisons.

In the pre-conception group, locomotor scores were positively associatiated with left caudopallidal FA; Personal social was negatively associated with right putamen- left pallidum; Language was

negatively associated with bilateral putamaopallidum; and Performance was positively associated with left pallidothalamic tract. None of the associations survived multiple comparisons.

In the post-conception group, Personal Social scores was negatively associated with MD in the left putamopallidal, left-pallidum- right thalamic, and right-putamen- left pallidal tracts; Language score was negatively associated with right caudopallidal MD; Eye & Head coordination score was negatively associated with left putamopallidal MD. Performance scores was negatively associated with MD in the following tracts:bilateral caudoputamen and putamopallidum, left caudopallidum, left caudate- right thalamus, left putamen- right thalamus, left pallidum- right thalamus, right putamen- left thalamus, right pallidum- left thalamus, and a trending right caudate- left thalamic connections.

General quotient score was negatively associated with left hemispheric putamopallidal tract's MD. None of these associations survived multiple comparisons.

Table 5.1 Sample characteristics and Neurodevelopmental scores (N = 61)

	HUU (n = 21)		**HEU (n = 40)**					
			Pre-conception ART (n = 18)		**Post-conception ART (n = 22)**			
	Mean±SD	**Range**	**Mean±SD**	**Range**	**Mean±SD**	**Range**	**X^2 or t or F**	***P (for* X^2 or t or F)**
Maternal indices								
Age at delivery (years)	27.8 ± 5.6	19.6 – 42.4	31.7 ± 6.5	20.6 – 46.3	28.8 ± 5.3	20.5 – 40.9	2.28	0.11
GA at enrolment (weeks)	20.6 ± 5.5	10.7 – 28.0	19.5 ± 7.5	7.1 – 35.1	21.7 ± 6.3	9.3 – 30.7	0.57	0.56
Highest school level completed (n, %)								
Grade 6	0 (0)	-	1 (5.5 %)	-	0 (0)	-	18.53	0.10
Grade 9	0 (0)	-	1 (5.5 %)	-	1 (4.5 %)	-		
Grade 10	0 (0)	-	0 (0)	-	4 (18.2 %)	-		
Grade 11	6 (28.6 %)	-	7 (39.0 %)	-	10 (45.4 %)	-		
Grade 12	15 (71.4 %)	-	9 (50.0 %)	-	7 (31.9 %)	-		
CD4 within 6 mo of enrolment (cells/µL)[1]	N/A	N/A	543 ± 187	108 – 816	408 ± 188	172 – 814	2.27	**0.03**
VL within 6 mo of enrolment								
Undetectable (n, %)	N/A	N/A	11 (61.1 %)	-	14 (63.6 %)	-	0.0	1.00
Detectable (n, %)	N/A	N/A	7 (38.9 %)	-	8 (36.4 %)	-		
VL (copies/mL)[2] Median[a] [IQR]	N/A	N/A	34 [27 – 55]	26 – 238	259 [45– 443]	35 – 16787	7.99	**0.009**
Substance use across pregnancy								

Alcohol (n; %)	10 (47.6 %)	-	6 (33.3 %)	-	9 (40.9 %)	-		
AA/day (oz)[3]	0.03 ± 0.02	0.001 x10^{-3} – 0.070	0.03 ± 0.01	0.017 – 0.048	0.04 ± 0.02	0.02 – 0.072	0.92	0.41
Cannabis (n; %)[4]	2 (9.5 %)	-	0 (0)	-	0 (0)	-	3.94	0.14
Methamphetamine (n; %)[4]	2 (9.5 %)	-	0 (0)	-	0 (0)	-	3.94	0.14
Methaqualone (n; %)[4]	1 (4.8 %)	-	0 (0)	-	0 (0)	-	1.94	0.38
Smoking (n; %)	0 (0)	-	0 (0)	-	0 (0)	-	-	NA
Infant indices								
Sex (n Female; %)	10 (47.6 %)	-	9 (50.0 %)	-	12 (54.5 %)	-	0.12	0.94
Delivery route:								
Vaginal (n, %)	17 (81.0%)	-	14 (77.8 %)		15 (68.2 %)	-	1.02	0.60
Caesarean (n, %)	4 (19.0%)	-	4 (22.2 %)		7 (31.8 %)	-		
Birth indices:								
GA (weeks)	39.6 ± 1.1	37.0 – 41.6	39.5 ± 1.5	36.6 – 41.6	39.7 ± 1.4	36.8 – 42.3	0.06	0.94
Weight (g)	3239 ± 434	2575 – 4180	3257 ± 290	2775 – 3750	3279 ± 426	2500 – 4230	0.05	0.95
Crown-to-heel length (cm)	50.1 ± 2.0	47.0 – 53.0	50.2 ± 2.0	47.0 – 54.0	50.4 ± 2.5	47.0 – 56.0	0.07	0.93
Head circumference (cm)	34.2 ± 1.4	32 – 37	34.2 ± 1.4	31 – 36	33.7 ± 1.5	32 – 39	0.72	0.49
ART exposure length (weeks)	N/A	N/A	39.5 ± 1.5	36.6 – 41.6	25.9 ± 5.7	14.0 – 35.6	9.90	**<0.0001**
MRI indices:								
GA Equivalent (weeks)	41.5 ± 0.9	40.0 – 43.9	41.3 ± 0.7	40.0 – 42.7	41.5 ± 1.1	39.3 – 43.1	0.22	0.81
Weight (g)[5]	3538 ± 398	2700 – 4250	3512 ± 380	2775 – 4200	3554 ± 400	2850 – 4450	0.06	0.94

Head circumference (cm)[5]	35.0 ± 1.2	33 – 37	36.0 ± 1.1	33 – 37	34.8 ± 1.3	31 – 36.5	5.49	**0.007**
Total ICV (x 10^5 mm^3)	4.85 ± 0.51	3.83 – 5.86	5.09 ± 0.48	4.42 – 6.40	5.07 ± 0.94	42.2 – 7.65	0.79	0.46
Age NP examination	9.50±0.97	8.60 – 13.10	9.60±0.83	8.96 – 12.10	9.9±1.22	8.70 – 12.6	0.81	0.45
Neuropsychological mean scores								
Locomotor	107.0±14.1	71 – 126	108.3±11.0	84 – 122	105.4±14.2	82 – 126	0.23	0.79
Personal Social	113.0±17.1	87 – 150	104.8±11.3	76 – 120	109.4±11.2	92 – 130	1.76	0.18
Language	106.5±13.2	85 – 138	104.8±11.2	77 – 127	109.1±13.1	89 – 138	0.61	0.54
Eye & Hand Coordination	108.0±17.9	74 – 150	105.7±15.0	78 – 133	104.0±13.5	84 – 133	0.36	0.70
Performance	92.9±15.8	67 – 133	92.5±12.1	72 – 120	92.4±15.3	50 – 110	0.01	1.00
General Quotient	109±19.6	82 – 177	104±8.4	86 – 118	105.7±8.9	86 – 124	0.82	0.44

[1]CD4 count missing for 2 mothers who started ART pre-conception; [2]Based only on mothers with detectable VL levels (9 mothers who started ART pre-conception; 14 mothers who started ART post-conception); [3]Based only on mothers who consumed alcohol; 1 oz absolute alcohol (AA) is equivalent to 2 standard drinks; [4]Numbers based on urine tests; [5]Data missing for 1 infant in the pre-conception group and 2 HUU infants. Bold indicates significance at $p \leq 0.05$. [a]Fisher exact test.

Table 5.2 Associations of WM-ROIs FAs with GMDS neuropsychological scores

	Locomotion						**Personal Social**					
	HUU		**HEU-preconception**		**HEU-postconception**		**HUU**		**HEU-preconception**		**HEU-postconception**	
	β (std err.)	**p**	**β (std err.)**	**p**	**β (std err.)**	**p**	**β (std err.)**	**p**	**β (std err.)**	**p**	**β (std err.)**	**p**
Intrinsic Basal ganglia connections												
L caudoputamen	185.8 (255.7)	0.50	-245 (357.1)	0.50	-68.5 (244.9)	0.80	**714.6 (246.8)**	**0.006**	230.9 (344.6)	0.50	-45.1 (236.4)	0.80
L caudopallidum	291.2 (217.5)	0.20	-338.5 9302.2)	0.30	-47.9 (196.7)	0.80	**537.0 (205.4)**	**0.01**	224.6 (285.4)	0.40	17.3 (185.7)	0.90
L putamopallidum	256.0 (187.7)	0.20	-190.1 (201.9)	0.30	-89.3 (219.9)	0.70	**435.8 (181.4)**	**0.02**	111.8 (195.2)	0.60	-45.6 (212.4)	0.80
R caudoputamen	17.6 (216.7)	0.90	-225.2 (383.9)	0.60	28.3 (269.8)	0.90	309.1 (199.8)	0.10	-86.6 (353.9)	0.80	-196.9 (248.6)	0.40
R caudopallidum	-79.8 (195.4)	0.70	-302.2 (286.1)	0.30	79.8 (280.2)	0.80	217.4 (187.5)	0.20	209.4 (274.5)	0.40	-170.5 (268.9)	0.50
R putamopallidum	46.9 (155.2),	0.80	-246.4 (248.4)	0.30	237.2 (171.0)	0.20	97.2 (156.1)	0.50	152.9 (249.7)	0.50	-17.1 (171.9)	0.70
Inter-caudate	344.4 (245.8)	0.20	105.7 (214.3)	0.60	-65.4 (183.9)	0.70	13.0 (253.4)	0.90	258.0 (220.9)	0.20	196.2 (189.6)	0.30
L putamen-R caudate	130.4 (136.1)	0.30	46.3 (141.5)	0.70	138.9 (117.1)	0.20	-63.7 (133.4)	0.60	210.4 (138.7)	0.10	-60.7 (114.8)	0.60
Extrinsic basal ganglia connections												
L caudothalamus	407.4 (241.7)	0.10	347.0 (337.5)	0.30	-37.1 (259.1)	0.90	**848.6 (214.3)**	**0.0002**	-27.7 (299.3)	0.90	150.2 (229.7)	0.50
L putamothalamus	407.4 (241.7)	0.10	247.0 (227.5)	0.30	-37.1 (259.1)	0.90	**848.6 (214.3)**	**0.0002**	-27.7 (299.3)	0.90	150.2 (229.7)	0.50
L pallidothalamus	175.1 (217.3)	0.40	-196.7 (303.9)	0.50	-157.8 (247.7)	0.50	**706.6 (191.7)**	**0.0006**	-4.2 (268.0)	1.00	64.3 (218.5)	0.80
R caudothalamus	347.9 (282,9)	0.20	99.2 (359.9)	0.80	-212.3 (297.1)	0.50	**769.2 (259.5)**	**0.005**	196.8 (330.2)	0.50	170.8 (272.50)	0.50
R putamothalamus	363.7 (339.2)	0.30	-19.0 (392.4)	0.90	-254.4 (378.1)	0.50	457.8 (323.5)	0.20	160.6 (374.3)	0.70	-332.7 (360.7)	0.40
R pallidothalamus	151.2 (295.3)	0.60	-198.5 (337.0)	0.50	41.8 (243.7)	0.90	134.7 (291.9)	0.60	109.1 (333.1)	0.70	21.7 (240.8)	0.90
L caudate-R thalamus	-39.4 (174.8)	0.80	152.4 (160.8)	0.30	143.3 (10.2)	0.30	110.7 (186.0)	0.50	124.2 (171.1)	0.50	46.8 (159.9)	0.80
L putamen-R thalamus	-132.7 (199.8)	0.30	194.8 (138.0)	0.20	170.9 (119.7)	0.20	-29.1 (128.4)	0.80	198.5 (147.9)	0.20	96.5 (128.3)	0.40
L pallidum-R thalamus	-42.5 (122.4)	0.30	97.7 (127.9)	0.40	114.7 (111.7)	0.30	-136.9 (127.6)	0.30	149.1 (133.5)	0.30	52.7 (116.5)	0.60
R caudate-L thalamus	272.5 (299.2)	0.40	124.7 (166.5)	0.40	157.1 (134.4)	0.20	393.7 (314.2)	0.20	32.3 (174.9)	0.80	-4.8 (141.2)	1.00
R putamen-L thalamus	106.1 (162.4)	0.50	183.6 (135.7)	0.20	85.1 (170.2)	0.60	36.8 (163.5)	0.80	90.2 (136.6)	0.50	-31.4 (171.4)	0.80

R pallidum-L thalamus	100.7 (181.1)	0.60	218.3 (158.4)	0.20	-26.8 (185.3)	0.90	-172.6 (171.9)	0.30	31.1 (150.4)	0.80	-181.7 (175.9)	0.30
R putamocerebellar	63.1 (136.6)	0.60	68.6 (253.9)	0.80	-80.3 (210.6)	0.70	132.2 (133.4)	0.30	80.1 (248.0)	0.70	-89.1 (105.6)	0.70
R pallidocerebellar	55.6 (173.4)	0.70	182.5 (226.1),	0.40	-180.3 (143.8)	0.20	**435.5 (162.1)**	**0.01**	-110.6 (211.4)	0.60	-21.1 (134.5)	0.90
Cerebellothalamic group												
L thalamocerebellar	-41.0 (189.8)	0.80	46.8 (226.3)	0.80	-169.9 (179.2)	0.30	230.1 (190.0)	0.20	-24.4 (226.6)	0.90	-147.1 (179.4)	0.40
R thalamocerebellar	67.9 (181.2)	0.70	642.5 (389.2)	0.10	-289.9 (162.7)	0.08	325.2 (182.2	0.08	24.9 (391.1)	0.90	162.9 (163.4)	0.30
L thalamo-vermis	138.1 (133.7)	0.30	34.5 (215.2)	0.90	122.3 (161.7)	0.40	18.0 (133.0)	0.90	169.1 (214.0)	0.40	-34.0 (160.8)	0.80
R thalamo-vermis	153.3 (163.1)	0.30	221.3 (200.5)	0.30	-127.4 (162.3),	0.60	15.1 (163.1)	0.90	195.9 (200.6)	0.30	168.4 (162.2)	0.30
Interthalami	-273.3 (294.9)	0.30	327.2 (224.1)	0.10	95.0 (173.5)	0.06	-313.6 (313.5)	0.30	64.9 (238.2)	0.80	-26.2 (184.4)	0.90
L cerebello-vermis	396.0 (203.2)	0.60	389.9 (508.6)	0.40	94.1 (261.3)	0.70	**686.3 (168.7)**	**0.0001**	246.7 (422.1)	0.60	-425.4 (216.8)	0.06
R cerebello-vermis	**450.2 (208.0)**	**0.03**	262.8 (278.2)	0.30	59.4 (207.9)	0.80	**848.6 (214.3)**	**0.0002**	176.1 (257.8)	0.50	-211.4 (192.7)	0.30
Intercerebelli	**428.9 (207.3)**	**0.04**	594.0 (368.2)	0.10	-5.4 (221.2)	1.00	**561.1 (199.8)**	**0.007**	407.2 (354.9)	0.20	71.6 (213.2)	0.70
	Language						**Eye & Hand coordination**					
	HUU		**HEU-preconception**		**HEU-postconception**		**HUU**		**HEU-preconception**		**HEU-postconception**	
	β (std err.)	**p**	**β (std err.)**	**p**	**β (std err.)**	**p**	**β (std err.)**	**p**	**β (std err.)**	**p**	**β (std err.)**	p
Intrinsic Basal ganglia connections												
L caudoputamen	434.5 (262.9)	0.10	-99.7 (367.1)	0.80	-106.7 (251.8)	0.70	**656.7 (322.6)**	0.05	262.0 (450.5)	0.60	65.6 (309.0)	0.80
L caudopallidum	207.7 (220.9)	0.30	-190.4 (307.1)	0.50	-11.6 (199.9)	0.90	**751.8 (266.0)**	0.007	31.7 (369.7)	0.90	112.5 (240.6)	0.60
L putamopallidum	218.3 (188.1)	0.20	-38.3 (202.4)	0.80	262.9 (220.3)	0.20	**717.6 (227.1)**	0.003	121.7 (244.4)	0.60	135.6 (265.9)	0.60
R caudoputamen	15.9 (210.5)	0.90	-181.4 (372.8)	0.60	-88.9 (262.0)	0.70	500.5 (262.1)	0.06	-248.0 (464.3)	0.60	438.9 (326.3)	0.20
R caudopallidum	-66.4 (197.2)	0.70	21.1 (288.7)	0.90	-120.3 (282.8)	0.70	331.3 (243.9)	0.20	84.7 (357.1)	0.80	478.6 (249.8)	0.20
R putamopallidum	-125.3 (158.2)	0.40	-99.2 (253.1)	0.70	19.2 (174.3)	0.90	288.1 (199.5)	0.10	203.5 (319.2)	0.50	101.6 (219.8)	0.60
Inter-caudate	-67.4 (247.9)	0.90	292.7 (216.1	0.20	159.7 (185.6)	0.40	434.5 (315.9)	0.20	628.2 (275.4)	0.03	46.8 (236.4)	0.80
L putamen-R caudate	-163.0 (135.6)	0.20	56.1 (140.9)	0.70	55.1 (116.7)	0.60	259.4 (173.8)	0.10	224.3 (180.7)	0.20	70.9 (149.3)	0.60

Extrinsic basal ganglia connections												
L caudothalamus	**506.1 (237.1)**	**0.04**	15.7 (331.0)	1.00	-247.4 (254.1)	0.30	**926.6 (290.2)**	**0.002**	388.4 (405.2)	0.30	-3.9 (311.1)	1.00
L putamothalamus	**506.1 (237.1)**	**0.04**	15.7 (331.0)	1.00	-247.4 (254.1)	0.30	**926.6 (290.2)**	**0.002**	388.6 (405.2)	0.30	13.9 (311.1)	1.00
L pallidothalamus	**419.2 (211.1)**	**0.05**	28.4 (295.2)	0.90	-82.9 (240.6)	0.70	**664.5 (260.7)**	**0.01**	440.1 (364.6)	0.20	187.5 (297.1)	0.50
R caudothalamus	501.2 (277.4)	0.08	141.1 (352.9)	0.70	-172.2 (291.1)	0.50	**804.3 (345.8)**	**0.02**	525.1 (440.0)	0.20	122.9 (363.1)	0.70
R putamothalamus	197.4 (343.1)	0.60	-79.5 (396.9)	0.80	11.4 (382.5)	1.00	**1001.2 (398.9)**	**0.01**	745.4 (461.5)	0.10	552.1 (444.7)	0.22
R pallidothalamus	-45.9 (295.3)	0.90	-93.6 (337.0)	0.80	126.9 (243.7)	0.60	567.1 (361.5)	0.10	604.9 (412.6)	0.10	240.6 (298.3)	0.40
L caudate-R thalamus	9.3 (178.2)	0.90	-26.5 (163.9)	0.90	226.2 (153.1)	0.10	305.4 (221.0)	0.20	392.1 (392.1	0.06	145.4 (189.9)	0.44
L putamen-R thalamus	-131.4 (130.5)	0.30	118.3 (150.4)	0.40	111.9 (130.5)	0.40	62.7 (162.8)	0.70	196.9 (187.6)	0.30	92.1 (162.7)	0.60
L pallidum-R thalamus	-207.0 (130.2)	0.10	71.8 (136.1)	0.60	78.5 (118.8)	0.50	33.8 (163.6)	0.80	232.5 (171.1)	0.20	4.6 (149.4)	1.00
R caudate-L thalamus	477.5 (292.6)	0.10	173.5 (162.9)	0.30	94.9 (131.3)	0.50	372.0 (389.3)	0.30	249.1 (215.7)	0.20	102.6 (174.9	0.60
R putamen-L thalamus	5.1 (162.1)	1.00	207.8 (135.4)	0.10	-90.0 (169.9)	0.60	67.7 (208.9)	0.70	255.7 (174.5)	0.10	38.6 (219.0)	0.90
R pallidum-L thalamus	-237.4 (173.1)	0.20	181.2 (151.3)	0.20	-125.5 (177.1)	0.50	96.9 (229.4)	0.70	315.4 (200.6)	0.10	190.1 (234.7)	0.40
R putamocerebellar	1.4 (136.2)	1.00	42.2 (253.2)	0.90	-135.6 (210.0)	0.50	281.0 (168.9)	0.10	326.9 (313.8)	0.30	-120.8 (260.3)	0.60
R pallidocerebellar	**347.9 (168.7)**	**0.04**	47.0 (219.9)	0.80	-98.3 (139.9)	0.50	**486.6 (213.3)**	**0.02**	399.5 (278.0)	0.10	-15.9 (176.9)	0.90
Cerebellothalamic group												
L thalamocerebellar	21.1 (199.8)	0.90	1.2 (238.2	1.00	-123.6 (188.6)	0.50	144.7 (244.8)	0.50	204.0 (291.9)	0.50	111.3 (231.0)	0.60
R thalamocerebellar	160.9 (190.9)	0.40	136.5 (410.0)	0.70	28.4 (171.4)	0.90	435.5 (228.1)	0.06	**1068.6 (489.7)**	**0.03**	98.9 (204.7)	0.60
L thalamo-vermis	-48.8 (134.5)	0.70	18.7 (216.5	0.90	-133.6 (162.6)	0.40	121.9 (173.0)	0.50	69.8 (278.3)	0.80	-101.0 (209.1)	0.60
R thalamo-vermis	-115.9 (168.9)	0.50	126.3 (207.6)	0.50	33.2 (168.0)	0.40	141.4 (208.4)	0.50	476.8 (256.3)	0.07	199.0 (207.4)	0.30
Interthalami	-314.3 (318.0)	0.30	115.0 (241.6)	0.60	-98.2 (187.0)	0.60	-303.4 (372.9)	0.40	511.5 (283.3)	0.08	-55.9 (219.3)	0.80
L cerebello-vermis	**481.9 (196.7)**	**0.02**	397.4 (492.2)	0.40	-159.2 (252.9)	0.50	**878.2 (225.0)**	**0.0003**	-154.0 (563.2)	0.80	-363.8 (289.3)	0.20
R cerebello-vermis	401.6 (210.4)	0.06	221.8 (281.4)	0.40	57.3 (210.3)	0.80	**377.4 (266.8)**	**0.03**	338.0 (356.8)	0.30	17.8 (266.6)	0.90
Intercerebelli	379.9 (212.6)	0.08	283.1 (377.7)	0.40	73.6 (226.9)	0.70	**915.0 (241.0)**	**0.0004**	**893.1 (428.2)**	**0.04**	-5.6 (257.2)	1.00

	Performance						General quotient					
	HUU		HEU-preconception		HEU-postconception		HUU		HEU-preconception		HEU-postconception	
	β (std err.)	p	β (std err.)	p	β (std err.)	p	β (std err.)	p	β (std err.)	p	β (std err.)	p
Intrinsic Basal ganglia connections												
L caudoputamen	311.6 (333.2)	0.30	-156.0 (142.3)	0.70	-220.8 (319.2)	0.50	215.2 (276.6)	0.40	112.4 (386.2)	0.80	-97.7 (264.9)	0.70
L caudopallidum	225.9 (274.5)	0.40	-161.3 (381.4)	0.70	-67.9 (248.2)	0.80	**488.1 (224.2)**	**0.03**	-31.5 (311.5)	0.90	-43.8 (202.7)	0.80
L putamopallidum	285.1 (237.7)	0.20	26.8 (255.8)	0.90	-99.0 (278.4)	0.70	332.0 (197.5)	0.09	37.9 (212.50)	0.80	16.1 (231.3)	0.90
R caudoputamen	182.0 (259.9)	0.50	-617.9 (460.4)	0.20	-188.8 (323.5)	0.70	118.8 (225.8)	0.60	-157.2 (399.9)	0.70	-7.5 (281.0)	1.00
R caudopallidum	130.4 (243.1)	0.60	-183.1 (355.9)	0.60	111.5 (348.5)	0.70	108.6 (207.1)	0.60	59.1 (303.2)	0.80	84.1 (297.0)	0.80
R putamopallidum	241.6 (189.0)	0.20	-16.6 (302.4)	0.90	-340.4 (208.2)	0.10	260.8 (163.3)	0.10	58.5 (261.2)	0.80	-14.6 (179.8)	0.90
Inter-caudate	400.9 (301.9)	0.20	269.6 (263.2)	0.30	121.7 (225.9)	0.60	203.0 (184.2)	0.30	**322.2 (160.6)**	**0.05**	90.2 (137.8)	0.50
L putamen-R caudate	92.0 (167.5)	0.60	148.9 (174.2)	0.40	-159.6 (144.2)	0.20	226.4 (141.8)	0.10	167.6 (147.4)	0.30	28.8 (122.0)	0.80
Extrinsic basal ganglia connections												
L caudothalamus	411.3 (304.1)	0.20	58.4 (424.6)	0.90	-132.7 (326.0)	0.70	**681.6 (242.1)**	**0.007**	247.3 (338.0)	0.50	-121.5 (259.5)	0.60
L putamothalamus	411.3 (304.1)	0.20	58.4 (424.6)	0.90	-132.7 (326.0)	0.70	**681.6 (242.1),**	**0.007**	247.3 (338.0)	0.50	-121.5 (259.5)	0.60
L pallidothalamus	294.5 (268.9)	0.30	122.2 (376.1)	0.70	3.7 (306.5)	1.00	**480.6 (220.2)**	**0.03**	123.7 (307.9)	0.70	-20.0 (250.9)	0.90
R caudothalamus	542.8 (347.6)	0.10	-154.3 (442.3)	0.70	26.9 (365.0)	0.90	450.7 (294.4)	0.10	244.9 (374.7)	0.50	-45.7 (309.2)	0.90
R putamothalamus	**965.2 (390.3)**	**0.02**	236.3 (451.5)	0.60	-662.7 (435.1)	0.10	**889.4 (335.0)**	**0.01**	281.1 (387.6)	0.50	-87.9 (373.5)	0.80
R pallidothalamus	546.7 (352.3)	0.10	257.4 (402.1)	0.50	-323.3 (290.7)	0.30	508.6 (301.3)	0.10	183.3 (343.8)	0.60	93.0 (248.6)	0.70
L caudate-R thalamus	183.8 (228.2)	0.40	246.2 (209.9)	0.20	126.5 (196.1)	0.50	3-5.6 (187.1)	0.10	196.3 (172.1)	0.30	139.3 (160.8)	0.40
L putamen-R thalamus	25.1 (157.5)	0.90	275.8 (181.5)	0.10	131.8 (157.4)	0.40	93.8 (131.8)	0.50	259.8 (151.8)	0.09	124.4 (131.7)	0.30
L pallidum-R thalamus	-58.8 (145.9)	0.70	198.1 (152.6)	0.20	84.6 (133.2)	0.50	-96.4 (98.4)	0.30	155.1 (103.0)	0.10	70.5 (89.9)	0.40
R caudate-L thalamus	**1087.3 (366.5)**	**0.005**	110.2 (204.0)	0.60	-186.4 (164.7)	0.30	**1201.0 (279.3)**	**<0.0001**	152.9 (155.5)	0.30	39.0 (125.5)	0.70
R putamen-L thalamus	259.4 (197.5)	0.20	252.1 (164.9),	0.10	-14.9 (207.0)	0.90	**348.7 (162.7)**	**0.04**	219.2 (135.9)	0.10	-24.1 (170.5)	0.90
R pallidum-L thalamus	138.1 (221.9)	0.50	248.4 (194.0)	0.20	-121.0 (226.9)	0.60	269.6 (185.4)	0.10	211.4 (162.1)	0.20	-69.3 (189.7)	0.70

R putamocerebellar	136.1 (159.0)	0.40	-4.8 (295.5)	1.00	**-571.1 (245.1)**	**0.02**	**347.6 (131.9)**	**0.01**	120.3 (245.2)	0.60	-241.7 (203.4)	0.20
R pallidocerebellar	362.1 (204.2)	0.08	133.6 (266.2),	0.60	-320.0 (169.3)	0.06	**601.0 (161.7)**	**<0.0001**	90.5 (210.8)	0.70	-144.5 (134.1)	0.30
Cerebellothalamic group												
L thalamocerebellar	71.9 (236.7)	0.80	-153.9 (282.3)	0.60	**-446.7 (223.4)**	**0.05**	62.9 (205.4)	0.80	45.9 (244.9)	0.80	-22.6 (193.9)	0.50
R thalamocerebellar	441.6 (225.5)	0.06	646.9 (484.1)	0.20	-3.7 (202.4)	1.00	**667.0 (174.5)**	**0.0004**	506.6 (374.7)	0.20	-2.8 (156.6)	1.00
L thalamo-vermis	91.7 (160.8)	0.60	-137.1 (258.7)	0.60	**-386.2 (194.4)**	**0.05**	-1.7 (141.4)	1.00	120.9 (227.5)	0.60	-118.9 (170.9)	0.50
R thalamo-vermis	19.5 (188.8)	0.90	333.9 (232.2)	0.10	-43.3 (187.9)	0.80	42.5 (127.5)	0.70	280.4 (156.7)	0.08	43.1 (126.8)	0.70
Interthalami	316.8 (376.5)	0.40	363.8 (286.1)	0.20	-196.6 (221.4)	0.40	330.5 (311.1)	0.30	303.1 (236.4)	0.20	-105.6 (182.9)	0.60
L cerebello-vermis	194.6 (229.0)	0.40	411.1 (573.2)	0.50	**-962.6 (294.5)**	**0.002**	**420.6 (203.3)**	0.04	452.0 (598.8)	0.40	-452.2 (261.4)	0.09
R cerebello-vermis	31.1 (258.4)	0.90	374.5 (345.6)	0.30	-504.2 (258.2)	0.06	233.8 (223.5)	0.30	361.5 (298.9)	0.20	-172.2 (223.3)	0.40
Intercerebelli	84.4 (262.5)	0.70	572.9 (466.4)	0.20	-433.5 (280.1)	0.10	294.6 (222.2)	0.30	625.4 (394.7)	0.10	-105.5 (237.1)	0.60

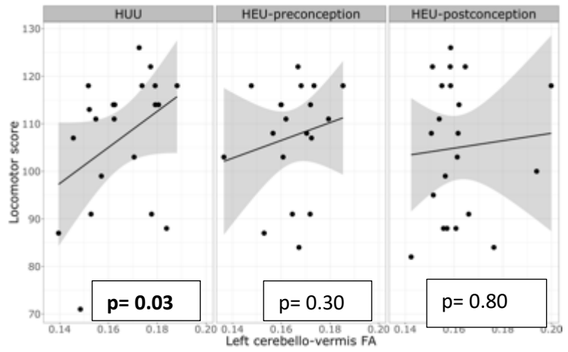
HUU
HEU-preconception
HEU-postconception
Locomotor score
Left cerebello-vermis FA
p= 0.03
p= 0.30
p= 0.80

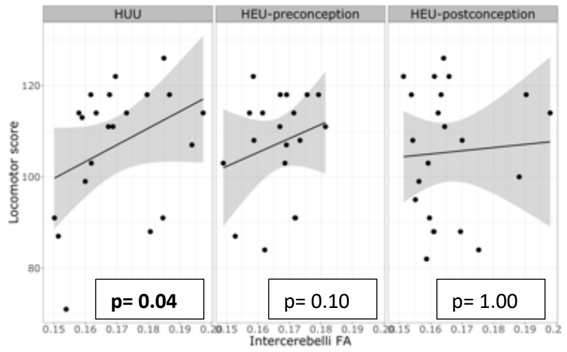
HUU
HEU-preconception
HEU-postconception
Locomotor score
Intercerebelli FA
p= 0.04
p= 0.10
p= 1.00

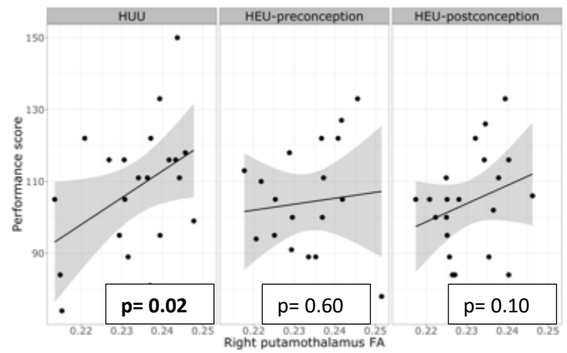
HUU
HEU-preconception
HEU-postconception
Performance score
Right putamothalamus FA
p= 0.02
p= 0.60
p= 0.10

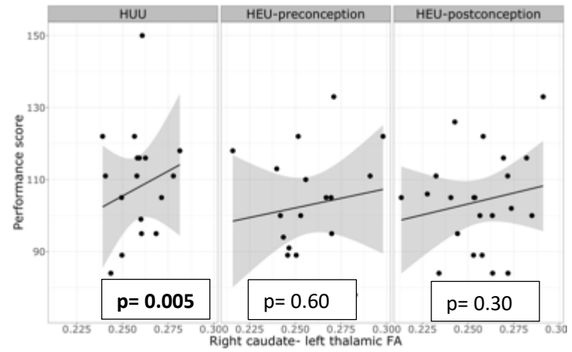
HUU
HEU-preconception
HEU-postconception
Performance score
Right caudate- left thalamic FA
p= 0.005
p= 0.60
p= 0.30

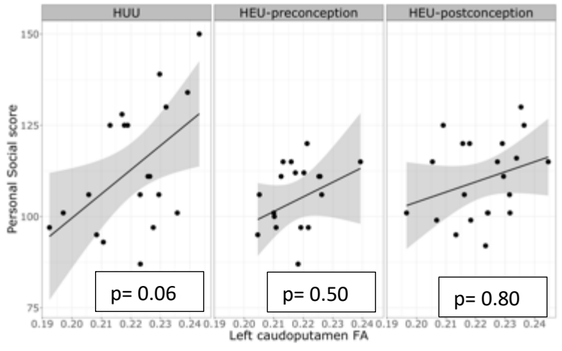
HUU
HEU-preconception
HEU-postconception
Personal Social score
Left caudoputamen FA
p= 0.06
p= 0.50
p= 0.80

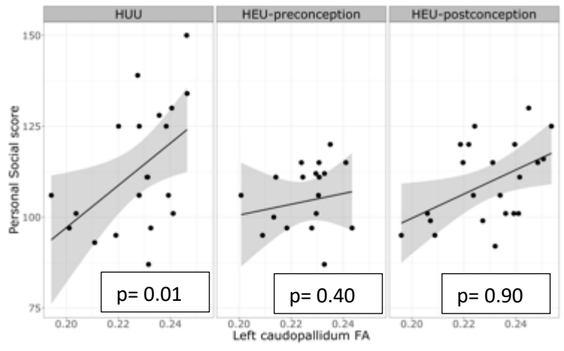
HUU
HEU-preconception
HEU-postconception
Personal Social score
Left caudopallidum FA
p= 0.01
p= 0.40
p= 0.90

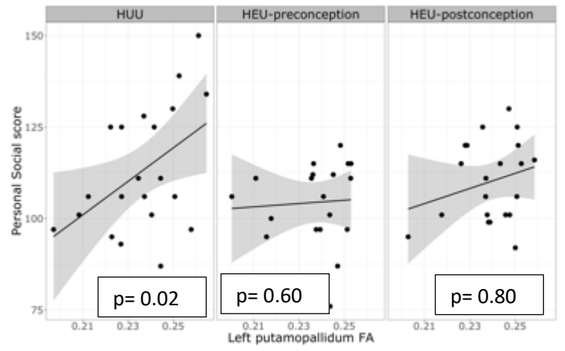
HUU
HEU-preconception
HEU-postconception
Personal Social score
Left putamopallidum FA
p= 0.02
p= 0.60
p= 0.80

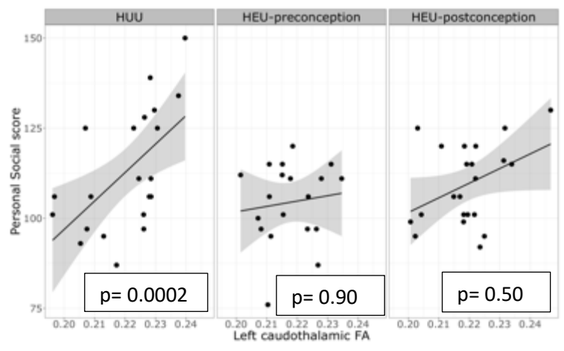
HUU
HEU-preconception
HEU-postconception
Personal Social score
Left caudothalamic FA
p= 0.0002
p= 0.90
p= 0.50

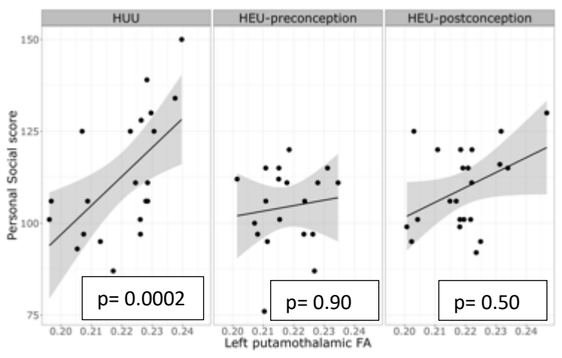
HUU
HEU-preconception
HEU-postconception
Personal Social score
Left putamothalamic FA
p= 0.0002
p= 0.90
p= 0.50

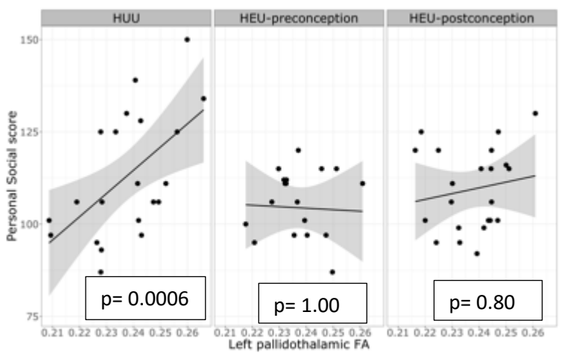
HUU
HEU-preconception
HEU-postconception
Personal Social score
Left pallidothalamic FA
p= 0.0006
p= 1.00
p= 0.80

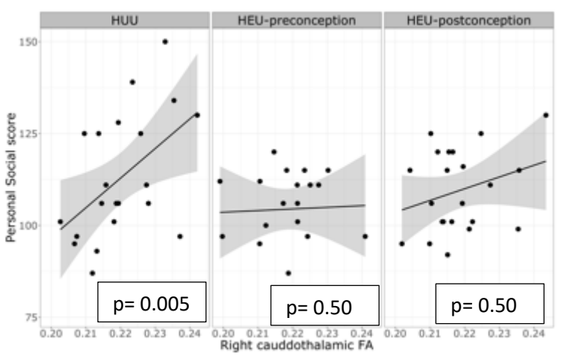
HUU
HEU-preconception
HEU-postconception
Personal Social score
Right cauddothalamic FA
p= 0.005
p= 0.50
p= 0.50

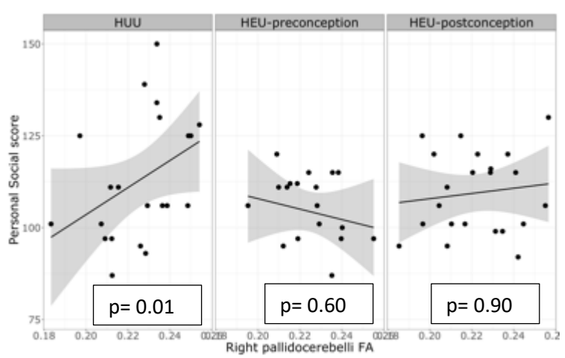
HUU
HEU-preconception
HEU-postconception
Personal Social score
Right pallidocerebelli FA
p= 0.01
p= 0.60
p= 0.90

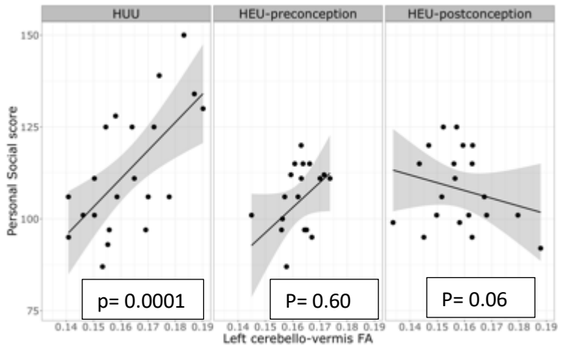
HUU
HEU-preconception
HEU-postconception
Personal Social score
Left cerebello-vermis FA
p= 0.0001
P= 0.60
P= 0.06

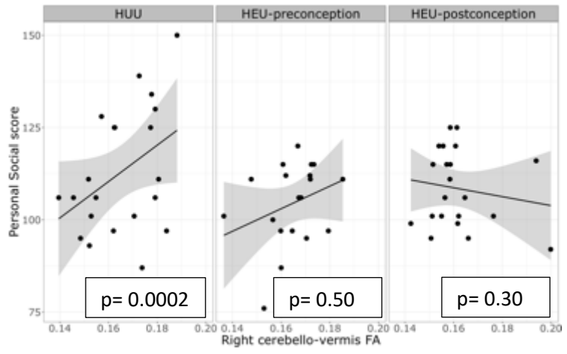
HUU
HEU-preconception
HEU-postconception
Personal Social score
Right cerebello-vermis FA
p= 0.0002
p= 0.50
p= 0.30

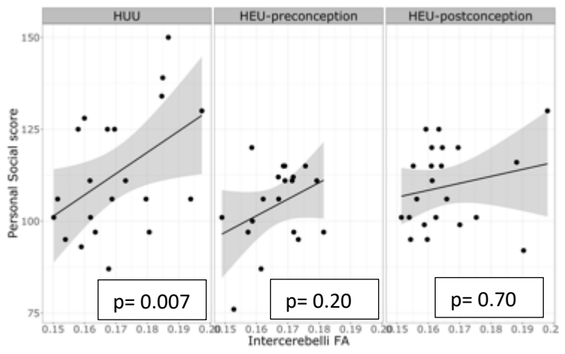
HUU
HEU-preconception
HEU-postconception
Personal Social score
Intercerebelli FA
p= 0.007
p= 0.20
p= 0.70

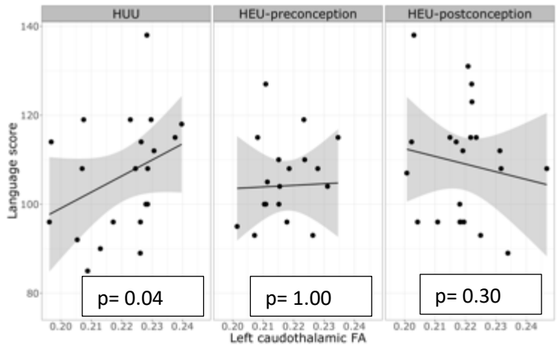
HUU
HEU-preconception
HEU-postconception
Language score
Left caudothalamic FA
p= 0.04
p= 1.00
p= 0.30

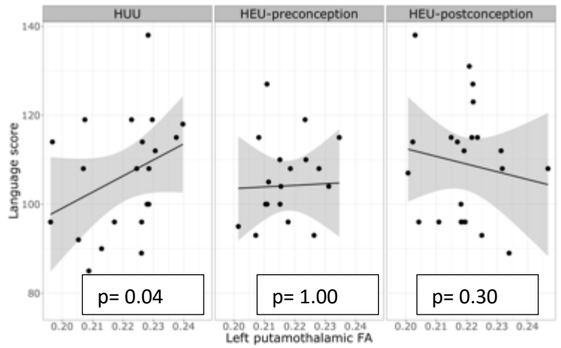
HUU
HEU-preconception
HEU-postconception
Language score
Left putamothalamic FA
p= 0.04
p= 1.00
p= 0.30

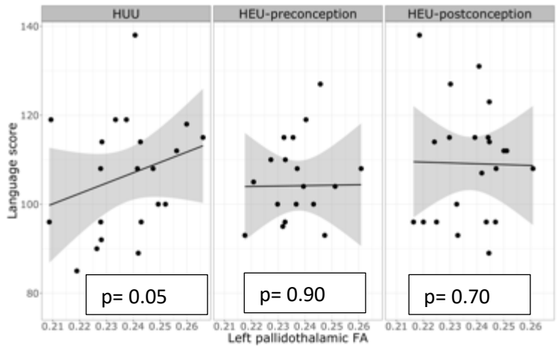
HUU
HEU-preconception
HEU-postconception
Language score
Left pallidothalamic FA
p= 0.05
p= 0.90
p= 0.70

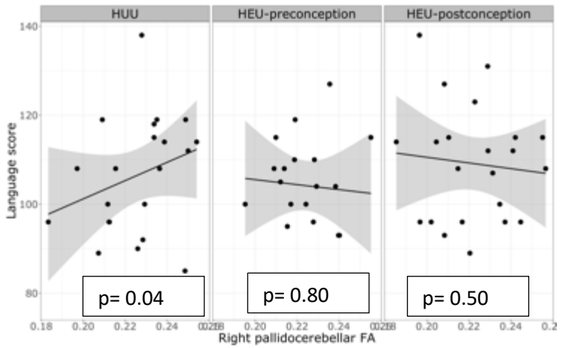
HUU
HEU-preconception
HEU-postconception
Language score
Right pallidocerebellar FA
p= 0.04
p= 0.80
p= 0.50

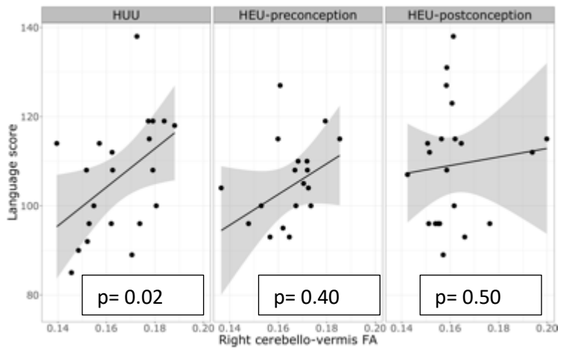
HUU
HEU-preconception
HEU-postconception
Language score
Right cerebello-vermis FA
p= 0.02
p= 0.40
p= 0.50

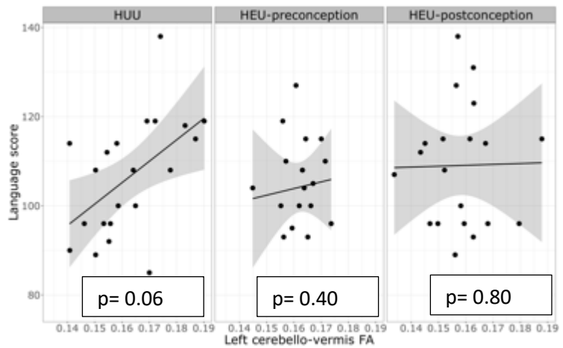
HUU
HEU-preconception
HEU-postconception
Language score
Left cerebello-vermis FA
p= 0.06
p= 0.40
p= 0.80

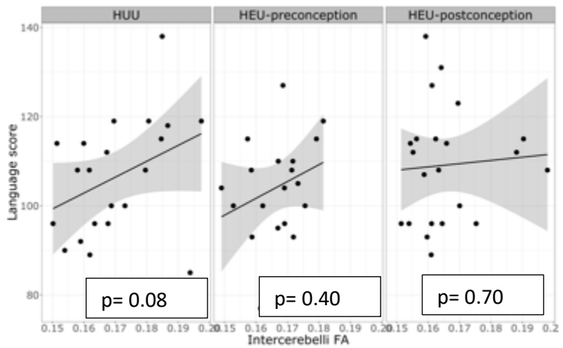
HUU
HEU-preconception
HEU-postconception
Language score
Intercerebelli FA
p= 0.08
p= 0.40
p= 0.70

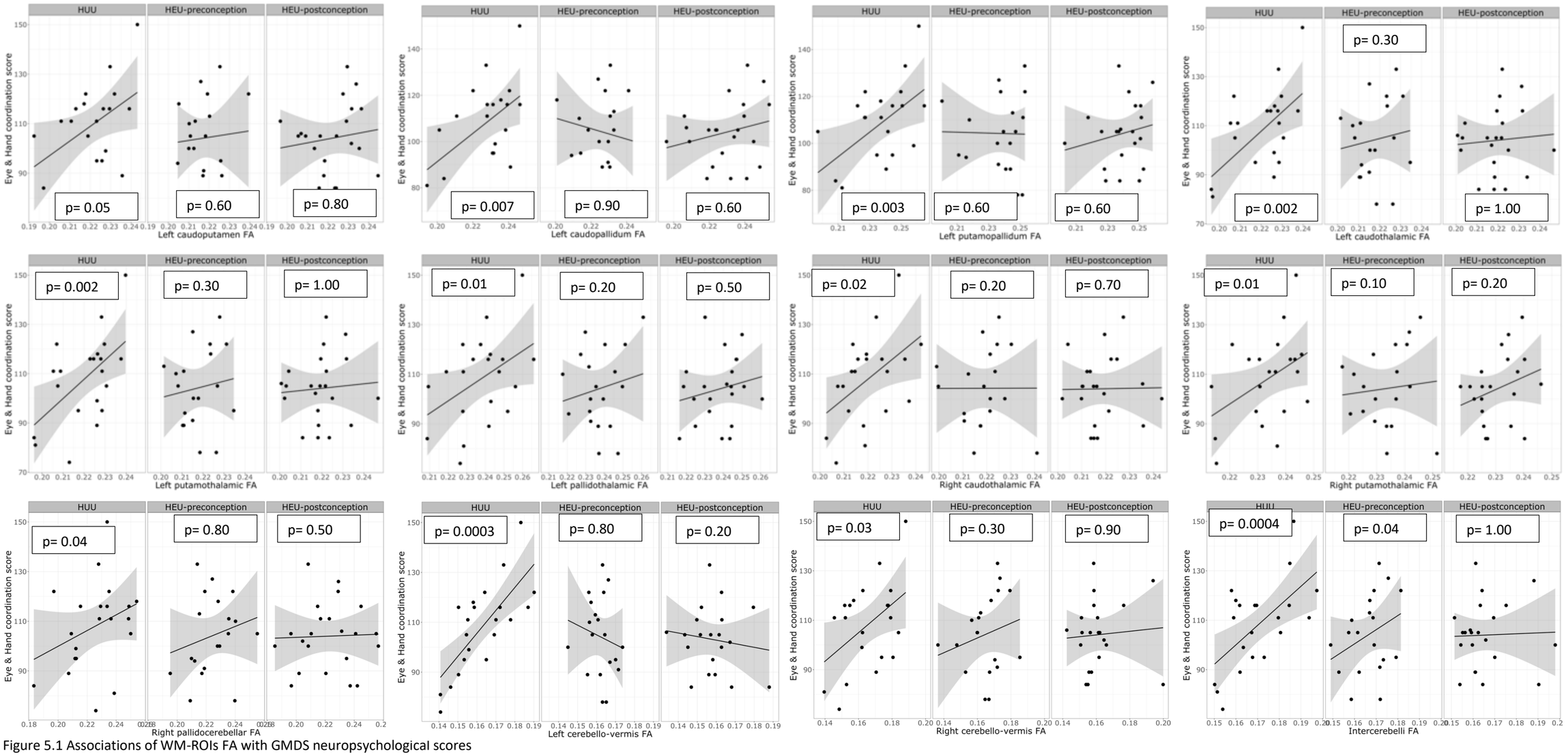

Figure 5.1 Associations of WM-ROIs FA with GMDS neuropsychological scores

Table 5.3 Associations of WM-ROIs MD with GMDS neuropsychological scores

	Locomotion						**Personal Social**					
	HUU		**HEU-preconception**		**HEU-postconception**		**HUU**		**HEU-preconception**		**HEU-postconception**	
	β (std err.)	**p**	**β (std err.)**	**p**	**β (std err.)**	**p**	**β (std err.)**	**p**	**β (std err.)**	**p**	**β (std err.)**	**p**
Intrinsic Basal ganglia connections												
L caudoputamen	29.4 (62.2)	0.60	-123.5 (72.2)	0.09	67.0 (64.4)	0.30	-71.3 (64.2)	0.30	7.6 (74.6)	0.90	-102.7 (66.5)	0.10
L caudopallidum	-4.1 (43.5)	0.90	**-133.9 (63.2)**	**0.04**	-17.4 (51.4)	0.70	-10.0 (43.8)	0.80	-7.3 (83.6)	0.90	-77.7 (51.7)	0.10
L putamopallidum	21.1 (50.5)	0.70	-97.7 (74.3)	0.20	1.9 (45.1)	1.00	-20.0 (47.5)	0.70	-34.1 (69.9)	0.60	**-106.6 (42.5)**	**0.01**
R caudoputamen	79.8 (50.4)	0.10	-124.7 (84.6)	0.10	91.5 (77.0)	0.20	-62.4 (55.9)	0.30	-32.6 (93.7)	0.70	-34.2 (85.3)	0.70
R caudopallidum	35.3 (52.3)	0.50	-102.3 (62.4)	0.10	58.7 (57.2)	0.30	25.3 (53.6)	0.60	-14.0 (63.9)	0.80	-51.9 (58.6)	0.40
R putamopallidum	41.7 (44.8)	0.30	-10.3 (67.1)	0.90	88.1 (46.9)	0.07	-5.6 (45.0)	0.90	-10.9 (67.4)	0.90	-73.3 (47.2)	0.10
Inter-caudate	-50.1 (39.1)	0.20	-18.2 (36.9)	0.60	-3.6 (44.9)	0.90	-29.7 (38.8)	0.40	-27.6 (36.6)	0.40	-15.0 (44.5)	0.70
L putamen-R caudate	109.8 (61.3)	0.08	-23.3 (55.9)	0.70	29.9 (53.6)	0.60	60.3 (63.5)	0.40	-58.7 (57.9)	0.30	-34.5 (55.6)	0.50
Extrinsic basal ganglia connections												
L caudothalamus	-4.1 (61.6)	0.90	-120.7 (75.7)	0.10	29.6 (68.8)	0.70	-25.0 (63.8)	0.70	0.9 (78.4)	1.00	-37.9 (71.2)	0.60
L putamothalamus	-4.1 (61.6)	0.90	-120.7 (75.7)	0.10	29.6 (68.8)	0.70	-25.0 (63.8)	0.70	0.9 (78.4)	1.00	-37.7 (71.2)	0.60
L pallidothalamus	-37.8 (72.6)	0.60	-122.1 (82.5)	0.10	35.4 (50.6)	0.50	89.4 (72.1)	0.20	-32.1 (81.9)	0.70	-90.2 (50.3)	0.08
R caudothalamus	114.0 (61.2)	0.07	-75.8 (72.6)	0.30	61.3 (77.5)	0.40	-0.8 (67.6)	1.00	-21.0 (80.2)	0.80	-51.6 (85.6)	0.50
R putamothalamus	**124.8 (55.9)**	**0.03**	-72.3 (59.3)	0.20	30.5 (59.8)	0.60	24.7 (58.3)	0.70	-5.4 (61.9)	0.90	-96.7 (62.4)	0.10
R pallidothalamus	-18.0 (112.2)	1.00	-52.9 (51.4)	0.30	16.5 (71.9)	0.80	-25.9 (64.0)	0.70	12.6 (53.1)	0.80	-69.9 (74.4)	0.30
L caudate-R thalamus	-29.2 (55.1)	0.60	-69.6 (60.3)	0.20	**117.8 (41.8)**	**0.007**	-63.0 (56.9)	0.30	24.4 (62.2)	0.70	-78.7 (43.2)	0.07
L putamen-R thalamus	25.3 (41.9)	0.50	-52.2 (70.4)	0.50	67.9 (38.5)	0.08	-15.7 (42.1)	0.70	-9.0 (70.7)	0.90	-61.4 (38.6)	0.10
L pallidum-R thalamus	-15.2 (45.3)	0.70	-54.3 (52.8)	0.30	74.9 (42.5)	0.08	-40.2 (46.0)	0.40	-5.4 (53.6)	0.90	**-93.2 (43.1)**	**0.03**
R caudate-L thalamus	17.9 (50.6)	0.70	-48.9 (85.9)	0.60	-39.5 (54.6)	0.50	44.2 (49.9)	0.40	-23.6 (47.1)	0.60	-67.4 (53.8)	0.20
R putamen-L thalamus	**126.9 (50.5)**	**0.01**	-66.7 (47.8)	0.20	71.4 (42.9)	0.10	-18.3 (52.3)	0.70	-15.6 (46.6)	0.70	**-87.5 (44.4)**	**0.05**

R pallidum-L thalamus	0.3 (46.5)	1.00	-24.6 (45.0)	0.60	77.4 (51.9)	0.10	-32.8 (47.7)	0.50	-9.9 (42.8)	0.80	-85.9 (53.3)	0.10
R putamocerebellar	24.8 (76.9)	0.70	-25.6 (41.7)	0.50	-29.6 (61.2)	0.60	-30.1 (74.9)	0.70	-35.9 (82.1)	0.70	-84.8 (59.6)	0.20
R pallidocerebellar	-22.2 (85.4)	0.80	-31.2 (84.3)	0.70	-31.1 (58.1)	0.60	-24.0 (84.2)	0.80	-89.0 (81.5)	0.30	-70.7 (57.3)	0.20
Cerebellothalamic group												
L thalamocerebellar	-27.6 (79.9)	0.70	-92.9 (70.7)	0.20	80.9 (59.7)	0.20	-51.2 (83.6)	0.50	42.1 (73.9)	0.60	-60.9 (62.5)	0.30
R thalamocerebellar	64.6 (65.5)	0.30	-91.7 (83.6)	0.30	22.2 (64.2)	0.70	-35.7 (66.3)	0.60	-51.3 (84.5)	0.50	-4.1 (64.9)	0.90
L thalamo-vermis	**96.1 (48.8)**	**0.05**	-111.2 (67.7)	0.10	42.6 (56.1)	0.40	59.7 (50.9)	0.20	48.4 (70.8)	0.50	-1.5 (58.7)	1.00
R thalamo-vermis	25.4 (66.3)	0.70	-5.7 (75.1)	0.90	-13.3 (50.5)	0.80	-28.3 (65.7)	1.00	19.6 (74.4)	0.80	24.9 (50.1)	0.60
Interthalami	9.1 (62.5)	0.90	-100.2 (73.0)	0.20	96.5 (51.5)	0.07	-101.2 (63.9)	0.10	41.6 (74.7)	0.60	-95.2 (52.7)	0.08
L cerebello-vermis	90.2 (56.2)	0.10	-68.7 (56.8)	0.20	56.9 (53.0)	0.30	-54.6 (60.2)	0.40	-8.9 (60.8)	0.90	18.5 (56.8)	0.70
R cerebello-vermis	78.3 (53.1)	0.10	-41.1 (62.6)	0.50	61.5 (49.8)	0.20	-55.7 (56.0)	0.30	-27.3 (66.0)	0.70	12.5 (52.5)	0.80
Intercerebelli	-45.6 (75.2)	0.50	-58.1 (52.2)	0.20	19.2 (56.3)	0.70	-32.5 (78.2)	0.70	-2.6 (54.3)	1.00	-10.5 (58.5)	0.80
	Language						**Eye & Hand coordination**					
	HUU		**HEU-preconception**		**HEU-postconception**		**HUU**		**HEU-preconception**		**HEU-postconception**	
	β (std err.)	**p**	**β (std err.)**	**p**	**β (std err.)**	**p**	**β (std err.)**	**p**	**β (std err.)**	**p**	**β (std err.)**	p
Intrinsic Basal ganglia connections												
L caudoputamen	-93.0 (63.7)	0.10	-117.2 (74.0)	0.10	-77.9 (66.0)	0.20	-29.7 (83.9)	0.70	-3.3 (97.4)	1.00	-85.9 (86.9)	0.30
L caudopallidum	-30.8 (43.6)	0.50	-80.1 (63.3)	0.20	-72.8 (51.5)	0.20	-30.2 (57.4)	0.60	-57.7 (83.3)	0.50	-69.5 (67.7)	0.30
L putamopallidum	-60.4 (47.2)	0.20	**-142.1 (69.4)**	**0.05**	-64.7 (42.1)	0.10	23.5 (63.6)	0.70	-66.1 (93.6)	0.50	**-119.2 (56.8)**	**0.04**
R caudoputamen	-97.8 (53.3)	0.07	-131.8 (89.4)	0.10	-67.7 (81.4)	0.40	38.3 (70.8)	0.60	-58.2 (118.8)	0.60	-96.4 (108.2)	0.40
R caudopallidum	-13.6 (50.5)	0.80	-104.1 (60.2)	0.09	**-125.0 (55.1)**	**0.03**	39.1 (67.1)	0.60	-82.6 (80.0)	0.30	-139.3 (73.3)	0.06
R putamopallidum	-41.4 (44.4)	0.30	**-135.6 (66.5)**	**0.05**	-17.5 (46.5)	0.70	33.8 (58.9)	0.60	-33.3 (88.2)	0.90	-78.3 (61.8)	0.20
Inter-caudate	5.8 (38.9)	0.90	-41.7 (36.7)	0.30	-42.8 (44.7)	0.30	**-97.3 (48.7)**	**0.05**	-15.8 (56.0)	0.70	-34.5 (56.0)	0.50
L putamen-R caudate	35.9 (62.3)	0.60	-59.6 (56.8)	0.30	-106.5 (54.5)	0.06	60.2 (80.4)	0.40	-80.0 (73.3)	0.30	-68.8 (70.3)	0.30

Extrinsic basal ganglia connections												
L caudothalamus	-21.2 (61.4)	0.70	-57.5 (75.4)	0.40	51.4 (68.5)	0.40	-38.5 (82.1)	0.60	-7.9 (100.1)	0.90	-74.1 (91.6)	0.40
L putamothalamus	-21.2 (61.4)	0.70	-57.5 (75.4)	0.40	51.4 (68.5)	0.40	-38.5 (82.1)	0.60	-7.9 (100.1)	0.90	-74.1 (91.6)	0.40
L pallidothalamus	47.8 (72.3)	0.50	-75.4 (82.1)	0.40	-60.5 (50.4)	0.20	-10.3 (93.1)	0.90	-141.9 (105.8)	0.20	-58.7 (64.9)	0.40
R caudothalamus	-43.7 (64.7)	0.50	-96.8 (76.8)	0.20	-96.4 (81.9)	0.20	104.9 (83.5)	0.20	-78.6 (99.0)	0.40	-90.6 (105.6)	0.40
R putamothalamus	-5.9 (54.8)	0.90	-108.2 (58.2)	0.07	-53.8 (58.6)	0.40	122.7 (75.1)	0.10	-51.1 (79.7)	0.50	-65.1 (80.3)	0.40
R pallidothalamus	-72.0 (63.2)	0.30	-57.9 (52.4)	0.30	-79.7 (73.5)	0.30	-15.5 (79.4)	0.80	-20.4 (65.8)	0.70	-32.8 (92.2)	0.70
L caudate-R thalamus	-79.5 (57.9)	0.20	-93.4 (63.5)	0.10	6.5 (44.0)	0.90	-119.6 (74.8)	0.10	-27.2 (81.9)	0.70	-58.7 (56.8)	0.30
L putamen-R thalamus	-57.4 (41.8)	0.20	-97.3 (70.2)	0.20	-15.1 (38.3)	0.70	10.5 (56.6)	0.80	46.6 (95.0)	0.60	-25.0 (51.9)	0.60
L pallidum-R thalamus	-75.8 (47.4)	0.10	-49.4 (55.2)	0.40	-33.7 (44.4)	0.40	-47.7 (61.2)	0.40	-19.3 (71.3)	0.80	-50.1 (57.4)	0.40
R caudate-L thalamus	19.6 (50.2)	0.70	-29.7 (47.4)	0.50	-87.3 (54.2)	0.10	8.9 (66.0)	0.90	-48.9 (62.3)	0.40	-41.8 (71.2)	0.60
R putamen-L thalamus	-22.4 (51.4)	0.70	-66.5 (45.8)	0.10	-31.8 (43.7)	0.50	70.0 (70.5)	0.30	2.1 (62.8)	1.00	-43.6 (60.0)	0.50
R pallidum-L thalamus	-47.7 (48.5)	0.30	-54.4 (43.5)	0.20	-27.9 (54.2)	0.60	-38.9 (60.2)	0.50	-8. 4 (54.0)	0.90	-95.9 (67.3)	0.20
R putamocerebellar	-22.2 (74.8)	0.80	-60.5 (82.0)	0.50	10.2 (59.5)	0.09	-5.0 (101.8)	1.00	32.7 (111.7)	0.80	15.2 (81.1)	0.80
R pallidocerebellar	-20.2 (84.2)	0.80	-61.5 (81.5)	0.40	-3.2 (57.3)	0.90	12.9 (113.6)	0.90	-58.8 (110.0)	0.60	-33.6 (77.3)	0.70
Cerebellothalamic group												
L thalamocerebellar	-39.5 (84.9)	0.60	-24.2 (75.2)	0.70	-57.7 (63.5)	0.40	-75.9 (105.5)	0.50	16.9 (93.3)	0.80	-106.2 (78.8)	0.20
R thalamocerebellar	-0.40 (67.1)	1.00	-45.9 (85.6)	0.60	-4.3 (65.8)	0.90	17.5 (86.1)	0.80	29.9 (109.8)	0.80	-11.6 (84.4)	0.90
L thalamo-vermis	97.4 (50.4)	0.06	-26.0 (70.0)	0.70	-28.9 (58.1)	0.60	71.5 (65.7)	0.30	19.5 (91.2)	0.80	-90.7 (75.6)	0.20
R thalamo-vermis	4.5 (66.8)	0.90	-19.2 (75.6)	0.80	-0.6 (50.9)	1.00	-68.3 (82.6)	0.40	155.2 (93.5)	0.10	14.0 (62.9)	0.80
Interthalami	-91.0 (63.9)	0.20	-70.7 (74.8)	0.30	29.3 (52.7)	0.60	-64.6 (85.2)	0.40	43.7 (99.6)	0.70	-40.4 (70.2)	0.60
L cerebello-vermis	-100.6 (59.5)	0.10	-33.6 (60.1)	0.60	-3.6 (56.2)	0.90	49.0 (76.5)	0.50	-53.6 (77.2)	0.50	-19.2 (72.1)	0.80
R cerebello-vermis	-95.8 (55.4)	0.90	-20.9 (65.3)	0.70	17.6 (51.9)	0.70	4.3 (71.2)	0.90	-89.3 (84.0)	0.30	6.5 (66.8)	0.80
Intercerebelli	**-154.5 (77.8)**	**0.05**	-17.9 (54.0)	0.70	36.7 (58.2)	0.50	-8.0 (102.0)	0.90	-66.4 (70.8)	0.30	27.0 (76.3)	0.70

	Performance						General quotient					
	HUU		HEU-preconception		HEU-postconception		HUU		HEU-preconception		HEU-postconception	
	β (std err.)	p	β (std err.)	p	β (std err.)	p	β (std err.)	p	β (std err.)	p	β (std err.)	p
Intrinsic Basal ganglia connections												
L caudoputamen	-29.9 (77.3)	0.70	-89.7 (89.8)	0.30	**-190.1 (80.1)**	**0.02**	-107.2 (67.0)	0.10	-74.1 (77.8)	0.30	-89.3 (69.4)	0.20
L caudopallidum	-15.6 (53.7)	0.80	-105.0 (77.0)	0.20	**-124.7 (62.6)**	**.05**	-54.8 (45.3)	0.20	-76.5 (65.8)	0.20	-82.7 (53.5)	0.10
L putamopallidum	-44.8 (56.1)	0.40	-148.7 (82.5)	0.08	**-155.7 (50.1)**	**0.003**	-54.6 (50.1)	0.30	-105.1 (73.7)	0.20	**-98.0 (44.8)**	**0.03**
R caudoputamen	5.4 (67.1)	0.90	-203.9 (112.5)	0.08	-121.2 (102.5)	0.20	-57.0 (58.2)	0.30	-120.2 (97.7)	0.20	-37.5 (89.0)	0.70
R caudopallidum	48.8 (62.0)	0.40	-138.3 (73.9)	0.07	**-157.4 (67.8)**	**0.02**	-15.6 (54.8)	0.80	-93.8 (65.3)	0.10	-101.1 (59.9)	0.10
R putamopallidum	43.4 (53.6)	0.40	-76.7 (80.2)	0.30	**-142.1 (56.1)**	**0.01**	-7.6 (48.3)	0.90	-53.4 (72.3)	0.50	-54.1 (50.6)	0.30
Inter-caudate	-69.9 (47.3)	0.10	-44.4 (44.6)	0.30	-3.8 (54.3)	0.90	-78.2 (39.9)	0.06	-29.5 (37.7)	0.40	-31.5 (35.8)	0.50
L putamen-R caudate	121.1 (73.8)	0.10	-108.1 (67.3)	0.10	-78.7 (64.6)	0.20	20.4 (66.8)	0.80	-80.5 (60.9)	0.20	-66.2 (58.4)	0.30
Extrinsic basal ganglia connections												
L caudothalamus	-24.3 (76.4)	0.70	-121.4 (93.9)	0.20	-121.6 (85.2)	0.20	-76.4 (66.6)	0.20	-79.6 (81.8)	0.30	-34.3 (74.3)	0.60
L putamothalamus	-24.3 (76.4)	0.70	-121.4 (93.9)	0.20	121.6 (85.2)	0.20	-76.4 (66.6)	0.20	-79.6 (81.8)	0.30	34.3 (74.3)	0.60
L pallidothalamus	-54.4 (81.6)	0.50	**-209.2 (92.7)**	**0.03**	-97.6 (56.9)	0.09	-81.3 (76.9)	0.30	-118.7 (87.4)	0.20	-54.6 (53.6)	0.30
R caudothalamus	26.6 (79.9)	0.70	-136.5 (94.7)	0.10	-170.2 (101.0)	0.10	-39.1 (69.7)	0.60	-88.7 (82.6)	0.30	-36.8 (88.1)	0.70
R putamothalamus	105.1 (65.9)	0.10	-104.4 (70.0)	0.10	**-221.2 (70.5)**	**0.003**	26.8 (61.5)	0.70	-62.1 (65.3)	0.30	-73.8 (65.8)	0.30
R pallidothalamus	27.4 (72.3)	0.70	-49.1 (59.9)	0.40	-152.8 (84.0)	0.07	-59.3 (65.5)	0.40	-24.2 (54.3)	0.60	52.0 (76.1)	0.50
L caudate-R thalamus	13.3 (71.1)	0.80	-70.0 (77.8)	0.40	**-110.0 (54.0)**	**0.04**	-44.1 (62.7)	0.50	-50.2 (68.6)	0.50	-23.4 (47.6)	0.60
L putamen-R thalamus	7.1 (50.4)	0.90	-97.9 (84.6)	0.20	**-118.7 (46.2)**	**0.01**	3.7 (45.7)	0.90	-62.5 (76.8)	0.40	-33.9 (42.0)	0.40
L pallidum-R thalamus	-24.0 (54.3)	0.70	-73.6 (63.3)	0.20	**-166.2 (51.0)**	**0.002**	-53.4 (49.5)	0.30	-51.3 (57.6)	0.40	-64.1 (46.4)	0.20
R caudate-L thalamus	74.7 (59.3)	0.20	-109.5 (56.0)	0.06	-109.6 (64.0)	0.09	18.9 (52.4)	0.70	-64.6 (49.4)	0.20	-83.2 (56.5)	0.10
R putamen-L thalamus	108.4 (62.9)	0.09	-58.8 (56.1)	0.30	**-126.0 (53.5)**	**0.02**	61.7 (56.5)	0.30	-39.4 (50.4)	0.40	54.0 (48.0)	0.30
R pallidum-L thalamus	33.4 (57.3)	0.60	-40.9 (51.4)	0.40	**-159.5 (64.0)**	**0.02**	-6.8 (50.3)	0.90	-30.0 (45.1)	0.50	-71.7 (56.2)	0.20

R putamocerebellar	59.7 (92.9)	0.50	-78.2 (101.9)	0.40	-103.2 (74.0)	0.20	-36.0 (82.2)	0.70	-81.3 (90.2)	0.40	-21.5 (65.4)	0.70
R pallidocerebellar	46.8 (106.5)	0.70	-159.9 (103.1)	0.10	-59.4 (72.4)	0.40	-22.5 (90.6)	0.80	-128.9 (87.8)	0.10	-43.1 (61.7)	0.50
Cerebellothalamic group												
L thalamocerebellar	-8.9 (101.7)	0.90	-87.6 (90.0)	0.30	-177.6 (76.0)	0.10	-125.0 (87.0)	0.10	-46.1 (77.0)	0.50	-52.1 (65.0)	0.40
R thalamocerebellar	26.7 (82.1)	0.70	-117.5 (104.7)	0.30	-34.2 (80.5)	0.70	-19.7 (69.8)	0.80	-95.9 (88.9)	0.30	0.33 (68.4)	1.00
L thalamo-vermis	45.4 (62.4)	0.50	-72.8 (86.6)	0.40	-71.4 (71.8)	0.30	2.8 (54.7)	0.90	-31.6 (75.9)	0.70	-37.9 (62.9)	0.50
R thalamo-vermis	-38.5 (80.3)	0.60	72.8 (90.9)	0.40	-22.3 (61.2)	0.70	-40.3 (69.5)	0.60	19.3 (78.7)	0.80	14.5 (52.9)	0.80
Interthalami	41.6 (82.8)	0.60	-56.2 (96.8)	0.60	-127.3 (68.3)	0.07	-23.8 (71.1)	0.70	-37.1 (83.1)	0.60	-24.8 (68.6)	0.70
L cerebello-vermis	41.3 (72.7)	0.60	-119.8 (73.4)	0.10	-44.4 (68.6)	0.50	17.9 (63.2)	0.80	-74.0 (63.8)	0.20	6.1 (59.6)	0.90
R cerebello-vermis	-7.6 (67.8)	0.90	-130.5 (79.9)	0.10	-59.9 (63.6)	0.30	-45.6 (58.8)	0.40	-75.5 (69.3)	0.30	2.8 (55.1)	0.90
Intercerebelli	-103.8 (95.3)	0.30	-114.2 (66.1)	0.09	-71.4 (71.3)	0.30	-122.7 (82.9)	0.20	-69.0 (57.6)	0.20	13.1 (62.1)	0.80

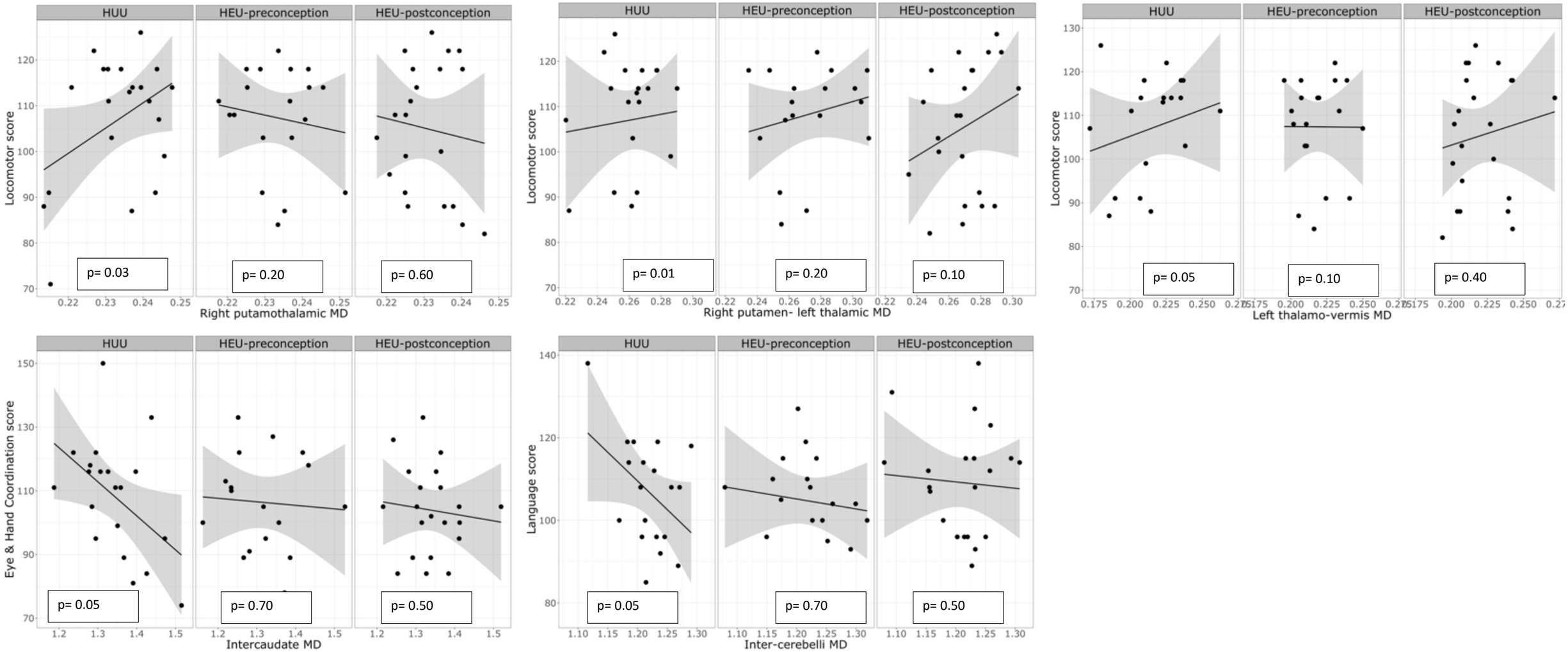

Figure 5.2 Associations of WM-ROIs MDs with GMDS neuropsychological scores.

5.3 Discussion

This chapter examined the prospective associations of WM DTI measures in neonates with neurodevelopmental outcomes at 9- to 12-months in typical development relative to in utero HIV and ART exposure. We hypothesized that tracts altered by HIV exposure would affect neuropsychological scores in HEU infants. And we expected associations would be independent of infants ART exposure duration. We report no associations between the compromised tracts, the R putamen – L thalamus and the R caudothalamus, and any GMDS domain. The lack of associations between the reported implicated WM tracts and cognitive domains may be due to the non-involvement of these tracts in any of the functional domains examined. This is supported by the observation that these tracts were not associated with any GMDS domain in typically developing infants.

In typically developed (HUU) infants, we found numerous WM tracts in early infancy to be associated with neurodevelopmental scores in late infancy. FA was positively associated with all domains of GMDS, suggesting a pivotal role of typical WM anisotropic diffusion in the developmental trajectory of infants. We found at least one white matter tract to be associated with all the assessed neurocognitive domains (table 5.2 and figure 5.1). By contrast, MD was prospectively associated with three of the six GMDS domains assessed.

Associations in typically developing infants

The late fetal period and early infancy are marked by rapid brain development (Stiles and Jernigan, 2010). These changes occur in tandem with the development of cognitive and behavioral functions shaped by environment and experience (Weisleder and Fernald, 2013). White matter maturation is dynamic - it is regional and functional network-specific, depending on the WM tracts recruited for a specific function or wide range of functions. Our focus is on WM tracts connecting BG to the thalamus, BG to the cerebellum, and the thalamus to cerebellar hemispheres and their relationship with neurodevelopmental domains in late infancy. In our cohort, HUU infants demonstrated positive associations between FA and neuropsychological scores in all domains. These results are similar to previous studies looking at FA and neurocognitive outcomes in healthy infants and children (Zuk et al., 2021, Meijer et al., 2021, Dowe et al., 2020, Sket et al., 2019, Feng et al., 2019, Schmithorst et al., 2005).

Typical white matter development and locomotor related skills

Two GMDS quotients are related to motor skills. The Locomotor quotient measures gross motor ability, and the Eye and Hand coordination domain measures fine motor-related skills. We identified two intrinsic cerebellar WM tracts where FA was positively associated with locomotor scores. This result suggests a role of cerebellar connectivity in gross motor control. Damage to the cerebellum is associated with impaired voluntary control of limb movement and predictive motor timing (Timmann et al., 2008, Bares

et al., 2007, Topka et al., 1998). Multiple WM tracts were positively associated with Eye & Hand coordination scores. These tracts included intrinsic basal ganglia circuitry, striatal-thalamic, and intrinsic cerebellar pathways. The association of the intrinsic basal ganglia circuit FA with Eye & Hand coordination scores was observed on the left hemisphere only. This suggests that the functional contribution of the intrinsic basal ganglia pathways in the control of Eye & Hand coordination is left hemispheric dominant. Gerardin and colleagues provide evidence of the role of the striatum in eye and hand movements (Gerardin et al., 2003), and a substantial body of evidence has documented the roles of the cerebellum in the control of eye movement (Beh et al., 2017, Patel and Zee, 2015, Kheradmand and Zee, 2011).

Typical WM development and language skills

Here, we found a few WM tracts in the extrinsic basal ganglia connections, mainly in the striatal-thalamic pathways, to be positively associated with language scores. In addition to striatal-thalamic connectivity, intrinsic cerebellar WM tracts were also positively related to language skills. These findings suggest the role of striatal-thalamic and intrinsic cerebellar pathways in language. Zuk et al. recently examined the associations between WM microstructure in early infancy and language ability at kindergarten in healthy subjects. They reported a positive association between arcuate fasciculus FA with phonological awareness and vocabulary knowledge; left corticospinal tract FA with phonological awareness, and bilateral corticospinal tract FA with phonological memory after controlling for age, cognitive, and environmental factors. They posited that the structural foundation of future language ability was present since infancy (Zuk et al., 2021). Although our WM-ROIs are different from that of Zuk et al.'s, our study suggests the involvement of basal ganglia and cerebellar pathways in language processing as previously reported by other studies (Crosson, 2021, Barbas et al., 2013, Ford et al., 2013, Gil Robles et al., 2005).

Cognitive ability and behaviour

Performance and Personal Social quotients of the GMDS measure cognition and behaviors, respectively. We observed two WM pathways associated with performance scores. The two WM pathways, the ipsilateral putamothalamic, and right caudate- left thalamic are right hemispheric domiciled with contribution from the left thalamus. This finding further substantiates a right hemispheric dominance of visuospatial skills in healthy patients (Everts et al., 2009). We found several WM pathways relating to Personal Social scores. The WM pathways recruited by HUU infants for this domain come from left hemispheric basal ganglia intrinsic pathways, left striatal-thalamic connections, and bilateral cerebellar WM connection. Attention is thought to precondition a better cognitive ability and behaviors (Pérez-Edgar et al., 2014). Dowe et al. found a positive association of WM microstructures in the neonatal period with attention at six-month postnatal life in healthy infants. Increased FA in the corpus callosum and anterior cingulum were associated with better orienting behaviors (Dowe et al., 2020).

In agreement with previous studies associating increased MD with lower cognitive scores in paediatric population (Schmithorst et al., 2005), we found increased MD to be negatively associated with lower scores in two GMDS subscales, language, and eye and hand coordination. We identified two pathways, intercerebelli and intercaudate, recruited for language and eye and hand coordination domains, respectively. By contrast, we found a positive association with language scores. The pathways involved included right putamothalamic and right putamen- left thalamic. However, this finding is counterintuitive given the empirical evidence that higher MD signifies compromised WM integrity (Alexander et al., 2011, Feldman et al., 2010, Alexander et al., 2007).

Associations in HEU infants

HEU infants did not recruit any of the WM pathways used by their HUU counterparts across all domains measured. This result suggests alternate pathways are employed since we report no HIV/ART exposure performance difference between groups. The alternate pathways used may involve the tracts reported to be associated with GMDS scores only in HEU infants. Surprisingly, these alternate pathways are dependent on ART exposure duration, as the associations differ between pre- and post-conception groups. However, these tracts were not associated with ART duration in the previous chapter. The left caudopallidum, one of the tracts associated with GMDS scores in the HEU group, was associated with maternal VL presenting a possible link to maternal immune health and alternate pathways. Our results may point to disruptions dependent on ART duration in utero to white matter development between the time of scan and neuropsychological testing.

In conclusion associations between tractography outcomes and neuropsychological scores show that HUU infants utilize white matter connections within the basal ganglia and cerebellum across cognitive domains. Further associations indicate HEU infants recruit alternate white matter pathways to perform neuropsychological tasks at the same level as their HUU peers.

CHAPTER SIX

6.0 Strengths, limitations and conclusion of the thesis

6.1 Strengths and limitations

6.1.1 Strengths

This work used manual segmentation, which is the most reliable technique for mapping grey matter structures in paediatric population (Morey et al., 2009, Yoon et al., 2009). The maternal-infant pairs recruited in this study are from the same community with a homogenous socio-cultural background. Lastly, we included both in utero ART exposure duration and maternal clinical data in our statistical models. The inclusion of these variables are uncommon in the literature, and likely play a role in grey and white matter-related abnormalities in HEU infants and children.

6.1.2 Limitations

A limitation of this study is the lack of maternal immune markers throughout pregnancy. We only report maternal CD4+ cell count and viral loads at one time point (within 6 months of enrolment). And, we did not consider the exact time within this 6-month period when these immune measures were collected which may be a source of potential bias. Another limitation is that we did not quantify migratory monocytes which may be used to infer the extent of neuroinflammation. An upsurge in infected migratory monocytes is thought to initiate a pro-inflammatory pathway (Anzinger et al., 2014, Valcour et al., 2012). We did not consider cortical projections to our ROIs seeds. Cortico-striato-thalamic loop may help in better understanding of HIV-exposure related WM pathology in the studied regions. Post infancy follow-up studies are needed to clarify if these changes represent damage or delayed development over a protractive period.

6.2 Conclusion

The results documented in this thesis points to the influence of HIV exposure, ART duration and maternal immune health on fetal brain development. However, these factors impact grey and white matter differently. ART initiated pre-conception was protective of caudate volumes but did not protect two white matter connections, the WM tract between right thalamus and right caudate, and WM that between left thalamus and right putamen. Within HUU neonates, basal ganglia and cerebellar volumes and white matter connections predicted neuropsychological outcomes in late infancy. However, HEU infants did not demonstrate the same associations suggesting they utilize alternate pathways from their HUU peers. While there were no exposure related differences across neuropsychological domains, the

long-term functional consequences of altered structural recruitment is unknown. Finally, this thesis adds to the body of literature that early ART in pregnancy is neuroprotective, and that HIV exposure related structural alterations are evident as early as 2 - 4 weeks after birth.

References

ABU-RAYA, B., KOLLMANN, T. R., MARCHANT, A. & MACGILLIVRAY, D. M. 2016a. The Immune System of HIV-Exposed Uninfected Infants. *Front Immunol,* 7**,** 383.

ABU-RAYA, B., SMOLEN, K. K., WILLEMS, F., KOLLMANN, T. R. & MARCHANT, A. 2016b. Transfer of Maternal Antimicrobial Immunity to HIV-Exposed Uninfected Newborns. *Front Immunol,* 7**,** 338.

AGABU, A., BAUGHMAN, A. L., FISCHER-WALKER, C., DE KLERK, M., MUTENDA, N., RUSBERG, F., DIERGAARDT, D., PENTIKAINEN, N., SAWADOGO, S., AGOLORY, S. & DINH, T. H. 2020. National-level effectiveness of ART to prevent early mother to child transmission of HIV in Namibia. *PLoS One,* 15**,** e0233341.

AGHAEEPOUR, N., GANIO, E. A., MCILWAIN, D., TSAI, A. S., TINGLE, M., VAN GASSEN, S., GAUDILLIERE, D. K., BACA, Q., MCNEIL, L., OKADA, R., GHAEMI, M. S., FURMAN, D., WONG, R. J., WINN, V. D., DRUZIN, M. L., EL-SAYED, Y. Y., QUAINTANCE, C., GIBBS, R., DARMSTADT, G. L., SHAW, G. M., STEVENSON, D. K., TIBSHIRANI, R., NOLAN, G. P., LEWIS, D. B., ANGST, M. S. & GAUDILLIERE, B. 2017. An immune clock of human pregnancy. *Sci Immunol,* 2.

AIZIRE, J., FOWLER, M. G. & COOVADIA, H. M. 2013. Operational issues and barriers to implementation of prevention of mother-to-child transmission of HIV (PMTCT) interventions in Sub-Saharan Africa. *Curr HIV Res,* 11**,** 144-59.

ALCOCK, K. J., ABUBAKAR, A., NEWTON, C. R. & HOLDING, P. 2016. The effects of prenatal HIV exposure on language functioning in Kenyan children: establishing an evaluative framework. *BMC Res Notes,* 9**,** 463.

ALEXANDER, A. L., HURLEY, S. A., SAMSONOV, A. A., ADLURU, N., HOSSEINBOR, A. P., MOSSAHEBI, P., TROMP DO, P. M., ZAKSZEWSKI, E. & FIELD, A. S. 2011. Characterization of cerebral white matter properties using quantitative magnetic resonance imaging stains. *Brain Connect,* 1**,** 423-46.

ALEXANDER, A. L., LEE, J. E., LAZAR, M. & FIELD, A. S. 2007. Diffusion tensor imaging of the brain. *Neurotherapeutics,* 4**,** 316-29.

ALIMENTI, A., FORBES, J. C., OBERLANDER, T. F., MONEY, D. M., GRUNAU, R. E., PAPSDORF, M. P., MAAN, E., COLE, L. J. & BURDGE, D. R. 2006. A prospective controlled study of neurodevelopment in HIV-uninfected children exposed to combination antiretroviral drugs in pregnancy. *Pediatrics,* 118**,** e1139-45.

ALTMAN, J. & BAYER, S. A. 1984. The development of the rat spinal cord. *Adv Anat Embryol Cell Biol,* 85**,** 1-164.

ALVAREZ-LINERA PRADO, J. 2012. [Structural magnetic resonance imaging in epilepsy]. *Radiologia,* 54**,** 9-20.

AMOD, Z., COCKCROFT, K. & SOELLAART, B. 2007a. Use of the 1996 Griffiths Mental Development Scales for infants: a pilot study with a Black, South African sample. *J Child Adolesc Ment Health,* 19**,** 123-30.

AMOD, Z., COCKCROFT, K. & SOELLAART, B. 2007b. Use of the 1996 Griffiths Mental Development Scales for infants: a pilot study with a Black, South African sample. *Journal of Cjild and Adolescent Health,* 19**,** 123-130.

ANAYA GARCÍA, M. S., HERNÁNDEZ ANAYA, J. S., MARRUFO MELÉNDEZ, O., VELÁZQUEZ RAMÍREZ, J. L. & PALACIOS AGUIAR, R. 2015. In vivo study of cerebral white matter in the dog using diffusion tensor tractography. *Vet Radiol Ultrasound,* 56**,** 188-95.

ANDREWS, D. S., LEE, J. K., SOLOMON, M., ROGERS, S. J., AMARAL, D. G. & NORDAHL, C. W. 2019. A diffusion-weighted imaging tract-based spatial statistics study of autism spectrum disorder in preschool-aged children. *Journal of Neurodevelopmental Disorders,* 11**,** 32.

ANDRONIKOU, S., ACKERMANN, C., LAUGHTON, B., COTTON, M., TOMAZOS, N., SPOTTISWOODE, B., MAUFF, K. & PETTIFOR, J. M. 2014. Correlating brain volume and callosal thickness with clinical and laboratory indicators of disease severity in children with HIV-related brain disease. *Childs Nerv Syst,* 30**,** 1549-57.

ANZINGER, J. J., BUTTERFIELD, T. R., ANGELOVICH, T. A., CROWE, S. M. & PALMER, C. S. 2014. Monocytes as regulators of inflammation and HIV-related comorbidities during cART. *J Immunol Res,* 2014**,** 569819.

ARCK, P. C. & HECHER, K. 2013. Fetomaternal immune cross-talk and its consequences for maternal and offspring's health. *Nat Med,* 19**,** 548-56.

ARISTIETA, A. & GITTIS, A. 2021. Distinct globus pallidus circuits regulate motor and cognitive functions. *Trends Neurosci,* 44**,** 597-599.

AVALOS, J. C., SANCHEZ, F., ROSSO, B., BESOCKE, A. G. & GARCIA, M. D. C. 2019. [Cerebral structural changes in generalized idiopathic epilepsy identified by automated magnetic resonance imaging analysis]. *Medicina (B Aires),* 79**,** 111-114.

AYLWARD, E. H., HENDERER, J. D., MCARTHUR, J. C., BRETTSCHNEIDER, P. D., HARRIS, G. J., BARTA, P. E. & PEARLSON, G. D. 1993. Reduced basal ganglia volume in HIV-1-associated dementia: results from quantitative neuroimaging. *Neurology,* 43**,** 2099-104.

BACHILLER, S., JIMÉNEZ-FERRER, I., PAULUS, A., YANG, Y., SWANBERG, M., DEIERBORG, T. & BOZA-SERRANO, A. 2018. Microglia in Neurological Diseases: A Road Map to Brain-Disease Dependent-Inflammatory Response. *Front Cell Neurosci,* 12**,** 488.

BACK, S. A., LUO, N. L., BORENSTEIN, N. S., LEVINE, J. M., VOLPE, J. J. & KINNEY, H. C. 2001. Late oligodendrocyte progenitors coincide with the developmental window of vulnerability for human perinatal white matter injury. *J Neurosci,* 21**,** 1302-12.

BAGENDA, D., NASSALI, A., KALYESUBULA, I., SHERMAN, B., DROTAR, D., BOIVIN, M. J. & OLNESS, K. 2006. Health, neurologic, and cognitive status of HIV-infected, long-surviving, and antiretroviral-naive Ugandan children. *Pediatrics,* 117**,** 729-40.

BALL, G., SRINIVASAN, L., ALJABAR, P., COUNSELL, S. J., DURIGHEL, G., HAJNAL, J. V., RUTHERFORD, M. A. & EDWARDS, A. D. 2013. Development of cortical microstructure in the preterm human brain. *Proc Natl Acad Sci U S A,* 110**,** 9541-6.

BARBAS, H., GARCÍA-CABEZAS, M. & ZIKOPOULOS, B. 2013. Frontal-thalamic circuits associated with language. *Brain Lang,* 126**,** 49-61.

BARES, M., LUNGU, O., LIU, T., WAECHTER, T., GOMEZ, C. M. & ASHE, J. 2007. Impaired predictive motor timing in patients with cerebellar disorders. *Exp Brain Res,* 180**,** 355-65.

BARRET, B., TARDIEU, M., RUSTIN, P., LACROIX, C., CHABROL, B., DESGUERRE, I., DOLLFUS, C., MAYAUX, M. J., BLANCHE, S. & FRENCH PERINATAL COHORT STUDY, G. 2003. Persistent mitochondrial dysfunction in HIV-1-exposed but uninfected infants: clinical screening in a large prospective cohort. *AIDS,* 17**,** 1769-85.

BASSER, P. J. & PIERPAOLI, C. 1996. Microstructural and physiological features of tissues elucidated by quantitative-diffusion-tensor MRI. *J Magn Reson B,* 111**,** 209-19.

BATTISTINI GARCIA, S. A. & GUZMAN, N. 2021. Acquired Immune Deficiency Syndrome CD4+ Count. *StatPearls.* Treasure Island (FL): StatPearls Publishing

BAUMAN, M. D., IOSIF, A. M., SMITH, S. E., BREGERE, C., AMARAL, D. G. & PATTERSON, P. H. 2014. Activation of the maternal immune system during pregnancy alters behavioral development of rhesus monkey offspring. *Biol Psychiatry,* 75**,** 332-41.

BAYLEY, N. 1993. Bayley Scales of Infant Development: Manual (2nd ed). *Harcourt Assessment, Tx: Psychological Corporation. St Antonio, TX*.

BAYLEY, N. 2006. Technical manual for the Bayley Scales of Infant Development (3rd ed). *Harcourt Assessment, Tx: Psychological Corporation. St Antonio, TX*.

BECKER, J. T., SANDERS, J., MADSEN, S. K., RAGIN, A., KINGSLEY, L., MARUCA, V., COHEN, B., GOODKIN, K., MARTIN, E., MILLER, E. N., SACKTOR, N., ALGER, J. R., BARKER, P. B., SAHARAN, P., CARMICHAEL, O. T. & THOMPSON, P. M. 2011. Subcortical brain atrophy persists even in HAART-regulated HIV disease. *Brain Imaging Behav,* 5**,** 77-85.

BEH, S. C., FROHMAN, T. C. & FROHMAN, E. M. 2017. Cerebellar Control of Eye Movements. *J Neuroophthalmol,* 37**,** 87-98.

BEN-ARI, Y., KHAZIPOV, R., LEINEKUGEL, X., CAILLARD, O. & GAIARSA, J. L. 1997. GABAA, NMDA and AMPA receptors: a developmentally regulated 'ménage à trois'. *Trends Neurosci,* 20**,** 523-9.

BLANCHE, S., TARDIEU, M., RUSTIN, P., SLAMA, A., BARRET, B., FIRTION, G., CIRARU-VIGNERON, N., LACROIX, C., ROUZIOUX, C., MANDELBROT, L., DESGUERRE, I., ROTIG, A., MAYAUX, M. J. & DELFRAISSY, J. F. 1999. Persistent mitochondrial dysfunction and perinatal exposure to antiretroviral nucleoside analogues. *Lancet,* 354**,** 1084-9.

BOIVIN, M. J., GREEN, S. D., DAVIES, A. G., GIORDANI, B., MOKILI, J. K. & CUTTING, W. A. 1995. A preliminary evaluation of the cognitive and motor effects of pediatric HIV infection in Zairian children. *Health Psychol,* 14**,** 13-21.

BOIVIN, M. J., MALIWICHI-SENGANIMALUNJE, L., OGWANG, L. W., KAWALAZIRA, R., SIKORSKII, A., FAMILIAR-LOPEZ, I., KUTEESA, A., NYAKATO, M., MUTEBE, A., NAMUKOOLI, J. L., MALLEWA, M., RUISEÑOR-ESCUDERO, H., AIZIRE, J., TAHA, T. E. & FOWLER, M. G. 2019. Neurodevelopmental effects of ante-partum and post-partum antiretroviral exposure in HIV-exposed and uninfected children versus HIV-unexposed and uninfected children in Uganda and Malawi: a prospective cohort study. *The Lancet HIV,* 6**,** e518 -e530.

BOUWMAN, J., MAIA, A. S., CAMOLETTO, P. G., POSTHUMA, G., ROUBOS, E. W., OORSCHOT, V. M., KLUMPERMAN, J. & VERHAGE, M. 2004. Quantification of synapse formation and maintenance in vivo in the absence of synaptic release. *Neuroscience,* 126**,** 115-26.

BOYLE, G. J., SAKLOFSKE, D. H. & MATHEWS, G. 2012. (Eds.), SAGE Benchmarks in Psychological Assesment *Clinical Neuropsychological Assessment. London: SAGE. ,* Vol. 3.

BRAHMBHATT, H., BOIVIN, M., SSEMPIJJA, V., KIGOZI, G., KAGAAYI, J., SERWADDA, D. & GRAY, R. H. 2014. Neurodevelopmental benefits of antiretroviral therapy in Ugandan children aged 0-6 years with HIV. *J Acquir Immune Defic Syndr,* 67**,** 316-22.

BROGLY, S. B., YLITALO, N., MOFENSON, L. M., OLESKE, J., VAN DYKE, R., CRAIN, M. J., ABZUG, M. J., BRADY, M., JEAN-PHILIPPE, P., HUGHES, M. D. & SEAGE, G. R., 3RD 2007. In utero nucleoside reverse transcriptase inhibitor exposure and signs of possible mitochondrial dysfunction in HIV-uninfected children. *AIDS,* 21**,** 929-38.

BROWN, A. S., BEGG, M. D., GRAVENSTEIN, S., SCHAEFER, C. A., WYATT, R. J., BRESNAHAN, M., BABULAS, V. P. & SUSSER, E. S. 2004. Serologic evidence of prenatal influenza in the etiology of schizophrenia. *Arch Gen Psychiatry,* 61**,** 774-80.

BROWN, C. J., MILLER, S. P., BOOTH, B. G., ANDREWS, S., CHAU, V., POSKITT, K. J. & HAMARNEH, G. 2014. Structural network analysis of brain development in young preterm neonates. *Neuroimage,* 101**,** 667-80.

BROWN-LUM, M., IZADI-NAJAFABADI, S., OBERLANDER, T. F., RAUSCHER, A. & ZWICKER, J. G. 2020. Differences in White Matter Microstructure Among Children With Developmental Coordination Disorder. *JAMA Network Open,* 3**,** e201184-e201184.

BUNDERS, M. J., VAN HAMME, J. L., JANSEN, M. H., BOER, K., KOOTSTRA, N. A. & KUIJPERS, T. W. 2014a. Fetal exposure to HIV-1 alters chemokine receptor expression by CD4+T cells and increases susceptibility to HIV-1. *Sci Rep,* 4**,** 6690.

BUNDERS, M. J., VAN HAMME, J. L., JANSEN, M. H., BOER, K., KOOTSTRA, N. A. & KUIJPERS, T. W. 2014b. Fetal exposure to HIV-1 alters chemokine receptor expression by CD4+T cells and increases susceptibility to HIV-1. *Scientific Reports,* 4**,** 6690.

C TE, J. 1967. The Circumference of The Head of Newborn Infants First Measured in 1785. *Pedriatrics,* 39**,** 883.

CASCIO, C., GRIBBIN, M., GOUTTARD, S., SMITH, R. G., JOMIER, M., FIELD, S., GRAVES, M., HAZLETT, H. C., MULLER, K., GERIG, G. & PIVEN, J. 2013. Fractional anisotropy distributions in 2- to 6-year-old children with autism. *J Intellect Disabil Res,* 57**,** 1037-49.

CASTELO, J. M. B., COURTNEY, M. G., MELROSE, R. J. & STERN, C. E. 2007. Putamen Hypertrophy in Nondemented Patients With Human Immunodeficiency Virus Infection and Cognitive Compromise. *Archives of Neurology,* 64**,** 1275-1280.

CATANI, M. & THIEBAUT DE SCHOTTEN, M. 2008. A diffusion tensor imaging tractography atlas for virtual in vivo dissections. *Cortex,* 44**,** 1105-32.
CAVALIERE, C., TRAMONTANO, L., FIORENZA, D., ALFANO, V., AIELLO, M. & SALVATORE, M. 2020. Gliosis and Neurodegenerative Diseases: The Role of PET and MR Imaging. *Front Cell Neurosci,* 14**,** 75.
CAVINESS, V. S., JR., KENNEDY, D. N., RICHELME, C., RADEMACHER, J. & FILIPEK, P. A. 1996a. The human brain age 7-11 years: a volumetric analysis based on magnetic resonance images. *Cereb Cortex,* 6**,** 726-36.
CAVINESS, V. S., JR., MEYER, J., MAKRIS, N. & KENNEDY, D. N. 1996b. MRI-Based Topographic Parcellation of Human Neocortex: An Anatomically Specified Method with Estimate of Reliability. *J Cogn Neurosci,* 8**,** 566-87.
CAVINESS, V. S., JR., MEYER, J., MAKRIS, N. & KENNEDY, D. N. 1996c. MRI-Based Topographic Parcellation of Human Neocortex: An Anatomically Specified Method with Estimate of Reliability. *J Cogn Neurosci,* 8**,** 566-87.
CHANG, L. & SHUKLA, D. K. 2018. Imaging studies of the HIV-infected brain. *Handb Clin Neurol,* 152**,** 229-264.
CHAUDHURY, S., WILLIAMS, P. L., MAYONDI, G. K., LEIDNER, J., HOLDING, P., TEPPER, V., NICHOLS, S., MAGETSE, J., SAKOI, M., MOABI, K., MAKHEMA, J., MDLULI, C., JIBRIL, H., SEAGE, G. R., 3RD, KAMMERER, B. & LOCKMAN, S. 2017. Neurodevelopment of HIV-Exposed and HIV-Unexposed Uninfected Children at 24 Months. *Pediatrics,* 140.
CHEN, J. Y., RIBAUDO, H. J., SOUDA, S., PAREKH, N., OGWU, A., LOCKMAN, S., POWIS, K., DRYDEN-PETERSON, S., CREEK, T., JIMBO, W., MADIDIMALO, T., MAKHEMA, J., ESSEX, M. & SHAPIRO, R. L. 2012. Highly active antiretroviral therapy and adverse birth outcomes among HIV-infected women in Botswana. *J Infect Dis,* 206**,** 1695-705.
CHEN, Z., NI, P., ZHANG, J., YE, Y., XIAO, H., QIAN, G., XU, S., WANG, J., YANG, X., CHEN, J., ZHANG, B. & ZENG, Y. 2008. Evaluating ischemic stroke with diffusion tensor imaging. *Neurol Res,* 30**,** 720-6.
CHOE, M. S., ORTIZ-MANTILLA, S., MAKRIS, N., GREGAS, M., BACIC, J., HAEHN, D., KENNEDY, D., PIENAAR, R., CAVINESS, V. S., JR., BENASICH, A. A. & GRANT, P. E. 2013. Regional infant brain development: an MRI-based morphometric analysis in 3 to 13 month olds. *Cereb Cortex,* 23**,** 2100-17.
CHOI, G. B., YIM, Y. S., WONG, H., KIM, S., KIM, H., KIM, S. V., HOEFFER, C. A., LITTMAN, D. R. & HUH, J. R. 2016. The maternal interleukin-17a pathway in mice promotes autism-like phenotypes in offspring. *Science,* 351**,** 933-9.
CICCARELLI, O., TOOSY, A. T., PARKER, G. J., WHEELER-KINGSHOTT, C. A., BARKER, G. J., MILLER, D. H. & THOMPSON, A. J. 2003. Diffusion tractography based group mapping of major white-matter pathways in the human brain. *Neuroimage,* 19**,** 1545-55.
CLERICI, M., SARESELLA, M., COLOMBO, F., FOSSATI, S., SALA, N., BRICALLI, D., VILLA, M. L., FERRANTE, P., DALLY, L. & VIGANO, A. 2000. T-lymphocyte maturation abnormalities in uninfected newborns and children with vertical exposure to HIV. *Blood,* 96**,** 3866-71.
COCKCROFT, K., AMOD, Z. & SOELLAART, B. 2008. Level of maternal education and performance of Black, South African infants on the 1996 Griffiths Mental Development Scales. *Afr J Psychiatry (Johannesbg),* 11**,** 44-50.
COPP, A. J., GREENE, N. D. & MURDOCH, J. N. 2003. The genetic basis of mammalian neurulation. *Nat Rev Genet,* 4**,** 784-93.
CORTEY, A., JARVIK, J. G., LENKINSKI, R. E., GROSSMAN, R. I., FRANK, I. & DELIVORIA-PAPADOPOULOS, M. 1994. Proton MR spectroscopy of brain abnormalities in neonates born to HIV-positive mothers. *AJNR Am J Neuroradiol,* 15**,** 1853-9.
CROSSON, B. 2021. The Role of Cortico-Thalamo-Cortical Circuits in Language: Recurrent Circuits Revisited. *Neuropsychol Rev,* 31**,** 516-533.
CULNANE, M., FOWLER, M., LEE, S. S., MCSHERRY, G., BRADY, M., O'DONNELL, K., MOFENSON, L., GORTMAKER, S. L., SHAPIRO, D. E., SCOTT, G., JIMENEZ, E., MOORE, E. C., DIAZ, C., FLYNN, P. M., CUNNINGHAM, B. & OLESKE, J. 1999. Lack of long-term effects of in utero exposure to

zidovudine among uninfected children born to HIV-infected women. Pediatric AIDS Clinical Trials Group Protocol 219/076 Teams. *JAMA,* 281**,** 151-7.
DAVENPORT, N. D., KARATEKIN, C., WHITE, T. & LIM, K. O. 2010. Differential fractional anisotropy abnormalities in adolescents with ADHD or schizophrenia. *Psychiatry Res,* 181**,** 193-8.
DAYMONT, C., HWANG, W. T., FEUDTNER, C. & RUBIN, D. 2010. Head-circumference distribution in a large primary care network differs from CDC and WHO curves. *Pediatrics,* 126**,** e836-42.
DE GRAAF-PETERS, V. B. & HADDERS-ALGRA, M. 2006. Ontogeny of the human central nervous system: what is happening when? *Early Hum Dev,* 82**,** 257-66.
DE MICCO, R., RUSSO, A. & TESSITORE, A. 2018. Structural MRI in Idiopathic Parkinson's Disease. *Int Rev Neurobiol,* 141**,** 405-438.
DEBEAUDRAP, P., BODEAU-LIVINEC, F., PASQUIER, E., GERMANAUD, D., NDIANG, S. T., NLEND, A. N., NDONGO, F. A., GUEMKAM, G., PENDA, C. I., WARSZAWSKI, J., KOECHER, D., FAYE, A. & TEJIOKEM, M. C. 2018. Neurodevelopmental outcomes in HIV-infected and uninfected African children. *Aids,* 32**,** 2749-2757.
DEL OLMO, E., LÓPEZ-GIMÉNEZ, J. F., VILARÓ, M. T., MENGOD, G., PALACIOS, J. M. & PAZOS, A. 1998. Early localization of mRNA coding for 5-HT1A receptors in human brain during development. *Brain Res Mol Brain Res,* 60**,** 123-6.
DELONG, M. & WICHMANN, T. 2010. Changing views of basal ganglia circuits and circuit disorders. *Clin EEG Neurosci,* 41**,** 61-7.
DESMONDE, S., GOETGHEBUER, T., THORNE, C. & LEROY, V. 2016. Health and survival of HIV perinatally exposed but uninfected children born to HIV-infected mothers. *Curr Opin HIV AIDS,* 11**,** 465-476.
DI SCLAFANI, V., MACKAY, R. D., MEYERHOFF, D. J., NORMAN, D., WEINER, M. W. & FEIN, G. 1997. Brain atrophy in HIV infection is more strongly associated with CDC clinical stage than with cognitive impairment. *J Int Neuropsychol Soc,* 3**,** 276-87.
DIETRICH, O., BIFFAR, A., BAUR-MELNYK, A. & REISER, M. F. 2010. Technical aspects of MR diffusion imaging of the body. *Eur J Radiol,* 76**,** 314-22.
DIVI, R. L., HAVERKOS, K. J., HUMSI, J. A., SHOCKLEY, M. E., THAMIRE, C., NAGASHIMA, K., OLIVERO, O. A. & POIRIER, M. C. 2007. Morphological and molecular course of mitochondrial pathology in cultured human cells exposed long-term to Zidovudine. *Environ Mol Mutagen,* 48**,** 179-89.
DORSEY, S., FOREHAND, R., ARMISTEAD, L. P., MORSE, E., MORSE, P. & STOCK, M. 1999. Mother Knows Best? Mother and Child Report of Behavioral Difficulties of Children of HIV-Infected Mothers. *Journal of Psychopathology and Behavioral Assessment,* 21**,** 191-206.
DOWE, K. N., PLANALP, E. M., DEAN, D. C., ALEXANDER, A. L., DAVIDSON, R. J. & GOLDSMITH, H. H. 2020. Early microstructure of white matter associated with infant attention. *Developmental Cognitive Neuroscience,* 45**,** 100815.
DOYA, K. 2000. Complementary roles of basal ganglia and cerebellum in learning and motor control. *Curr Opin Neurobiol,* 10**,** 732-9.
DROTAR, D., OLNESS, K., WIZNITZER, M., SCHATSCHNEIDER, C., MARUM, L., GUAY, L., FAGAN, J., HOM, D., SVILAR, G., NDUGWA, C. & MAYENGO, R. K. 1999. Neurodevelopmental outcomes of Ugandan infants with HIV infection: an application of growth curve analysis. *Health Psychol,* 18**,** 114-21.
DUBOWITZ, L., RICCIW, D. & MERCURI, E. 2005. The Dubowitz neurological examination of the full-term newborn. *Mental Retardation and Developmental Disabilities Research Reviews,* 11**,** 1080-4013.
DUKE UNIVERSITY 2016. Understanding Fetal Alcohol Spectrum Disorders (FASD): Normal Brain Development *Duke Wordpress,* Chapter 3.
DZANIBE, S., JASPAN, H. B., ZULU, M. Z., KIRAVU, A. & GRAY, C. M. 2019. Impact of maternal HIV exposure, feeding status, and microbiome on infant cellular immunity. *J Leukoc Biol,* 105**,** 281-289.
ELLMAN, L. M., YOLKEN, R. H., BUKA, S. L., TORREY, E. F. & CANNON, T. D. 2009. Cognitive functioning prior to the onset of psychosis: the role of fetal exposure to serologically determined influenza infection. *Biol Psychiatry,* 65**,** 1040-7.

ESPOSITO, S., MUSETTI, L., MUSETTI, M. C., TORNAGHI, R., CORBELLA, S., MASSIRONI, E., MARCHISIO, P., GUARESCHI, A. & PRINCIPI, N. 1999. Behavioral and psychological disorders in uninfected children aged 6 to 11 years born to human immunodeficiency virus-seropositive mothers. *J Dev Behav Pediatr,* 20**,** 411-7.

EVERTS, R., LIDZBA, K., WILKE, M., KIEFER, C., MORDASINI, M., SCHROTH, G., PERRIG, W. & STEINLIN, M. 2009. Strengthening of laterality of verbal and visuospatial functions during childhood and adolescence. *Hum Brain Mapp,* 30**,** 473-83.

FAMILIAR, I., COLLINS, S. M., SIKORSKII, A., RUISENOR-ESCUDERO, H., NATAMBA, B., BANGIRANA, P., WIDEN, E. M., ACHIDRI, D., ACHOLA, H., ONEN, D., BOIVIN, M. & YOUNG, S. L. 2018. Quality of Caregiving is Positively Associated With Neurodevelopment During the First Year of Life Among HIV-Exposed Uninfected Children in Uganda. *J Acquir Immune Defic Syndr,* 77**,** 235-242.

FELDMAN, H. M., YEATMAN, J. D., LEE, E. S., BARDE, L. H. & GAMAN-BEAN, S. 2010. Diffusion tensor imaging: a review for pediatric researchers and clinicians. *J Dev Behav Pediatr,* 31**,** 346-56.

FENG, K., ROWELL, A. C., ANDRES, A., BELLANDO, B. J., LOU, X., GLASIER, C. M., RAMAKRISHNAIAH, R. H., BADGER, T. M. & OU, X. 2019. Diffusion Tensor MRI of White Matter of Healthy Full-term Newborns: Relationship to Neurodevelopmental Outcomes. *Radiology,* 292**,** 179-187.

FORD, A. A., TRIPLETT, W., SUDHYADHOM, A., GULLETT, J., MCGREGOR, K., FITZGERALD, D. B., MARECI, T., WHITE, K. & CROSSON, B. 2013. Broca's area and its striatal and thalamic connections: a diffusion-MRI tractography study. *Front Neuroanat,* 7**,** 8.

FOREHAND, R., STEELE, R., ARMISTEAD, L., MORSE, E., SIMON, P. & CLARK, L. 1998. The Family Health Project: psychosocial adjustment of children whose mothers are HIV infected. *J Consult Clin Psychol,* 66**,** 513-20.

FOWLER, K. B., STAGNO, S., PASS, R. F., BRITT, W. J., BOLL, T. J. & ALFORD, C. A. 1992. The outcome of congenital cytomegalovirus infection in relation to maternal antibody status. *N Engl J Med,* 326**,** 663-7.

FOXCROFT, C. D. & ROODT, G. 2006. An Introduction to Psychological Assessment in the South African Context (2nd ed). *Cape Town: Oxford University Press*.

GERARDIN, E., LEHÉRICY, S., POCHON, J. B., TÉZENAS DU MONTCEL, S., MANGIN, J. F., POUPON, F., AGID, Y., LE BIHAN, D. & MARSAULT, C. 2003. Foot, hand, face and eye representation in the human striatum. *Cereb Cortex,* 13**,** 162-9.

GIL ROBLES, S., GATIGNOL, P., CAPELLE, L., MITCHELL, M. C. & DUFFAU, H. 2005. The role of dominant striatum in language: a study using intraoperative electrical stimulations. *J Neurol Neurosurg Psychiatry,* 76**,** 940-6.

GILLIES, M. J., HYAM, J. A., WEISS, A. R., ANTONIADES, C. A., BOGACZ, R., FITZGERALD, J. J., AZIZ, T. Z., WHITTINGTON, M. A. & GREEN, A. L. 2017. The Cognitive Role of the Globus Pallidus interna; Insights from Disease States. *Exp Brain Res,* 235**,** 1455-1465.

GILMORE, J. H., JARSKOG, L. F. & VADLAMUDI, S. 2003. Maternal infection regulates BDNF and NGF expression in fetal and neonatal brain and maternal-fetal unit of the rat. *J Neuroimmunol,* 138**,** 49-55.

GILMORE, J. H., LIN, W., PRASTAWA, M. W., LOONEY, C. B., VETSA, Y. S., KNICKMEYER, R. C., EVANS, D. D., SMITH, J. K., HAMER, R. M., LIEBERMAN, J. A. & GERIG, G. 2007. Regional gray matter growth, sexual dimorphism, and cerebral asymmetry in the neonatal brain. *J Neurosci,* 27**,** 1255-60.

GOMEZ, C., ARCHILA, M. E., RUGELES, C., CARRIZOSA, J., RUGELES, M. T. & CORNEJO, J. W. 2009. [A prospective study of neurodevelopment of uninfected children born to human immunodeficiency virus type 1 positive mothers]. *Rev Neurol,* 48**,** 287-91.

GRAHAM, A. S., HOLMES, M. J., LITTLE, F., DOBBELS, E., COTTON, M. F., LAUGHTON, B., VAN DER KOUWE, A., MEINTJES, E. M. & ROBERTSON, F. C. 2020. MRS suggests multi-regional inflammation and white matter axonal damage at 11 years following perinatal HIV infection. *Neuroimage Clin,* 28**,** 102505.

GRUVER, R. S., MALL, S., KVALSVIG, J. D., KNOX, J. R., MELLINS, C. A., DESMOND, C., KAUCHALI, S., ARPADI, S. M., TAYLOR, M. & DAVIDSON, L. L. 2020. Cognitive and Language Development at Age 4-6 Years in Children HIV-Exposed But Uninfected Compared to Those HIV-Unexposed and to Children Living With HIV. *New Dir Child Adolesc Dev,* 2020**,** 39-54.

GUY-EVANAS, O. 2021. Lateralization of brain function. *Simply Psychology*

GUZMAN-MARTINEZ, L., MACCIONI, R. B., ANDRADE, V., NAVARRETE, L. P., PASTOR, M. G. & RAMOS-ESCOBAR, N. 2019. Neuroinflammation as a Common Feature of Neurodegenerative Disorders. *Front Pharmacol,* 10**,** 1008.

HAARTSEN, R., JONES, E. J. H. & JOHSON, M. H. 2016. Human brain development over the early years. *Current Opinion in Behavioral Sciences* 10**,** 149 - 154.

HABBEN, N. & MILLBERG, W. 2009. Essentials of Neuropsychological Assessment (2nd ed.). *New Jersey: John Wiley & Sons***,** 127.

HAGMANN, P., JONASSON, L., MAEDER, P., THIRAN, J. P., WEDEEN, V. J. & MEULI, R. 2006. Understanding diffusion MR imaging techniques: from scalar diffusion-weighted imaging to diffusion tensor imaging and beyond. *Radiographics,* 26 Suppl 1**,** S205-23.

HASHEMI, R. H., BRADLEY JR, W. G. & LISANTI, C. J. 2010. MRI: The basics *Philadelphia, PA: Lippincott Williams and Wilkins*.

HATTEN, M. E. 1999. Central nervous system neuronal migration. *Annu Rev Neurosci,* 22**,** 511-39.

HELLSTRÖM-LINDAHL, E., GORBOUNOVA, O., SEIGER, A., MOUSAVI, M. & NORDBERG, A. 1998. Regional distribution of nicotinic receptors during prenatal development of human brain and spinal cord. *Brain Res Dev Brain Res,* 108**,** 147-60.

HERLENIUS, E. & LAGERCRANTZ, H. 2001. Neurotransmitters and neuromodulators during early human development. *Early Hum Dev,* 65**,** 21-37.

HESTAD, K., MCARTHUR, J. H., DAL PAN, G. J., SELNES, O. A., NANCE-SPROSON, T. E., AYLWARD, E., MATHEWS, V. P. & MCARTHUR, J. C. 1993. Regional brain atrophy in HIV-1 infection: association with specific neuropsychological test performance. *Acta Neurol Scand,* 88**,** 112-8.

HIMES, S. K., HUO, Y., SIBERRY, G. K., WILLIAMS, P. L., RICE, M. L., SIROIS, P. A., FREDERICK, T., HAZRA, R., HUESTIS, M. A. & PEDIATRIC, H. C. S. 2015. Meconium Atazanavir Concentrations and Early Language Outcomes in HIV-Exposed Uninfected Infants With Prenatal Atazanavir Exposure. *J Acquir Immune Defic Syndr,* 69**,** 178-86.

HOEFT, F., BARNEA-GORAY, N., HAAS, B. W., GOLARAI, G., NG, D., MILLS, D., KORENBERG, J., BELLUGI, U., GALABURDA, A. & REISS, A. 2007. More Is Not Always Better: Increased Fractional Anisotropy of Superior Longitudinal Fasciculus Associated with Poor Visuospatial Abilities in Williams Syndrome. *J Neurosci,* 27**,** 11960 - 11965

HOFER, C. B., KEISER, O., ZWAHLEN, M., LUSTOSA, C. S., FROTA, A. C., DE OLIVEIRA, R. H., ABREU, T. F., CARVALHO, A. W., ARAUJO, L. E. & EGGER, M. 2016. In Utero Exposure to Antiretroviral Drugs: Effect on Birth Weight and Growth Among HIV-exposed Uninfected Children in Brazil. *Pediatr Infect Dis J,* 35**,** 71-7.

HOLLAND, D., CHANG, L., ERNST, T. M., CURRAN, M., BUCHTHAL, S. D., ALICATA, D., SKRANES, J., JOHANSEN, H., HERNANDEZ, A., YAMAKAWA, R., KUPERMAN, J. M. & DALE, A. M. 2014. Structural growth trajectories and rates of change in the first 3 months of infant brain development. *JAMA Neurol,* 71**,** 1266-74.

HOLMES, M. J., ROBERTSON, F. C., LITTLE, F., RANDALL, S. R., COTTON, M. F., VAN DER KOUWE, A. J. W., LAUGHTON, B. & MEINTJES, E. M. 2017. Longitudinal increases of brain metabolite levels in 5-10 year old children. *PLoS One,* 12**,** e0180973.

HORTA, B. L., LORET DE MOLA, C. & VICTORA, C. G. 2015. Breastfeeding and intelligence: a systematic review and meta-analysis. *Acta Paediatr,* 104**,** 14-9.

HUANG, H., SHU, N., MISHRA, V., JEON, T., CHALAK, L., WANG, Z. J., ROLLINS, N., GONG, G., CHENG, H., PENG, Y., DONG, Q. & HE, Y. 2015. Development of human brain structural networks through infancy and childhood. *Cereb Cortex,* 25**,** 1389-404.

HUPPI, P. S., WARFIELD, S., KIKINIS, R., BARNES, P. D., ZIENTARA, G. P., JOLESZ, F. A., TSUJI, M. K. & VOLPE, J. J. 1998. Quantitative magnetic resonance imaging of brain development in premature and mature newborns. *Ann Neurol,* 43**,** 224-35.

HUTTENLOCHER, P. R. & DABHOLKAR, A. S. 1997. Regional differences in synaptogenesis in human cerebral cortex. *J Comp Neurol,* 387**,** 167-78.

INNOCENTI, G. M. & PRICE, D. J. 2005. Exuberance in the development of cortical networks. *Nat Rev Neurosci,* 6**,** 955-65.

INGLESE, M. & BESTER, M. 2010. Diffusion imaging in multiple sclerosis: research and clinical implications. NMR in Biomedicine, 23(7), 865-872.

JACOBSON, S. W., CHIODO, L. M., SOKOL, R. J. & JACOBSON, J. L. 2002. Validity of maternal report of prenatal alcohol, cocaine, and smoking in relation to neurobehavioral outcome. *Pediatrics,* 109**,** 815-25.

JACOBSON, S. W., STANTON, M. E., MOLTENO, C. D., BURDEN, M. J., FULLER, D. S., HOYME, H. E., ROBINSON, L. K., KHAOLE, N. & JACOBSON, J. L. 2008. Impaired eyeblink conditioning in children with fetal alcohol syndrome. *Alcohol Clin Exp Res,* 32**,** 365-72.

JAHANSHAD, N., COUTURE, M. C., PRASITSUEBSAI, W., NIR, T. M., AURPIBUL, L., THOMPSON, P. M., PRUKSAKAEW, K., LERDLUM, S., VISRUTARATNA, P., CATELLA, S., DESAI, A., KERR, S. J., PUTHANAKIT, T., PAUL, R., ANANWORANICH, J. & VALCOUR, V. G. 2015. Brain Imaging and Neurodevelopment in HIV-uninfected Thai Children Born to HIV-infected Mothers. *Pediatr Infect Dis J,* 34**,** e211-6.

JANKIEWICZ, M., HOLMES, M. J., TAYLOR, P. A., COTTON, M. F., LAUGHTON, B., VAN DER KOUWE, A. J. W. & MEINTJES, E. M. 2017. White Matter Abnormalities in Children with HIV Infection and Exposure. *Frontiers in Neuroanatomy,* 11.

JAO, J. & ABRAMS, E. J. 2014. Metabolic complications of in utero maternal HIV and antiretroviral exposure in HIV-exposed infants. *Pediatr Infect Dis J,* 33**,** 734-40.

JAO, J., KACANEK, D., YU, W., WILLIAMS, P. L., PATEL, K., BURCHETT, S., SCOTT, G., ABRAMS, E. J., SPERLING, R. S., VAN DYKE, R. B., SMITH, R., MALEE, K. & PEDIATRIC, H. I. V. A. C. S. 2020. Neurodevelopment of HIV-Exposed Uninfected Infants Born to Women With Perinatally Acquired HIV in the United States. *J Acquir Immune Defic Syndr,* 84**,** 213-219.

JELLISON, B. J., FIELD, A. S., MEDOW, J., LAZAR, M., SALAMAT, M. S. & ALEXANDER, A. L. 2004. Diffusion tensor imaging of cerebral white matter: a pictorial review of physics, fiber tract anatomy, and tumor imaging patterns. *AJNR Am J Neuroradiol,* 25**,** 356-69.

JUDAS, M., RASIN, M. R., KRUSLIN, B., KOSTOVIĆ, K., JUKIĆ, D., PETANJEK, Z. & KOSTOVIĆ, I. 2003. Dendritic overgrowth and alterations in laminar phenotypes of neocortical neurons in the newborn with semilobar holoprosencephaly. *Brain Dev,* 25**,** 32-9.

KACANEK, D., WILLIAMS, P. L., MAYONDI, G., HOLDING, P., LEIDNER, J., MOABI, K., TEPPER, V., NICHOLS, S., MAKHEMA, J., JIBRIL, H., MADIDIMALO, T., SHAPIRO, R., LOCKMAN, S. & KAMMERER, B. 2018. Pediatric Neurodevelopmental Functioning After In Utero Exposure to Triple-NRTI vs. Dual-NRTI + PI ART in a Randomized Trial, Botswana. *J Acquir Immune Defic Syndr,* 79**,** e93-e100.

KANDAWASVIKA, G. Q., OGUNDIPE, E., GUMBO, F. Z., KUREWA, E. N., MAPINGURE, M. P. & STRAY-PEDERSEN, B. 2011. Neurodevelopmental impairment among infants born to mothers infected with human immunodeficiency virus and uninfected mothers from three peri-urban primary care clinics in Harare, Zimbabwe. *Dev Med Child Neurol,* 53**,** 1046-52.

KARUBE, F., TAKAHASHI, S., KOBAYASHI, K. & FUJIYAMA, F. 2019. Motor cortex can directly drive the globus pallidus neurons in a projection neuron type-dependent manner in the rat. *Elife,* 8.

KATO, T., YOSHIHARA, Y., WATANABE, D., FUKUMOTO, M., WADA, K., NAKAKURA, T., KURIYAMA, K., SHIRASAKA, T. & MURAI, T. 2020. Neurocognitive impairment and gray matter volume reduction in HIV-infected patients. *J Neurovirol,* 26**,** 590-601.

KERR, S. J., PUTHANAKIT, T., VIBOL, U., AURPIBUL, L., VONTHANAK, S., KOSALARAKSA, P., KANJANAVANIT, S., HANSUDEWECHAKUL, R., WONGSAWAT, J., LUESOMBOON, W., RATANADILOK, K., PRASITSUEBSAI, W., PRUKSAKAEW, K., VAN DER LUGT, J., PAUL, R.,

ANANWORANICH, J. & VALCOUR, V. G. 2014. Neurodevelopmental outcomes in HIV-exposed-uninfected children versus those not exposed to HIV. *AIDS Care,* 26**,** 1327 - 35.
KHERADMAND, A. & ZEE, D. S. 2011. Cerebellum and ocular motor control. *Front Neurol,* 2**,** 53.
KNICKMEYER, R. C., GOUTTARD, S., KANG, C., EVANS, D., WILBER, K., SMITH, J. K., HAMER, R. M., LIN, W., GERIG, G. & GILMORE, J. H. 2008. A structural MRI study of human brain development from birth to 2 years. *J Neurosci,* 28**,** 12176-82.
KOLASA, M., HAKULINEN, U., BRANDER, A., HAGMAN, S., DASTIDAR, P., ELOVAARA, I. & SUMELAHTI, M. L. 2019. Diffusion tensor imaging and disability progression in multiple sclerosis: A 4-year follow-up study. *Brain Behav,* 9**,** e01194.
KOSTOVIC, I. & GOLDMAN-RAKIC, P. S. 1983. Transient cholinesterase staining in the mediodorsal nucleus of the thalamus and its connections in the developing human and monkey brain. *J Comp Neurol,* 219**,** 431-47.
KOSTOVIĆ, I. & JOVANOV-MILOSEVIĆ, N. 2006. The development of cerebral connections during the first 20-45 weeks' gestation. *Semin Fetal Neonatal Med,* 11**,** 415-22.
KOSTOVIĆ, I. & JUDAS, M. 2002. Correlation between the sequential ingrowth of afferents and transient patterns of cortical lamination in preterm infants. *Anat Rec,* 267**,** 1-6.
KÜPER, M., RABE, K., ESSER, S., GIZEWSKI, E. R., HUSSTEDT, I. W., MASCHKE, M. & OBERMANN, M. 2011. Structural gray and white matter changes in patients with HIV. *J Neurol,* 258**,** 1066-75.
LANCIEGO, J. L., LUQUIN, N. & OBESO, J. A. 2012. Functional neuroanatomy of the basal ganglia. *Cold Spring Harb Perspect Med,* 2**,** a009621.
LANMAN, T., LETENDRE, S., MA, Q., BANG, A. & ELLIS, R. 2021. CNS Neurotoxicity of Antiretrovirals. *J Neuroimmune Pharmacol,* 16**,** 130-143.
LAUGHTON, B., CORNELL, M., GROVE, D., KIDD, M., SPRINGER, P. E., DOBBELS, E., VAN RENSBURG, A. J., VIOLARI, A., BABIKER, A. G., MADHI, S. A., JEAN-PHILIPPE, P., GIBB, D. M. & COTTON, M. F. 2012. Early antiretroviral therapy improves neurodevelopmental outcomes in infants. *AIDS,* 26**,** 1685-90.
LAUGHTON, B., CORNELL, M., KIDD, M., SPRINGER, P. E., DOBBELS, E. F. M., RENSBURG, A. J. V., OTWOMBE, K., BABIKER, A., GIBB, D. M., VIOLARI, A., KRUGER, M. & COTTON, M. F. 2018. Five year neurodevelopment outcomes of perinatally HIV-infected children on early limited or deferred continuous antiretroviral therapy. *J Int AIDS Soc,* 21**,** e25106.
LAUGHTON, B., NAIDOO, S., DOBBELS, E., BOIVIN, M. J., VAN RENSBURG, A. J., GLASHOFF, R. H., VAN ZYL, G. U., KRUGER, M. & COTTON, M. F. 2019. Neurodevelopment at 11 months after starting antiretroviral therapy within 3 weeks of life. *South Afr J HIV Med,* 20**,** 1008.
LAUGHTON, B., SPRINGER, P., GROVE, D., SEEDAT, S., CORNELL, M., KIDD, M., MADHI, S. & COTTON, M. 2010. Longitudinal developmental profile of children from low socio-economic circumstances in Cape Town, using the 1996 Griffiths Mental Development Scales. *SAJCH,* 4**,** 106-111.
LE DOARE, K., BLAND, R. & NEWELL, M. L. 2012. Neurodevelopment in children born to HIV-infected mothers by infection and treatment status. *Pediatrics,* 130**,** e1326-44.
LE ROUX, S. M., DONALD, K. A., BRITTAIN, K., PHILLIPS, T. K., ZERBE, A., NGUYEN, K. K., STRANDVIK, A., KROON, M., ABRAMS, E. J. & MYER, L. 2018. Neurodevelopment of breastfed HIV-exposed uninfected and HIV-unexposed children in South Africa. *AIDS,* 32**,** 1781-1791.
LEBEL, C., WALKER, L., LEEMANS, A., PHILLIPS, L. & BEAULIEU, C. 2008. Microstructural maturation of the human brain from childhood to adulthood. *Neuroimage,* 40**,** 1044-55.
LEE, B. N., HAMMILL, H., POPEK, E. J., CRON, S., KOZINETZ, C., PAUL, M., SHEARER, W. T. & REUBEN, J. M. 2001. Production of interferons and beta-chemokines by placental trophoblasts of HIV-1-infected women. *Infect Dis Obstet Gynecol,* 9**,** 95-104.
LEISMAN, G., BRAUN-BENJAMIN, O. & MELILLO, R. 2014. Cognitive-motor interactions of the basal ganglia in development. *Front Syst Neurosci,* 8**,** 16.
LENROOT, R. K., GOGTAY, N., GREENSTEIN, D. K., WELLS, E. M., WALLACE, G. L., CLASEN, L. S., BLUMENTHAL, J. D., LERCH, J., ZIJDENBOS, A. P., EVANS, A. C., THOMPSON, P. M. & GIEDD, J. N.

2007. Sexual dimorphism of brain developmental trajectories during childhood and adolescence. *Neuroimage,* 36**,** 1065-73.

LEWIS-DE LOS ANGELES, C. P., WILLIAMS, P. L., HUO, Y., WANG, S. D., UBAN, K. A., HERTING, M. M., MALEE, K., YOGEV, R., CSERNANSKY, J. G., NICHOLS, S., VAN DYKE, R. B., SOWELL, E. R. & WANG, L. 2017. Lower total and regional grey matter brain volumes in youth with perinatally-acquired HIV infection: Associations with HIV disease severity, substance use, and cognition. *Brain, Behavior, and Immunity,* 62**,** 100-109.

LEYDEN, K. M., KUCUKBOYACI, N. E., PUCKETT, O. K., LEE, D., LOI, R. Q., PAUL, B. & MCDONALD, C. R. 2015. What does diffusion tensor imaging (DTI) tell us about cognitive networks in temporal lobe epilepsy? *Quant Imaging Med Surg,* 5**,** 247-63.

LEZAK, M. D., HOWIESON, D. B., ERIN, D. & TRANEL, D. 2012. Neuropsychological Assessment (5th Ed). *Oxford: Oxford University Press*.

LI, J., GAO, L., WEN, Z., ZHANG, J., WANG, P., TU, N., LEI, H., LIN, F., GUI, X. & WU, G. 2018. Structural Covariance of Gray Matter Volume in HIV Vertically Infected Adolescents. *Sci Rep,* 8**,** 1182.

LIU, Y. & RAO, M. 2004. Glial progenitors in the CNS and possible lineage relationships among them. *Biology of the cell,* 96 4**,** 279-90.

LUIZ, D. M., STEWART, R., BARNARD, A., COLLIER, P. T. & KOTRAS, N. 2000a. Revision and Standardization of the Griffiths Extended Scales of Mental Development: A Working Document: Department off Psychology, University of Port Elizabeth.

LYALL, A. E., SHI, F., GENG, X., WOOLSON, S., LI, G., WANG, L., HAMER, R. M., SHEN, D. & GILMORE, J. H. 2015. Dynamic Development of Regional Cortical Thickness and Surface Area in Early Childhood. *Cereb Cortex,* 25**,** 2204-12.

MACKIEWICH, B. 1995. Basic Principles of MRI. *University of Leeds*.

MADLALA, H. P., MYER, L., MALABA, T. R. & NEWELL, M. L. 2020. Neurodevelopment of HIV-exposed uninfected children in Cape Town, South Africa. *PLoS One,* 15**,** e0242244.

MADZIME, J., HOLMES, M., COTTON, M., LAUGHTON, B., VAN DER KOUWE, A. J. W., MEINTJES, E. & JANKIEWICZ, M. 2021. ALTERED WHITE MATTER TRACTS IN THE SOMATOSENSORY, SALIENCE, MOTOR AND DEFAULT MODE NETWORKS IN 7-year old CHILDREN LIVING WITH HIV - A TRACTOGRAPHIC ANALYSIS. *Brain Connect*.

MAHARAJ, N. R., PHULUKDAREE, A., NAGIAH, S., RAMKARAN, P., TILOKE, C. & CHUTURGOON, A. A. 2017. Pro-Inflammatory Cytokine Levels in HIV Infected and Uninfected Pregnant Women with and without Preeclampsia. *PLoS One,* 12**,** e0170063.

MANDELBROT, L., TUBIANA, R., LE CHENADEC, J., DOLLFUS, C., FAYE, A., PANNIER, E., MATHERON, S., KHUONG, M. A., GARRAIT, V., RELIQUET, V., DEVIDAS, A., BERREBI, A., ALLISY, C., ELLEAU, C., ARVIEUX, C., ROUZIOUX, C., WARSZAWSKI, J. & BLANCHE, S. 2015. No perinatal HIV-1 transmission from women with effective antiretroviral therapy starting before conception. *Clin Infect Dis,* 61**,** 1715-25.

MARTIN, H. J. 2013. Neuroanatomy: text and atlas. *McGraw-Hill Medical Publishing Division* 3rd ed.**,** 1-488.

MARZBAN, E. N., ELDEIB, A. M., YASSINE, I. A. & KADAH, Y. M. 2020. Alzheimer's disease diagnosis from diffusion tensor images using convolutional neural networks. *PLoS One,* 15**,** e023409.

MEDNICK, S. A., MACHON, R. A., HUTTUNEN, M. O. & BONETT, D. 1988. Adult schizophrenia following prenatal exposure to an influenza epidemic. *Arch Gen Psychiatry,* 45**,** 189-92.

MEIJER, A., POUWELS, P. J. W., SMITH, J., VISSCHER, C., BOSKER, R. J., HARTMAN, E., OOSTERLAAN, J. & KÖNIGS, M. 2021. The relationship between white matter microstructure, cardiovascular fitness, gross motor skills, and neurocognitive functioning in children. *J Neurosci Res,* 99**,** 2201-2215.

MELIEF, E. J., MCKINLEY, J. W., LAM, J. Y., WHITELEY, N. M., GIBSON, A. W., NEUMAIER, J. F., HENSCHEN, C. W., PALMITER, R. D., BAMFORD, N. S. & DARVAS, M. 2018. Loss of glutamate signaling from the thalamus to dorsal striatum impairs motor function and slows the execution of learned behaviors. *NPJ Parkinsons Dis,* 4**,** 23.

MELILLO, R. 2011. Primitive reflexes and their relationship to delayed cortical maturation, underconnectivity and functional disconnection in childhood neurobehavioral disorders. *Funct Neurol Rehabil Ergon,* 1**,** 279-314.
MELLINS, C. A., LEVENSON, R. L., JR., ZAWADZKI, R., KAIRAM, R. & WESTON, M. 1994. Effects of pediatric HIV infection and prenatal drug exposure on mental and psychomotor development. *J Pediatr Psychol,* 19**,** 617-27.
MEYER, U. 2014. Prenatal poly(i:C) exposure and other developmental immune activation models in rodent systems. *Biol Psychiatry,* 75**,** 307-15.
MEYER, U., NYFFELER, M., ENGLER, A., URWYLER, A., SCHEDLOWSKI, M., KNUESEL, I., YEE, B. K. & FELDON, J. 2006. The time of prenatal immune challenge determines the specificity of inflammation-mediated brain and behavioral pathology. *J Neurosci,* 26**,** 4752-62.
MINK, J. W. 1996. The basal ganglia: focused selection and inhibition of competing motor programs. *Prog Neurobiol,* 50**,** 381-425.
MINK, J. W. 2003. The Basal Ganglia and involuntary movements: impaired inhibition of competing motor patterns. *Arch Neurol,* 60**,** 1365-8.
MOESKOPS, P., BENDERS, M. J., KERSBERGEN, K. J., GROENENDAAL, F., DE VRIES, L. S., VIERGEVER, M. A. & ISGUM, I. 2015. Development of Cortical Morphology Evaluated with Longitudinal MR Brain Images of Preterm Infants. *PLoS One,* 10**,** e0131552.
MOLTENO, C. D., JACOBSON, J. L., CARTER, R. C., DODGE, N. C. & JACOBSON, S. W. 2014. Infant emotional withdrawal: a precursor of affective and cognitive disturbance in fetal alcohol spectrum disorders. *Alcohol Clin Exp Res,* 38**,** 479-88.
MOREY, R. A., PETTY, C. M., XU, Y., HAYES, J. P., WAGNER, H. R., 2ND, LEWIS, D. V., LABAR, K. S., STYNER, M. & MCCARTHY, G. 2009. A comparison of automated segmentation and manual tracing for quantifying hippocampal and amygdala volumes. *Neuroimage,* 45**,** 855-66.
MORI, S., CRAIN, B. J., CHACKO, V. P. & VAN ZIJL, P. C. 1999. Three-dimensional tracking of axonal projections in the brain by magnetic resonance imaging. *Ann Neurol,* 45**,** 265-9.
MORI, S. & VAN ZIJL, P. C. 2002. Fiber tracking: principles and strategies - a technical review. *NMR Biomed,* 15**,** 468-80.
MSELLATI, P., LEPAGE, P., HITIMANA, D. G., VAN GOETHEM, C., VAN DE PERRE, P. & DABIS, F. 1993. Neurodevelopmental testing of children born to human immunodeficiency virus type 1 seropositive and seronegative mothers: a prospective cohort study in Kigali, Rwanda. *Pediatrics,* 92**,** 843-8.
NAMBU, A., TOKUNO, H., HAMADA, I., KITA, H., IMANISHI, M., AKAZAWA, T., IKEUCHI, Y. & HASEGAWA, N. 2000. Excitatory cortical inputs to pallidal neurons via the subthalamic nucleus in the monkey. *J Neurophysiol,* 84**,** 289-300.
NATIONAL DEPARTMENT OF HEALTH 2019. Annual Report (2019-2020): Department of Health, Republic of South Africa. 177 pages.
NGOMA, M. S., HUNTER, J. A., HARPER, J. A., CHURCH, P. T., MUMBA, S., CHANDWE, M., COTE, H. C., ALBERT, A. Y., SMITH, M. L., SELEMANI, C., SANDSTROM, P. A., BANDENDUCK, L., NDLOVU, U., KHAN, S., ROA, L. & SILVERMAN, M. S. 2014. Cognitive and language outcomes in HIV-uninfected infants exposed to combined antiretroviral therapy in utero and through extended breast-feeding. *AIDS,* 28 Suppl 3**,** S323-30.
NIGRO, G., ADLER, S. P., LA TORRE, R., BEST, A. M. & CONGENITAL CYTOMEGALOVIRUS COLLABORATING, G. 2005. Passive immunization during pregnancy for congenital cytomegalovirus infection. *N Engl J Med,* 353**,** 1350-62.
NOZYCE, M., HITTELMAN, J., MUENZ, L., DURAKO, S. J., FISCHER, M. L. & WILLOUGHBY, A. 1994. Effect of perinatally acquired human immunodeficiency virus infection on neurodevelopment in children during the first two years of life. *Pediatrics,* 94**,** 883-91.
NOZYCE, M. L., HUO, Y., WILLIAMS, P. L., KAPETANOVIC, S., HAZRA, R., NICHOLS, S., HUNTER, S., SMITH, R., SEAGE, G. R., 3RD & SIROIS, P. A. 2014. Safety of in utero and neonatal antiretroviral

exposure: cognitive and academic outcomes in HIV-exposed, uninfected children 5-13 years of age. *Pediatr Infect Dis J,* 33**,** 1128-33.

NTOZINI, R., CHANDNA, J., EVANS, C., CHASEKWA, B., MAJO, F. D., KANDAWASVIKA, G., TAVENGWA, N. V., MUTASA, B., MUTASA, K., MOULTON, L. H., HUMPHREY, J. H., GLADSTONE, M. J., PRENDERGAST, A. J. & TEAM, S. T. 2020. Early child development in children who are HIV-exposed uninfected compared to children who are HIV-unexposed: observational sub-study of a cluster-randomized trial in rural Zimbabwe. *J Int AIDS Soc,* 23**,** e25456.

NUNTA-AREE, S., OHATA, K., SOARES JR, S. B., HAGUE, M., TAKAMI, Y., INOUE, A., HAKUBA, A. & HARA, M. 2001. The morphological development of human basal ganglia. *Congenital Anomalies***,** 177-186.

O'DONNELL, L. J. & WESTIN, C. F. 2011. An introduction to diffusion tensor image analysis. *Neurosurg Clin N Am,* 22**,** 185-96, viii.

PANG, Y., FAN, L. W., TIEN, L. T., DAI, X., ZHENG, B., CAI, Z., LIN, R. C. & BHATT, A. 2013. Differential roles of astrocyte and microglia in supporting oligodendrocyte development and myelination in vitro. *Brain Behav,* 3**,** 503-14.

PARBOOSING, R., BAO, Y., SHEN, L., SCHAEFER, C. A. & BROWN, A. S. 2013. Gestational influenza and bipolar disorder in adult offspring. *JAMA Psychiatry,* 70**,** 677-85.

PATEL, V. R. & ZEE, D. S. 2015. The cerebellum in eye movement control: nystagmus, coordinate frames and disconjugacy. *Eye,* 29**,** 191-195.

PAUS, T., CASTRO-ALAMANCOS, M. A. & PETRIDES, M. 2001. Cortico-cortical connectivity of the human mid-dorsolateral frontal cortex and its modulation by repetitive transcranial magnetic stimulation. *Eur J Neurosci,* 14**,** 1405-11.

PEKNY, M. & PEKNA, M. 2016. Reactive gliosis in the pathogenesis of CNS diseases. *Biochim Biophys Acta,* 1862**,** 483-91.

PENG, S. J., HARNOD, T., TSAI, J. Z., KER, M. D., CHIOU, J. C., CHIUEH, H., WU, C. Y. & HSIN, Y. L. 2014. Evaluation of subcortical grey matter abnormalities in patients with MRI-negative cortical epilepsy determined through structural and tensor magnetic resonance imaging. *BMC Neurol,* 14**,** 104.

PÉREZ-EDGAR, K., TABER-THOMAS, B., AUDAY, E. & MORALES, S. 2014. Temperament and Attention as Core Mechanisms in the Early Emergence of Anxiety. *Contrib Hum Dev,* 26**,** 42-56.

PETERSON, D. J., RYAN, M., RIMRODT, S. L., CUTTING, L. E., DENCKLA, M. B., KAUFMANN, W. E. & MAHONE, E. M. 2011. Increased regional fractional anisotropy in highly screened attention-deficit hyperactivity disorder (ADHD). *J Child Neurol,* 26**,** 1296-302.

PFEFFERBAUM, A., MATHALON, D. H., SULLIVAN, E. V., RAWLES, J. M., ZIPURSKY, R. B. & LIM, K. O. 1994. A quantitative magnetic resonance imaging study of changes in brain morphology from infancy to late adulthood. *Arch Neurol,* 51**,** 874-87.

PFEIFER, C. & BUNDERS, M. J. 2016. Maternal HIV infection alters the immune balance in the mother and fetus; implications for pregnancy outcome and infant health. *Curr Opin HIV AIDS,* 11**,** 138-45.

PHELPS, B. R., AHMED, S., AMZEL, A., DIALLO, M. O., JACOBS, T., KELLERMAN, S. E., KIM, M. H., SUGANDHI, N., TAM, M. & WILSON-JONES, M. 2013. Linkage, initiation and retention of children in the antiretroviral therapy cascade: an overview. *AIDS,* 27 Suppl 2**,** S207-13.

PIERPAOLI, C. & BASSER, P. J. 1996. Toward a quantitative assessment of diffusion anisotropy. *Magn Reson Med,* 36**,** 893-906.

PIERRE, W. C., SMITH, P. L. P., LONDONO, I., CHEMTOB, S., MALLARD, C. & LODYGENSKY, G. A. 2017. Neonatal microglia: The cornerstone of brain fate. *Brain Behav Immun,* 59**,** 333-345.

PISKE, M., BUDD, M. A., QIU, A. Q., MAAN, E. J., SAUVÉ, L. J., FORBES, J. C., ALIMENTI, A., JANSSEN, P. & CÔTÉ, H. C. F. 2018. Neurodevelopmental outcomes and in-utero antiretroviral exposure in HIV-exposed uninfected children. *Aids,* 32**,** 2583-2592.

POWIS, K. M., SMEATON, L., OGWU, A., LOCKMAN, S., DRYDEN-PETERSON, S., VAN WIDENFELT, E., LEIDNER, J., MAKHEMA, J., ESSEX, M. & SHAPIRO, R. L. 2011. Effects of in utero antiretroviral

exposure on longitudinal growth of HIV-exposed uninfected infants in Botswana. *J Acquir Immune Defic Syndr,* 56**,** 131-8.
PURVES, D., AUGUSTINE, G. J., FITZPATRICK, D., HALL, W. C., LAMANTIA, A. S., MCNAMARA, J. O. & WHITE, L. E. 2008. Neuroscience (4th ed). *Sinauer Associates***,** pp. 15-16.
QI, Y., XU, M., WANG, W., WANG, Y. Y., LIU, J. J., REN, H. X., LIU, M. M., LI, R. L. & LI, H. J. 2021. Early prediction of putamen imaging features in HIV-associated neurocognitive impairment syndrome. *BMC Neurol,* 21**,** 106.
RAJAN, R., SETH, A., MUKHERJEE, S. B. & CHANDRA, J. 2017. Development assessment of HIV exposed children aged 6-18 months: a cohort study from North India. *AIDS Care,* 29**,** 1404-1409.
RAKIC, S. & ZECEVIC, N. 2000. Programmed cell death in the developing human telencephalon. *Eur J Neurosci,* 12**,** 2721-34.
RAMANOËL, S., HOYAU, E., KAUFFMANN, L., RENARD, F., PICHAT, C., BOUDIAF, N., KRAINIK, A., JAILLARD, A. & BACIU, M. 2018. Gray Matter Volume and Cognitive Performance During Normal Aging. A Voxel-Based Morphometry Study. *Front Aging Neurosci,* 10**,** 235.
RANDALL, S. R., WARTON, C. M. R., HOLMES, M. J., COTTON, M. F., LAUGHTON, B., VAN DER KOUWE, A. J. W. & MEINTJES, E. M. 2017. Larger Subcortical Gray Matter Structures and Smaller Corpora Callosa at Age 5 Years in HIV Infected Children on Early ART. *Front Neuroanat,* 11**,** 95.
REEMST, K., NOCTOR, S. C., LUCASSEN, P. J. & HOL, E. M. 2016. The Indispensable Roles of Microglia and Astrocytes during Brain Development. *Front Hum Neurosci,* 10**,** 566.
REES, S. & HARDING, R. 2004. Brain development during fetal life: influences of the intra-uterine environment. *Neurosci Lett,* 361**,** 111-4.
RICE, M. L., ZELDOW, B., SIBERRY, G. K., PURSWANI, M., MALEE, K., HOFFMAN, H. J., FREDERICK, T., BUCHANAN, A., SIROIS, P. A., ALLISON, S. M., WILLIAMS, P. L. & PEDIATRIC, H. C. S. 2013. Evaluation of risk for late language emergence after in utero antiretroviral drug exposure in HIV-exposed uninfected infants. *Pediatr Infect Dis J,* 32**,** e406-13.
RICH, K. C., SIEGEL, J. N., JENNINGS, C., RYDMAN, R. J. & LANDAY, A. L. 1997. Function and phenotype of immature CD4+ lymphocytes in healthy infants and early lymphocyte activation in uninfected infants of human immunodeficiency virus-infected mothers. *Clin Diagn Lab Immunol,* 4**,** 358-61.
RITTER, D. A., BHATT, D. H. & FETCHO, J. R. 2001. In vivo imaging of zebrafish reveals differences in the spinal networks for escape and swimming movements. *J Neurosci,* 21**,** 8956-65.
ROBERTSON, F. C., HOLMES, M. J., COTTON, M. F., DOBBELS, E., LITTLE, F., LAUGHTON, B., VAN DER KOUWE, A. J. W. & MEINTJES, E. M. 2018. Perinatal HIV Infection or Exposure Is Associated With Low N-Acetylaspartate and Glutamate in Basal Ganglia at Age 9 but Not 7 Years. *Front Hum Neurosci,* 12**,** 145.
RODIER, P. M. & HYMAN, S. M. 1998. Early environmental factors in autism. *Men Retard Dev Disabil Res Rev* 121-128.
ROMIJN, H. J., HOFMAN, M. A. & GRAMSBERGEN, A. 1991. At what age is the developing cerebral cortex of the rat comparable to that of the full-term newborn human baby? *Early Hum Dev,* 26**,** 61-7.
ROTHERAM-BORUS, M. J., CHRISTODOULOU, J., HAYATI REZVAN, P., COMULADA, W. S., GORDON, S., SKEEN, S., STEWART, J., ALMIROL, E. & TOMLINSON, M. 2019. Maternal HIV does not affect resiliency among uninfected/HIV exposed South African children from birth to 5 years of age. *Aids,* 33 Suppl 1**,** S5-s16.
SALEMI, J. L., WHITEMAN, V. E., AUGUST, E. M., CHANDLER, K., MBAH, A. K. & SALIHU, H. M. 2014. Maternal hepatitis B and hepatitis C infection and neonatal neurological outcomes. *J Viral Hepat,* 21**,** e144-53.
SAMRC. 2016. *Early mother-to-child transmission of HIV stats plunge.pdf* [Online]. South African Medical Research Council. Available: http://www.mrc.ac.za/Media/2016/13press2016.htm [Accessed 2 November 2017].
SANAC, S. A. N. A. C. 2018. Let our actions count: National Strategic Plan on HIV, TB and STIs (2017-2022).

SANMANEECHAI, O., PUTHANAKIT, T., LOUTHRENOO, O. & SIRISANTHANA, V. 2005. Growth, Developmental, and Behavioral Outcomes of HIV-Affected Preschool Children in Thailand. *J Med Assoc Thai,* 88**,** 1873-9.

SAPPENFIELD, E., JAMIESON, D. J. & KOURTIS, A. P. 2013. Pregnancy and susceptibility to infectious diseases. *Infect Dis Obstet Gynecol,* 2013**,** 752852.

SARMA, M. K., NAGARAJAN, R., KELLER, M. A., KUMAR, R., NIELSEN-SAINES, K., MICHALIK, D. E., DEVILLE, J., CHURCH, J. A. & THOMAS, M. A. 2014. Regional brain gray and white matter changes in perinatally HIV-infected adolescents. *Neuroimage Clin,* 4**,** 29-34.

SBARDELLA, E., TONA, F., PETSAS, N. & PANTANO, P. 2013. DTI Measurements in Multiple Sclerosis: Evaluation of Brain Damage and Clinical Implications. *Mult Scler Int,* 2013**,** 671730.

SCHMITHORST, V. J., WILKE, M., DARDZINSKI, B. J. & HOLLAND, S. K. 2005. Cognitive functions correlate with white matter architecture in a normal pediatric population: a diffusion tensor MRI study. *Hum Brain Mapp,* 26**,** 139-47.

SCHRODER, I. A. 2004. The Performance of Hearing Impaired Children on the Revised Extended Griffiths Sclaes (unublished Master's thesis). University of Port Elizabet, South Africa.

SCIACCA, F. & JONES, J. Thalamus. *Radiopaedia*.

SCIENCES, N. A. O. 2000. Technologies for Studying the Developing Human Brain *In:* SHONKOFF, J. P. & PHILLIPS, D. A. (eds.) *From Neurons to Neighborhoods: The Science of Early Childhood Development.* Washington (DC).

SEIDMAN, L. J. 1998. Neuropsychological testing. *Harvard Mental Health Letter,* 14 4-6.

SHERMAN, S. M. 2006. Thalamus. *Scholarpedia,* 1**,** 1583.

SHETTY, A. K. & MALDONADO, Y. 2013. Antiretroviral drugs to prevent mother-to-child transmission of HIV during breastfeeding. *Curr HIV Res,* 11**,** 102-25.

SHIGEMOTO-MOGAMI, Y., HOSHIKAWA, K., GOLDMAN, J. E., SEKINO, Y. & SATO, K. 2014. Microglia enhance neurogenesis and oligodendrogenesis in the early postnatal subventricular zone. *J Neurosci,* 34**,** 2231-43.

SHIMIZU, I., YOSHIMOTO, M., KOJIMA, T. & OKADO, N. 1984. Development of retinohypothalamic projections in the chick embryo. *Neurosci Lett,* 50**,** 43-7.

SHIMONY, J. S., BURTON, H., EPSTEIN, A. A., MCLAREN, D. G., SUN, S. W. & SNYDER, A. Z. 2006. Diffusion tensor imaging reveals white matter reorganization in early blind humans. *Cereb Cortex,* 16**,** 1653-61.

SHORT, S. J., LUBACH, G. R., KARASIN, A. I., OLSEN, C. W., STYNER, M., KNICKMEYER, R. C., GILMORE, J. H. & COE, C. L. 2010. Maternal influenza infection during pregnancy impacts postnatal brain development in the rhesus monkey. *Biol Psychiatry,* 67**,** 965-73.

SIROIS, P. A., HUO, Y., WILLIAMS, P. L., MALEE, K., GARVIE, P. A., KAMMERER, B., RICH, K., VAN DYKE, R. B. & NOZYCE, M. L. 2013. Safety of perinatal exposure to antiretroviral medications: developmental outcomes in infants. *Pediatr Infect Dis J,* 32**,** 648-55.

SKET, G. M., OVERFELD, J., STYNER, M., GILMORE, J. H., ENTRINGER, S., WADHWA, P. D., RASMUSSEN, J. M. & BUSS, C. 2019. Neonatal White Matter Maturation Is Associated With Infant Language Development. *Front Hum Neurosci,* 13**,** 434.

SMITH, S. E., LI, J., GARBETT, K., MIRNICS, K. & PATTERSON, P. H. 2007. Maternal immune activation alters fetal brain development through interleukin-6. *J Neurosci,* 27**,** 10695-702.

SNIJDEWIND, I. J. M., SMIT, C., GODFRIED, M. H., BAKKER, R., NELLEN, J., JADDOE, V. W. V., VAN LEEUWEN, E., REISS, P., STEEGERS, E. A. P. & VAN DER ENDE, M. E. 2018. Preconception use of cART by HIV-positive pregnant women increases the risk of infants being born small for gestational age. *PLoS One,* 13**,** e0191389.

SOWELL, E. R., TRAUNER, D. A., GAMST, A. & JERNIGAN, T. L. 2002. Development of cortical and subcortical brain structures in childhood and adolescence: a structural MRI study. *Dev Med Child Neurol,* 44**,** 4-16.

SPAULDING, A. B., YU, Q., CIVITELLO, L., MUSSI-PINHATA, M. M., PINTO, J., GOMES, I. M., ALARCÓN, J. O., SIBERRY, G. K., HARRIS, D. R. & HAZRA, R. 2016. Neurologic Outcomes in HIV-

Exposed/Uninfected Infants Exposed to Antiretroviral Drugs During Pregnancy in Latin America and the Caribbean. *AIDS Res Hum Retroviruses,* 32**,** 349-56.

SPRINGER, P. E., SLOGROVE, A. L., KIDD, M., KALK, E., BETTINGER, J. A., ESSER, M. M., COTTON, M. F., ZUNZA, M., MOLTENO, C. D. & KRUGER, M. 2020. Neurodevelopmental and behavioural outcomes of HIV-exposed uninfected and HIV-unexposed children at 2-3 years of age in Cape Town, South Africa. *AIDS Care,* 32**,** 411-419.

SPRINGER, P. E., SLOGROVE, A. L., LAUGHTON, B., BETTINGER, J. A., SAUNDERS, H. H., MOLTENO, C. D. & KRUGER, M. 2018. Neurodevelopmental outcome of HIV-exposed but uninfected infants in the Mother and Infants Health Study, Cape Town, South Africa. *Trop Med Int Health,* 23**,** 69-78.

STILES, J. 2008. The fundamentals of brain development: Integrating nature and nurture. *Cambridge: MA, Harvard University Press*.

STILES, J. & JERNIGAN, T. L. 2010. The basics of brain development. *Neuropsychol Rev,* 20**,** 327-48.

STREHLAU, R., VAN ASWEGEN, T., BURKE, M., KUHN, L. & POTTERTON, J. 2020. A description of early neurodevelopment in a cohort of HIV-exposed uninfected children. *AIDS Care,* 32**,** 1421-1428.

SUPÈR, H., SORIANO, E. & UYLINGS, H. B. 1998. The functions of the preplate in development and evolution of the neocortex and hippocampus. *Brain Res Brain Res Rev,* 27**,** 40-64.

SYMMS, M., JAGER, H. R., SCHMIERER, K. & YOUSRY, T. A. 2004. A review of structural magnetic resonance neuroimaging. *J Neurol Neurosurg Psychiatry,* 75**,** 1235-44.

TIMMANN, D., BRANDAUER, B., HERMSDÖRFER, J., ILG, W., KONCZAK, J., GERWIG, M., GIZEWSKI, E. R. & SCHOCH, B. 2008. Lesion-symptom mapping of the human cerebellum. *Cerebellum,* 7**,** 602-6.

TIWARI, N., PATASKAR, A., PÉRON, S., THAKURELA, S., SAHU, S. K., FIGUERES-OÑATE, M., MARICHAL, N., LÓPEZ-MASCARAQUE, L., TIWARI, V. K. & BERNINGER, B. 2018. Stage-Specific Transcription Factors Drive Astrogliogenesis by Remodeling Gene Regulatory Landscapes. *Cell Stem Cell,* 23**,** 557-571.e8.

TOPKA, H., KONCZAK, J. & DICHGANS, J. 1998. Coordination of multi-joint arm movements in cerebellar ataxia: analysis of hand and angular kinematics. *Exp Brain Res,* 119**,** 483-92.

TORTORA, G. J. & ANAGNOSTAKOS, N. P. 1987. Principles of anatomy and physiology. 5th Edition.

TRAN, L. T., ROOS, A., FOUCHE, J. P., KOEN, N., WOODS, R. P., ZAR, H. J., NARR, K. L., STEIN, D. J. & DONALD, K. A. 2016. White Matter Microstructural Integrity and Neurobehavioral Outcome of HIV-Exposed Uninfected Neonates. *Medicine (Baltimore),* 95**,** e2577.

TROMP, D. 2016. DTI Scalars (FA, MD, AD, RD) - How do they relate to brain structure? *The Winnower*.

URAKUBO, A., JARSKOG, L. F., LIEBERMAN, J. A. & GILMORE, J. H. 2001. Prenatal exposure to maternal infection alters cytokine expression in the placenta, amniotic fluid, and fetal brain. *Schizophr Res,* 47**,** 27-36.

UTHMAN, O. A., NACHEGA, J. B., ANDERSON, J., KANTERS, S., MILLS, E. J., RENAUD, F., ESSAJEE, S., DOHERTY, M. C. & MOFENSON, L. M. 2017. Timing of initiation of antiretroviral therapy and adverse pregnancy outcomes: a systematic review and meta-analysis. *Lancet HIV,* 4**,** e21-e30.

VALCOUR, V., CHALERMCHAI, T., SAILASUTA, N., MAROVICH, M., LERDLUM, S., SUTTICHOM, D., SUWANWELA, N. C., JAGODZINSKI, L., MICHAEL, N., SPUDICH, S., VAN GRIENSVEN, F., DE SOUZA, M., KIM, J. & ANANWORANICH, J. 2012. Central nervous system viral invasion and inflammation during acute HIV infection. *J Infect Dis,* 206**,** 275-82.

VAN DEN HEUVEL, M. P., KERSBERGEN, K. J., DE REUS, M. A., KEUNEN, K., KAHN, R. S., GROENENDAAL, F., DE VRIES, L. S. & BENDERS, M. J. 2015. The Neonatal Connectome During Preterm Brain Development. *Cereb Cortex,* 25**,** 3000-13.

VAN RIE, A., DOW, A., MUPUALA, A. & STEWART, P. 2009. Neurodevelopmental trajectory of HIV-infected children accessing care in Kinshasa, Democratic Republic of Congo. *J Acquir Immune Defic Syndr,* 52**,** 636-42.

VAN RIE, A., MUPUALA, A. & DOW, A. 2008. Impact of the HIV/AIDS epidemic on the neurodevelopment of preschool-aged children in Kinshasa, Democratic Republic of the Congo. *Pediatrics,* 122**,** e123-8.

VAN SCHALKWYK, C., MNDZEBELE, S., HLOPHE, T., GARCIA CALLEJA, J. M., KORENROMP, E. L., STONEBURNER, R. & PERVILHAC, C. 2013. Outcomes and impact of HIV prevention, ART and TB programs in Swaziland--early evidence from public health triangulation. *PLoS One,* 8**,** e69437.

VERNEY, C., LEBRAND, C. & GASPAR, P. 2002. Changing distribution of monoaminergic markers in the developing human cerebral cortex with special emphasis on the serotonin transporter. *Anat Rec,* 267**,** 87-93.

VERNEY, C., MILOSEVIC, A., ALVAREZ, C. & BERGER, B. 1993. Immunocytochemical evidence of well-developed dopaminergic and noradrenergic innervations in the frontal cerebral cortex of human fetuses at midgestation. *J Comp Neurol,* 336**,** 331-44.

VICTORA, C. G., BAHL, R., BARROS, A. J., FRANCA, G. V., HORTON, S., KRASEVEC, J., MURCH, S., SANKAR, M. J., WALKER, N., ROLLINS, N. C. & LANCET BREASTFEEDING SERIES, G. 2016. Breastfeeding in the 21st century: epidemiology, mechanisms, and lifelong effect. *Lancet,* 387**,** 475-90.

VIGANO, A., SARESELLA, M., SCHENAL, M., ERBA, P., PIACENTINI, L., TORNAGHI, R., NADDEO, V., GIACOMET, V., BORELLI, M., TRABATTONI, D. & CLERICI, M. 2007. Immune activation and normal levels of endogenous antivirals are seen in healthy adolescents born of HIV-infected mothers. *Aids,* 21**,** 245-8.

VISENTIN, S., MANARA, R., MILANESE, L., DA ROIT, A., FORNER, G., SALVIATO, E., CITTON, V., MAGNO, F. M., ORZAN, E., MORANDO, C., CUSINATO, R., MENGOLI, C., PALU, G., ERMANI, M., RINALDI, R., COSMI, E. & GUSSETTI, N. 2012. Early primary cytomegalovirus infection in pregnancy: maternal hyperimmunoglobulin therapy improves outcomes among infants at 1 year of age. *Clin Infect Dis,* 55**,** 497-503.

VYAS, P., MATHAD, J. S., LEU, C. S., NAIK, S., ALEXANDER, M., ARAUJO-PEREIRA, M., KULKARNI, V., DESHPANDE, P., YADANA, S., ANDRADE, B. B., BHOSALE, R., KUMAR, P., BABU, S., GUPTA, A. & SHIVAKOTI, R. 2021a. Impact of HIV status on systemic inflammation during pregnancy. *Aids*.

VYAS, P., MATHAD, J. S., LEU, C. S., NAIK, S., ALEXANDER, M., ARAÚJO-PEREIRA, M., KULKARNI, V., DESHPANDE, P., YADANA, S., ANDRADE, B. B., BHOSALE, R., KUMAR, P., BABU, S., GUPTA, A. & SHIVAKOTI, R. 2021b. Impact of HIV status on systemic inflammation during pregnancy. *Aids,* 35**,** 2259-2268.

WALKER, K. A. 2018. Inflammation and neurodegeneration: chronicity matters. *Aging (Albany NY),* 11**,** 3-4.

WANG, L., SHI, F., LI, G., GAO, Y., LIN, W., GILMORE, J. H. & SHENA, D. 2014. Segmentation of Neonatal Brain MR Images using Patch-Driven Level Sets. *Neuroimage Clin,* 84**,** 141 - 158.

WEDDERBURN, C. J., YEUNG, S., REHMAN, A. M., STADLER, J. A. M., NHAPI, R. T., BARNETT, W., MYER, L., GIBB, D. M., ZAR, H. J., STEIN, D. J. & DONALD, K. A. 2019. Neurodevelopment of HIV-exposed uninfected children in South Africa: outcomes from an observational birth cohort study. *Lancet Child Adolesc Health,* 3**,** 803-813.

WEISLEDER, A. & FERNALD, A. 2013. Talking to children matters: early language experience strengthens processing and builds vocabulary. *Psychol Sci,* 24**,** 2143-52.

WELNIARZ, Q., WORBE, Y. & GALLEA, C. 2021. The Forward Model: A Unifying Theory for the Role of the Cerebellum in Motor Control and Sense of Agency. *Front Syst Neurosci,* 15**,** 644059.

WHITE, M., FEUCHT, U. D., DUFFLEY, E., MOLOKOANE, F., DURANDT, C., CASSOL, E., ROSSOUW, T. & CONNOR, K. L. 2020. Does in utero HIV exposure and the early nutritional environment influence infant development and immune outcomes? Findings from a pilot study in Pretoria, South Africa. *Pilot Feasibility Stud,* 6**,** 192.

WICHMANN, T. & DELONG, M. R. 2007. Anatomy and physiology of the basal ganglia: relevance to Parkinson's disease and related disorders. *Handb Clin Neurol,* 83**,** 1-18.

WILLIAMS, P. L., MARINO, M., MALEE, K., BROGLY, S., HUGHES, M. D. & MOFENSON, L. M. 2010. Neurodevelopment and in utero antiretroviral exposure of HIV-exposed uninfected infants. *Pediatrics,* 125**,** e250-60.

WORLD-HEALTH-OGANIZATION 2007. WHO Child Growth Standards: Head Circumference-for-age, arm circumference-for-age, tricepts skinfold-forage and subscapula skinfold-for-age. *World Health Organization*.

WRIGHT, P. W., PYAKUREL, A., VAIDA, F. F., PRICE, R. W., LEE, E., PETERSON, J., FUCHS, D., ZETTERBERG, H., ROBERTSON, K. R., WALTER, R., MEYERHOFF, D. J., SPUDICH, S. S. & ANCES, B. M. 2016. Putamen volume and its clinical and neurological correlates in primary HIV infection. *Aids,* 30**,** 1789-94.

WU, J., LI, J., LI, Y., LOO, K. K., YANG, H., WANG, Q., DUAN, R., XIAO, X., SONG, X., YANG, S. & SUN, L. 2018. Neurodevelopmental outcomes in young children born to HIV-positive mothers in rural Yunnan, China. *Pediatr Int,* 60**,** 618-625.

XUE, H., SRINIVASAN, L., JIANG, S., RUTHERFORD, M., EDWARDS, A. D., RUECKERT, D. & HAJNAL, J. V. 2007. Automatic segmentation and reconstruction of the cortex from neonatal MRI. *Neuroimage,* 38**,** 461-77.

XUE, R., VAN ZIJL, P. C., CRAIN, B. J., SOLAIYAPPAN, M. & MORI, S. 1999. In vivo three-dimensional reconstruction of rat brain axonal projections by diffusion tensor imaging. *Magn Reson Med,* 42**,** 1123-7.

YADAV, S. K., GUPTA, R. K., GARG, R. K., VENKATESH, V., GUPTA, P. K., SINGH, A. K., HASHEM, S., AL-SULAITI, A., KAURA, D., WANG, E., MARINCOLA, F. M. & HARIS, M. 2017. Altered structural brain changes and neurocognitive performance in pediatric HIV. *Neuroimage Clin,* 14**,** 316-322.

YADAV, S. K., GUPTA, R. K., HASHEM, S., NISAR, S., AZEEM, T., BHAT, A. A., SYED, N., GARG, R. K., VENKATESH, V., KAMAL, M., FAKHRO, K., FRENNEAUX, M. P. & HARIS, M. 2020. Brain microstructural changes support cognitive deficits in HIV uninfected children born to HIV infected mothers. *Brain Behav Immun Health,* 2**,** 100039.

YAMADA, K., SAKAI, K., AKAZAWA, K., YUEN, S. & NISHIMURA, T. 2009. MR tractography: a review of its clinical applications. *Magn Reson Med Sci,* 8**,** 165-74.

YOON, U., FONOV, V. S., PERUSSE, D., EVANS, A. C. & BRAIN DEVELOPMENT COOPERATIVE, G. 2009. The effect of template choice on morphometric analysis of pediatric brain data. *Neuroimage,* 45**,** 769-77.

YOUNG, C. B., REDDY, V. & SONNE, J. 2020. Neuroanatomy, Basal Ganglia. *StatPearls.* Treasure Island (FL).

YU, H., STERNAD, D., CORCOS, D. M. & VAILLANCOURT, D. E. 2007. Role of hyperactive cerebellum and motor cortex in Parkinson's disease. *Neuroimage,* 35**,** 222-33.

YU, X., GAO, L., WANG, H., YIN, Z., FANG, J., CHEN, J., LI, Q., XU, H. & GUI, X. 2019. Neuroanatomical Changes Underlying Vertical HIV Infection in Adolescents. *Front Immunol,* 10**,** 814.

ZECEVIC, N. 1998. Synaptogenesis in layer I of the human cerebral cortex in the first half of gestation. *Cereb Cortex,* 8**,** 245-52.

ZECEVIC, N. & VERNEY, C. 1995. Development of the catecholamine neurons in human embryos and fetuses, with special emphasis on the innervation of the cerebral cortex. *J Comp Neurol,* 351**,** 509-35.

ZUENA, A. R., GIULI, C., VENEROSI PESCIOLINI, A., TRAMUTOLA, A., AJMONE-CAT, M. A., CINQUE, C., ALEMÀ, G. S., GIOVINE, A., PELUSO, G., MINGHETTI, L., NICOLAI, R., CALAMANDREI, G. & CASOLINI, P. 2013. Transplacental exposure to AZT induces adverse neurochemical and behavioral effects in a mouse model: protection by L-acetylcarnitine. *PLoS One,* 8**,** e55753.

ZUK, J., YU, X., SANFILIPPO, J., FIGUCCIO, M. J., DUNSTAN, J., CARRUTHERS, C., SIDERIDIS, G., TURESKY, T. K., GAGOSKI, B., GRANT, P. E. & GAAB, N. 2021. White matter in infancy is prospectively associated with language outcomes in kindergarten. *Dev Cogn Neurosci,* 50**,** 100973.

Supplementary analysis 1

Table 1. Intra-ratter reliability

Region	Agreement		Consistency	
	ICC (C, 1)	p value	ICC (C, 1)	p value
Left caudate	0.999	<0.0001	0.999	<0.0001
Right caudate	0.874	0.0001	0.873	0.0002
Left putamen	0.877	0.0002	0.867	0.0003
Right putamen	0.999	<0.0001	0.999	<0.0001
Left pallidum	0.923	0.002	0.958	<0.0001
Right pallidum	0.962	0.0002	0.976	<0.0001
Left thalamus	0.962	<0.0001	0.974	<0.0001
Right thalamus	0.916	<0.0001	0.923	<0.0001
Left cerebellum	0.999	<0.0001	0.999	<0.0001
Right cerebellum	0.999	<0.0001	0.999	<0.0001
Vermis	0.999	<0.0001	0.999	<0.0001

Table 2. Associations of regional volumes with potential confounding variables

ROI	Infant indices at MRI				Maternal indices	
	Sex	**GA**	**Weight[1]**	**Head Circum-ference[1]**	**Weight change per week**	**Age at delivery**
L caudate	-0.08 (0.37)	0.05 (0.55)	**0.21 (0.02)**	0.14 (0.13)	-0.04 (0.63)	-0.04 (0.64)
R caudate	-0.04 (0.69)	-0.01 (0.95)	**0.18 (0.05)**	0.10 (0.28)	-0.04 (0.65)	0.004 (0.96)
L putamen	0.02 (0.80)	0.09 (0.35)	**0.30 (<0.001)**	**0.20 (0.03)**	**0.16 (0.09)**	-0.01 (0.90)
R putamen	0.04 (0.64)	0.09 (0.32)	**0.30 (<0.001)**	**0.24 (0.009)**	0.12 (0.19)	-0.02 (0.82)
L pallidum	-0.05 (0.56)	-0.12 (0.19)	0.05 (0.53)	**0.21 (0.02)**	-0.01 (0.92)	-0.01 (0.93)
R pallidum	-0.13 (0.17)	0.04 (0.70)	**0.17 (0.07)**	**0.16 (0.09**)	-0.01 (0.95)	-0.09 (0.33)
L thalamus	-0.14 (0.13)	0.13 (0.15)	**0.38 (<0.001)**	0.09 (0.29)	-0.02 (0.86)	0.07 (0.44)
R thalamus	-0.14 (0.14)	**0.16 (0.08)**	**0.38 (<0.001)**	0.09 (0.31)	-0.02 (0.84)	0.08 (0.38)
L cerebellum	-0.09 (0.31)	**0.20 (0.03)**	**0.51 (<0.001)**	0.09 (0.35)	0.10 (0.28)	-0.03 (0.76)
R cerebellum	-0.13 (0.14)	**0.20 (0.03)**	**0.48 (<0.001)**	0.07 (0.43)	0.11 (0.22)	-0.03 (0.76)
Vermis	0.11 (0.23)	**0.17 (0.07)**	**0.31 (<0.001**)	-0.11 (0.24)	0.10 (0.28)	-0.09 (0.29)

Values are Pearson correlation coefficients, *r* (p-value); GA = gestational age; L left; R right;
Bold indicates significance at $p<0.10$; [1]Data missing for 1 infant in the HEU pre-conception ART group and 2 HUU infants.

Table 3. Associations of regional volumes among HEU infants with maternal clinical and treatment variables

Region	**Maternal CD4 within 6 mo of enrolment (n = 77)[a]**		**Maternal VL within 6 mo of enrolment (n = 23)[b]**		**Maternal VL within 6 mo of enrolment (n = 79)[c]**		**Infant ART Exposure duration (n = 79)**	
	***r* (*p*)**	**β (*p*)**	***r* (*p*)**	**β (*p*)**	***r* (*p*)**	**β (*p*)**	***r* (*p*)**	**β (*p*)**
Left caudate[2]	**0.28 (0.01)**	**0.35 (0.01)**	0.19 (0.39)	0.009 (0.53)	-0.07 (0.54)	0.007 (0.61)	**0.38 (<0.001)**	**10.74 (<0.001)**
Right caudate[2]	0.16 (0.18)	0.19 (0.16)	0.19 (0.38)	0.009 (0.56)	-0.08 (0.50)	0.008 (0.56)	**0.35 (0.002)**	**9.43 (0.001)**
Left putamen[2,3,4]	0.09 (0.43)	0.09 (0.48)	-0.03 (0.88)	-0.002 (0.89)	-0.05 (0.66)	-0.005 (0.71)	0.09 (0.44)	-0.03 (0.99)
Right putamen[2,3]	0.09 (0.44)	0.10 (0.41)	-0.11 (0.61)	-0.01 (0.50)	-0.10 (0.40)	-0.01 (0.31)	0.14 (0.23)	2.33 (0.41)
Left pallidum[3]	0.02 (0.84)	0.01 (0.89)	0.24 (0.26)	-0.26 (0.30)	-0.14 (0.22)	-0.24 (0.14)	0.13 (0.26)	1.80 (0.28)
Right pallidum[3,4]	-0.00 (0.99)	-0.01 (0.57)	0.20 (0.37)	0.01 (0.72)	0.11 (0.34)	-0.13 (0.42)	0.04 (0.71)	0.28 (0.87)
Left thalamus[2]	0.01 (0.95)	0.09 (0.70)	-0.14 (0.52)	-0.03 (0.36)	-0.09 (0.41)	-0.03 (0.20)	0.05 (0.68)	3.44 (0.53)
Right thalamus[2,3]	-0.03 (0.79)	-0.10 (0.96)	-0.17 (0.44)	-0.03 (0.22)	-0.11 (0.34)	-0.03 (0.18)	0.01 (0.93)	1.38 (0.78)
Left cerebellum[2,3]	0.03 (0.78)	0.62 (0.44)	0.003 (0.99)	-0.03 (0.71)	-0.02 (0.84)	-0.05 (0.51)	0.11 (0.33)	25.41 (0.16)
Right cerebellum[2,3]	0.05 (0.65)	0.73 (0.36)	0.02 (0.94)	-0.006 (0.95)	-0.02 (0.87)	-0.05 (0.55)	0.14 (0.22)	29.45 (0.10)
Vermis[2,3]	-0.04 (0.74)	-0.01 (0.96)	-0.08 (0.71)	-0.02 (0.37)	-0.05 (0.67)	-0.01 (0.49)	-0.10 (0.38)	-2.97 (0.98)

r is Pearson correlation coefficient; **β** is unstandardised regression coefficient after controlling for potential confounders related to the outcome at $p<0.10$: 1 = equivalent GA of infant at MRI; 2 = infant weight at MRI; 3 = infant head circumference at MRI; 4 = maternal weight change per week. Bold indicates significance at $p\leq0.05$. [a]CD4 count missing for 2 mothers who started ART pre-conception; [b]Only for mothers with detectable viral load (VL); [c]Associations among all HEU infants; VL set to zero for mothers with undetectable levels

Table 4. Comparison of regional volumes among HEU infants between those whose mothers had detectable or undetectable viral loads within 6 months of enrolment. We present the comparison for all HEU infants combined, and separately for those in the pre- and post-conception ART groups.

	HEU (n = 79)		**HEU pre-conception ART (n = 40)**		**HEU post-conception ART (n = 39)**	
Region	**Detectable vs undetectable maternal VL**		**Detectable vs undetectable maternal VL**		**Detectable vs undetectable maternal VL**	
	t (*p*)	**β (*p*)**	**t (*p*)**	**β (*p*)**	**t (*p*)**	**β (*p*)**
Left caudate[1]	-1.28 (0.21)	0.80 (0.16)	0.01 (0.99)	14.9 (0.88)	-1.45 (0.16)	0.74 (0.20)
Right caudate[1]	-1.47 (0.14)	0.80 (0.16)	-0.16 (0.87)	26.6 (0.79)	-1.54 (0.13)	0.96 (0.16)
Left putamen[1,2,3]	-1.42 (0.16)	61.3 (0.24)	-0.80 (0.43)	112.0 (0.18)	-0.99 (0.33)	49.2 (0.49)
Right putamen[1,2]	-1.63 (0.11)	72.8 (0.16)	-0.56 (0.58)	66.2 (0.42)	-1.40 (0.17)	79.9 (0.26)
Left pallidum[2,4]	-0.34 (0.74)	8.09 (0.79)	-0.51 (0.62)	40.8 (0.39)	0.54 (0.59)	-27.9 (0.46)
Right pallidum[1,2,4]	-0.60 (0.55)	16.9 (0.59)	-0.10 (0.92)	14.4 (0.81)	-0.65 (0.52)	0.16 (0.64)
Left thalamus[1]	-0.90 (0.38)	64.5 (0.68)	0.69 (0.49)	-205.8 (0.26)	**-2.50 (0.02)**	**270.4 (0.02)**
Right thalamus[1,5]	-1.04 (0.30)	69.4 (0.56)	0.20 (0.84)	-100.3 (0.53)	-1.95 (0.06)	198.3 (0.11)
Left cerebellum[1,5]	-1.00 (0.33)	217.1 (0.52)	-0.28 (0.78)	-40.0 (0.95)	-1.07 (0.29)	233.5 (0.56)
Right cerebellum[1,5]	-1.14 (0.26)	280.6 (0.40)	0.03 (0.98)	-260.5 (0.65)	-1.45 (0.15)	444.5 (0.30)
Vermis[1,5]	-0.38 (0.70)	11.8 (0.88)	0.09 (0.32)	-152.3 (0.20)	-1.69 (0.10)	144.7 (0.18)

Independent one-tail t-test; **β** is unstandardised regression coefficient after controlling for potential confounders related to the outcome at $p<0.10$: 1 = infant weight at MRI; 2 = infant head circumference at MRI; 3 = maternal weight change per week; 4 = maternal alcohol consumption averaged across pregnancy; 5 = Equivalent GA of infant at MRI. Bold indicates significance at $p \leq 0.05$.

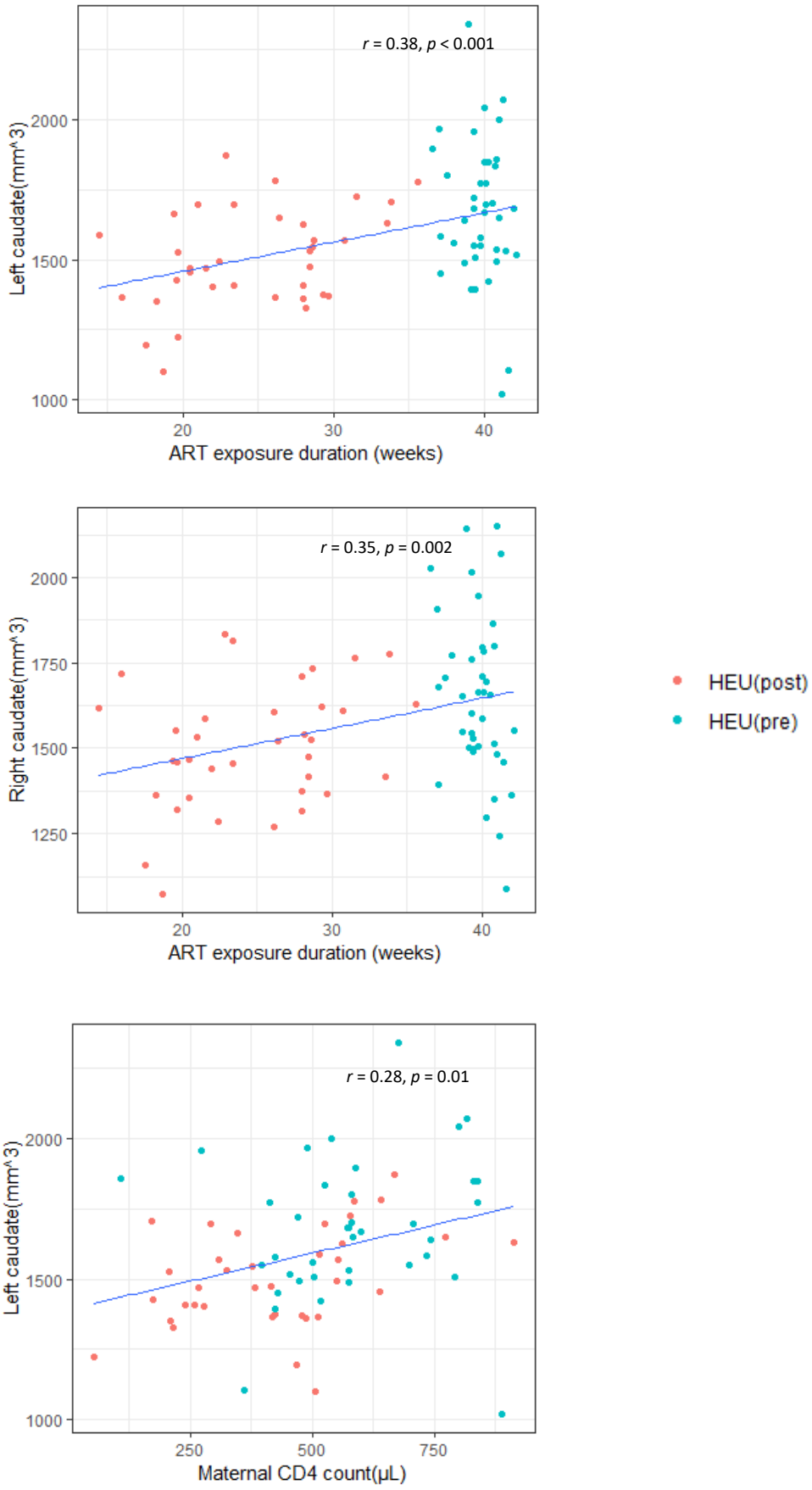

Figure 1. plots showing associations of the regional volumes among infants with maternal clinical and treatment variables.

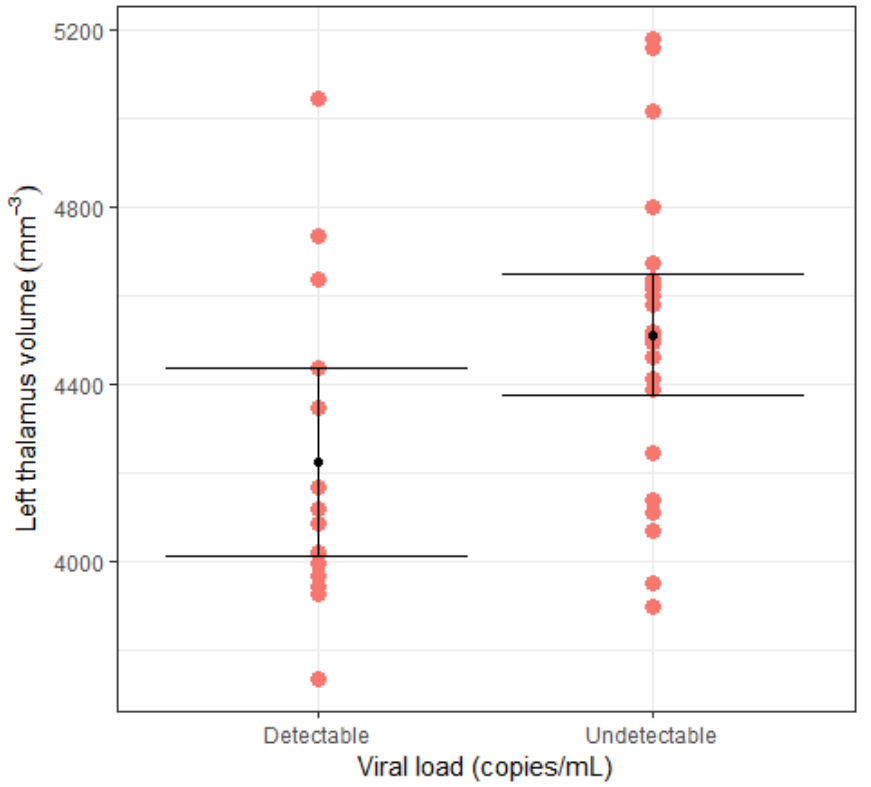

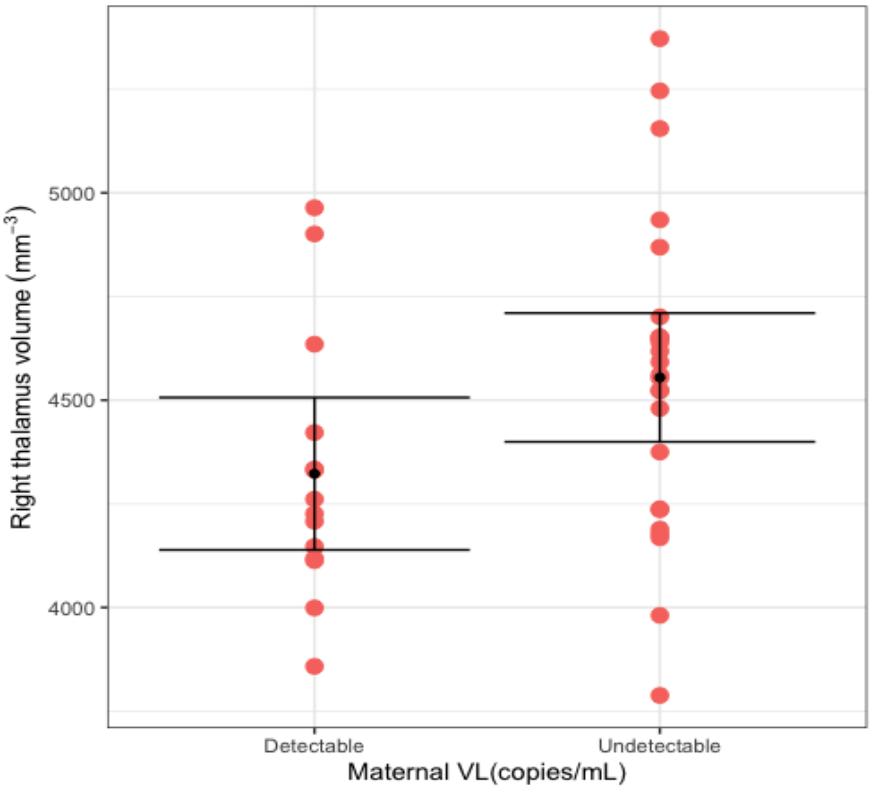

Figure 2. Comparison (mean and quartile) of left thalamic volumes by maternal viral load detectability within HEU post-conception infants.

Supplementary analysis 2

Fractional anisotropy (FA)	Mean diffusivity (MD)	Axial diffusivity (AD)	Radial diffusivity (RD)	
Intrinsic basal ganglia connections				
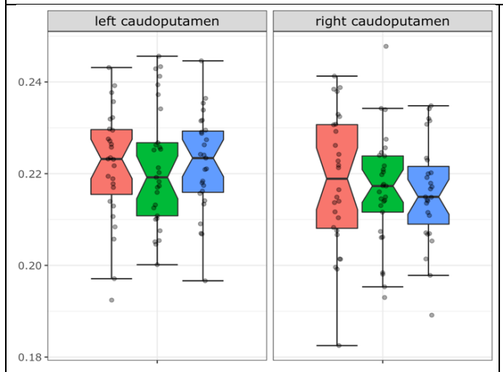	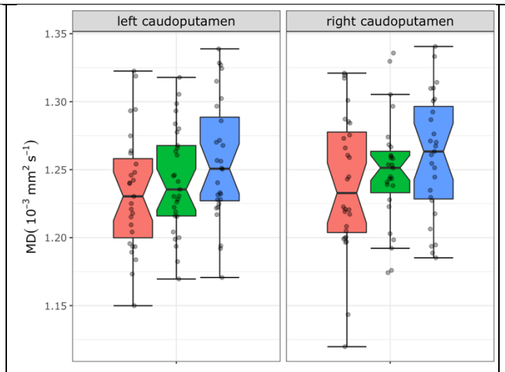	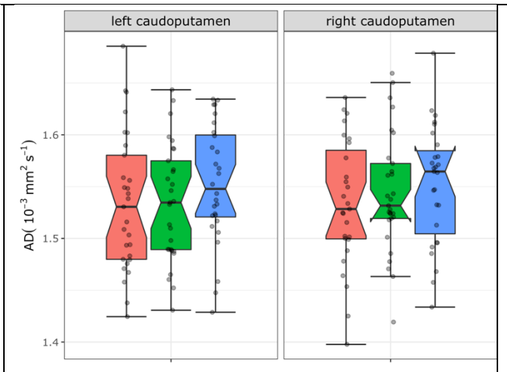	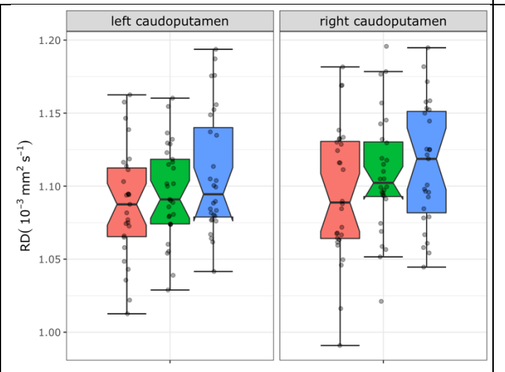	
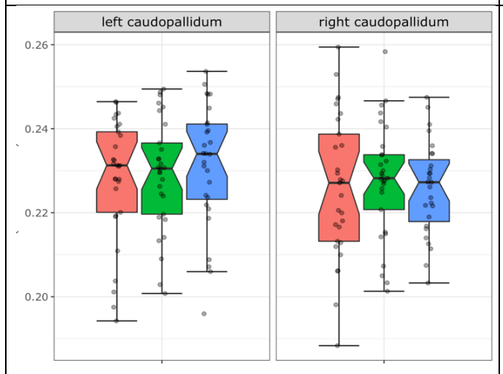	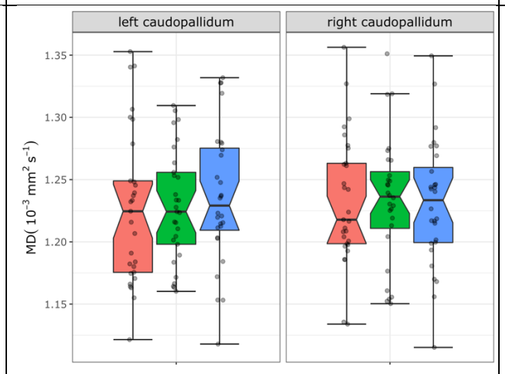	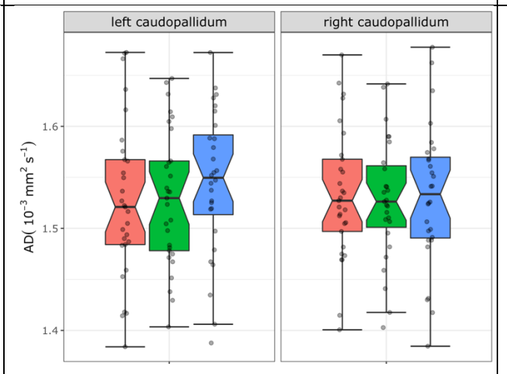	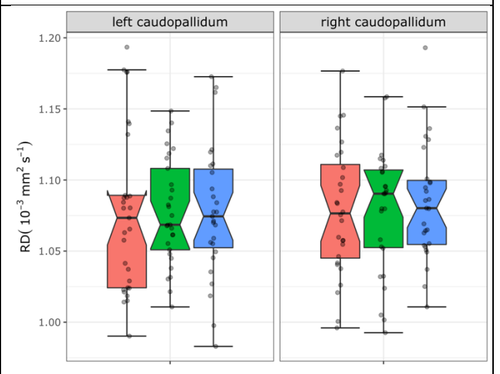	
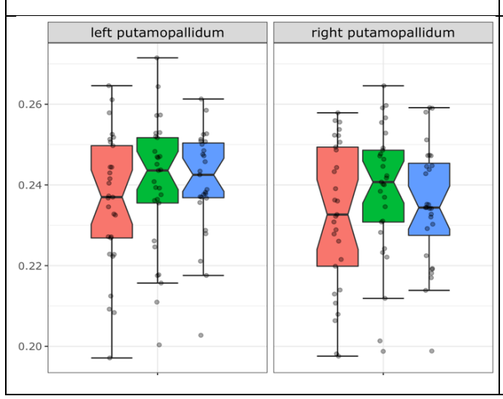	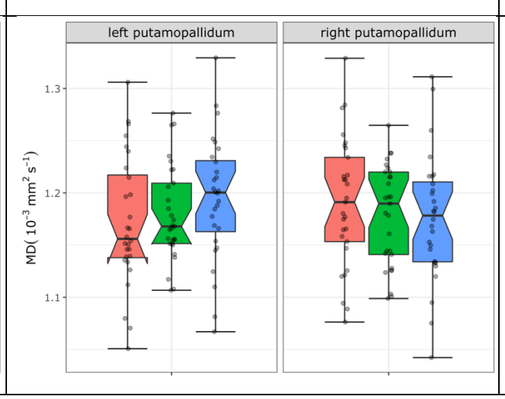	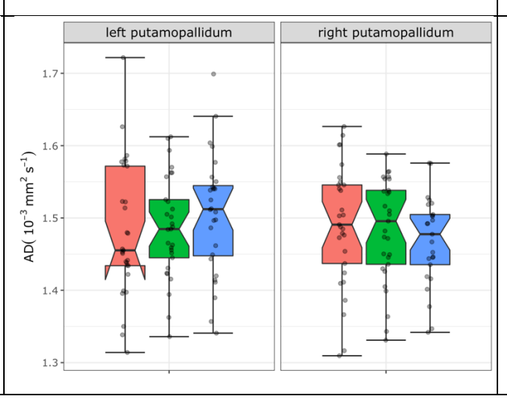	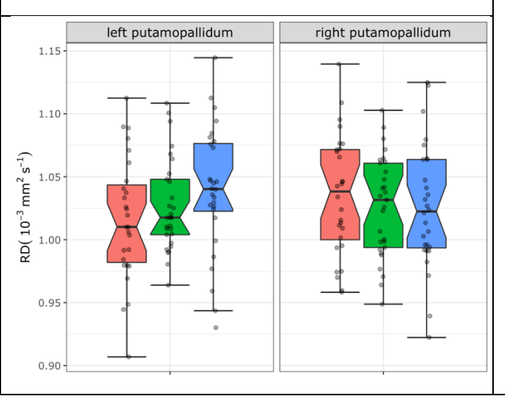	

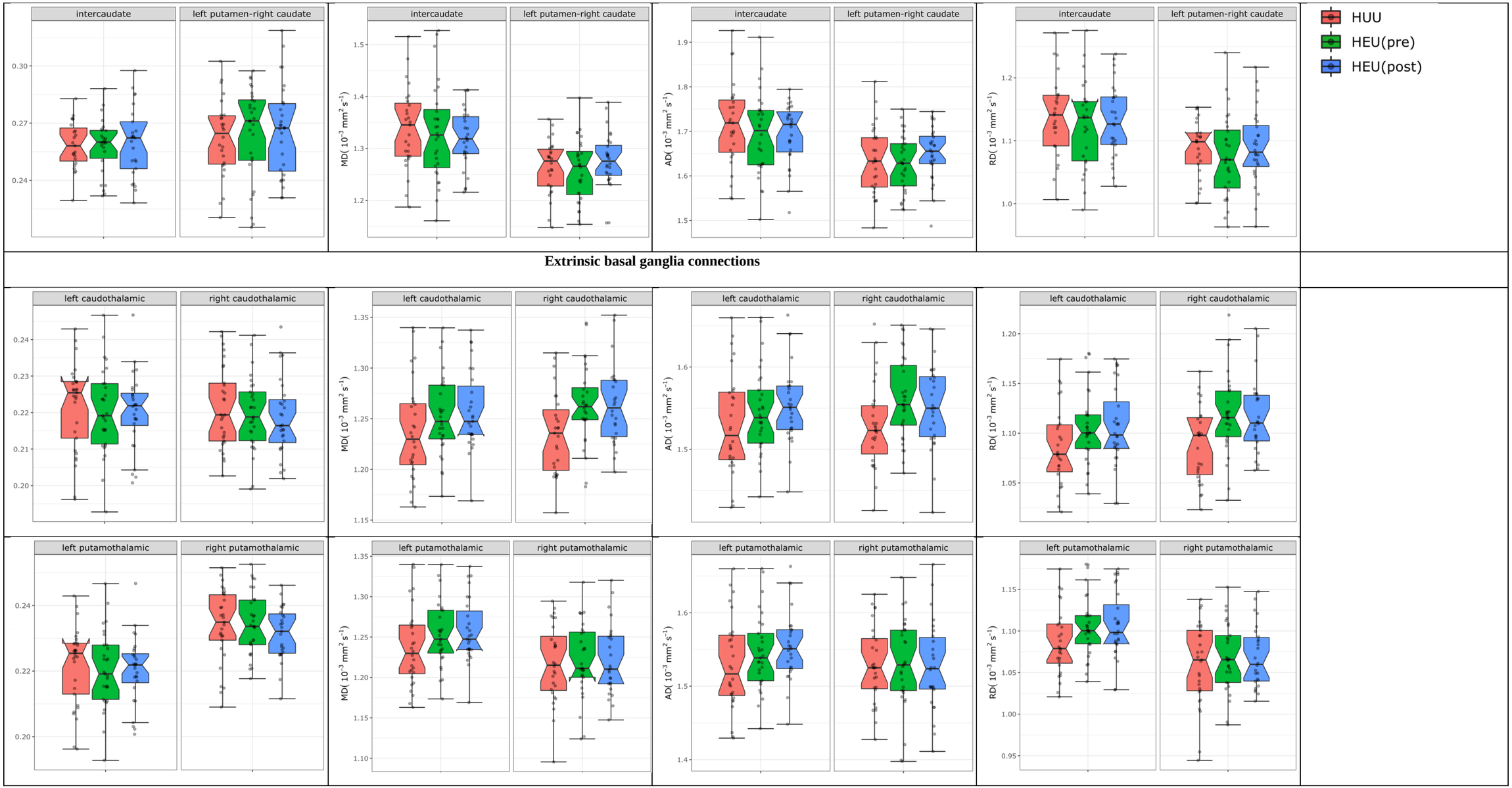
intercaudate
left putamen-right caudate
MD(10^{-3} mm^2 s^{-1})
AD(10^{-3} mm^2 s^{-1})
RD(10^{-3} mm^2 s^{-1})
HUU
HEU(pre)
HEU(post)
Extrinsic basal ganglia connections
left caudothalamic
right caudothalamic
left putamothalamic
right putamothalamic

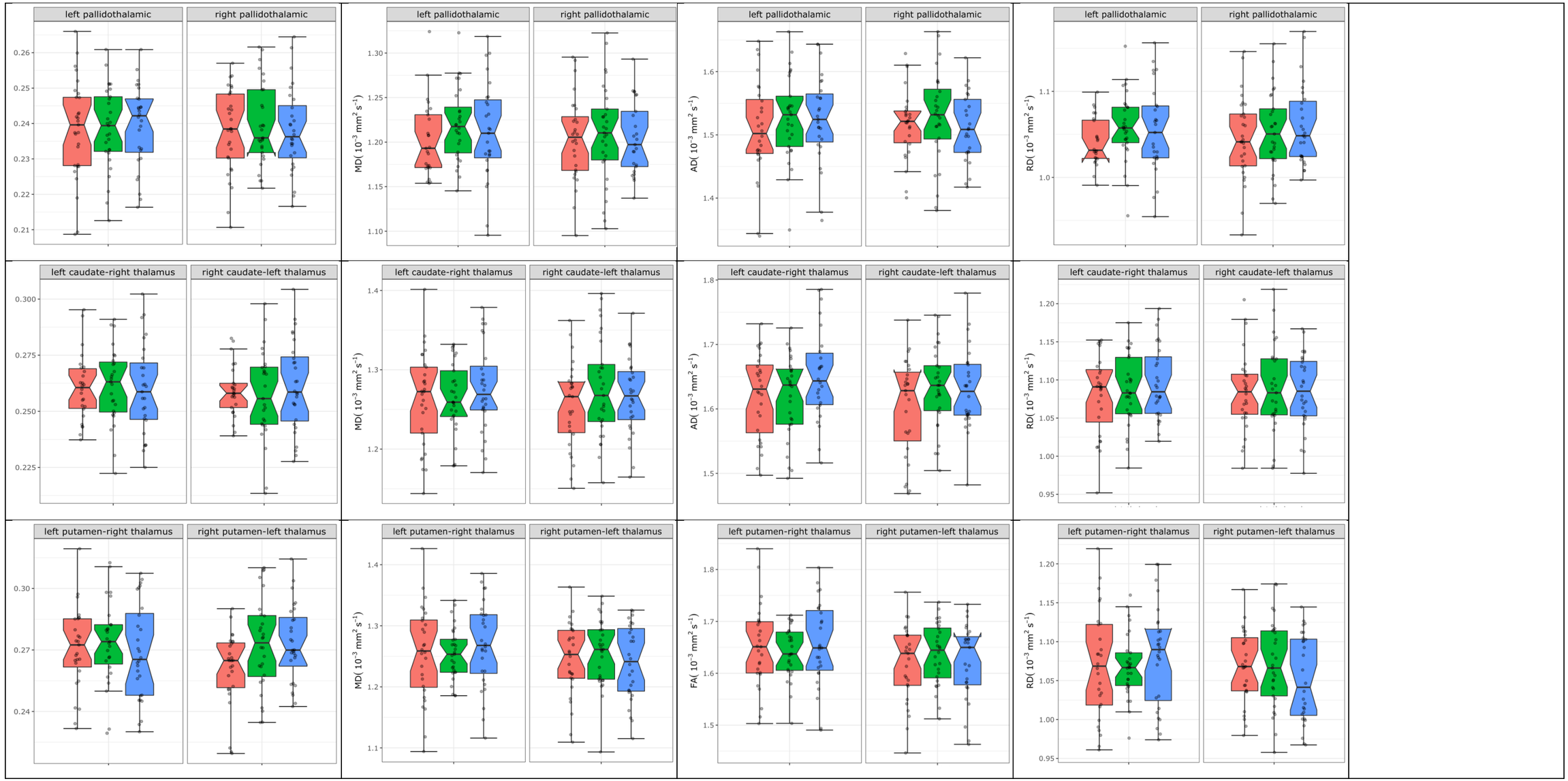
left pallidothalamic
right pallidothalamic
MD(10^{-3} mm^2 s^{-1})
AD(10^{-3} mm^2 s^{-1})
RD(10^{-3} mm^2 s^{-1})
left caudate-right thalamus
right caudate-left thalamus
left putamen-right thalamus
right putamen-left thalamus
FA(10^{-3} mm^2 s^{-1})

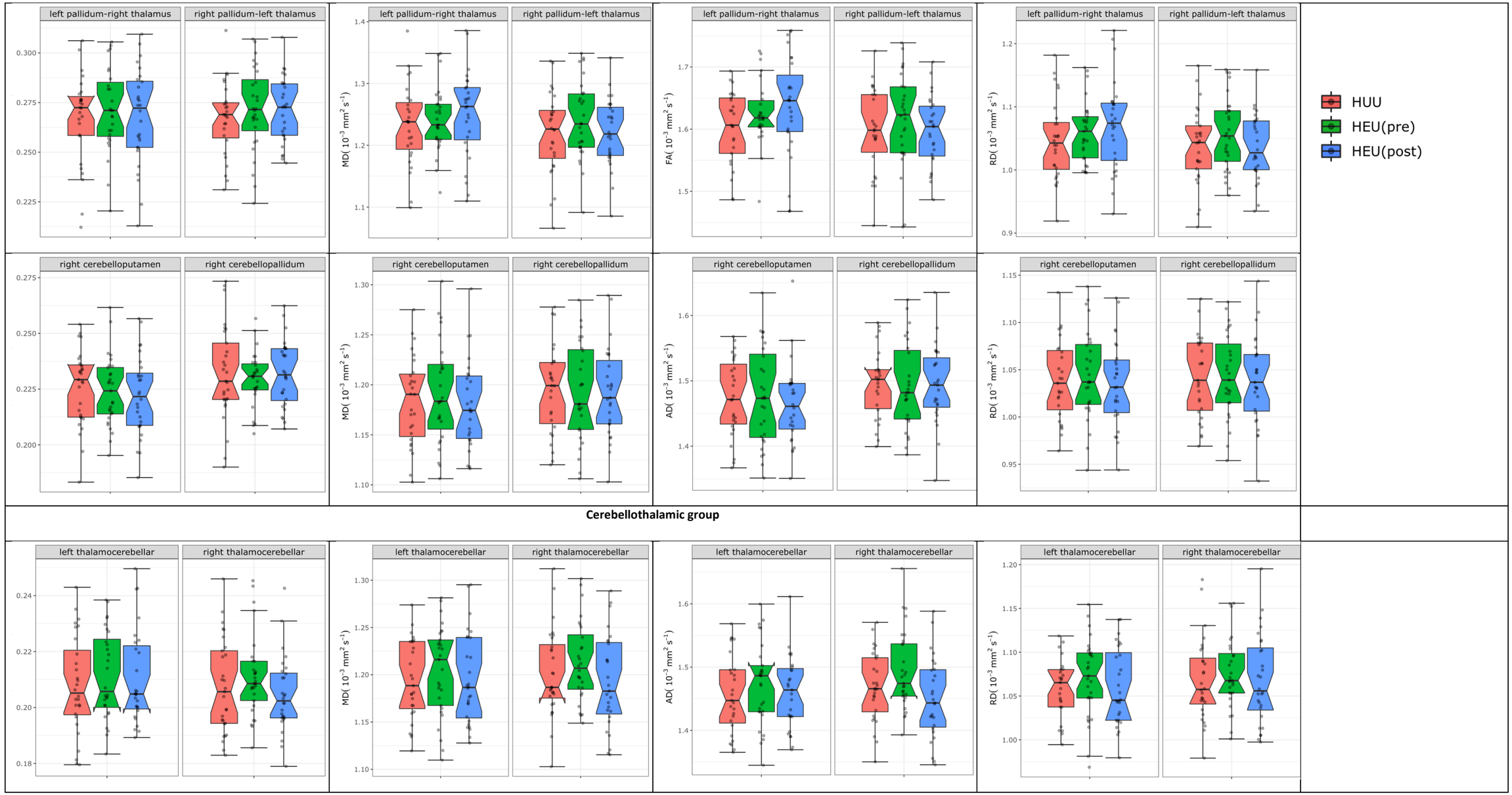
left pallidum-right thalamus
right pallidum-left thalamus
MD(10^{-3} mm^2 s^{-1})
FA(10^{-3} mm^2 s^{-1})
RD(10^{-3} mm^2 s^{-1})
right cerebelloputamen
right cerebellopallidum
AD(10^{-3} mm^2 s^{-1})
Cerebellothalamic group
left thalamocerebellar
right thalamocerebellar
HUU
HEU(pre)
HEU(post)

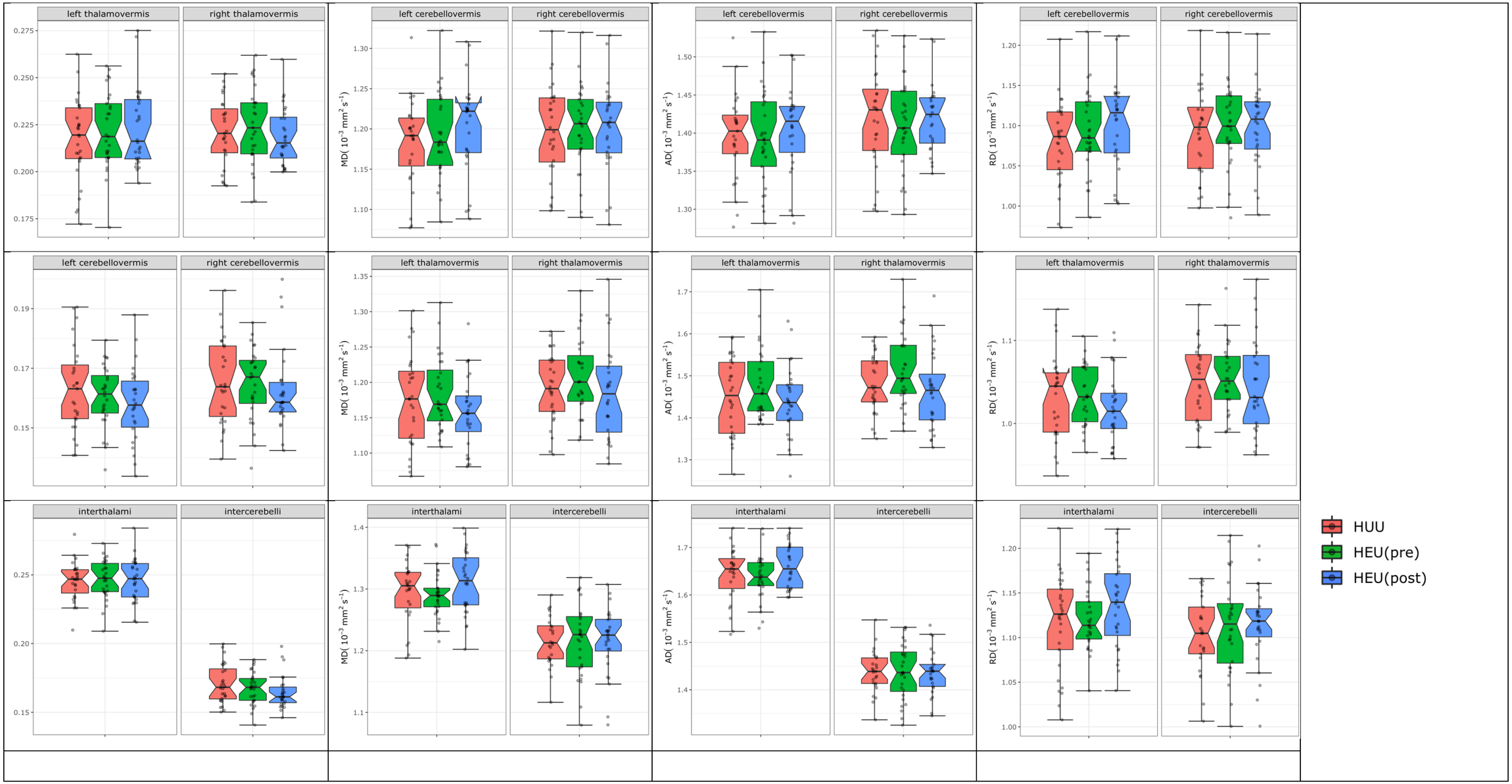

Figure 1. comparison of DTI parameters by group. The HEU group comprised exposed uninfected infants born to mothers who had either initiated ART **pre**-conception or during gestation (**post**-conception); HUU are unexposed uninfected controls. Hourglasses show median and interquartile ranges; whiskers are upper and lower extremes. Values above and below the whiskers are outliers, defined as data points more than 1.5 times the interquartile range above (or below) the upper (or lower) quartile. *p* values from independent one-tail student t-test.

Table 2.1a Associations of WM-ROIs FA with potential confounding variables

WM-ROI	Infant indices at MRI				Maternal indices	
	Sex	**GA**	**Weight[1]**	**Head Circumference[1]**	**Weight change per week**	**Age at delivery**
Intrinsic basal ganglia connections						
L caudoputamen	0.02 (0.80)	**0.32 (0.003)**	-0.05 (0.60)	-0.14 (0.20)	0.01 (0.90)	-0.03 (0.80)
L caudopallidum	0.03 (0.80)	**0.31 (0.003)**	-0.03 (0.80)	-0.09 (0.40)	-0.02 (0.80)	-0.11 (0.30)
L putamopallidum	-0.07 (0.50)	**0.27 (0.01)**	-0.01 (0.90)	-0.02 (0.80)	-0.05 (0.60)	-0.09 (0.40)
R caudoputamen	0.01(0.90)	**0.30 (0.005)**	-0.06 (0.60)	**-0.19 (0.09)**	0.09 (0.40)	-0.10 (0.40)
R caudopallidum	0.03 (0.80)	**0.31 (0.004)**	-0.02 (0.80)	-0.10 (0.30)	0.05 (0.60)	-0.09 (0.40)
R putamopallidum	-0.001 (1.00)	**0.23 (0.04)**	0.01 (0.90)	0.07 (0.50)	-0.07 (0.50)	-0.07 (0.50)
Inter-caudate	0.04 (0.70)	**0.27 (0.02)**	-0.02 (0.90)	-0.03 (0.80)	0.10 (0.40)	-0.08 (0.40)
L putamen-R caudate	-0.11 (0.30)	0.09 (0.40)	-0.04 (0.70)	-0.02 (0.80)	-0.001 (1.00)	-0.05 (0.60)
Extrinsic basal ganglia connections						
L caudothalamus	0.13 (0.20)	**0.27 (0.01)**	0.004 (1.00)	-0.03 (0.80)	0.03 (0.80)	-0.03 (0.80)
L putamothalamus	0.13 (0.20)	**0.27 (0.01)**	0.004 (1.00)	-0.03 (0.80)	0.03 (0.80)	-0.03 (0.80)
L pallidothalamus	0.03 (0.70)	**0.29 (0.007)**	0.10 (0.40)	0.16 (0.10)	-0.01 (0.90)	-0.06 (0.60)
R caudothalamus	0.06 (0.60)	**0.37 (0.0004)**	0.12 (0.30)	-0.05 (0.60)	0.13 (0.20)	-0.002 (1.00)
R putamothalamus	0.06 (0.60)	**0.26 (0.01)**	0.10 (0.40)	0.02 (0.80)	0.06 (0.60)	-0.04 (0.70)
R pallidothalamus	-0.01 (0.90)	0.14 (0.20)	0.10 (0.40)	0.14 (0.20)	-0.01 (0.90)	-0.05 (0.60)
L caudate-R thalamus	-0.09 (0.40)	**0.19 (0.08)**	0.06 (0.60)	0.16 (0.20)	-0.01 (0.90)	0.01 (0.90)
L putamen-R thalamus	-0.01 (0.90)	0.16 (0.10)	-0.07 (0.50)	0.05 (0.70)	-0.03 (0.80)	-0.15 (0.20)
L pallidum-R thalamus	-0.04 (0.70)	0.16 (0.10)	0.05 (0.70)	0.09 (0.40)	0.05 (0.60)	-0.18 (0.10)
R caudate-L thalamus	-0.11 (0.30)	0.18 (0.10)	0.06 (0.60)	0.04 (0.70)	-0.01 (0.90)	-0.03 (0.80)
R putamen-L thalamus	0.001 (1.00)	**0.29 (0.07)**	-0.03 (0.80)	0.03 (0.80)	-0.02 (0.80)	-0.18 (0.10)
R pallidum-L thalamus	-0.01 (0.90)	**0.24 (0.03)**	-0.05 (0.60)	-0.002 (1.00)	0.06 (0.60)	**-0.19 (0.09)**

R putamocerebellar	0.15 (0.20)	0.13 (0.20)	0.02 (0.80)	-0.05 (0.60)	-0.01 (0.90)	**-0.20 (0.02)**
R pallidocerebellar	**0.28 (0.009)**	0.10 (0.30)	0.17 (0.10)	0.10 (0.30)	0.05 (0.60)	-0.05 (0.60)
Cerebellothalamic group						
L thalamocerebellar	0.07 (0.50)	**0.23 (0.03)**	-0.07 (0.50)	0.12 (0.30)	-0.02 (0.80)	-0.06 (0.60)
R thalamocerebellar	**0.19 (0.08)**	**0.23 (0.03)**	0.01 (0.90)	0.04 (0.70)	0.001 (1.00)	0.007 (0.90)
L thalamo-vermis	0.16 (0.10)	0.11 (0.30)	-0.02 (0.80)	0.13 (0.20)	-0.06 (0.60)	0.02 (0.80)
R thalamo-vermis	0.09 (0.40)	0.15 (0.10)	-0.04 (0.70)	0.09 (0.40)	-0.08 (0.40)	0.04 (0.70)
Interthalami	-0.04 (0.70)	**0.28 (0.01)**	0.11 (0.30)	0.09 (0.40)	0.09 (0.40)	0.03 (0.80)
L cerebello-vermis	**0.26 (0.02)**	0.04 (0.70)	-0.02 (0.90)	0.05 (0.70)	0.16 (0.10)	0.01 (0.90)
R cerebello-vermis	**0.20 (0.07)**	**0.20 (0.06)**	0.01 (0.90)	0.03 (0.80)	0.005 (1.00)	0.10 (0.40)
Intercerebelli	**0.30 (0.007)**	0.13 (0.20)	-0.09 (0.40)	-0.06 (0.60)	0.13 (0.20)	0.08 (0.40)

Values are Pearson correlation coefficients, *r* (p-value); GA = gestational age; AA = absolute alcohol (oz); L left; R right; Bold indicates significance at $p<0.10$; [1]Data missing for 1 infant in the HEU pre-conception ART group and 2 HUU infants.

Table 2.1b Associations of WM-ROIs MD with potential confounding variables

WM-ROI	Infant indices at MRI				Maternal indices	
	Sex	**GA**	**Weight[1]**	**Head Circumference[1]**	**Weight change per week**	**Age at delivery**
Intrinsic basal ganglia connections						
L caudoputamen	**-0.22 (0.04)**	**-0.22 (0.04)**	0.06 (0.60)	0.16 (0.20)	-0.13 (0.20)	-0.08 (0.40)
L caudopallidum	-0.11 (0.30)	-0.17 (0.10)	0.03 (0.80)	0.09 (0.40)	-0.04 (0.70)	-0.05 (0.60)
L putamopallidum	0.01 (0.90)	**-0.26 (0.01)**	0.03 (0.80)	0.02 (0.80)	-0.07 (0.50)	0.01 (0.90)
R caudoputamen	-0.14 (0.20)	-0.08 (0.50)	-0.01 (0.90)	0.11 (0.30)	**-0.18 (0.09)**	0.17 (0.10)
R caudopallidum	-0.06 (0.50)	-0.05 (0.60)	0.02 (0.80)	0.08 (0.50)	-0.04 (0.70)	0.17 (0.10)
R putamopallidum	-0.12 (0.30)	-0.17 (0.10)	0.03 (0.70)	0.05 (0.60)	0.03 (0.80)	0.13 (0.20)
Inter-caudate	-0.06 (0.60)	-0.06 (0.60)	0.15 (0.20)	0.17 (0.10)	0.02 (0.90)	**0.19 (0.09)**
L putamen-R caudate	0.01 (0.90)	-0.05 (0.60)	0.15 (0.20)	0.15 (0.20)	**-0.18 (0.09)**	0.03 (0.80)
Extrinsic basal ganglia connections						
L caudothalamus	**-0.27 (0.01)**	**-0.23 (0.03)**	0.15 (0.20)	**0.20 (0.07)**	-0.14 (0.20)	-0.04 (0.70)
L putamothalamus	**-0.27 (0.01)**	**-0.23 (0.03)**	0.15 (0.20)	**0.20 (0.07)**	-0.14 (0.20)	-0.04 (0.70)
L pallidothalamus	0.02 (0.80)	-0.16 (0.10)	-0.10 (0.40)	0.003 (1.00)	-0.07 (0.50)	-0.08 (0.40)
R caudothalamus	-0.18 (0.10)	**-0.25 (0.02)**	0.07 (0.50)	0.13 (0.20)	-0.14 (0.20)	**0.24 (0.02)**
R putamothalamus	-0.11 (0.30)	-0.18 (0.10)	-0.12 (0.30)	0.02 (0.80)	-0.09 (0.40)	**0.23 (0.03)**
R pallidothalamus	-0.03 (0.80)	-0.09 (0.40)	-0.12 (0.30)	-0.09 (0.40)	-0.01 (0.90)	0.11 (0.30)
L caudate-R thalamus	**-0.21 (0.05)**	-0.17 (0.10)	**0.33 (0.002)**	0.12 (0.30)	-0.07 (0.50)	0.08 (0.40)
L putamen-R thalamus	-0.08 (0.50)	-0.14 (0.20)	0.09 (0.40)	-0.01 (0.90)	-0.08 (0.40)	0.02 (0.80)
L pallidum-R thalamus	-0.04 (0.70)	**-0.22 (0.04)**	0.03 (0.80)	0.03 (0.80)	-0.11 (0.30)	-0.03 (0.80)
R caudate-L thalamus	0.01 (0.90)	-0.08 (0.40)	0.15 (0.20)	0.12 (0.30)	0.009 (0.90)	0.17 (0.10)
R putamen-L thalamus	-0.10 (0.40)	-0.08 (0.40)	0.09 (0.40)	0.02 (0.90)	-0.09 (0.40)	**0.20 (0.06)**
R pallidum-L thalamus	-0.09 (0.40)	-0.16 (0.10)	0.15 (0.20)	0.05 (0.70)	0.02 (0.90)	0.08 (0.40)

R putamocerebellar	**-0.20 (0.07)**	**-0.31 (0.005)**	0.02 (0.80)	-0.07 (0.50)	0.03 (0.80)	0.06 (0.60)
R pallidocerebellar	-0.13 (0.20)	**-0.38 (0.0005)**	0.07 (0.50)	-0.03 (0.70)	0.01 (0.90)	0.15 (0.20)
Cerebellothalamic group						
L thalamocerebellar	**-0.23 (0.04)**	-0.18 (0.10)	0.14 (0.20)	-0.04 (0.70)	0.03 (0.80)	0.01 (0.90)
R thalamocerebellar	-0.14 (0.20)	**-0.34 (0.001)**	-0.04 (0.70)	-0.10 (0.40)	-0.08 (0.40)	0.12 (0.20)
L thalamo-vermis	-0.01 (0.90)	-0.11 (0.30)	0.07 (0.50)	-0.05 (0.60)	-0.004 (1.00)	0.18 (1.00)
R thalamo-vermis	-0.03 (0.80)	-0.08 (0.50)	0.13 (0.20)	-0.02 (0.90)	**-0.23 (0.03)**	**0.19 (0.09)**
Interthalami	-0.14 (0.20)	**-0.36 (0.0008)**	0.04 (0.70)	0.03 (0.80)	-0.14 (0.20)	0.01 (0.90)
L cerebello-vermis	**-0.20 (0.07)**	**-0.34 (0.002)**	-0.03 (0.80)	-0.11 (0.30)	-0.04 (0.70)	-0.17 (0.10)
R cerebello-vermis	-0.14 (0.20)	**-0.32 (0.003)**	-0.01 (0.90)	-0.13 (0.20)	-0.02 (0.90)	-0.08 (0.50)
Intercerebelli	**-0.13 (0.04)**	**-0.24 (0.03)**	0.01 (0.90)	-0.15 (0.20)	-0.01 (0.90)	-0.15 (0.20)

Values are Pearson correlation coefficients, *r* (p-value); GA = gestational age; AA = absolute alcohol (oz); L left; R right; Bold indicates significance at $p<0.10$; [1]Data missing for 1 infant in the HEU pre-conception ART group and 2 HUU infants.

Table 2.1c Associations of WM-ROIs AD with potential confounding variables

WM-ROI	Infant indices at MRI				Maternal indices	
	Sex	**GA**	**Weight[1]**	**Head Circumference[1]**	**Weight change per week**	**Age at delivery**
Intrinsic Basal ganglia connections						
L caudoputamen	-0.15 (0.10)	-0.13 (0.20)	0.02 (0.90)	0.07 (0.50)	-0.08 (0.50)	-0.03 (0.70)
L caudopallidum	-0.09 (0.40)	-0.07 (0.50)	0.01 (0.90)	0.04 (0.70)	-0.04 (0.70)	-0.08 (0.50)
L putamopallidum	0.03 (0.70)	-0.13 (0.20)	0.06 (0.60)	0.04 (0.70)	-0.02 (0.80)	-0.02 (0.80)
R caudoputamen	-0.16 (0.10)	0.006 (0.90)	0.09 (0.40)	0.10 (0.40)	-0.11 (0.30)	0.15 (0.20)
R caudopallidum	-0.02 (0.80)	0.06 (0.50)	0.05 (0.70)	0.002 (1.00)	-0.02 (0.80)	0.11 (0.30)
R putamopallidum	-0.10 (0.40)	-0.09 (0.40)	0.03 (0.80)	0.05 (0.60)	0.006 (0.90)	0.09 (0.40)
Inter-caudate	-0.06 (0.60)	0.01 (0.90)	0.15 (0.20)	0.16 (0.20)	0.02 (0.80)	0.11 (0.30)
L putamen-R caudate	-0.5 (0.60)	-0.11 (0.30)	0.17 (0.10)	0.17 (0.10)	-0.15 (0.20)	0.07 (0.50)
Extrinsic basal ganglia connections						
L caudothalamus	**-0.22 (0.04)**	-0.15 (0.20)	0.14 (0.20)	0.16 (0.10)	-0.12 (0.30)	-0.05 (0.60)
L putamothalamus	**-0.22 (0.04)**	-0.15 (0.20)	0.14 (0.20)	0.16 (0.10)	-0.12 (0.30)	-0.05 (0.60)
L pallidothalamus	0.001 (1.00)	-0.14 (0.20)	-0.02 (0.90)	0.05 (0.60)	-0.07 (0.50)	-0.06 (0.60)
R caudothalamus	-0.15 (0.20)	**-0.22 (0.04)**	0.09 (0.40)	0.09 (0.40)	-0.07 (0.50)	**0.28 (0.01)**
R putamothalamus	-0.12 (0.20)	-0.16 (0.10)	-0.07 (0.50)	0.008 (0.90)	-0.03 (0.80)	**0.22 (0.04)**
R pallidothalamus	-0.02 (0.20)	-0.05 (0.70)	-0.09 (0.40)	-0.05 (0.70)	-0.002 (1.00)	0.09 (0.40)
L caudate-R thalamus	-0.16 (0.80)	-0.04 (0.70)	**0.27 (0.01)**	0.11 (0.30)	-0.13 (0.20)	0.07 (0.50)
L putamen-R thalamus	-0.02 (0.10)	0.005 (1.00)	0.15 (0.20)	0.04 (0.70)	-0.05 (0.70)	-0.04 (0.70)
L pallidum-R thalamus	0.02 (0.90)	**-0.19 (0.09)**	0.14 (0.20)	0.09 (0.40)	-0.15 (0.20)	-0.03 (0.80)
R caudate-L thalamus	-0.06 (0.80)	-0.02 (0.80)	0.16 (0.10)	0.10 (0.30)	-0.04 (0.70)	0.17 (0.10)
R putamen-L thalamus	-0.12 (0.60)	-0.04 (0.70)	**0.23 (0.04)**	0.19 (0.10)	-0.07 (0.50)	0.17 (0.10)
R pallidum-L thalamus	-0.03 (0.80)	-0.15 (0.20)	0.15 (0.20)	0.03 (0.80)	0.03 (0.80)	0.09 (0.40)

R putamocerebellar	-0.11 (0.30)	**-0.26 (0.02)**	0.02 (0.80)	-0.11 (0.30)	0.006 (0.90)	-0.002 (1.00)
R pallidocerebellar	0.02 (0.80)	**-0.25 (0.02)**	0.10 (0.30)	-0.004 (0.10)	-0.01 (0.90)	0.10 (0.40)
Cerebellothalamic group						
L thalamocerebellar	-0.10 (0.30)	-0.09 (0.40)	0.03 (0.80)	-0.03 (0.80)	0.01 (0.90)	0.006 (0.90)
R thalamocerebellar	-0.10 (0.30)	**-0.22 (0.04)**	-0.01 (0.90)	-0.11 (0.30)	-0.06 (0.60)	0.14 (0.20)
L thalamo-vermis	0.01 (0.90)	-0.06 (0.60)	0.07 (0.50)	0.05 (0.60)	-0.02 (0.80)	0.16 (0.10)
R thalamo-vermis	-0.06 (0.60)	0.01 (0.90)	0.13 (0.20)	0.04 (0.70)	**-0.20 (0.7)**	0.17 (0.10)
Interthalami	-0.04 (0.70)	-0.13 (0.20)	0.14 (0.20)	0.20 (0.08)	-0.07 (0.50)	-0.09 (0.40)
L cerebello-vermis	-0.10 (0.40)	**-0.29 (0.008)**	-0.02 (0.80)	-0.11 (0.30)	0.004 (1.00)	**-0.20 (0.06)**
R cerebello-vermis	-0.06 (0.60)	**-0.25 (0.02)**	-0.005 (1.00)	-0.12 (0.30)	-0.002 (1.00)	-0.08 (0.80)
Intercerebelli	**-0.23 (0.04)**	-0.18 (0.10)	0.03 (0.80)	-0.15 (0.20)	0.04 (0.70)	-0.07 (0.60)

Values are Pearson correlation coefficients, *r* (p-value); GA = gestational age; AA = absolute alcohol (oz); L left; R right; Bold indicates significance at $p<0.10$; [1]Data missing for 1 infant in the HEU pre-conception ART group and 2 HUU infants.

Table 2.1d Associations of WM-ROIs RD with potential confounding variables

WM-ROI	Infant indices at MRI				Maternal indices	
	Sex	**GA**	**Weight[1]**	**Head Circumference[1]**	**Weight change per week**	**Age at delivery**
Intrinsic basal ganglia connections						
L caudoputamen	**-0.23 (0.03)**	**-0.30 (0.005)**	0.07 (0.50)	**0.20 (0.07)**	-0.14 (0.20)	-0.08 (0.40)
L caudopallidum	-0.11 (0.30)	**-0.23 (0.03)**	0.04 (0.70)	0.12 (0.30)	-0.03 (0.80)	-0.02 (0.80)
L putamopallidum	-0.02 (0.90)	**-0.36 (0.001)**	0.03 (0.80)	0.03 (0.70)	-0.08 (0.40)	0.004 (1.00)
R caudoputamen	-0.14 (0.20)	-0.15 (0.20)	-0.03 (0.80)	0.14 (0.20)	**-0.20 (0.07)**	0.17 (0.10)
R caudopallidum	-0.11 (0.30)	-0.08 (0.40)	0.08 (0.50)	0.14 (0.20)	-0.09 (0.40)	**0.18 (0.09)**
R putamopallidum	-0.17 (0.10)	**-0.25 (0.02)**	-0.001 (1.00)	0.01 (0.90)	-0.009 (0.9)	0.18 (0.10)
Inter-caudate	-0.03 (0.80)	-011 (0.30)	0.12 (0.30)	0.11 (0.30)	0.02 (0.80)	0.09 (0.40)
L putamen-R caudate	0.05 (0.60)	-0.05 (0.70)	0.11 (0.30)	0.12 (0.30)	-0.15 (0.20)	0.03 (0.80)
Extrinsic basal ganglia connections						
L caudothalamus	**-0.27 (0.01)**	**-0.26 (0.01)**	0.12 (0.30)	**0.20 (0.07)**	-0.14 (0.20)	-0.07 (0.50)
L putamothalamus	**-0.28 (0.01)**	**-0.26 (0.01)**	0.12 (0.30)	**0.20 (0.07)**	-0.14 (0.20)	-0.07 (0.50)
L pallidothalamus	0.01 (0.90)	**-0.23 (0.03)**	-0.14 (0.20)	-0.05 (0.60)	-0.11 (0.30)	-0.05 (0.60)
R caudothalamus	-0.17 (0.10)	**-0.28 (0.008)**	0.05 (0.60)	0.15 (0.20)	-0.17 (0.10)	**0.23 (0.04)**
R putamothalamus	-0.15 (0.20)	**-0.21 (0.05)**	-0.10 (0.30)	0.06 (0.60)	-0.09 (0.40)	0.17 (0.10)
R pallidothalamus	-0.08 (0.40)	**-0.23 (0.03)**	-0.09 (0.40)	**-0.23 (0.03)**	-0.03 (0.70)	0.10 (0.30)
L caudate-R thalamus	-0.15 (0.10)	-0.17 (0.10)	**0.29 (0.007)**	0.08 (0.50)	-0.05 (0.60)	0.06 (0.60)
L putamen-R thalamus	-0.09 (0.40)	**-0.18 (0.09)**	0.12 (0.30)	-0.02 (0.90)	-0.08 (0.50)	0.08 (0.50)
L pallidum-R thalamus	0.003 (1.00)	**-0.23 (0.03)**	-0.007 (0.90)	-0.04 (0.70)	-0.12 (0.30)	0.02 (0.80)
R caudate-L thalamus	0.07 (0.50)	-0.14 (0.20)	0.10 (0.30)	0.12 (0.30)	0.004 (1.00)	0.15 (0.10)
R putamen-L thalamus	-0.14 (0.20)	-0.14 (0.20)	0.12 (0.30)	0.03 (0.80)	-0.07 (0.50)	**0.20 (0.07)**
R pallidum-L thalamus	-0.04 (0.70)	**-0.20 (0.06)**	0.07 (0.50)	-0.01 (0.90)	-0.02 (0.80)	0.13 (0.20)

R putamocerebellar	-0.16 (0.10)	**-0.27 (0.01)**	0.01 (0.90)	0.03 (0.80)	0.04 (0.70)	0.14 (0.20)
R pallidocerebellar	-0.16 (0.10)	**-032 (0.003)**	0.01 (0.90)	-0.04 (0.7)	-0.03 (0.80)	0.13 (0.20)
Cerebellothalamic group						
L thalamocerebellar	**-0.26 (0.02)**	**-0.23 (0.03)**	**0.20 (0.08)**	-0.04 (0.70)	0.05 (0.60)	0.03 (0.90)
R thalamocerebellar	-0.14 (0.20)	**-0.30 (0.005)**	-0.04 (0.70)	-0.08 (0.50)	-0.11 (0.30)	0.08 (0.40)
L thalamo-vermis	-0.06 (0.60)	**-0.19 (0.08)**	0.09 (0.40)	-0.03 (0.80)	0.02 (0.80)	0.10 (0.40)
R thalamo-vermis	-0.04 (0.70)	-0.13 (0.20)	0.15 (0.20)	-0.04 (0.70)	**-0.21 (0.06)**	0.17 (0.10)
Interthalami	-0.14 (0.20)	**-0.35 (0.001)**	-0.01 (0.90)	-0.004 (1.00)	-0.17 (0.10)	0.01 (0.90)
L cerebello-vermis	**-0.25 (0.02)**	**-0.35 (0.001)**	-0.01 (0.90)	-0.08 (0.40)	-0.06 (0.60)	-0.17 (0.10)
R cerebello-vermis	**-0.19 (0.07)**	**-0.35 (0.001)**	0.01 (0.90)	-0.10 (0.40)	-0.02 (0.80)	-0.10 (0.40)
Intercerebelli	**-0.30 (0.005)**	**-0.26 (0.02)**	0.03 (0.80)	-0.08 (0.50)	-0.06 (0.60)	-0.15 (0.20)

Values are Pearson correlation coefficients, *r* (p-value); GA = gestational age; L left; R right; Bold indicates significance at $p<0.10$; [1]Data missing for 1 infant in the HEU pre-conception ART group and 2 HUU infants.

Table 2.2a Associations among HEU infants of DTI parameters (FA, MD, AD and RDin WM tracts connecting manually traced seeds/targets with maternal clinical and treatment variables (CD 4 counts)

	FA		**MD**		**AD**		**RD**	
WM-ROI	**Maternal CD4 within 6 mo of enrolment (n = 57)[x]**		**Maternal CD4 within 6 mo of enrolment (n = 57)[x]**		**Maternal CD4 within 6 mo of enrolment (n = 57)[x]**		**Maternal CD4 within 6 mo of enrolment (n = 57)[x]**	
	r *(p)*	**β *(p)***	**r *(p)***	**β *(p)***	**r *(p)***	**β *(p)***	**r *(p)***	**β *(p)***
Intrinsic basal ganglia connections								
L caudoputamen[2, a, b, *, †, §]	0.09 (0.50)	0.00001 (0.40)	-0.06 (0.70)	-0.00002 (0.40)	-0.03 (0.80)	-0.00001 (0.80)	-0.07 (0.60)	-0.00002 (0.30)
L caudopallidum[2, †]	0.11 (0.40)	0.00001 (0.30)	-0.07 (0.60)	-0.00002 (0.60)	-0.04 (0.80)	-0.00001 (0.80)	-0.09 (0.50)	-0.00002 (0.40)
L putamopallidum[2, b, †]	0.15 (0.30)	0.00001 (0.20)	-0.02 (0.90)	-0.00001 (0.80)	0.01 (0.90)	0.000005 (0.90)	-0.04 (0.70)	-0.00001 (0.60)
R caudoputamen[2, e, †, ¶]	0.09 (0.50)	0.00001 (0.30)	0.02 (0.90)	0.000006 (0.80)	0.03 (0.80)	0.00001 (0.80)	0.02 (0.90)	0.000004 (0.90)
R caudopallidum[2, #, ¶]	0.17 (0.20)	0.00001 (0.10)	-0.01 (1.00)	-0.000001 (1.00)	-0.04 (0.80)	-0.00001 (0.80)	-0.04 (0.80)	-0.00002 (0.60)
R putamopallidum[2]	0.09 (0.50)	0.00001 (0.40)	0.08 (0.60)	0.00002 (0.60)	0.08 (0.53)	0.00003 (0.50)	0.07 (0.60)	0.00001 (0.70)
Inter-caudate[2, f]	0.20 (0.10)	0.00002 (0.10)	-0.08 (0.50)	-0.00003 (0.50)	-0.07 (0.60)	-0.00003 (0.60)	-0.16 (0.30)	-0.00005 (0.30)
L putamen-R caudate[e]	0.11 (0.40)	0.00001 (0.40)	**-0.32 (0.01)**	**-0.0001 (0.02)**	**-0.27 (0.04)**	**-0.00008 (0.04)**	**-0.30 (0.03)**	**-0.0001 (0.03)**
Extrinsic basal ganglia connections								
L caudothalamus[2, a, b, d, A, *, †, §]	0.10 (0.50)	0.00001 (0.40)	0.01 (0.90)	-0.000005 (0.80)	0.03 (0.80)	0.00001 (0.8)	-0.004 (1.00)	-0.00001 (0.70)
L putamothalamus[2, a, b, d, A, *, †, §]	0.10 (0.50)	0.00001 (0.40)	0.01 (0.90)	-0.000005 (0.80)	0.03 (0.80)	0.000001 (1.00)	-0.004 (1.00)	-0.00001 (0.70)
L pallidothalamus[2, †]	0.10 (0.40)	0.00001 (0.40)	-0.004 (1.00)	-0.000001 (1.00)	-0.02 (0.90)	-0.00001 (0.80)	-0.02 (0.90)	-0.00001 (0.70)
R caudothalamus[2, a, b, f, B, F, †, #]	0.03 (0.80)	0.000003 (0.70)	0.08 (0.50)	0.0000005 (1.00)	0.08 (0.50)	0.000004 (0.90)	0.07 (0.60)	0.000003 (0.90)
R putamothalamus[2, f, F, †]	0.08 (0.50)	0.000004 (0.40)	0.06 (0.60)	0.000002 (0.90)	0.15 (0.20)	0.00003 (0.40)	0.05 (0.70)	0.00001 (0.70)
R pallidothalamus[†, §]	0.13 (0.30)	0.00001 (0.30)	0.05 (0.70)	0.00001 (0.70)	0.09 (0.50)	0.00003 (0.50)	-0.02 (0.80)	-0.000002 (0.90)
L caudate-R thalamus[2, a, c, C, ‡]	0.10 (0.50)	0.00001 (0.40)	0.05 (0.70)	0.00002 (0.60)	0.007 (1.00)	0.00001 (0.80)	0.01 (0.90)	0.00001 (0.80)
L putamen-R thalamus[†]	0.06 (0.60)	0.00001 (0.60)	-0.12 (0.40)	-0.00004 (0.30)	-0.18 (0.20)	-0.00007 (0.20)	-0.14 (0.30)	-0.00004 (0.20)
L pallidum-R thalamus[b, B, †]	0.12 (0.40)	0.00001 (0.40)	-0.17 (0.10)	-0.00006 (0.20)	-0.22 (0.10)	-0.00008 (0.10)	-0.18 (0.20)	-0.00006 (0.10)
R caudate-L thalamus	-0.006 (1.00)	-0.000001 (1.00)	-0.11 (0.40)	-0.00003 (0.40)	-0.15 (0.30)	-0.00005 (0.30)	-0.11 (0.40)	-0.00003 (0.40)
R putamen-L thalamus[2, f, C, #]	-0.05 (0.70)	-0.000001 (0.80)	0.06 (0.70)	0.00002 (0.60)	-0.04 (0.80)	-0.000005 (0.90)	0.08 (0.50)	0.00001 (0.80)
R pallidum-L thalamus[2, 6, †]	-0.01 (0.90)	0.000003 (0.80)	0.06 (0.70)	0.00002 (0.70)	-0.02 (0.90)	-0.000006 (0.90)	0.06 (0.60)	0.00001 (0.70)
R putamocerebellar[6, a, b, B, †]	0.09 (0.50)	0.00001 (0.40)	0.01 (0.90)	-0.000001 (1.00)	0.03 (0.80)	0.000005 (0.90)	0.03 (0.80)	0.000004 (0.90)
R pallidocerebellar[1, b, B, †]	-0.01 (0.90)	0.000002 (0.80)	0.03 (0.80)	0.000005 (0.90)	-0.05 (0.70)	-0.00002 (0.60)	-0.05 (0.70)	-0.00002 (0.60)
Cerebellothalamic group								
L thalamocerebellar[2, a, *, †, ‡]	-0.10 (0.50)	-0.00001 (0.50)	0.001 (1.00)	-0.000001 (0.80)	-0.05 (0.70)	-0.00001 (0.70)	0.04 (0.80)	0.000002 (0.90)
R thalamocerebellar[1,2, b, B, †]	0.05 (0.70)	0.00001 (0.40)	0.11 (0.40)	0.00003 (0.40)	0.16 (0.20)	0.00005 (0.20)	-0.004 (1.00)	-0.00001 (0.80)
L thalamo-vermis[†]	0.03 (0.80)	0.000003 (0.80)	0.17 (0.20)	0.00005 (0.20)	0.21 (0.10)	0.0001 (0.10)	0.13 (0.30)	0.00002 (0.40)
R thalamo-vermis[e, f, E, ¶]	0.01 (0.90)	0.000001 (0.90)	0.06 (0.70)	0.00001 (0.80)	0.14 (0.30)	0.00007 (0.20)	0.04 (0.80)	0.00001 (0.70)
Interthalami[2, b, †]	0.09 (0.50)	0.00001 (0.40)	-0.10 (0.40)	-0.00003 (0.30)	-0.19 (0.20)	-0.00004 (0.20)	-0.11 (0.40)	-0.00003 (0.30)
L cerebello-vermis[1, a, b, B, F, *, †]	0.12 (0.40)	0.00001 (0.20)	-0.08 (0.50)	-0.00003 (0.40)	-0.12 (0.40)	-0.00004 (0.30)	-0.10 (0.50)	-0.00004 (0.30)
R cerebello-vermis[1, 2, b, B, *, †]	0.05 (0.70)	0.000006 (0.60)	-0.05 (0.70)	-0.00002 (0.50)	-0.11 (0.40)	-0.00004 (0.40)	-0.05 (0.70)	-0.00002 (0.50)
Intercerebelli[1, a, b, A, *, †]	0.13 (0.30)	0.00001 (0.20)	-0.04 (0.70)	-0.00002 (0.50)	-0.01 (0.90)	-0.00001 (0.80)	-0.05 (0.70)	-0.00003 (0.40)

r is Pearson correlation coefficient; **β** is unstandardised regression coefficient after controlling for potential confounders related to the outcome at $p<0.10$: The model includes potential confounders related to the outcome at $p<0.1$: FA:- 1 = infant sex; 2 = Equivalent GA of infant at MRI; 3 = infant weight at MRI; 4 = infant head circumference at MRI; 5 = maternal weight change per week; 6 = maternal age at delivery; MD:- a = infant sex; b = Equivalent GA of infant at MRI; c = infant weight at MRI; d = infant head circumference at MRI; e maternal weight change per week; f = maternal age at delivery; AD:- A = infant sex; B = Equivalent GA of infant at MRI; C = infant weight at MRI; D = infant head circumference at MRI; E = maternal weight change per week; F = maternal age at delivery; RD:- ∗ = infant sex; † = Equivalent GA of infant at MRI; ‡ = infant weight at MRI, § = infant head circumference at MRI; ¶ = maternal weight change per week; # = maternal age at delivery; [x]CD4 count missing for 1 mother who started ART pre-conception. Bold indicates significance at $p\leq0.05$.

Table 2.2b Associations of WM-ROIs DTI parameters (FA, MD, AD and RD) in HEU infants with maternal clinical and treatment variables (maternal viral loads)

WM-ROI	FA				MD				AD				RD			
	Maternal VL within 6 mo of enrolment (n = 17)[y]		Maternal VL within 6 mo of enrolment (n = 57)[z]		Maternal VL within 6 mo of enrolment (n = 17)[y]		Maternal VL within 6 mo of enrolment (n = 57)[z]		Maternal VL within 6 mo of enrolment (n = 17)[y]		Maternal VL within 6 mo of enrolment (n = 57)[z]		Maternal VL within 6 mo of enrolment (n = 17)[y]		Maternal VL within 6 mo of enrolment (n = 57)[z]	
	r *(p)*	β (x 10^{-3}) *(p)*	r *(p)*	β (x 10^{-3}) *(p)*	r *(p)*	β (x 10^{-3}) *(p)*	r *(p)*	β (x 10^{-3}) *(p)*	r *(p)*	β (x 10^{-3}) *(p)*	r *(p)*	β (x 10^{-3}) *(p)*	r *(p)*	β (x 10^{-3}) *(p)*	r *(p)*	β (x 10^{-3}) *(p)*
Intrinsic basal ganglia connections																
L caudoputamen[2, a, b, *, †, §]	**-0.62 (0.01)**	**-0.002 (0.01)**	**-0.28 (0.04)**	**-0.001 (0.04)**	0.34 (0.20)	0.003 (0.20)	0.25 (0.06)	0.004 (0.10)	0.17 (0.50)	0.002 (0.50)	0.13 (0.30)	0.003 (0.30)	0.44 (0.08)	0.004 (0.10)	**0.31 (0.02)**	**0.004 (0.04)**
L caudopallidum[2, †]	-0.46 (0.06)	-0.001 (0.08)	-0.23 (0.08)	-0.001 (0.10)	0.45 (0.07)	0.005 (0.07)	**0.26 (0.05)**	**0.06 (0.05)**	0.28 (0.30)	0.005 (0.30)	0.17 (0.20)	0.005 (0.20)	**0.55 (0.02)**	**0.006 (0.03)**	**0.32 (0.02)**	**0.006 (0.02)**
L putamopallidum[2, b, †]	**-0.066 (0.005)**	**-0.001 (0.01)**	-0.20 (0.10)	-0.001 (0.20)	0.17 (0.50)	0.001 (0.60)	0.08 (0.50)	0.001 (0.60)	0.02 (0.90)	0.0004 (0.90)	0.02 (0.90)	0.001 (0.90)	0.27 (0.30)	0.002 (0.40)	0.13 (0.30)	0.002 (0.40)
R caudoputamen[2, e, †, ¶]	0.05 (0.80)	0.0003 (0.60)	0.03 (0.80)	0.0003 (0.60)	-0.04 (0.90)	-0.001 (0.90)	0.03 (0.80)	0.0004 (0.90)	-0.02 (0.90)	-0.0003 (0.90)	0.05 (0.70)	0.001 (0.70)	-0.06 (0.80)	-0.001 (0.70)	0.02 (0.90)	-0.0002 (0.90)
R caudopallidum[2, #, ¶]	-0.15 (0.50)	-0.0002 (0.70)	-0.05 (0.70)	0.0001 (0.90)	0.03 (0.90)	0.0005 (0.90)	0.03 (0.80)	0.01 (0.80)	0.05 (0.80)	0.0007 (0.80)	0.02 (0.80)	0.001 (0.80)	0.06 (0.80)	0.001 (0.70)	0.03 (0.80)	0.001 (0.70)
R putamopallidum[2]	-0.36 (0.10)	-0.0001 (0.20)	-0.15 (0.30)	-0.001 (0.30)	0.09 (0.70)	0.001 (0.70)	0.11 (0.40)	0.003 (0.40)	-0.06 (0.80)	-0.001 (0.80)	0.05 (0.70)	0.002 (0.70)	0.19 (0.40)	0.001 (0.60)	0.15 (0.20)	0.002 (0.30)
Inter-caudate[2, f]	-0.33 (0.20)	-0.001 (0.30)	-0.10 (0.50)	-0.0006 (0.60)	0.17 (0.50)	0.003 (0.50)	0.06 (0.70)	0.002 (0.70)	0.12 (0.60)	0.002 (0.60)	0.06 (0.70)	0.002 (0.70)	0.19 (0.50)	0.003 (0.50)	0.11 (0.40)	0.003 (0.40)
L putamen-R caudate[e]	**-0.58 (0.01)**	**-0.003 (0.01)**	-0.19 (0.20)	-0.002 (0.20)	0.33 (0.20)	0.004 (0.30)	0.13 (0.30)	0.003 (0.40)	0.10 (0.70)	0.002 (0.70)	0.04 (0.80)	0.001 (0.80)	0.43 (0.09)	0.006 (0.09)	0.17 (0.20)	0.005 (0.20)
Extrinsic basal connections																
L caudothalamus[2, a, b, d, A, *, †, §]	-0.43 (0.08)	-0.001 (0.10)	-0.19 (0.10)	-0.001 (0.20)	0.27 (0.30)	0.003 (0.30)	0.15 (0.20)	0.002 (0.40)	0.16 (0.50)	0.002 (0.50)	0.09 (0.50)	0.002 (0.50)	0.33 (0.20)	0.003 (0.20)	0.19 (0.20)	0.002 (0.30)
L putamothalamus[2, a, b, d, A, *, †, §]	-0.43 (0.08)	-0.001 (0.10)	-0.20 (0.10)	-0.001 (0.20)	0.27 (0.30)	0.003 (0.30)	0.15 (0.20)	0.002 (0.40)	0.16 (0.50)	0.002 (0.50)	0.09 (0.50)	0.002 (0.60)	0.33 (0.20)	0.003 (0.20)	0.19 (0.20)	0.002 (0.30)
L pallidothalamus[2, †]	-0.45 (0.07)	-0.001 (0.09)	-0.22 (0.10)	-0.001 (0.10)	0.10 (0.70)	0.001 (0.70)	0.08 (0.50)	0.002 (0.50)	-0.03 (0.90)	0.0006 (0.90)	0.02 (0.90)	0.0002 (0.90)	0.19 (0.50)	0.001 (0.60)	0.12 (0.40)	0.002 (0.40)
R caudothalamus[2, a, b, f, B, F, †, #]	-0.18 (0.50)	-0.0002 (0.60)	-0.08 (0.60)	-0.0002 (0.70)	0.12 (0.70)	0.002 (0.50)	0.06 (0.70)	0.001 (0.60)	0.08 (0.80)	0.001 (0.80)	0.05 (0.70)	0.001 (0.60)	0.14 (0.60)	0.001 (0.60)	0.06 (0.70)	0.0001 (0.70)
R putamothalamus[2, f, F, †]	-0.37 (0.10)	-0.0005 (0.20)	-0.12 (0.40)	-0.0004 (0.50)	0.08 (0.80)	0.001 (0.80)	0.08 (0.50)	0.002 (0.50)	0.004 (1.00)	0.001 (0.80)	0.05 (0.70)	0.002 (0.50)	0.13 (0.60)	0.0003 (0.90)	0.11 (0.40)	0.001 (0.50)
R pallidothalamus[†, §]	-0.34 (0.20)	-0.001 (0.20)	-0.11 (0.40)	-0.0006 (0.40)	0.03 (0.90)	0.0003 (0.90)	0.06 (0.60)	0.001 (0.60)	-0.04 (0.90)	-0.0007 (0.90)	0.03 (0.80)	0.0008 (0.80)	0.04 (0.90)	-0.0004 (0.90)	0.07 (0.60)	0.001 (0.70)
L caudate-R thalamus[2, a, c, C, ‡]	-0.43 (0.08)	-0.002 (0.10)	-0.19 (0.20)	-0.001 (0.20)	0.03 (0.90)	-0.001 (0.80)	0.05 (0.70)	0.0006 (0.80)	-0.16 (0.50)	-0.0006 (0.90)	-0.02 (0.90)	-0.001 (0.70)	0.15 (0.60)	0.0008 (0.80)	0.09 (0.50)	0.001 (0.60)
L putamen-R thalamus[†]	**-0.50 (0.04)**	**-0.003 (0.04)**	-0.19 (0.10)	-0.002 (0.20)	-0.13 (0.60)	-0.001 (0.60)	-0.0002 (1.00)	-0.0001 (1.00)	-0.46 (0.06)	-0.006 (0.06)	-0.11 (0.40)	-0.003 (0.40)	0.07 (0.80)	0.0006 (0.80)	0.06 (0.60)	0.001 (0.70)
L pallidum-R thalamus[b, B, †]	-0.45 (0.07)	-0.002 (0.07)	-0.18 (0.20)	-0.002 (0.20)	0.06 (0.80)	-0.00002 (1.00)	0.05 (0.70)	0.001 (0.80)	-0.27 (0.30)	-0.004 (0.20)	-0.06 (0.70)	-0.002 (0.60)	0.15 (0.60)	0.001 (0.70)	0.09 (0.50)	0.002 (0.60)
R caudate-L thalamus	-0.39 (0.10)	-0.002 (0.10)	-0.17 (0.20)	-0.002 (0.20)	0.13 (0.60)	0.002 (0.60)	0.07 (0.60)	0.002 (0.60)	-0.03 (0.90)	0.001 (0.80)	0.01 (0.90)	0.0002 (0.90)	0.22 (0.40)	0.003 (0.40)	0.10 (0.40)	0.003 (0.40)
R putamen-L thalamus[2, f, C, #]	-0.16 (0.50)	-0.0006 (0.70)	-0.04 (0.70)	- 0.0002 (0.90)	0.07 (0.80)	0.001 (0.70)	0.08 (0.50)	0.002 (0.50)	-0.01 (1.00)	-0.001 (0.60)	0.07 (0.60)	0.0001 (0.70)	0.11 (0.70)	0.002 (0.50)	0.08 (0.50)	0.003 (0.40)
R pallidum-L thalamus[2, 6, †]	-0.12 (0.60)	-0.0005 (0.70)	-0.03 (0.80)	-0.0001 (0.90)	0.12 (0.60)	0.001 (0.60)	0.08 (0.50)	0.002 (0.50)	0.11 (0.70)	0.001 (0.70)	0.08 (0.50)	0.002 (0.50)	0.12 (0.60)	0.001 (0.80)	0.08 (0.60)	0.001 (0.70)

R putamocerebellar[6, a, b, B, †]	-0.19 (0.50)	-0.001 (0.30)	-0.07 (0.60)	-0.0004 (0.60)	0.21 (0.40)	0.002 (0.50)	0.12 (0.40)	-0.002 (0.50)	0.11 (0.70)	-0.001 (0.80)	0.08 (0.60)	0.002 (0.70)	0.27 (0.30)	0.002 (0.40)	0.10 (040)	0.002 (0.50)
R pallidocerebellar[1, b, B, †]	-0.07 (0.80)	0.0002 (0.80)	-0.05 (0.70)	-0.0002 (0.80)	0.21 (0.40)	0.002 (0.50)	0.09 (0.50)	0.001 (0.60)	0.14 (0.60)	0.002 (0.70)	0.05 (0.70)	0.001 (0.80)	0.25 (0.30)	0.002 (0.40)	0.10 (0.40)	0.002 (0.50)
Cerebellothalamic group																
L thalamocerebellar[2, a, *, †, ‡]	-0.27 (0.30)	-0.001 (0.40)	-0.16 (0.20)	-0.000001 (0.30)	0.08 (0.70)	0.000001 (0.80)	0.06 (0.60)	0.001 (0.70)	-0.02 (0.90)	-0.0003 (0.90)	-0.002 (1.00)	-0.00005 (1.00)	0.19 (0.40)	0.001 (0.60)	0.10 (0.40)	0.001 (0.70)
R thalamocerebellar[1,2, b, B, †]	-0.52 (0.03)	-0.006 (0.05)	-0.28 (0.04)	-0.001 (0.06)	0.13 (0.60)	0.001 (0.70)	0.04 (0.80)	0.0004 (0.90)	-0.05 (0.80)	-0.0007 (0.80)	-0.06 (0.60)	-0.002 (0.60)	0.23 (0.40)	0.001 (0.60)	0.09 (0.50)	0.001 (0.60)
L thalamo-vermis[†]	-0.19 (0.50)	-0.001 (0.50)	-0.07 (0.60)	-0.001 (0.60)	-0.14 (0.60)	-0.002 (0.60)	-0.08 (0.50)	-0.002 (0.50)	-0.17 (0.50)	-0.004 (0.50)	-0.09 (0.50)	-0.003 (0.50)	-0.10 (0.70)	-0.001 (0.60)	-0.06(0.70)	-0.001 (0.50)
R thalamo-vermis[e, f, E, ¶]	-0.33 (0.20)	-0.001 (0.20)	-0.15 (0.20)	-0.001 (0.20)	0.06 (0.80)	-0.0001 (1.00)	0.02 (0.90)	0.0004 (0.90)	-0.03 (0.90)	-0.001 (0.90)	-0.04 (0.70)	-0.002 (0.70)	0.14 (0.60)	0.001 (0.70)	0.06 (0.70)	0.001 (0.70)
Interthalami[2, b, †]	-0.39 (0.10)	-0.001 (0.20)	-0.16 (0.20)	-0.001 (0.30)	-0.08 (0.70)	-0.001 (0.40)	0.04 (0.80)	0.0002 (0.90)	-0.26 (0.30)	-0.003 (0.30)	-0.03 (0.80)	-0.0007 (0.80)	0.02 (0.90)	-0.001 (0.70)	0.07 (0.60)	0.001 (0.70)
L cerebello-vermis[1, a, b, B, F, *, †]	-0.27 (0.30)	-0.0003 (0.50)	-0.12 (0.40)	-0.0004 (0.50)	0.21 (0.40)	0.02 (0.50)	0.10 (0.40)	0.002 (0.60)	0.14 (0.60)	0.002 (0.60)	0.07 (0.60)	0.002 (0.60)	0.24 (0.30)	0.002 (0.50)	0.12 (0.40)	0.002 (0.50)
R cerebello-vermis[1, 2, b, B, *, †]	-0.28 (0.30)	-0.0007 (0.30)	-0.10 (0.40)	-0.0005 (0.60)	0.09 (0.70)	0.001 (0.80)	0.08 (0.60)	0.001 (0.70)	0.02 (0.90)	0.000004 (1.00)	0.03 (0.80)	0.0002 (0.90)	0.14 (0.60)	0.001 (0.70)	0.10 (0.50)	0.001 (0.60)
Intercerebelli[1, a, b, A, *, †]	-0.40 (0.10)	-0.0008 (0.20)	-0.16 (0.20)	-0.001 (0.30)	0.15 (0.50)	0.002 (0.70)	0.08 (0.50)	0.001 (0.70)	-0.01 (0.90)	-0.0006 (0.90)	0.03 (0.80)	0.00003 (1.00)	0.21 (0.40)	0.001 (0.70)	0.11 (0.40)	0.001 (0.60)

r is Pearson correlation coefficient; **β** is unstandardised regression coefficient after controlling for potential confounders related to the outcome at $p<0.10$: The model includes potential confounders related to the outcome at $p<0.1$:

FA:- 1 = infant sex; 2 = Equivalent GA of infant at MRI; 3 = infant weight at MRI; 4 = infant head circumference at MRI; 5 = maternal weight change per week; 6 = maternal age at delivery;

MD:- a = infant sex; b = Equivalent GA of infant at MRI; c = infant weight at MRI; d = infant head circumference at MRI; e maternal weight change per week; f = maternal age at delivery;

AD:- A = infant sex; B = Equivalent GA of infant at MRI; C = infant weight at MRI; D = infant head circumference at MRI; E = maternal weight change per week; F = maternal age at delivery;

RD:- ∗ = infant sex; † = Equivalent GA of infant at MRI; ‡ = infant weight at MRI, § = infant head circumference at MRI; ¶ = maternal weight change per week; # = maternal age at delivery.

[b]Only for mothers with detectable viral load (VL); [c]Associations among all HEU infants; VL set to zero for mothers with undetectable levels. Bold indicates significance at $p\leq0.05$. [y]Only for mothers with detectable viral load (VL); [z]Associations among all HEU infants; VL set to zero for mothers with undetectable levels.

Table 2.2c. Associations of WM-ROIs DTI parameters (FA, MD, AD and RD) in HEU infants with maternal clinical and treatment variables (Infant ART exposure duration)

	FA		**MD**		**AD**		**RD**	
WM-ROI	**Infant ART Exposure duration (n = 57)**		**Infant ART Exposure duration (n = 57)**		**Infant ART Exposure duration (n = 57)**		**Infant ART Exposure duration (n = 57)**	
	r *(p)*	**β *(p)***	**r *(p)***	**β *(p)***	**r *(p)***	**β *(p)***	**r *(p)***	**β *(p)***
Intrinsic basal ganglia connections								
L caudoputamen[2, a, b, *, †, §]	-0.06 (0.70)	-0.00006 (0.70)	-0.18 (0.20)	-0.001 (0.20)	-0.18 (0.20)	-0.001 (0.20)	-0.17 (0.20)	-0.0007 (0.20)
L caudopallidum[2, †]	-0.17 (0.20)	-0.0002 (0.20)	-0.08 (0.50)	-0.0005 (0.50)	-0.14 (0.30)	-0.001 (0.30)	-0.03 (0.80)	-0.0002 (0.80)
L putamopallidum[2, b, †]	-0.06 (0.70)	-0.0001 (0.80)	-0.16 (0.20)	-0.001 (0.20)	-0.15 (0.20)	-0.001 (0.20)	-0.16 (0.20)	-0.0009 (0.20)
R caudoputamen[2, e, †, ¶]	-0.05 (0.70)	-0.00005 (0.80)	-0.07 (0.60)	-0.0001 (0.80)	-0.10 (0.50)	-0.0006 (0.50)	-0.04 (0.80)	-0.0001 (0.90)
R caudopallidum[2, #, ¶]	0.003 (1.00)	0.00003 (0.90)	-0.04 (0.70)	-0.0002 (0.70)	-0.09 (0.50)	-0.0007 (0.50)	-0.03 (0.80)	-0.0003 (0.60)
R putamopallidum[2]	-0.01 (0.90)	-0.000002 (1.00)	-0.07 (0.60)	-0.0004 (0.60)	-0.07 (0.60)	-0.0007 (0.60)	-0.07 (0.60)	-0.0004 (0.50)
Inter-caudate[2, f]	0.06 (0.70)	0.0002 (0.50)	0.09 (0.50)	0.001 (0.50)	0.04 (0.80)	0.0003 (0.80)	-0.04 (0.80)	-0.0003 (0.80)
L putamen-R caudate[e]	-0.07 (0.60)	-0.0002 (0.60)	-0.20 (0.10)	-0.001 (0.30)	**-0.27 (0.04)**	**-0.002 (0.04)**	-0.13 (0.30)	-0.0009 (0.30)
Extrinsic basal connections								
L caudothalamus[2, a, b, d, A, *, †, §]	-0.03 (0.80)	-0.00003 (0.90)	-0.03 (0.80)	0.00004 (1.00)	-0.05 (0.70)	-0.0003 (0.70)	-0.01 (0.90)	0.0001 (0.80)

L putamothalamus[2, a, b, d, A, *, †, §]	-0.03 (0.80)	-0.00003 (0.90)	-0.03 (0.80)	0.00003 (1.00)	-0.05 (0.70)	-0.0002 (0.80)	-0.01 (0.90)	0.00002 (1.00)
L pallidothalamus[2, †]	-0.07 (0.60)	-0.0001 (0.60)	-0.04 (0.70)	-0.0002 (0.70)	-0.09 (0.50)	-0.0006 (0.60)	-0.02 (0.90)	-0.0002 (0.80)
R caudothalamus[2, a, b, f, B, F, †, #]	0.08 (0.08)	0.0001 (0.40)	-0.03 (0.80)	-0.0003 (0.60)	-0.02 (0.80)	-0.0006 (0.40)	-0.02 (0.80)	-0.0004 (0.50)
R putamothalamus[2, f, F, †]	0.13 (0.30)	0.0001 (0.20)	-0.06 (0.60)	-0.0005 (0.50)	-0.04 (0.80)	-0.0007 (0.50)	-0.08 (0.60)	-0.0005 (0.40)
R pallidothalamus[†, §]	0.12 (0.40)	0.0002 (0.30)	0.005 (1.00)	0.00003 (1.00)	0.04 (0.80)	0.0003 (0.80)	-0.07 (0.60)	-0.0004 (0.50)
L caudate-R thalamus[2, a, c, C, ‡]	0.05 (0.70)	0.0001 (0.70)	-0.17 (0.20)	-0.001 (0.20)	-0.19 (0.10)	-0.001 (0.20)	-0.12 (0.30)	-0.006 (0.40)
L putamen-R thalamus[†]	-0.003 (1.00)	0.000003 (1.00)	-0.21 (0.10)	-0.001 (0.10)	-0.17 (0.20)	-0.001 (0.20)	-0.19 (0.10)	-0.001 (0.10)
L pallidum-R thalamus[b, B, †]	0.05 (0.70)	0.0001 (0.70)	-0.19 (0.20)	-0.001 (0.10)	-0.13 (0.30)	-0.001 (0.30)	-0.16 (0.20)	-0.001 (0.20)
R caudate-L thalamus	-0.03 (0.80)	-0.00007 (0.80)	-0.03 (0.80)	-0.0002 (0.80)	-0.10 (0.50)	-0.0007 (0.50)	-0.04 (0.80)	-0.0002 (0.80)
R putamen-L thalamus[2, f, C, #]	0.05 (0.70)	0.0002 (0.40)	-0.02 (0.90)	-0.00003 (1.00)	-0.01 (0.90)	0.0001 (0.90)	-0.001 (1.00)	-0.0003 (0.70)
R pallidum-L thalamus[2, 6, †]	0.04 (0.80)	0.0001 (0.60)	0.04 (0.70)	0.0003 (0.70)	0.06 (0.60)	0.0005 (0.60)	0.06 (0.70)	0.0003 (0.70)
R putamocerebellar[6, a, b, B, †]	-0.01 (0.90)	-0.00003 (0.90)	0.02 (0.90)	0.00003 (1.00)	0.02 (0.90)	0.00007 (0.90)	0.07 (0.60)	0.0004 (0.60)
R pallidocerebellar[1, b, B, †]	0.14 (0.30)	0.0002 (0.40)	0.02 (0.90)	-0.00002 (1.00)	0.07 (0.60)	0.0005 (0.70)	-0.007 (0.90)	-0.0001 (0.80)
Cerebellothalamic group								
L thalamocerebellar[2, a, *, †, ‡]	-0.01 (0.90)	-0.00002 (1.00)	-0.01 (0.90)	0.00003 (1.00)	0.05 (0.70)	0.0003 (0.70)	0.01 (0.90)	0.0001 (0.80)

R thalamocerebellar[1,2, b, B, †]	0.25 (0.06)	**0.0004 (0.05)**	0.13 (0.30)	0.0006 (0.40)	0.24 (0.07)	0.002 (0.07)	0.06 (0.60)	0.0004 (0.60)
L thalamo-vermis[†]	-0.06 (0.60)	-0.0001 (0.60)	0.16 (0.20)	0.001 (0.20)	0.11 (0.40)	0.001 (0.40)	0.15 (0.30)	0.0006 (0.30)
R thalamo-vermis[e, f, E, ¶]	0.14 (0.30)	0.0003 (0.30)	0.13 (0.30)	0.001 (0.20)	0.21 (0.10)	**0.003 (0.04)**	0.09 (0.50)	0.0008 (0.30)
Interthalami[2, b, †]	0.03 (0.80)	0.00007 (0.70)	**-0.30 (0.02)**	**-0.002 (0.01)**	**-0.30 (0.03)**	**-0.002 (0.03)**	**-0.26 (0.05)**	**-0.001 (0.02)**
L cerebello-vermis[1, a, b, B, F, *, †]	0.10 (0.50)	0.00007 (0.70)	-0.08 (0.50)	-0.0006 (0.40)	-0.09 (0.50)	-0.0008 (0.30)	-0.07 (0.60)	-0.0005 (0.50)
R cerebello-vermis[1, 2, b, B, *, †]	-0.05 (0.70)	-0.0001 (0.60)	-0.02 (0.90)	-0.0002 (0.70)	-0.04 (0.80)	-0.0004 (0.70)	-0.005 (1.00)	-0.0001 (0.80)
Intercerebelli[1, a, b, A, *, †]	0.13 (0.30)	0.0001 (0.40)	-0.04 (0.70)	-0.0003 (0.70)	-0.10 (0.40)	-0.0004 (0.60)	-0.01 (0.90)	-0.00001 (1.00)

r is Pearson correlation coefficient; **β** is unstandardised regression coefficient after controlling for potential confounders related to the outcome at $p<0.10$: The model includes potential confounders related to the outcome at $p<0.1$:

FA:- 1 = infant sex; 2 = Equivalent GA of infant at MRI; 3 = infant weight at MRI; 4 = infant head circumference at MRI; 5 = maternal weight change per week; 6 = maternal age at delivery;

MD:- a = infant sex; b = Equivalent GA of infant at MRI; c = infant weight at MRI; d = infant head circumference at MRI; e maternal weight change per week; f = maternal age at delivery;

AD:- A = infant sex; B = Equivalent GA of infant at MRI; C = infant weight at MRI; D = infant head circumference at MRI; E = maternal weight change per week; F = maternal age at delivery;

RD:- ∗ = infant sex; † = Equivalent GA of infant at MRI; ‡ = infant weight at MRI, § = infant head circumference at MRI; ¶ = maternal weight change per week; # = maternal age at delivery. Bold indicates significance at $p \leq 0.05$.

Table 2.3a Comparison of WM-ROIs DTI parameters (FA, MD, AD and RD) among HEU infants between those whose mothers had detectable or undetectable viral loads within 6 months of enrolment for all HEU infants combined

	FA		**MD**		**AD**		**RD**	
WM-ROI	**HEU (n = 57)**		**HEU (n = 57)**		**HEU (n = 57)**		**HEU (n = 57)**	
	Detectable vs Undetectable maternal VL		**Detectable vs Undetectable maternal VL**		**Detectable vs Undetectable maternal VL**		**Detectable vs Undetectable maternal VL**	
	t *(p)*	**β *(p)***	**t *(p)***	**β *(p)***	**t *(p)***	**β *(p)***	**t *(p)***	**β *(p)***
Intrinsic basal ganglia connections								
L caudoputamen[2, a, b, *, †, §]	0.01 (0.90)	-0.0004 (0.90)	-1.84 (0.07)	0.021 (0.07)	-1.39 (0.20)	0.022 (0.20)	**-2.01 (0.05)**	**0.21 (0.04)**
L caudopallidum[2, †]	0.19 (0.80)	-0.0005 (0.90)	-0.72 (0.50)	0.01 (0.50)	-0.61 (0.50)	0.012 (0.50)	-1.01 (0.40)	0.009 (0.50)
L putamopallidum[2, b, †]	-0.71 (0.50)	0.003 (0.50)	-0.41 (0.70)	0.006 (0.70)	-0.39 (0.70)	0.009 (0.70)	-0.41 (0.70)	0.004 (0.70)
R caudoputamen[2, e, †, ¶]	-0.10 (0.90)	0.0004 (0.90)	-1.88 (0.06)	0.020 (0.06)	-1.86 (0.07)	0.030 (0.07)	-1.76 (0.08)	0.021 (0.08)
R caudopallidum[2, #, ¶]	-0.74 (0.50)	0.003 (0.40)	-0.24 (0.80)	0.004 (0.80)	-0.07 (0.90)	0.001 (0.90)	0.005 (1.00)	0.004 (1.00)
R putamopallidum[2]	-1.08 (0.30)	0.005 (0.30)	**-2.24 (0.03)**	**0.033 (0.03)**	**-2.32 (0.02)**	**0.050 (0.02)**	**-2.02 (0.05)**	**0.24 (0.04)**
Inter-caudate[2, f]	-1.12 (0.30)	0.006 (0.30)	0.82 (0.40)	-0.018 (0.40)	0.25 (0.80)	-0.006 (0.80)	0.40 (0.70)	-0.006 (0.70)
L putamen-R caudate[e]	-1.94 (0.06)	0.010 (0.06)	1.29 (0.20)	-0.020 (0.06)	0.56 (0.60)	-0.010 (0.60)	1.60 (0.10)	-0.028 (0.10)

Extrinsic basal connections								
L caudothalamus[2, a, b, d, A, *, †, §]	0.60 (0.50)	-0.002 (0.60)	-0.59 (0.50)	0.006 (0.60)	-0.39 (0.70)	0.006 (0.70)	-0.70 (0.50)	0.007 (0.50)
L putamothalamus[2, a, b, d, A, *, †, §]	0.60 (0.50)	-0.002 (0.60)	-0.59 (0.50)	0.006 (0.60)	-0.39 (0.70)	0.006 (0.70)	-0.70 (0.50)	0.007 (0.50)
L pallidothalamus[2, †]	-0.44 (0.60)	0.002 (0.60)	-1.17 (0.20)	0.015 (0.20)	-0.92 (0.40)	0.019 (0.40)	-1.01 (0.30)	0.013 (0.30)
R caudothalamus[2, a, b, f, B, F, †, #]	0.07 (0.90)	0.00002 (1.00)	-0.06 (0.90)	-0.0004 (1.00)	-0.25 (0.80)	0.003 (0.80)	0.06 (0.90)	-0.0007 (0.90)
R putamothalamus[2, f, F, †]	-0.51 (0.60)	0.002 (0.50)	-1.33 (0.20)	0.017 (0.20)	-1.63 (0.10)	0.029 (0.10)	-1.15 (0.20)	0.015 (0.20)
R pallidothalamus[†, §]	-0.58 (0.60)	0.002 (0.60)	-1.47 (0.10)	0.021 (0.10)	-1.56 (0.10)	0.031 (0.10)	-1.47 (0.10)	0.019 (0.10)
L caudate-R thalamus[2, a, c, C, ‡]	-1.55 (0.10)	0.008 (0.10)	-1.16 (0.20)	0.024 (0.09)	-1.87 (0.07)	**0.048 (0.02)**	-0.27 (0.80)	0.008 (0.50)
L putamen-R thalamus[†]	-1.63 (0.10)	0.011 (0.10)	-1.64 (0.10)	0.027 (0.10)	**-2.14 (0.04)**	**0.043 (0.04)**	-0.87 (0.40)	0.014 (0.40)
L pallidum-R thalamus[b, B, †]	-1.50 (0.10)	0.010 (0.10)	-1.11 (0.30)	0.020 (0.30)	-1.87 (0.07)	0.036 (0.07)	-0.72 (0.50)	0.012 (0.50)
R caudate-L thalamus	-1.73 (0.09)	0.010 (0.09)	0.22 (0.80)	-0.004 (0.80)	-0.88 (0.40)	0.016 (0.40)	0.56 (0.60)	-0.010 (0.50)
R putamen-L thalamus[2, f, C, #]	-1.27 (0.20)	0.008 (0.20)	-1.83 (0.07)	0.031 (0.07)	**-2.40 (0.02)**	**0.052 (0.007)**	0.09 (0.30)	0.017 (0.30)
R pallidum-L thalamus[2, 6, †]	-1.01 (0.30)	0.006 (0.20)	-1.10 (0.30)	0.019 (0.30)	-1.34 (0.20)	0.026 (0.20)	-0.59 (0.50)	0.008 (0.60)
R putamocerebellar[6, a, b, B, †]	-1.00 (0.30)	0.004 (0.30)	-0.38 (0.70)	0.005 (0.70)	-0.56 (0.60)	0.010 (0.60)	0.21 (0.80)	-0.004 (0.80)
R pallidocerebellar[1, b, B, †]	-0.50 (0.60)	0.002 (0.60)	0.07 (0.90)	-0.001 (0.90)	0.43 (0.70)	-0.010 (0.60)	0.20 (0.80)	-0.003 (0.80)

Cerebellothalamic group								
L thalamocerebellar[2, a, *, †, ‡]	-0.32 (0.70)	0.001 (0.80)	0.81 (0.40)	0.011 (0.40)	-0.28 (0.80)	0.005 (0.80)	0.68 (0.50)	0.008 (0.50)
R thalamocerebellar[1,2, b, B, †]	-1.76 (0.08)	0.007 (0.07)	-0.74 (0.40)	-0.010 (0.40)	1.43 (0.10)	-0.027 (0.10)	-0.55 (0.60)	-0.008 (0.50)
L thalamo-vermis[†]	0.53 (0.60)	-0.003 (0.60)	0.02 (1.00)	0.0004 (1.00)	-0.04 (1.00)	0.001 (1.00)	0.11 (0.90)	0.001 (0.90)
R thalamo-vermis[e, f, E, ¶]	0.22 (0.80)	-0.001 (0.80)	-0.61 (0.50)	-0.010 (0.50)	0.82 (0.40)	-0.021 (0.40)	-0.66 (0.50)	-0.007 (0.60)
Interthalami[2, b, †]	0.87 (0.40)	-0.004 (0.30)	**2.61 (0.01)**	**0.031 (0.008)**	**-2.56 (0.01)**	**0.035 (0.01)**	**1.95 (0.05)**	**0.022 (0.04)**
L cerebello-vermis[1, a, b, B, F, *, †]	0.10 (0.90)	-0.001 (0.90)	0.003 (1.00)	-0.001 (0.90)	0.17 (0.90)	-0.005 (0.70)	-0.03 (1.00)	-0.001 (0.90)
R cerebello-vermis[1, 2, b, B, *, †]	1.05 (0.30)	-0.004 (0.30)	0.68 (0.50)	0.009 (0.50)	-0.74 (0.50)	0.013 (0.40)	0.48 (0.60)	0.006 (0.60)
Intercerebelli[1, a, b, A, *, †]	0.30 (0.70)	-0.001 (0.80)	-0.14 (0.90)	-0.003 (0.80)	-1.06 (0.30)	0.017 (0.30)	0.28 (0.80)	0.004 (0.80)

Independent one-tail t-test; **β** is unstandardised regression coefficient after controlling for potential confounders related to the outcome at $p<0.10$: The model includes potential confounders related to the outcome at $p<0.1$:

FA:- 1 = infant sex; 2 = Equivalent GA of infant at MRI; 3 = infant weight at MRI; 4 = infant head circumference at MRI; 5 = maternal weight change per week; 6 = maternal age at delivery;

MD:- a = infant sex; b = Equivalent GA of infant at MRI; c = infant weight at MRI; d = infant head circumference at MRI; e maternal weight change per week; f = maternal age at delivery;

AD:- A = infant sex; B = Equivalent GA of infant at MRI; C = infant weight at MRI; D = infant head circumference at MRI; E = maternal weight change per week; F = maternal age at delivery;

RD:- ∗ = infant sex; † = Equivalent GA of infant at MRI; ‡ = infant weight at MRI, § = infant head circumference at MRI; ¶ = maternal weight change per week; # = maternal age at delivery; Bold indicates significance at $p\leq0.05$. Bold indicates significance at $p\leq0.05$.

Table 2.3b Comparison of DT parameters (FA, MD, AD and RD) in WM tracts connecting manually traced seeds/targets among HEU infants between those whose mothers had detectable or undetectable viral loads within 6 months of enrolment. We present the comparison for all HEU infants separately for those in the pre- and post-conception ART groups.

WM-ROI	FA				MD				AD				RD			
	HEU pre-conception ART (n = 29)		HEU post-conception ART (n = 28)		HEU pre-conception ART (n = 29)		HEU post-conception ART (n = 28)		HEU pre-conception ART (n = 29)		HEU post-conception ART (n = 28)		HEU pre-conception ART (n = 29)		HEU post-conception ART (n = 28)	
	Detectable vs Undetectable maternal VL		Detectable vs Undetectable maternal VL		Detectable vs Undetectable maternal VL		Detectable vs Undetectable maternal VL		Detectable vs Undetectable maternal VL		Detectable vs Undetectable maternal VL		Detectable vs Undetectable maternal VL		Detectable vs Undetectable maternal VL	
	t *(p)*	β *(p)*	t *(p)*	β *(p)*	t *(p)*	β *(p)*	t *(p)*	β *(p)*	t *(p)*	β *(p)*	t *(p)*	β *(p)*	t *(p)*	β *(p)*	t *(p)*	β *(p)*
Intrinsic basal ganglia connections																
L caudoputamen[2, a, b, *, †, §]	-0.05 (0.90)	-0.001 (0.80)	0.19 (0.80)	-0.00004 (1.00)	-0.41 (0.70)	0.011 (0.50)	-1.85 (0.08)	0.03 (0.10)	-0.28 (0.80)	0.007 (0.80)	-1.44 (0.20)	0.032 (0.20)	-0.47 (0.60)	0.011 (0.40)	-1.96 (0.06)	0.029 (0.08)
L caudopallidum[2, †]	-0.19 (0.80)	-0.0002 (1.00)	0.49 (0.60)	-0.001 (0.90)	0.37 (0.70)	-0.007 (0.70)	-1.10 (0.30)	0.023 (0.30)	0.28 (0.80)	-0.008 (0.80)	-0.91 (0.40)	0.026 (0.40)	0.43 (0.70)	0.0001 (1.00)	-1.15 (0.20)	0.022 (0.30)
L putamopallidum[2, b, †]	-0.73 (0.50)	0.003 (0.70)	-0.21 (0.80)	0.002 (0.70)	0.55 (0.60)	-0.004 (0.80)	-0.73 (0.50)	0.010 (0.60)	0.23 (0.80)	-0.007 (0.80)	-0.51 (0.60)	0.017 (0.60)	0.82 (0.40)	-0.005 (0.70)	-0.87 (0.40)	0.010 (0.60)
R caudoputamen[2, e, †, ¶]	-0.07 (0.90)	-0.001 (0.80)	-0.10 (0.90)	0.003 (0.40)	-1.15 (0.30)	0.02 (0.30)	-1.42 (0.20)	0.020 (0.20)	-1.10 (0.30)	0.027 (0.30)	-1.39 (0.20)	0.031 (0.20)	-1.11 (0.30)	0.027 (0.10)	-1.32 (0.20)	0.019 (0.30)
R caudopallidum[2, #, ¶]	-0.78 (0.40)	0.003 (0.60)	-0.30 (0.80)	0.005 (0.30)	-0.16 (0.90)	0.004 (0.90)	-0.21 (0.80)	0.004 (0.80)	0.55 (0.60)	-0.012 (0.60)	-0.40 (0.70)	0.011 (0.70)	0.012 (1.00)	0.001 (0.90)	-0.04 (1.00)	-0.002 (0.90)
R putamopallidum[2]	-1.57 (0.10)	0.009 (0.20)	-0.15 (0.90)	0.002 (0.70)	-1.31 (0.20)	0.027 (0.20)	-1.80 (0.08)	0.041 (0.08)	-1.69 (0.10)	0.050 (0.10)	-1.64 (0.10)	0.055 (0.10)	-0.88 (0.40)	0.022 (0.20)	-1.85 (0.07)	0.027 (0.10)
Inter-caudate[2, f]	**-2.26 (0.03)**	0.01 (0.07)	0.30 (0.80)	-0.002 (0.80)	1.25 (0.20)	-0.050 (0.20)	-0.44 (0.60)	0.010 (0.60)	0.82 (0.40)	-0.003 (0.40)	-0.59 (0.60)	0.016 (0.60)	0.90 (0.40)	-0.029 (0.40)	-0.32 (0.70)	0.009 (0.70)
L putamen-R caudate[e]	**-2.85 (0.008)**	**0.027 (0.008)**	-0.17 (0.80)	0.002 (0.90)	**2.85 (0.008)**	**-0.065 (0.01)**	-0.51 (0.60)	0.007 (0.70)	1.89 (0.07)	-0.050 (0.07)	-0.71 (0.50)	0.017 (0.50)	**3.12 (0.004)**	**-0.078 (0.004)**	-0.34 (0.70)	0.008 (0.70)
Extrinsic basal ganglia connections																
L caudothalamus[2, a, b, d, A, *, †, §]	0.17 (0.90)	-0.002 (0.70)	0.70 (0.50)	-0.001 (0.70)	0.59 (0.50)	-0.009 (0.60)	-1.26 (0.20)	0.018 (0.30)	0.63 (0.50)	-0.010 (0.50)	-1.03 (0.30)	0.022 (0.30)	0.51 (0.60)	-0.007 (0.70)	-1.35 (0.20)	0.017 (0.30)
L putamothalamus[2, a, b, d, A, *, †, §]	0.17 (0.90)	-0.002 (0.70)	0.70 (0.50)	-0.001 (0.70)	0.59 (0.50)	-0.009 (0.60)	-1.26 (0.20)	0.019 (0.30)	0.63 (0.50)	-0.018 (0.40)	-1.03 (0.30)	0.23 (0.30)	0.51 (0.60)	-0.007 (0.70)	-1.35 (0.20)	0.017 (0.30)
L pallidothalamus[2, †]	-0.99 (0.30)	0.004 (0.40)	0.33 (0.70)	0.0001 (1.90)	-0.28 (0.80)	0.006 (0.80)	-1.31 (0.20)	0.028 (0.20)	-0.46 (0.60)	0.012 (0.70)	-0.75 (0.40)	0.025 (0.40)	-0.11 (0.90)	0.005 (0.80)	-1.30 (0.20)	0.019 (0.40)
R caudothalamus[2, a, b, f, B, F, †, #]	-1.25 (0.20)	0.004 (0.40)	1.12 (0.30)	-0.002 (0.60)	0.12 (0.90)	-0.004 (0.80)	-0.28 (0.80)	0.001 (0.90)	-0.26 (0.80)	0.015 (0.40)	-0.18 (0.90)	-0.005 (0.80)	0.36 (0.70)	0.001 (0.90)	-0.32 (0.70)	-0.001 (0.90)
R putamothalamus[2, f, F, †]	-1.49 (0.10)	0.004 (0.30)	0.50 (0.60)	-0.0007 (0.80)	-1.28 (0.20)	0.026 (0.20)	-0.60 (0.50)	0.011 (0.50)	-1.58 (0.10)	0.041 (0.10)	-0.86 (0.40)	0.014 (0.60)	-1.01 (0.30)	0.025 (0.10)	-0.59 (0.50)	0.009 (0.60)
R pallidothalamus[‡, §]	-0.96 (0.30)	0.004 (0.30)	-0.02 (1.00)	0.00001 (1.00)	-1.78 (0.08)	0.041 (0.08)	-0.26 (0.80)	0.004 (0.80)	-1.86 (0.07)	0.060 (0.07)	-0.36 (0.70)	0.008 (0.70)	-1.64 (0.10)	**0.040 (0.05)**	-0.41 (0.70)	-0.003 (0.90)
L caudate-R thalamus[2, a, c, C, ‡]	**-3.14 (0.004)**	**0.016 (0.008)**	0.10 (0.90)	-0.001 (0.90)	0.24 (0.80)	0.006 (0.80)	-1.51 (0.10)	0.039 (0.10)	-1.36 (0.20)	0.048 (0.09)	-1.06 (0.30)	0.040 (0.20)	1.27 (0.20)	-0.009 (0.60)	-1.39 (0.20)	0.021 (0.30)
L putamen-R thalamus[†]	**-2.71 (0.01)**	**0.026 (0.01)**	0.11 (0.90)	-0.001 (0.90)	-0.46 (0.60)	0.009 (0.60)	-1.45 (0.10)	0.039 (0.10)	-1.80 (0.08)	0.046 (0.08)	-1.14 (0.30)	0.037 (0.30)	0.78 (0.40)	-0.014 (0.40)	-1.34 (0.20)	0.03 (0.20)
L pallidum-R thalamus[b, B, †]	**-2.31 (0.03)**	**0.020 (0.03)**	-0.26 (0.80)	0.002 (0.80)	0.31 (0.70)	-0.003 (0.90)	-1.51 (0.10)	0034 (0.20)	-0.17 (0.90)	0.008 (0.70)	**-2.02 (0.05)**	0.055 (0.09)	1.30 (0.20)	-0.022 (0.30)	-1.57 (0.10)	0.04 (0.20)
R caudate-L thalamus	**-2.09 (0.04)**	**0.019 (0.04)**	-0.36 (0.70)	0.003 (0.70)	1.36 (0.20)	-0.036 (0.20)	-1.38 (0.20)	0.026 (0.20)	0.43 (0.70)	-0.011 (0.70)	-1.69 (0.10)	0.040 (0.10)	1.54 (0.10)	-0.004 (0.10)	-1.00 (0.30)	0.018 (0.40)
R putamen-L thalamus[2, f, C, #]	-1.56 (0.10)	0.009 (0.30)	-0.20 (0.80)	0.003 (0.70)	-0.12 (0.90)	-0.002 (0.90)	**-2.65 (0.01)**	**0.053 (0.02)**	-0.83 (0.40)	0.029 (0.30)	**-2.61 (0.01)**	**0.076 (0.005)**	0.51 (0.60)	-0.012 (0.60)	**-2.32 (0.03)**	**0.042 (0.04)**
R pallidum-L thalamus[2, 6, †]	-1.11 (0.30)	0.005 (0.50)	-0.26 (0.80)	0.004 (0.60)	-0.25 (0.80)	0.007 (0.80)	-1.63 (0.10)	0.034 (0.10)	-0.53 (0.60)	0.017 (0.60)	-1.79 (0.08)	0.038 (0.08)	-0.16 (0.90)	0.005 (0.80)	1.30 (0.20)	0.018 (0.40)

R putamocerebellar[6, a, b, B, †]	-0.66 (0.50)	0.004 (0.50)	-0.64 (0.50)	0.002 (0.70)	0.26 (0.80)	0.004 (0.80)	-0.78 (0.40)	0.010 (0.60)	0.16 (0.90)	0.006 (0.80)	-0.93 (0.40)	0.019 (0.50)	0.61 (0.50)	-0.007 (0.80)	-0.53 (0.60)	0.008 (0.70)
R pallidocerebellar[1, b, B, †]	0.39 (0.70)	-0.002 (0.80)	0.24 (0.80)	-0.002 (0.70)	0.96 (0.30)	-0.011 (0.60)	-1.02 (0.30)	0.013 (0.50)	0.98 (0.30)	-0.018 (0.60)	-0.37 (0.70)	0.008 (0.80)	0.90 (0.40)	-0.008 (0.70)	-0.55 (0.60)	0.008 (0.70)
Cerebellothalamic group																
L thalamocerebellar[2, a, *, †, ‡]	0.31 (0.80)	-0.005 (0.40)	0.18 (0.80)	-0.00004 (1.00)	-0.58 (0.60)	0.011 (0.60)	-0.68 (0.50)	0.016 (0.40)	-0.68 (0.50)	0.019 (0.50)	0.19 (0.80)	-0.004 (0.80)	-0.42 (0.70)	0.014 (0.50)	-0.68 (0.50)	0.013 (0.50)
R thalamocerebellar[1,2, b, B, †]	0.38 (0.70)	-0.004 (0.50)	1.88 (0.07)	-0.009 (0.09)	1.41 (0.20)	-0.019 (0.30)	-0.37 (0.70)	0.003 (0.90)	1.60 (0.10)	-0.041 (0.10)	0.14 (0.90)	-0.007 (0.80)	1.21 (0.20)	-0.015 (0.40)	-0.27 (0.80)	0.006 (0.80)
L thalamo-vermis[†]	-0.40 (0.70)	0.004 (0.70)	-0.29 (0.80)	0.002 (0.80)	-0.25 (0.80)	0.006 (0.80)	-0.09 (0.90)	0.002 (0.90)	-0.090 (0.90)	0.003 (0.90)	-0.26 (0.80)	0.009 (0.80)	-0.58 (0.60)	0.010 (0.60)	0.10 (0.90)	-0.003 (0.80)
R thalamo-vermis[e, f, E, ¶]	-0.85 (0.40)	0.008 (0.40)	0.44 (0.60)	-0.003 (0.60)	0.82 (0.40)	-0.019 (0.40)	-0.01 (1.00)	-0.006 (0.80)	-0.81 (0.40)	-0.030 (0.40)	0.06 (0.90)	-0.012 (0.70)	1.01 (0.30)	-0.008 (0.70)	-0.07 (0.90)	0.00004 (1.00)
Interthalami[2, b, †]	-1.53 (0.10)	0.007 (0.30)	0.09 (0.90)	0.001 (0.90)	-1.09 (0.30)	0.020 (0.20)	-2.17 (0.04)	0.028 (0.10)	-1.69 (0.10)	0.034 (0.10)	-1.69 (0.10)	0.031 (0.10)	-0.38 (0.70)	0.010 (0.50)	-1.89 (0.07)	0.022 (0.20)
L cerebello-vermis[1, a, b, B, F, *, †]	-0.90 (0.30)	0.006 (0.20)	0.48 (0.60)	-0.003 (0.60)	0.06 (0.90)	0.006 (0.80)	0.06 (0.90)	-0.015 (0.50)	-0.02 (1.00)	0.007 (0.80)	0.45 (0.60)	0.026 (0.30)	0.11 (0.90)	0.005 (0.80)	0.05 (1.00)	-0.014 (0.50)
R cerebello-vermis[1, 2, b, B, *, †]	-0.89 (0.40)	0.005 (0.30)	-0.59 (0.60)	0.003 (0.60)	-0.26 (0.80)	0.016 (0.50)	-0.61 (0.50)	0.001 (0.90)	-0.49 (0.60)	0.024 (0.30)	-0.46 (0.60)	0.002 (0.90)	-0.11 (0.90)	0.013 (0.50)	-0.55 (0.60)	0.001 (1.00)
Intercerebelli[1, a, b, A, *, †]	-0.92 (0.40)	0.006 (0.30)	0.29 (0.80)	-0.002 (0.60)	0.76 (0.40)	-0.014 (0.60)	-0.58 (0.60)	0.004 (0.80)	-0.16 (0.90)	0.004 (0.90)	-1.36 (0.20)	0.030 (0.10)	0.04 (1.00)	0.006 (0.80)	-0.47 (0.60)	0.001 (0.100)

Independent one-tail t-test; **β** is unstandardised regression coefficient after controlling for potential confounders related to the outcome at $p<0.10$: The model includes potential confounders related to the outcome at $p<0.1$:

FA:- 1 = infant sex; 2 = Equivalent GA of infant at MRI; 3 = infant weight at MRI; 4 = infant head circumference at MRI; 5 = maternal weight change per week; 6 = maternal age at delivery;

MD:- a = infant sex; b = Equivalent GA of infant at MRI; c = infant weight at MRI; d = infant head circumference at MRI; e maternal weight change per week; f = maternal age at delivery;

AD:- A = infant sex; B = Equivalent GA of infant at MRI; C = infant weight at MRI; D = infant head circumference at MRI; E = maternal weight change per week; F = maternal age at delivery;

RD:- ∗ = infant sex; † = Equivalent GA of infant at MRI; ‡ = infant weight at MRI, § = infant head circumference at MRI = maternal weight change per week; # = maternal age at delivery. Bold indicates significance at *p-value.*